NTP
National Toxicology Program
U.S. Department of Health and Human Services

NTP Technical Report on the Toxicology and Carcinogenesis Studies of Antimony Trioxide (CASRN 1309-64-4) in Wistar Han [Crl:WI(Han)] Rats and B6C3F1/N Mice (Inhalation Studies)

NTP TR 590

DECEMBER 2017

NTP Technical Report on the Toxicology and Carcinogenesis Studies of Antimony Trioxide (CASRN 1309-64-4) in Wistar Han [Crl:WI(Han)] Rats and B6C3F1/N Mice (Inhalation Studies)

Technical Report 590

December 2017

National Toxicology Program
Public Health Service
U.S. Department of Health and Human Services
ISSN: 2378-8925

Research Triangle Park, North Carolina, USA

Foreword

The National Toxicology Program (NTP) is an interagency program within the Public Health Service (PHS) of the Department of Health and Human Services (HHS) and is headquartered at the National Institute of Environmental Health Sciences of the National Institutes of Health (NIEHS/NIH). Three agencies contribute resources to the program: NIEHS/NIH, the National Institute for Occupational Safety and Health of the Centers for Disease Control and Prevention (NIOSH/CDC), and the National Center for Toxicological Research of the Food and Drug Administration (NCTR/FDA). Established in 1978, NTP is charged with coordinating toxicological testing activities, strengthening the science base in toxicology, developing and validating improved testing methods, and providing information about potentially toxic substances to health regulatory and research agencies, scientific and medical communities, and the public.

The Technical Report series began in 1976 with carcinogenesis studies conducted by the National Cancer Institute. In 1981, this bioassay program was transferred to NTP. The studies described in the Technical Report series are designed and conducted to characterize and evaluate the toxicologic potential, including carcinogenic activity, of selected substances in laboratory animals (usually two species, rats and mice). Substances selected for NTP toxicity and carcinogenicity studies are chosen primarily on the basis of human exposure, level of production, and chemical structure. The interpretive conclusions presented in NTP Technical Reports are based only on the results of these NTP studies. Extrapolation of these results to other species, including characterization of hazards and risks to humans, requires analyses beyond the intent of these reports. Selection per se is not an indicator of a substance's carcinogenic potential.

NTP conducts its studies in compliance with its laboratory health and safety guidelines and FDA Good Laboratory Practice Regulations and must meet or exceed all applicable federal, state, and local health and safety regulations. Animal care and use are in accordance with the Public Health Service Policy on Humane Care and Use of Animals. Studies are subjected to retrospective quality assurance audits before being presented for public review.

The NTP Technical Reports are available free of charge on the NTP website and cataloged in PubMed, a free resource developed and maintained by the National Library of Medicine (part of the National Institutes of Health). Data for these studies are included in NTP's Chemical Effects in Biological Systems database.

For questions about the reports and studies, please email NTP or call 984-287-3211.

Table of Contents

Foreword ii
Tables v
Figures vi
About This Report viii
Explanation of Levels of Evidence of Carcinogenic Activity xi
Peer Review xiii
Publication Details xiv
Abstract xv
Two-week Study in Rats xv
Two-week Study in Mice xv
Two-year Study in Rats xv
Two-year Study in Mice xvii
Genetic Toxicology xix
Tissue Burden xix
Molecular Pathology xix
Conclusions xix
Introduction 1
Chemical and Physical Properties 1
Production, Use, and Human Exposure 1
Regulatory Status 3
Absorption, Distribution, Metabolism, and Excretion 3
Experimental Animals 3
Humans 4
Toxicity 4
Experimental Animals 4
Humans 5
Reproductive and Developmental Toxicity 6
Experimental Animals 6
Humans 6
Carcinogenicity 6
Experimental Animals 6
Humans 7
Genetic Toxicity 7
Study Rationale 8
Materials and Methods 9
Procurement and Characterization of Antimony Trioxide 9
Aerosol Generation and Exposure System 9
Aerosol Concentration Monitoring 10
Chamber Atmosphere Characterization 10
Animal Source 12

Animal Welfare 12
Two-week Studies 12
Two-year Studies 13
Study Design 13
Clinical Examinations and Pathology 14
Tissue Burden Study 15
Mutation Analysis of Alveolar/Bronchiolar Adenomas and Carcinomas 15
Statistical Methods 19
Survival Analyses 19
Calculation of Incidence 19
Analysis of Neoplasm and Nonneoplastic Lesion Incidences 19
Analysis of Continuous Variables 20
Historical Control Data 20
Quality Assurance Methods 20
Genetic Toxicology 21

Results 22
Data Availability 22
Rats 22
Two-week Study 22
Two-year Study 25
Mice 46
Two-week Study 46
Two-year Study 48
Genetic Toxicology 71
Tissue Burden 71
Two-week Tissue Burden Results in Rats and Mice 72
Two-year Tissue Burden Results in Rats and Mice 73
Molecular Pathology 75

Discussion 89

Conclusions 97

References 98

Appendix A. Summary of Lesions in Male Rats in the Two-year Inhalation Study of Antimony Trioxide A-1

Appendix B. Summary of Lesions in Female Rats in the Two-year Inhalation Study of Antimony Trioxide B-1

Appendix C. Summary of Lesions in Male Mice in the Two-year Inhalation Study of Antimony Trioxide C-1

Appendix D. Summary of Lesions in Female Mice in the Two-year Inhalation Study of Antimony Trioxide D-1

Appendix E. Genetic Toxicology E-1

Appendix F. Organ Weights and Organ-Weight-To-Body-Weight Ratios F-1

Appendix G. Tissue Burden Results G-1

Appendix H. Chemical Characterization and Generation of Chamber Concentrations H-1

Appendix I. Ingredients, Nutrient Composition, and Contaminant Levels in NTP-2000 Rat and Mouse Ration.....I-1

Appendix J. Sentinel Animal Program J-1

Appendix K. Analysis of *Kras* and *Egfr* Mutations in Wistar Han Rat and B6C3F1/N Mouse Alveolar/Bronchiolar Tumors Resulting from Chronic Inhalation Exposure to Antimony Trioxide..... K-1

Appendix L. Summary of Peer Review Panel Comments.....L-1

Tables

Summary of the Two-year Carcinogenesis and Genetic Toxicology Studies of Antimony Trioxide xxi
Table 1. Experimental Design and Materials and Methods in the Inhalation Studies of Antimony Trioxide 16
Table 2. Survival and Body Weights of Rats in the Two-week Inhalation Study of Antimony Trioxide 22
Table 3. Selected Organ Weights and Organ-Weight-to-Body-Weight Ratios for Rats in the Two-week Inhalation Study of Antimony Trioxide 23
Table 4. Incidences of Selected Nonneoplastic Lesions of the Respiratory System in Rats in the Two-week Inhalation Study of Antimony Trioxide 24
Table 5. Survival of Rats in the Two-year Inhalation Study of Antimony Trioxide 26
Table 6. Mean Body Weights and Survival of Male Rats in the Two-year Inhalation Study of Antimony Trioxide 28
Table 7. Mean Body Weights and Survival of Female Rats in the Two-year Inhalation Study of Antimony Trioxide 29
Table 8. Selected Organ Weights and Organ-Weight-to-Body-Weight Ratios for Rats at the Twelve-month Interim Evaluation in the Two-year Inhalation Study of Antimony Trioxide 31
Table 9. Incidences of Neoplasms and Nonneoplastic Lesions of the Lung in Rats in the Two-year Inhalation Study of Antimony Trioxide.....33
Table 10. Incidences of Neoplasms and Nonneoplastic Lesions of the Adrenal Medulla in Rats in the Two-year Inhalation Study of Antimony Trioxide.....37
Table 11. Incidences of Nonneoplastic Lesions of the Upper Respiratory Tract in Rats in the Two-year Inhalation Study of Antimony Trioxide.....39
Table 12. Incidences of Nonneoplastic Lesions of the Hematopoietic System in Rats in the Two-year Inhalation Study of Antimony Trioxide.....41
Table 13. Incidences of Nonneoplastic Lesions in the Arterial Vessels of Rats in the Two-year Inhalation Study of Antimony Trioxide.....42
Table 14. Incidences of Selected Nonneoplastic Lesions in Rats in the Two-year Inhalation Study of Antimony Trioxide 45
Table 15. Survival and Body Weights of Mice in the Two-week Inhalation Study of Antimony Trioxide 46

Table 16. Lung Weights and Lung-Weight-to-Body-Weight Ratios for Mice in the Two-week Inhalation Study of Antimony Trioxide 47
Table 17. Incidences of Selected Nonneoplastic Lesions of the Respiratory System in Mice in the Two-week Inhalation Study of Antimony Trioxide 48
Table 18. Survival of Mice in the Two-year Inhalation Study of Antimony Trioxide 49
Table 19. Mean Body Weights and Survival of Male Mice in the Two-year Inhalation Study of Antimony Trioxide 52
Table 20. Mean Body Weights and Survival of Female Mice in the Two-year Inhalation Study of Antimony Trioxide 53
Table 21. Selected Organ Weights and Organ-Weight-to-Body-Weight Ratios for Mice at the Twelve-month Interim Evaluation in the Two-year Inhalation Study of Antimony Trioxide 55
Table 22. Incidences of Neoplasms and Nonneoplastic Lesions of the Lung in Mice in the Two-year Inhalation Study of Antimony Trioxide 58
Table 23. Incidences of Malignant Lymphoma in Female Mice in the Two-year Inhalation Study of Antimony Trioxide 62
Table 24. Incidences of Neoplasms of the Skin in Mice in the Two-year Inhalation Study of Antimony Trioxide 63
Table 25. Incidences of Nonneoplastic Lesions of the Upper Respiratory Tract in Mice in the Two-year Inhalation Study of Antimony Trioxide 65
Table 26. Incidences of Nonneoplastic Lesions of the Hematopoietic System in Mice in the Two-year Inhalation Study of Antimony Trioxide 68
Table 27. Incidences of Selected Nonneoplastic Lesions in Mice in the Two-year Inhalation Study of Antimony Trioxide 70

Figures

Figure 1. Antimony Trioxide (CASRN 1309-64-4; Chemical Formula: Sb_2O_3; Molecular Weight: 291.5) 1
Figure 2. Kaplan-Meier Survival Curves for Rats Exposed to Antimony Trioxide by Inhalation for Two Years 27
Figure 3. Growth Curves for Rats Exposed to Antimony Trioxide by Inhalation for Two Years 30
Figure 4. Kaplan-Meier Survival Curves for Mice Exposed to Antimony Trioxide by Inhalation for Two Years 50
Figure 5. Growth Curves for Mice Exposed to Antimony Trioxide by Inhalation for Two Years 54
Figure 6. Epithelial Hyperplasia and Neoplasia in the Rat Lung (H&E) 76
Figure 7. Foreign Body (Presumed Test Article) in the Lung of a Male Wistar Han Rat Exposed to 30 mg Antimony Trioxide/m^3 by Inhalation for Two Years (H&E) 77
Figure 8. Nonneoplastic Changes in the Lung of a Male Wistar Han Rat Exposed to 30 mg Antimony Trioxide/m^3 by Inhalation for Two Years (H&E) 78
Figure 9. Inflammation in the Lung of a Male Wistar Han Rat Exposed to 30 mg Antimony Trioxide/m^3 by Inhalation for Two Years (H&E) 78
Figure 10. Alveolar Proteinosis in the Rat Lung 79
Figure 11. Fibrosis in the Lung 80

Figure 12. Hyperplasia and Neoplasia of the Adrenal Medulla (H&E) 81
Figure 13. Respiratory Epithelial Hyperplasia of the Ventral Septum of the Nose (Level I) (H&E) 82
Figure 14. Arterial Inflammation (A, B, and C) and Plexiform Vasculopathy (D) (H&E).....83
Figure 15. Epithelial Neoplasia in the Mouse Lung (H&E) 84
Figure 16. Lymphoid Hyperplasia in the Mouse Lung.....85
Figure 17. Epithelial Hyperplasia and Fibrosis in the Lung (H&E) 86
Figure 18. Malignant Lymphoma in the Mouse Lung.....87
Figure 19. Squamous Metaplasia of the Base of the Epiglottis (H&E).....88

This report has been reformatted to meet new NTP publishing requirements;
its content has not changed.

About This Report

National Toxicology Program[1]

[1]Division of the National Toxicology Program, National Institute of Environmental Health Sciences, Research Triangle Park, North Carolina, USA

Collaborators

M.D. Stout, B.C. Sayers, G.P. Flake, G.L. Baker, C.R. Blystone, J.A. Dill, P.M. Foster, S.L. Grumbein, B.K. Hayden, R.A. Herbert, J.S. Hoane, M.J. Hooth, A.P. King-Herbert, G.E. Kissling, D.E. Malarkey, R.A. Miller, A.R. Pandiri, K.M. Patton, S.L. Smith-Roe, L.M. Staska, K.A. Szabo, G.S. Travlos, M.K. Vallant, S. Waidyanatha, N.J. Walker, K.L. Witt

Division of the National Toxicology Program, National Institute of Environmental Health Sciences, Research Triangle Park, North Carolina, USA
Evaluated and interpreted results and reported findings
M.D. Stout, Ph.D., Co-Study Scientist
B.C. Sayers, Ph.D., Co-Study Scientist
G.P. Flake, M.D., Study Pathologist
C.R. Blystone, Ph.D.
P.M. Foster, Ph.D.
R.A. Herbert, D.V.M., Ph.D.
M.J. Hooth, Ph.D.
A.P. King-Herbert, D.V.M.
G.E. Kissling, Ph.D.
D.E. Malarkey, D.V.M., Ph.D.
A.R. Pandiri, B.V.Sc. & A.H., Ph.D.
S.L. Smith-Roe, Ph.D.
G.S. Travlos, D.V.M.
M.K. Vallant, M.S., MT
S. Waidyanatha, Ph.D.
N.J. Walker, Ph.D.
K.L. Witt, M.S.

Battelle Toxicology Northwest, Richland, Washington, USA
Conducted studies and evaluated pathology findings
J.A. Dill, Ph.D., Principal Investigator
G.L. Baker, Ph.D., Study Director
S.L. Grumbein, D.V.M., Ph.D.
B.K. Hayden
K.M. Patton, D.V.M., Ph.D.
L.M. Staska, D.V.M., Ph.D.

Experimental Pathology Laboratories, Inc., Research Triangle Park, North Carolina, USA
Conducted pathology review
R.A. Miller, D.V.M., Ph.D.
A.R. Pandiri, B.V.Sc. & A.H., Ph.D.

Pathology Associates International, A Charles River Company, Research Triangle Park, North Carolina, USA
Coordinated NTP Pathology Working Groups
J.S. Hoane, D.V.M., Coordinated 2-year rats (October 17, 2013, and November 14, 2013)
K.A. Szabo, D.V.M., M.S., Coordinated 2-year mice (December 10, 2013)

Contributors

Experimental Pathology Laboratories, Inc., Research Triangle Park, North Carolina, USA
Supervised pathology review
M.H. Hamlin, II, D.V.M., Principal Investigator

NTP Pathology Working Group, National Institute of Environmental Health Sciences, Research Triangle Park, North Carolina, USA
Participated in NTP Pathology Working Group on 2-year rats (October 17, 2013, and November 14, 2013)
M.F. Cesta, D.V.M., Ph.D., National Toxicology Program
S.A. Elmore, D.V.M., M.S., National Toxicology Program
G.P. Flake, M.D., National Toxicology Program
R.A. Herbert, D.V.M., Ph.D., National Toxicology Program
M.P. Jokinen, D.V.M., ILS, Inc.
R.A. Miller, D.V.M., Ph.D., Experimental Pathology Laboratories, Inc.
A.R. Pandiri, B.V.Sc. & A.H., Ph.D., Experimental Pathology Laboratories, Inc.
L.M. Staska, D.V.M., Ph.D., ILS, Inc.

Participated in NTP Pathology Working Group on 2-year mice (December 10, 2013)
M.F. Cesta, D.V.M., Ph.D., National Toxicology Program
S.A. Elmore, D.V.M., M.S., National Toxicology Program
G.P. Flake, M.D., National Toxicology Program
M.P. Jokinen, D.V.M., ILS, Inc.
R.A. Miller, D.V.M., Ph.D., Experimental Pathology Laboratories, Inc.
A.R. Pandiri, B.V.Sc. & A.H., Ph.D., Experimental Pathology Laboratories, Inc.
E.M. Quist, D.V.M., M.S., National Toxicology Program
D.B. Rao, B.V.Sc., Ph.D., ILS, Inc.

Social & Scientific Systems, Inc., Research Triangle Park, North Carolina, USA
Provided statistical analyses
M.V. Smith, Ph.D., Principal Investigator
L.J. Betz, M.S.
S.F. Harris, B.S.

Dynamac Corporation, Research Triangle Park, North Carolina, USA
Prepared quality assessment audits
S. Brecher, Ph.D., Principal Investigator
S. Iyer, B.S.
V.S. Tharakan, D.V.M.

Biotechnical Services, Inc., Little Rock, Arkansas, USA
Prepared Technical Report
S.R. Gunnels, M.A., Principal Investigator
P.A. Gideon, B.A.
B.F. Hall, M.S.
L.M. Harper, B.S.
D.C. Serbus, Ph.D.

Explanation of Levels of Evidence of Carcinogenic Activity

The National Toxicology Program describes the results of individual experiments on a chemical agent and notes the strength of the evidence for conclusions regarding each study. Negative results, in which the study animals do not have a greater incidence of neoplasia than control animals, do not necessarily mean that a chemical is not a carcinogen, inasmuch as the experiments are conducted under a limited set of conditions. Positive results demonstrate that a chemical is carcinogenic for laboratory animals under the conditions of the study and indicate that exposure to the chemical has the potential for hazard to humans. Other organizations, such as the International Agency for Research on Cancer, assign a strength of evidence for conclusions based on an examination of all available evidence, including animal studies such as those conducted by NTP, epidemiologic studies, and estimates of exposure. Thus, the actual determination of risk to humans from chemicals found to be carcinogenic in laboratory animals requires a wider analysis that extends beyond the purview of these studies.

Five categories of evidence of carcinogenic activity are used in the Technical Report series to summarize the strength of evidence observed in each experiment: two categories for positive results **(clear evidence and some evidence)**; one category for uncertain findings **(equivocal evidence)**; one category for no observable effects **(no evidence)**; and one category for experiments that cannot be evaluated because of major flaws **(inadequate study)**. These categories of interpretative conclusions were first adopted in June 1983 and then revised on March 1986 for use in the Technical Report series to incorporate more specifically the concept of actual weight of evidence of carcinogenic activity. For each separate experiment (male rats, female rats, male mice, female mice), one of the following five categories is selected to describe the findings. These categories refer to the strength of the experimental evidence and not to potency or mechanism.

- **Clear evidence** of carcinogenic activity is demonstrated by studies that are interpreted as showing a dose-related (i) increase of malignant neoplasms, (ii) increase of a combination of malignant and benign neoplasms, or (iii) marked increase of benign neoplasms if there is an indication from this or other studies of the ability of such tumors to progress to malignancy.
- **Some evidence** of carcinogenic activity is demonstrated by studies that are interpreted as showing a chemical-related increased incidence of neoplasms (malignant, benign, or combined) in which the strength of the response is less than that required for clear evidence.
- **Equivocal evidence** of carcinogenic activity is demonstrated by studies that are interpreted as showing a marginal increase of neoplasms that may be chemical related.
- **No evidence** of carcinogenic activity is demonstrated by studies that are interpreted as showing no chemical-related increases in malignant or benign neoplasms.
- **Inadequate study** of carcinogenic activity is demonstrated by studies that, because of major qualitative or quantitative limitations, cannot be interpreted as valid for showing either the presence or absence of carcinogenic activity.

For studies showing multiple chemical-related neoplastic effects that if considered individually would be assigned to different levels of evidence categories, the following convention has been

adopted to convey completely the study results. In a study with clear evidence of carcinogenic activity at some tissue sites, other responses that alone might be deemed some evidence are indicated as "were also related" to chemical exposure. In studies with clear or some evidence of carcinogenic activity, other responses that alone might be termed equivocal evidence are indicated as "may have been" related to chemical exposure.

When a conclusion statement for a particular experiment is selected, consideration must be given to key factors that would extend the actual boundary of an individual category of evidence. Such consideration should allow for incorporation of scientific experience and current understanding of long-term carcinogenesis studies in laboratory animals, especially for those evaluations that may be on the borderline between two adjacent levels. These considerations should include:

- adequacy of the experimental design and conduct;
- occurrence of common versus uncommon neoplasia;
- progression (or lack thereof) from benign to malignant neoplasia as well as from preneoplastic to neoplastic lesions;
- some benign neoplasms have the capacity to regress but others (of the same morphologic type) progress. At present, it is impossible to identify the difference. Therefore, where progression is known to be a possibility, the most prudent course is to assume that benign neoplasms of those types have the potential to become malignant;
- combining benign and malignant tumor incidence known or thought to represent stages of progression in the same organ or tissue;
- latency in tumor induction;
- multiplicity in site-specific neoplasia;
- metastases;
- supporting information from proliferative lesions (hyperplasia) in the same site of neoplasia or other experiments (same lesion in another sex or species);
- presence or absence of dose relationships;
- statistical significance of the observed tumor increase;
- concurrent control tumor incidence as well as the historical control rate and variability for a specific neoplasm;
- survival-adjusted analyses and false positive or false negative concerns;
- structure-activity correlations; and
- in some cases, genetic toxicology.

Peer Review

The members of the Peer Review Panel who evaluated the draft *NTP Technical Report on the Toxicology and Carcinogenesis Studies of Antimony Trioxide (CASRN 1309-64-4) in Wistar Han [Crl:WI(Han)] Rats and B6C3F1/N Mice (Inhalation Studies)* on February 16, 2016, are listed below. Panel members served as independent scientists, not as representatives of any institution, company, or governmental agency. In this capacity, reviewers had five major responsibilities in reviewing the NTP studies:

- to ascertain that all relevant literature data have been adequately cited and interpreted,
- to determine if the design and conditions of the NTP studies were appropriate,
- to ensure that the Technical Report presents the experimental results and conclusions fully and clearly,
- to judge the significance of the experimental results by scientific criteria, and
- to assess the evaluation of the evidence of carcinogenic activity and other observed toxic responses.

Peer Reviewers

Jon C. Mirsalis, Ph.D. (Chair)
SRI International
Menlo Park, California, USA

William J. Brock, Ph.D.
Brock Scientific Consulting, LLC
Montgomery Village, Maryland, USA

Michael R. Elwell, D.V.M., Ph.D.
Nonclinical Safety Assessment
Covance Laboratories, Inc.
Chantilly, Virginia, USA

Kent E. Pinkerton, Ph.D. (Primary Reviewer)
Center for Health and the Environment
University of California
Davis, California, USA

Michael V. Pino, D.V.M., Ph.D. (Primary Reviewer)
Veterinary Toxicologic Pathology and Preclinical Drug Development
Albuquerque, New Mexico, USA

Tara Sabo-Attwood, Ph.D.
Department of Environmental and Global Health
University of Florida
Gainesville, Florida, USA

Madhuri Singal, Ph.D. (Primary Reviewer)
Global Regulatory Compliance
Reckitt Benckiser
Montvale, New Jersey, USA

Publication Details

Publisher: National Toxicology Program

Publishing Location: Research Triangle Park, NC

ISSN: 2378-8925

DOI: https://doi.org/10.22427/NTP-TR-590

Report Series: NTP Technical Report Series

Report Series Number: 590

Official citation: National Toxicology Program (NTP). 2017. NTP technical report on the toxicology and carcinogenesis studies of antimony trioxide (CASRN 1309-64-4) in Wistar Han [Crl:WI(Han)] rats and B6C3F1/N mice (inhalation studies). Research Triangle Park, NC: National Toxicology Program. Technical Report 590.

Abstract

Antimony trioxide (Sb_2O_3) is used as a flame retardant in canvas, textiles, paper, and plastics and in combination with some chlorinated or brominated flame retardants on commercial furniture, draperies, wall coverings, and carpets. It is also used in batteries, enamels and paint pigment, and ceramics and fiberglass. Occupationally, the major sources of exposure to antimony exist in the metal ore smelting and mining industries. Antimony trioxide was nominated by the Consumer Products Safety Commission and The National Institute of Environmental Health Sciences for National Toxicology Program testing due to the potential for substantial human exposure in occupational settings and the lack of adequate 2-year exposure carcinogenicity studies. Male and female Wistar Han [Crl:WI(Han)] rats and B6C3F1/N mice were exposed to antimony trioxide (greater than 99.9% pure) by inhalation for 2 weeks or 2 years. Genetic toxicology studies were conducted in rat and mouse peripheral blood erythrocytes, peripheral blood leukocytes, and lung cells.

Two-week Study in Rats

Groups of five male and five female core study rats were exposed by whole body inhalation to antimony trioxide aerosol at concentrations of 0, 3.75, 7.5, 15, 30, or 60 mg/m^3 for 6 hours plus T_{90} (12 minutes) per day, 5 days per week for 12 exposure days during a 16-day period. Additional groups of five female tissue burden study rats were exposed to the same concentrations for 16 days then held for 28 days without exposure. All rats survived to the end of the study. The mean body weights of exposed groups of males and females were similar to those of the respective chamber control groups. Lung weights of 60 mg/m^3 males and 30 and 60 mg/m^3 females were significantly greater than those of the chamber controls.

Incidences of chronic active inflammation in the lungs were significantly increased in 30 and 60 mg/m^3 males and females.

Two-week Study in Mice

Groups of five male and five female core study mice were exposed by whole body inhalation to antimony trioxide aerosol at concentrations of 0, 3.75, 7.5, 15, 30, or 60 mg/m^3 for 6 hours plus T_{90} (12 minutes) per day, 5 days per week for 13 exposure days during a 17-day period. Additional groups of five female tissue burden study mice were exposed to the same concentrations for 17 days then held for 28 days without exposure. All mice survived to the end of the study. The mean body weights of exposed groups of males and females were similar to those of the respective chamber control groups. Lung weights were significantly increased in 60 mg/m^3 males and 15 mg/m^3 or greater females.

In the larynx, there were significantly increased incidences of squamous metaplasia of the epiglottis in the 30 and 60 mg/m^3 males and females compared to those in the chamber control groups.

Two-year Study in Rats

Groups of 60 male and 60 female rats were exposed by whole body inhalation to antimony trioxide aerosol at concentrations of 0, 3, 10, or 30 mg/m^3 for 6 hours plus T_{90} (12 minutes) per day, 5 days per week for up to 105 weeks. Additional groups of 25 tissue burden study female rats were exposed to the same concentrations of antimony trioxide for up to 79 weeks. Survival of 10 and 30 mg/m^3 females was significantly less than that of the chamber control group. The decreased survival in females was attributed primarily to lung proteinosis. In males, the trend

towards reduced survival was attributed primarily to lung inflammation and proteinosis. Mean body weights of 30 mg/m^3 males were at least 10% less than those of the chamber control group after week 69 and decreased to 80% of that of the chamber controls by the end of the study. Mean body weights of 3, 10, and 30 mg/m^3 females were at least 10% less than those of the chamber control group after weeks 99, 81, and 65, respectively, and those of 10 and 30 mg/m^3 females were 20% and 28% less, respectively, than that of the chamber control group by the end of the study. Exposure-related clinical findings included abnormal breathing, cyanosis, and thinness in males and females. Lung weights were significantly increased in all exposed groups of males and females at the 12-month interim evaluation.

At the 12-month interim evaluation, a single incidence of alveolar/bronchiolar adenoma of the lung occurred in a 30 mg/m^3 female. There was a positive trend in the incidences of alveolar/bronchiolar adenoma in females in the 2-year study, and the incidences were significantly increased in females exposed to 10 or 30 mg/m^3; 30 mg/m^3 females also had one squamous cell carcinoma and two cystic keratinizing epitheliomas. In all exposed groups of males, the incidences of alveolar/bronchiolar adenoma and of alveolar/bronchiolar adenoma or carcinoma (combined) exceeded the historical control ranges for inhalation studies and for all routes of administration.

Incidences of chronic active inflammation, alveolar epithelium hyperplasia, proteinosis, and fibrosis in the lung were significantly increased in all exposed groups of males and females at the 12-month interim evaluation and in the 2-year study. Foreign body, presumed to be the test article, was identified in the larynges and lungs of all exposed male and female rats in both the 12-month and 2-year evaluations, and was also seen in the trachea and bronchial and mediastinal lymph nodes of most exposed male and female rats at each time point. Incidences of lymphocytic perivascular cellular infiltration were significantly increased in 3 and 10 mg/m^3 males and females at the 12-month interim evaluation and in 3 and 10 mg/m^3 males and all exposed groups of females in the 2-year study. Incidences of bronchiole epithelium hyperplasia were significantly increased in all exposed groups of males at the 12-month interim evaluation and in all exposed groups of males and females in the 2-year study. The incidences of suppurative alveolar inflammation were significantly increased in all exposed groups of males and females in the 2-year study. The incidence of squamous metaplasia of the alveolar epithelium was significantly increased in 3 mg/m^3 females in the 2-year study.

In the adrenal medulla, the incidences of benign pheochromocytoma were significantly increased in 30 mg/m^3 males and females and the incidence of benign or malignant pheochromocytoma (combined) was significantly increased in 30 mg/m^3 females in the 2-year study. Incidences of adrenal medullary hyperplasia occurred with a positive trend in both males and females in the 2-year study, and the incidences were significantly increased in 30 mg/m^3 males and females.

In the 2-year study, incidences of respiratory epithelium hyperplasia in the nose were significantly increased in 3 and 30 mg/m^3 males and 30 mg/m^3 females. The incidences of respiratory epithelium squamous metaplasia in 30 mg/m^3 males and females were significantly increased in the 2-year study.

In the 2-year study, the incidence of chronic active inflammation was significantly increased in the larynx of 3 mg/m^3 females.

In the bone marrow, incidences of hyperplasia, predominantly due to increased erythroid precursors, were significantly increased in 30 mg/m^3 males and females in the 2-year study.

Incidences of lymphoid hyperplasia in the bronchial and mediastinal lymph nodes were significantly increased in 10 mg/m^3 males and 3 mg/m^3 females at the 12-month interim evaluation and in all exposed groups of males and females in the 2-year study. The incidence of pigmentation was significantly increased in the bronchial lymph nodes of 30 mg/m^3 males in the 2-year study.

Chronic active arterial inflammation was observed in multiple tissues in males and females in the 2-year study, including the mediastinum, pancreas, mesentery, lung, and kidney. The combined incidences of chronic active arterial inflammation in all tissues were increased in 10 and 30 mg/m^3 males and females. These increases were significant in 30 mg/m^3 males and 10 and 30 mg/m^3 females.

In the kidney, the incidences of renal tubule hyaline droplet accumulation were significantly increased in 30 mg/m^3 males and 10 and 30 mg/m^3 females in the 2-year study. The incidence of nephropathy was significantly increased in 30 mg/m^3 females in the 2-year study.

Incidences of retinal atrophy were significantly increased in all exposed groups of females in the 2-year study. Incidences of acute inflammation of the ciliary body of the eye were significantly increased in 30 mg/m^3 males and females in the 2-year study.

Two-year Study in Mice

Groups of 60 male and 60 female mice were exposed by whole body inhalation to antimony trioxide aerosol at concentrations of 0, 3, 10, or 30 mg/m^3 for 6 hours plus T_{90} (12 minutes) per day, 5 days per week for up to 105 weeks. Additional groups of 25 tissue burden study female mice were exposed to the same concentrations of antimony trioxide for up to 79 weeks. Survival of 10 and 30 mg/m^3 males and females was significantly less than that of the chamber control groups. Decreases in survival were attributed primarily to alveolar/bronchiolar carcinomas and inflammation of the lung in males and malignant lymphoma and lung inflammation in females. Mean body weights of 30 mg/m^3 males were 10% to 25% less than those of the chamber control group after week 73; mean body weights of 30 mg/m^3 females were at least 10% less than those of the chamber control group after week 85. Exposure-related clinical findings included abnormal breathing and thinness in males and females.

Lung weights were significantly increased in all exposed groups of males and in 10 and 30 mg/m^3 females at the 12-month interim evaluation. Thymus weights of 10 and 30 mg/m^3 males and females were significantly increased at the 12-month interim evaluation.

Significantly increased incidences of alveolar/bronchiolar carcinoma and alveolar/bronchiolar adenoma or carcinoma (combined) occurred in all exposed groups of males in the 2-year study; these incidences occurred with a positive trend and exceeded the historical control ranges for inhalation studies and for all routes of administration. The incidences of multiple alveolar/bronchiolar carcinoma were also significantly increased in exposed male mice. In female mice, incidences of alveolar/bronchiolar adenoma, alveolar/bronchiolar carcinoma, and alveolar/bronchiolar adenoma or carcinoma (combined) were significantly increased in all exposed groups in the 2-year study and exceeded the historical control ranges for inhalation studies and for all routes of administration. The incidences of multiple alveolar/bronchiolar carcinoma were significantly increased in all exposed groups of females.

In the lung, incidences of lymphocytic cellular infiltration, chronic active inflammation, pleura fibrosis, pleura inflammation, alveolar epithelium hyperplasia, and bronchiole epithelium

hyperplasia were significantly increased in all exposed groups of males and females at the 12-month interim evaluation and in the 2-year study. Incidences of alveolus fibrosis were significantly increased in all exposed groups of males and in 10 and 30 mg/m^3 females at the 12-month interim evaluation; incidences of this lesion were significantly increased in all exposed groups of males and females in the 2-year study. Foreign body, presumed to be the test article, was identified in the lungs of all exposed male and female mice in both the 12-month and 2-year evaluations, and was also seen in the nose, larynx, trachea, and bronchial and mediastinal lymph nodes of many exposed male and female mice at each time point.

Incidences of malignant lymphoma occurred with a positive trend in females, and were significantly increased in all exposed groups in the 2-year study.

In the skin, the incidences of fibrous histiocytoma and fibrous histiocytoma or fibrosarcoma (combined) were significantly increased in 30 mg/m^3 males in the 2-year study. In females, the incidence of squamous cell carcinoma was slightly increased at 30 mg/m^3.

In the nose, incidences of chronic active inflammation of the respiratory epithelium were significantly increased in 3 and 10 mg/m^3 males in the 2-year study. The incidence of squamous metaplasia of the respiratory epithelium was significantly increased in 30 mg/m^3 females in the 2-year study.

In the larynx, incidences of respiratory epithelium hyperplasia were significantly increased in 10 and 30 mg/m^3 males and 10 mg/m^3 females at the 12-month interim evaluation and in 10 and 30 mg/m^3 males and females in the 2-year study. Incidences of respiratory epithelium squamous metaplasia were significantly increased in 30 mg/m^3 females at the 12-month interim evaluation and in 10 and 30 mg/m^3 males and 30 mg/m^3 females in the 2-year study. Incidences of squamous epithelium hyperplasia were significantly increased in 30 mg/m^3 males and females in the 2-year study.

In the trachea, the incidence of epithelium hyperplasia was significantly increased in 30 mg/m^3 males in the 2-year study.

In the hematopoietic system, incidences of lymphoid hyperplasia in the bronchial lymph nodes were significantly increased in all exposed groups of males and females at the 12-month interim evaluation and in the 2-year study. Incidences of this lesion in the mediastinal lymph node were significantly increased in 30 mg/m^3 males at the 12-month interim evaluation and in 10 and 30 mg/m^3 males and females in the 2-year study. Incidences of this lesion were also significantly increased in the spleen of all exposed groups of females at the 12-month interim evaluation. The incidences of histiocytic cellular infiltration were significantly increased in the bronchial lymph node of 10 mg/m^3 females at the 12-month interim evaluation and 30 mg/m^3 males and 10 and 30 mg/m^3 females in the 2-year study. Incidences of this lesion were also significantly increased in the mediastinal lymph node of 10 and 30 mg/m^3 males and all exposed groups of females in the 2-year study. The incidence of hematopoietic cell proliferation was significantly increased in the spleen of 30 mg/m^3 females in the 2-year study. Incidences of bone marrow hyperplasia, predominantly due to increased myelopoiesis, were significantly increased in all exposed groups of males and in 10 and 30 mg/m^3 females in the 2-year study. Incidences of cellular depletion were significantly increased in the thymus of 10 and 30 mg/m^3 males and all exposed groups of females in the 2-year study.

In the heart, incidences of chronic active inflammation of the epicardium were significantly increased in 10 and 30 mg/m^3 males and females in the 2-year study.

The incidence of chronic active inflammation of the forestomach was significantly increased in 30 mg/m^3 males in the 2-year study.

Genetic Toxicology

Antimony trioxide induced small but significant increases in micronucleated erythrocytes in male and female B6C3F1/N mice following exposure for 12 months by inhalation. Significant increases in the percentage of reticulocytes (immature erythrocytes) were also seen in both male and female mice. In addition, increased levels of DNA damage, assessed using the comet assay, were observed in these same male and female mice in lung tissue samples, but not in peripheral blood leukocytes. No increases in micronucleated red blood cells, percentage of reticulocytes, or DNA damage in lung tissue samples or blood leukocytes were observed in male or female Wistar Han rats following exposure to antimony trioxide for 12 months.

Tissue Burden

Total antimony trioxide lung burdens and blood antimony concentrations increased with increasing exposure concentration in rats and mice in the 2-week and 2-year studies. Based on the observed deposition of antimony trioxide in the lung, it is presumed that foreign body observed in the lungs of rats and mice in the 2-week studies and the lungs, nose, larynx, trachea, bronchial and mediastinal lymph nodes, and mandibular lymph node (mice only) in the 2-year studies is consistent with the presence of antimony trioxide particles in these tissues.

Molecular Pathology

In Wistar Han rats exposed to antimony trioxide by inhalation for 2 years, there was a high incidence of *Egfr* mutations (13/26) but not *Kras* mutations (1/26) in alveolar/bronchiolar tumors. The *Egfr* mutations were localized within exons 18 to 21 and all of them were transition mutations. No *Kras* or *Egfr* mutations were noted in the alveolar/bronchiolar tumors that arose spontaneously or in age-matched nontumor lung tissues.

Compared to the rats, the mice had higher frequencies of point mutations within hot spot regions of *Kras* (34/80) in alveolar/bronchiolar tumors. However, the mice also had a relatively high incidence of *Kras* mutations in the spontaneous alveolar/bronchiolar carcinomas in the chamber controls (3/9), and as a result, the increased incidences of *Kras* mutations within the exposed groups did not achieve statistical significance. In addition, the majority of *Kras* mutations in both spontaneous and chemically induced alveolar/bronchiolar tumors were within codon 12 and were G to A transitions. Incidences of *Egfr* mutations increased with exposure concentration and occurred with a positive trend across the exposure concentration groups. The *Egfr* mutations were mainly located within exons 18 and 20, and were transition mutations.

Conclusions

Under the conditions of these 2-year inhalation studies, there was *some evidence of carcinogenic activity* (see Explanation of Levels of Evidence of Carcinogenic Activity; see a summary of the Peer Review Panel comments and the public discussion on this Technical Report in Appendix L) of antimony trioxide in male Wistar Han rats based on increased combined incidences of alveolar/bronchiolar adenoma or carcinoma in the lung and on increased incidences of benign pheochromocytoma of the adrenal medulla. There was *some evidence of carcinogenic activity* of antimony trioxide in female Wistar Han rats based on increased incidences of

alveolar/bronchiolar adenoma in the lung and on increased combined incidences of benign or malignant pheochromocytoma of the adrenal medulla. The combined occurrence of cystic keratinizing epithelioma and squamous cell carcinoma in the lung may have been related to exposure. There was *clear evidence of carcinogenic activity* of antimony trioxide in male B6C3F1/N mice based on increased incidences of alveolar/bronchiolar carcinoma of the lung. Increases in the incidences of fibrous histiocytoma in the skin, as well as the combined incidences of fibrous histiocytoma or fibrosarcoma in the skin of male mice were also considered to be related to exposure. There was *clear evidence of carcinogenic activity* in female B6C3F1/N mice based on increases in the incidences of alveolar/bronchiolar adenoma and alveolar/bronchiolar carcinoma of the lung and on increased incidences of malignant lymphoma. The occurrence of squamous cell carcinoma of the skin may have been related to exposure.

Exposure to antimony trioxide resulted in increased incidences of nonneoplastic findings of the lung, nose, larynx, trachea, bronchial and mediastinal lymph nodes, and bone marrow of male and female rats and mice; the adrenal medulla, arteries of multiple tissues (mesentery, pancreas, mediastinum, kidney, and lung), kidney, and eye of male and female rats; the thymus and heart of male and female mice; the forestomach of male mice; and the spleen of female mice.

Synonyms: A1530; A1582; a1588 lp; antimonious oxide; antimony oxide; antimony (III) oxide; antimony peroxide; antimony sesquioxide; antimony white; AP 50; biantimony trioxide; C.I. pigment white 11; dechlorane a-o; diantimony trioxide; exitelite; flowers of antimony; nyacol a 1530; senarmontite; valentinite; weisspiessglanz

Trade names: FireShield®, Microfine®, Montana Brand, Thermoguard®, Timonox, TMS®, Trutint®, Ultrafine®, White Star

Summary of the Two-year Carcinogenesis and Genetic Toxicology Studies of Antimony Trioxide

	Male Wistar Han Rats	Female Wistar Han Rats	Male B6C3F1/N Mice	Female B6C3F1/N Mice
Concentrations in Air	0, 3, 10, or 30 mg/m^3	0, 3, 10, or 30 mg/m^3	0, 3, 10, or 30 mg/m^3	0, 3, 10, or 30 mg/m^3
Survival Rates	30/50, 30/50, 28/50, 18/50	39/50, 38/50, 28/50, 20/50	38/50, 30/50, 27/50, 17/50	36/50, 31/50, 26/50, 15/50
Body Weights	30 mg/m^3 group at least 10% less than the chamber control group after week 69 and decreased to 80% of that of the chamber controls by the end of the exposure.	3, 10, and 30 mg/m^3 groups at least 10% less than the chamber control group after weeks 99, 81, and 65, respectively; the 10 and 30 mg/m^3 groups were 20% and 28% less, respectively, than the chamber control group by the end of the exposure.	30 mg/m^3 group at least 10% less than the chamber control group after week 73 and 25% less than the chamber control group by the end of the exposure.	30 mg/m^3 group at least 10% less than the chamber control group after week 85 and 21% less than the chamber control group by the end of the exposure.
Nonneoplastic Effects	Lung: foreign body (1/50, 50/50, 50/50, 50/50); inflammation, chronic active (18/50, 50/50, 50/50, 50/50); alveolus, inflammation, suppurative (0/50, 12/50, 24/50, 28/50); perivascular, infiltration cellular, lymphocyte (3/50, 25/50, 19/50, 9/50); proteinosis (0/50, 47/50, 50/50, 50/50); alveolar epithelium, hyperplasia (4/50, 50/50, 48/50, 49/50); bronchiole, epithelium, hyperplasia (3/50, 34/50, 36/50, 33/50); fibrosis (2/50, 50/50, 49/50, 49/50) Adrenal medulla: hyperplasia (1/49, 2/50, 4/49, 8/50) Nose: foreign body (0/50, 0/49, 17/50, 40/50); respiratory epithelium, hyperplasia (6/50, 15/49, 13/50, 25/50); respiratory	Lung: foreign body (0/50, 50/50, 50/50, 50/50); inflammation, chronic active (21/50, 50/50, 50/50, 50/50); alveolus, inflammation, suppurative (0/50, 5/50, 6/50, 5/50); perivascular, infiltration cellular, lymphocyte (0/50, 18/50, 11/50, 8/50); proteinosis (0/50, 50/50, 50/50, 50/50); alveolar epithelium, hyperplasia (5/50, 50/50, 49/50, 50/50); bronchiole, epithelium, hyperplasia (6/50, 26/50, 25/50, 27/50); alveolar epithelium, metaplasia, squamous (0/50, 5/50, 3/50, 1/50); fibrosis (1/50, 50/50, 50/50, 49/50) Adrenal medulla: hyperplasia (0/49, 0/49, 3/49, 5/50) Nose: foreign body (0/50, 5/50, 26/50, 45/50); respiratory	Lung: infiltration cellular, lymphocyte (13/50, 47/50, 48/50, 45/50); foreign body (0/50, 50/50, 50/50, 50/50); inflammation, chronic active (0/50, 48/50, 50/50, 50/50); alveolus, fibrosis (0/50, 12/50, 30/50, 37/50); pleura, fibrosis (0/50, 36/50, 46/50, 50/50); pleura, inflammation (1/50, 40/50, 47/50, 48/50); alveolar epithelium, hyperplasia (6/50, 39/50, 45/50, 49/50); bronchiole, epithelium, hyperplasia (0/50, 32/50, 44/50, 44/50) Bone marrow: hyperplasia (10/49, 19/50, 27/48, 33/50) Thymus: depletion cellular (15/41, 14/38, 32/43, 32/39) Nose: foreign body (0/50, 48/49, 48/49, 49/50); respiratory epithelium, inflammation,	Lung: infiltration cellular, lymphocyte (7/50, 37/50, 37/50, 26/50); foreign body (0/50, 50/50, 50/50, 50/50); inflammation, chronic active (1/50, 50/50, 50/50, 50/50); alveolus, fibrosis (0/50, 13/50, 30/50, 38/50); pleura, fibrosis (1/50, 39/50, 50/50, 50/50); pleura, inflammation (4/50, 27/50, 42/50, 38/50); alveolar epithelium, hyperplasia (1/50, 36/50, 49/50, 48/50); bronchiole, epithelium, hyperplasia (1/50, 34/50, 48/50, 45/50) Spleen: hematopoietic cell proliferation (17/50, 19/50, 20/50, 35/50) Bone marrow: hyperplasia (3/50, 5/50, 15/50, 28/50) Thymus: depletion cellular (9/47, 18/49, 23/49, 29/49) Nose: foreign body (1/50, 44/49, 45/50, 48/50); respiratory

	Male Wistar Han Rats	Female Wistar Han Rats	Male B6C3F1/N Mice	Female B6C3F1/N Mice
	epithelium, metaplasia, squamous (0/50, 0/49, 2/50, 6/50) Larynx: foreign body (0/50, 50/50, 50/50, 50/50)	epithelium, hyperplasia (4/50, 6/50, 7/50, 16/50); respiratory epithelium, metaplasia, squamous (0/50, 2/50, 3/50, 5/50) Larynx: foreign body (0/50, 50/50, 50/50, 50/50); inflammation, chronic active (0/50, 8/50, 0/50, 3/50)	chronic active (3/50, 9/49, 9/49, 6/50)	epithelium, metaplasia, squamous (0/50, 3/49, 2/50, 4/50)
	Trachea: foreign body (0/50, 28/50, 43/50, 48/50) Bone marrow: hyperplasia (0/50, 3/50, 4/50, 8/50) Lymph node, bronchial: foreign body (0/41, 35/40, 45/48, 42/47); hyperplasia, lymphoid (0/41, 21/40, 29/48, 26/47); pigmentation (1/41, 4/40, 5/48, 10/47) Lymph node, mediastinal: foreign body (0/42, 41/45, 41/49, 43/49); hyperplasia, lymphoid (1/42, 24/45, 30/49, 26/49) Mediastinum: artery, inflammation, chronic active (0/0, 1/1, 2/2, 10/10) Pancreas: artery, inflammation, chronic active (1/50, 0/50, 2/50, 8/50) Mesentery: artery, inflammation, chronic active (0/50, 0/50, 0/50, 6/50) Lung: artery, inflammation, chronic active (0/50, 0/50, 1/50, 1/50)	Trachea: foreign body (0/50, 39/50, 47/50, 49/50) Bone marrow: hyperplasia (8/50, 5/50, 11/50, 20/50) Lymph node, bronchial: foreign body (0/35, 35/36, 23/28, 36/41); hyperplasia, lymphoid (0/35, 21/36, 9/28, 11/41) Lymph node, mediastinal: foreign body (0/46, 27/46, 32/46, 33/46); hyperplasia, lymphoid (0/46, 14/46, 10/46, 15/46) Mediastinum: artery, inflammation, chronic active (0/0, 0/0, 2/2, 9/9) Pancreas: artery, inflammation, chronic active (0/50, 0/50, 3/50, 8/50); artery, necrosis (0/50, 0/50, 0/50, 4/50) Mesentery: artery, inflammation, chronic active (0/50, 0/50, 0/50, 6/50) Lung: artery, inflammation, chronic active (0/50, 0/50, 1/50, 2/50)	Larynx: foreign body (0/50, 15/50, 29/50, 44/50); respiratory epithelium, hyperplasia (1/50, 3/50, 15/50, 30/50); respiratory epithelium, metaplasia, squamous (0/50, 0/50, 8/50, 18/50); squamous epithelium, hyperplasia (2/50, 0/50, 4/50, 13/50) Trachea: foreign body (0/49, 3/50, 1/50, 20/50); epithelium, hyperplasia (0/49, 0/50, 2/50, 5/50) Lymph node, bronchial: hyperplasia, lymphoid (2/30, 21/43, 26/47, 13/41); foreign body (0/30, 34/43, 47/47, 38/41); infiltration cellular, histiocyte (0/30, 2/43, 4/47, 6/41) Lymph node, mediastinal: hyperplasia, lymphoid (2/37, 8/45, 17/48, 34/49); foreign body (0/37, 32/45, 42/48, 48/49); infiltration cellular,	Larynx: foreign body (0/50, 25/50, 39/50, 48/50); respiratory epithelium, hyperplasia (2/50, 0/50, 14/50, 18/50); respiratory epithelium, metaplasia, squamous (1/50, 0/50, 5/50, 24/50); squamous epithelium, hyperplasia (4/50, 1/50, 1/50, 12/50) Trachea: foreign body (0/50, 7/50, 14/50, 20/50) Lymph node, bronchial: hyperplasia, lymphoid (2/41, 15/47, 17/48, 11/49); foreign body (0/41, 34/47, 46/48, 43/49); infiltration cellular, histiocyte (0/41, 2/47, 7/48, 7/49) Lymph node, mediastinal: hyperplasia, lymphoid (0/46, 3/48, 16/49, 18/50); foreign body (0/46, 28/48, 45/49, 44/50); infiltration cellular, histiocyte (0/46, 6/48, 11/49, 16/50) Heart: epicardium, inflammation, chronic

	Male Wistar Han Rats	Female Wistar Han Rats	Male B6C3F1/N Mice	Female B6C3F1/N Mice
	Kidney: renal tubule, accumulation, hyaline droplet (0/50, 1/50, 3/50, 14/50); artery, inflammation, chronic active (0/50, 0/50, 1/50, 4/50) Artery (all tissues combined): inflammation, chronic active (1/50, 1/50, 5/50, 16/50) Eye: ciliary body, inflammation, acute (0/49, 0/49, 1/50, 6/49)	Kidney: renal tubule, accumulation, hyaline droplet (0/50, 0/50, 5/50, 11/50); nephropathy (16/50, 15/50, 20/50, 24/50); artery, inflammation, chronic active (0/50, 0/50, 0/50, 2/50) Artery (all tissues combined): inflammation, chronic active (0/50, 0/50, 5/50, 15/50) Eye: retina, atrophy (6/49, 21/50, 18/49, 19/49); ciliary body, inflammation, acute (0/49, 0/50, 1/49, 6/49)	histiocyte (0/37, 4/45, 13/48, 34/49) Heart: epicardium, inflammation, chronic active (0/50, 2/50, 7/50, 16/50) Stomach, forestomach: inflammation, chronic active (2/50, 4/50, 4/49, 7/50)	active (0/50, 2/50, 7/50, 7/50)
Neoplastic Effects	Lung: Alveolar/Bronchiolar Adenoma (3/50, 4/50, 6/50, 8/50); Alveolar/Bronchiolar Adenoma Or Carcinoma (3/50, 4/50, 8/50, 8/50) Adrenal Medulla: Benign Pheochromocytoma (1/49, 0/50, 2/49, 7/50)	Lung: alveolar/bronchiolar adenoma (0/50, 2/50, 6/50, 5/50) Adrenal medulla: benign pheochromocytoma (0/49, 2/49, 2/49, 6/50); benign or malignant pheochromocytoma (0/49, 2/49, 2/49, 7/50)	Lung: alveolar/bronchiolar carcinoma (4/50, 18/50, 20/50, 27/50) Skin: fibrous histiocytoma (0/50, 1/50, 1/50, 4/50); fibrous histiocytoma or fibrosarcoma (0/50, 1/50, 3/50, 4/50)	Lung: alveolar/bronchiolar adenoma (1/50, 10/50, 19/50, 8/50); alveolar/bronchiolar carcinoma (2/50, 14/50, 11/50, 11/50); alveolar/bronchiolar adenoma or carcinoma (3/50, 22/50, 27/50, 18/50) All organs: malignant lymphoma (7/50, 17/50, 20/50, 27/50)
Equivocal Findings	None	Lung: cystic keratinizing epithelioma or squamous cell carcinoma (0/50, 0/50, 0/50, 3/50)	None	Skin: squamous cell carcinoma (0/50, 0/50, 0/50, 2/50)
Level of Evidence of Carcinogenic Activity	Some evidence	Some evidence	Clear evidence	Clear evidence
Genetic Toxicology				
Micronucleated Erythrocytes				
Rat Peripheral Blood in vivo:		Negative in males and females		
Mouse Peripheral Blood in vivo:		Positive in males and females		
DNA Damage				
Rat		Negative in lung cells and leukocytes (males and females)		
Mouse		Positive in lung cells (males and females); negative in leukocytes (males and females)		

Introduction

Figure 1. Antimony Trioxide (CASRN 1309-64-4; Chemical Formula: Sb_2O_3; Molecular Weight: 291.5)

Synonyms: A1530; A1582; a1588 lp; antimonious oxide; antimony oxide; antimony (III) oxide; antimony peroxide; antimony sesquioxide; antimony white; AP 50; biantimony trioxide; C.I. pigment white 11; dechlorane a-o; diantimony trioxide; exitelite; flowers of antimony; nyacol a 1530; senarmontite; valentinite; weisspiessglanz.
Trade names: FireShield®, Microfine®, Montana Brand, Thermoguard®, Timonox, TMS®, Trutint®, Ultrafine®, White Star.

Chemical and Physical Properties

Antimony trioxide (Sb_2O_3) is the primary form of antimony in the atmosphere and also occurs naturally as the ores of valentinite, senarmontite, exitelite, and weisspiessglanz. At 1,500°C, antimony trioxide exists in vapor phase as dimeric Sb_4O_6[1]. Commercially, antimony trioxide is available as an odorless, white crystalline powder. Antimony trioxide has minimal solubility (0.017 mg/L) in water and is amphoteric with solubility in alkaline hydroxide solutions as well as in hydrochloric, tartaric, and acetic acids[1; 2]. While typically white in color, suspensions of antimony trioxide develop a darker color following absorption of ultraviolet radiation below 325 nm, possibly due to peroxide radical formation on the crystal surface[3]. The white color of the suspension slowly returns when light is removed.

Aerosolized antimony trioxide particles do not readily change chemical composition, particle size, or morphology after emission, although a coating of sulfate may form on the particle surface[3]. Methylation of antimony trioxide may occur in water-logged soil. Three organoantimony biotransformation products have been identified in natural sediment containing antimony trioxide (10 or 100 ppm) following incubation for 60 days under aerobic and anaerobic conditions. Two of the organoantimony products, methylstibonic acid and dimethylstibonic acid were identified, and less than 0.1% of the antimony in the incubates was transformed.

Antimony is a group 15 metalloid that occurs in the earth's crust at 0.2 to 1 mg/kg and in seawater at approximately 2×10^{-4} mg/kg[4]. Four allotropes of antimony have been identified with metallic antimony being the only stable allotrope. Metallic antimony is a brittle, silver-white shiny metal[4]. Although native antimony occurs naturally, antimony predominantly exists as a mineral with over 100 mineral species identified[5]. Stibnite (Sb_2S_3) is the primary ore for industrial purposes[5]. Antimony has three oxidation states, +3, −3, and +5[3]. When metallic antimony (0) is burned in air, it oxidizes to antimony (+3) trioxide[3]. Aerosolized antimony reacts with atmospheric oxidants and rapidly oxidizes to antimony trioxide. Antimony oxidation generally occurs in aerobic surface soils as well.

Production, Use, and Human Exposure

Antimony trioxide is the most commercially significant form of antimony. Antimony trioxide is predominantly produced by two methods: 1) oxidation of stibnite ore via furnace roasting or 2) furnace oxidation of metallic antimony. Antimony trioxide can also be produced from the

reaction of antimony trichloride ($SbCl_3$) with water or by alkaline hydrolysis of stibene (SbH_3). Commercially available antimony trioxide typically has a purity between 99.2% and 99.5%[5]. Trace impurities include arsenic, copper, iron, lead, and nickel with up to 0.3% of both lead and arsenic[6; 7].

Antimony trioxide is used as a flame retardant in canvas, textiles, paper, and plastics and in combination with some chlorinated or brominated flame retardants on commercial furniture, draperies, wall coverings, and carpets (typically 2% to 10% by weight)[1; 8]. It is commonly used with tetrabromobisphenol-A to enhance flame retardancy in printed circuit boards[7]. Antimony trioxide is also used as a catalyst in the production of polyethylene terephthalate (PET) plastic[5]. Antimony trioxide is added to phosphorescent light sources (fluorescent tubes and television/computer screens) to reinforce the photogenic capacity of phosphorus[8].

Antimony metal is used in the electronics industry in the production of silicon wafers and diodes[5]. Lead-antimony alloys have a variety of uses including use in batteries, ammunition, corrosion resistant pumps and pipes, tank linings, roofing sheets, solder, cable sheaths, and antifriction bearings[5]. Medicinally, antimony compounds have been historically used as emetics and to treat protozoan and parasitic infections. Potassium antimonyl tartrate is a powerful emetic that was once used to treat schistosomiasis. Currently, pentavalent antimonials are used to treat leishmaniasis[9]. The estimated worldwide distribution of antimony uses is: flame retardants, 72%; transportation, including batteries, 10%; chemicals, 10%; ceramics and fiberglass, 4%; and other, 4%[5].

Most atmospheric releases of antimony substances result from high-temperature industrial processes, the combustion of petroleum, petroleum products, and coal and the incineration of products that contain antimony. Antimony is oxidized at the high temperatures used in these processes resulting in the formation of antimony trioxide and possibly antimony tetraoxide and antimony pentoxide[6]. Antimony compounds can also leach from mining and smelting waste products discarded in large tailing piles. Acid conditions, often created in the tailing piles by the oxidation of pyrites, increase the potential for leaching[3]. High levels of antimony trioxide (>300 ppm) have been detected in ambient air downwind from a copper smelting plant[6]. The mean concentration of antimony in rainwater downwind from a copper smelting plant was 1.3 ppb compared with 0.03 ppb in rainwater collected upwind from the plant[3].

Occupationally, the major sources of exposure to antimony exist in the metal ore smelting and mining industries. Additional worker exposure potential exists in industries where antimony trioxide is used in the production of ceramics, glass, and alloys. Inhalation and dermal contact with dusts are the most common routes of exposure[6]. For workers exposed to antimony, a mean body burden of 7.9 mg antimony has been estimated[3]. Antimony concentrations up to 600 mg/L were measured in urine samples collected from workers at a smelter plant. Firemen and emergency workers may also be exposed to antimony that is released from the combustion of materials containing antimony trioxide associated with flame retardants. Up to 543 ppm antimony has been identified in soot and tracheal specimens collected from cadavers of fire victims[3].

The average daily intake of antimony from food and water has been estimated to be 100 μg/day[3]. Another evaluation reported that the antimony concentration for a mixed diet is 9.3 ppb, which corresponds to 4.6 μg antimony per day based on consumption of approximately 3,000 g

diet/day[10]. Separate reports indicate that antimony concentrations in a variety of foods including meats, seafood, and vegetables range from 0.22 to 2.81 ppb, while another evaluation study reported that median levels of antimony in eight food groups were less than 10 ppb (wet weight)[3]. In pooled human milk, antimony concentration has been reported to be 13 ppm[3]. For drinking water, the USEPA maximum contaminant level is 6 μg/L[6]. A mean body burden of 0.7 mg antimony has been reported based on autopsy data from unexposed Japanese adults. In urine samples collected from the National Health and Nutrition Examination Survey, the geometric mean antimony concentration was 0.133 μg/L with 0.380 μg/L for the 95th percentile[11].

Regulatory Status

An occupational exposure limit of 0.5 mg/m^3 has been established for antimony [8-hour time-weighted average (TWA) threshold limit value[12]; NIOSH 10-hour TWA recommended exposure limit and OSHA 8-hour TWA permissible exposure limit[13]]. The current United States Environmental Protection Agency[14] inhalation reference concentration for antimony trioxide is 0.2 μg/m^3.

Absorption, Distribution, Metabolism, and Excretion

Experimental Animals

In laboratory animals, the lung deposition, retention, and clearance of aerosols containing antimony following inhalation exposure depend on particle size and solubility[15]. In general, aerosols of antimony oxides with small particle sizes and low water solubility are retained in the lungs longer than larger particles with high water solubility (antimony tartrates). In a chronic inhalation study, Fischer 344 rats were exposed to antimony trioxide for 12 months at 0.06, 0.51, or 4.50 mg/m^3 followed by a 12-month observation period[16]. At the end of the 12-month exposure period, antimony lung burdens in female rats were approximately 11.3, 129.5, and 2,010 μg in the 0.06, 0.51, and 4.50 mg/m^3 exposure groups, respectively, and declined to approximately 2%, 15%, or 44% of the original lung burden. The resulting half-lives were 2.3, 3.6, and 9.5 months, respectively, for the 0.06, 0.51, and 4.50 mg/m^3 groups, suggesting that the clearance is dependent on the lung burden.

Experiments in laboratory animals have shown that aerosols of trivalent antimony (tartrate) are distributed primarily to the lung, bone, liver, pelt, and thyroid gland following inhalation exposure and are excreted both in the feces and in the urine[17; 18]. In a comparison of the distribution of trivalent versus pentavalent antimony inhaled as the tartrate in hamsters, trivalent antimony accumulated in liver greater than pentavalent antimony. The opposite pattern was observed in the skeleton. Trivalent antimony in blood concentrated almost exclusively in the erythrocytes, whereas pentavalent antimony in blood was found to a greater extent in the plasma during the first 2 hours postexposure, after which, pentavalent antimony also concentrated in the erythrocytes[19]. Following intratracheal instillation of antimony trioxide (1.52 mg/kg) in hamsters, the clearance of antimony from the lung was biphasic with half-lives of 40 hours and 20 to 40 days for the first and second phases, respectively[15].

Humans

Antimony trioxide is absorbed after inhalation exposure as indicated by elevated blood and urine levels of antimony measured in occupationally exposed workers[6]. Urine concentrations of antimony remained elevated in smelter plant workers after exposure had ceased[20-23]. Samples collected from retired (for approximately 20 years) and deceased smelter plant workers suggest that antimony has a long biological half-life in the lung. Antimony measured in the lungs of deceased smelter workers (n = 40) was 12 times greater (312 mg/kg) than control samples, and antimony concentration in the lungs did not decrease with length of exposure cessation[24]. A separate series of studies evaluated trace elements in human lung tissue collected from deceased individuals not occupationally exposed to antimony[25-27]. In these studies, antimony accumulation in lung tissue correlated with age, presumably due to inhalation of environmental contaminants. Antimony trioxide is poorly absorbed from the gastrointestinal tract in humans[6].

Antimony compounds are eliminated mainly in the urine, with small amounts appearing in feces via bile after conjugation with glutathione. A significant amount of antimony excreted in bile undergoes enterohepatic circulation. A renal elimination half-life of 4 days following inhalation of antimony trioxide was estimated in 21 employees of a starter battery manufacturing plant[6].

Toxicity

Experimental Animals

In one study, Fischer 344 rats were exposed via whole body inhalation to target concentrations of up to 25 mg antimony trioxide/m^3 (measured concentrations of up to 23.46 mg/m^3) for 13 weeks (6 hours per day, 5 days per week) with some animals held for 27 weeks postexposure[16]. In this study, particle sizes were considerably higher in the exposure atmospheres [mass median aerodynamic particle diameter (MMAD) 5.7 µm] than in the test material prior to exposure (MMAD 3.4 µm). Body weights in animals exposed to 23.46 mg/m^3 during the exposure and most of the recovery periods were lower than controls; however, the differences were less than 10%. Nonneoplastic lesions that were found at higher incidences in exposed animals included the presence of particulate material in alveolar/intra-alveolar macrophages and perivascular and/or peribronchial lymph node aggregates at the end of exposure and in the recovery period. In addition, incidences of chronic inflammation of the interstitium, granulomatous inflammation, interstitial fibrosis, and alveolar/bronchiolar hyperplasia were higher in exposed animals following the recovery period; increases in these lesions were primarily limited to the two highest exposure concentrations. In an extended study by these investigators, Fischer 344 rats were exposed via whole body inhalation to antimony trioxide target concentrations up to 5.0 mg/m^3 (measured concentrations of up to 4.5 mg/m^3) for 1 year (6 hours per day, 5 days per week) with some animals held for 1 year postexposure[16]. Depending on the method used, the particle size was 3.76 ± 0.84 µm with a geometric standard deviation (GSD) of 1.79 ± 0.32 (TSI Aerodynamic Particle Sizer) or 4.55 µm with a GSD of 1.80 (Cascade Impactor). Following the 1-year exposure, exposure-related lesions were limited primarily to increases in particle-laden alveolar/intraalveolar macrophages, and the presence of foreign particulate material in perivascular/peribronchiolar aggregates of lymphoid cells and in peribronchial lymph node macrophages. After the 1-year postexposure period, relatively modest exposure-related increases in chronic inflammation of the interstitium were also observed. Mild, compound-related ocular

irritation was noted at 6 months, but no indications of compound-related ocular disease were noted at 12 or 18 months.

Hext et al.[28] reported a subchronic study in which male and female Wistar rats of the Alpk:APSD strain were fed diets containing 0, 1,000, 5,000, or 20,000 ppm antimony trioxide. No in-life toxicity was observed. Some small (≤10%) changes in hematology and clinical chemistry parameters and liver weights and slight increases in histopathologic findings, including pituitary cysts and plasma cell infiltration in the cervical lymph node, were observed; however, the relationship of these changes to toxicity was uncertain.

Humans

Antimony trioxide dust and fumes cause irritation to the respiratory tract and mucous membranes[6]. Chronic occupational exposure to antimony trioxide is associated with antimony pneumoconiosis characterized on chest X rays by the presence of diffuse, densely distributed punctate opacities that are round, polygonal, or irregular in shape[21; 29; 30]. In a study by McCallum[23], pneumoconiosis was identified in asymptomatic antimony smelter workers and the degree of radiographic abnormalities was correlated with the amount of antimony retained in the lungs and duration of exposure. In a study by McCallum et al.[31], radiographic abnormalities were observed after just a few years of exposure. In this study, antimony (as antimony trioxide) aerosol concentrations averaged 5 mg/m^3 with concentrations up to 37 mg/m^3 measured during tapping operations. In the Cooper et al.[21] study, antimony pneumoconiosis was diagnosed in three of the 13 smelter workers exposed to antimony ore and antimony trioxide (0.08 to 138 mg antimony/m^3) for 1 to 15 years. Pulmonary function examinations were also conducted in this study, and no consistent pattern of abnormalities was observed. The Potkonjak and Pavlovich[30] study evaluated smelter workers (n = 51) who had been employed for 9 to 31 years. The evaluation included physical examination, laboratory analysis, chest X ray, and pulmonary function studies. In this study, the airborne dust concentrations measured 17 to 86 mg/m^3 and were composed of 39% to 89% antimony trioxide, 2% to 8% antimony pentoxide and less than 5% free silica. Other agents present in the dust included less than 4% ferric trioxide and less than 7% arsenic oxide. Pulmonary function testing identified no specific pattern of abnormalities. Chronic coughing was identified in 61% of the workers and antimony pneumoconiosis was identified by chest X ray in 67% of the smelter workers. The chest X ray lesions in smelter workers (dense, irregular opacities with diameters < 1 mm in mid and lower lung) differ from the chest X ray lesions of silicosis observed in antimony miners (round opacities with diameters >3 mm in upper and mid lung) where airborne dust samples containing nearly 80% free silica have been identified[30].

Antimony toxicity following oral exposure in humans has been reported following medicinal use of potassium antimonyl tartrate[32]. Accidental ingestion of antimony has been reported due to leaching from ceramic containers into acidic beverages. In one incident, more than 50 people were hospitalized after consuming a beverage contaminated with antimony (13 mg/L). Symptoms included a burning sensation in the stomach, colic, nausea, vomiting, and collapse[6].

Chronic occupational exposure to antimony trioxide on exposed skin causes dermatitis with papular and pustular lesions developing on the arms and legs[6]. The skin lesions primarily occur during the summer and develop around sweat and sebaceous glands with areas of eczema. The lesions invaginate, crust, and eventually desquamate with residual hyperpigmentation[30].

Reproductive and Developmental Toxicity

Experimental Animals

Female rats were exposed by inhalation to antimony trioxide at 250 mg/m^3 for up to 2 months (4 hours per day)[33]. Exposure began 3 to 5 days before estrus and continued through mating and gestation until 3 to 5 days prior to delivery. All of the chamber control rats (n = 10) and 16 of 24 exposed rats became pregnant. The average litter size was 6.2 in the exposed rats and 8.3 in the chamber control rats. No data were presented on the incidences of postimplantation loss. No teratogenic effects were observed in the fetuses of the exposed animals. No testicular toxicity was identified in rats or mice following oral gavages of antimony trioxide or antimony potassium tartrate up to 1,200 mg/kg body weight[34].

Humans

Women (number not specified) occupationally exposed to dust containing metallic antimony, antimony trioxide, and antimony pentasulfide were evaluated over a period of 2 years[33]. The level of exposure and selection criteria of the control group were not specified. Disturbances of the menstrual cycle and increased incidences of spontaneous abortion and premature birth were reported in exposed women. Antimony was detected in the blood of the exposed workers at levels 10 times higher than in the controls. Antimony also was measured in the urine, breast milk, amniotic fluid, placental tissue, and umbilical cord blood of the exposed workers.

Carcinogenicity

Experimental Animals

Inhalation studies of antimony trioxide have identified increased incidences of lung tumors in rats[14; 35]. In one study, female CR Fischer rats (n = 50) were exposed to 1.9 or 5.0 mg/m^3 antimony trioxide (6 hours per day, 5 days per week) for 1 year followed by a postexposure period of 1 year or longer[14]. In this study, antimony trioxide exposure resulted in the induction of lung tumors including adenomas, scirrhous carcinomas, and squamous cell carcinomas. Other reports have indicated that, while the reported high exposure concentration was 5.0 mg/m^3, the actual exposure concentration based on histopathologic examination in comparison to another study of antimony trioxide was probably considerably higher and that the MMAD and GSD for that study were 5.06 μm and 2.13, respectively[16]. In another study[35], male and female Wistar rats (n = 90/sex) were exposed via whole body inhalation to either antimony trioxide (45 mg/m^3; MMAD: 2.80 μm) or antimony ore (36 to 40 mg/m^3; MMAD: 4.78 μm) for up to 1 year (7 hours per day, 5 days per week) with a 20-week postexposure period. Increases in lung tumor incidences (squamous cell carcinomas, scirrhous carcinomas, and bronchoalveolar adenomas and carcinomas with antimony trioxide) over controls were observed in female rats exposed to antimony trioxide (19/70) or antimony ore (17/68). In the Newton et al.[16] whole body inhalation study, antimony trioxide exposure at concentrations of 0.05, 0.5 and 5.0 mg/m^3 (measured at 0.06, 0.51 and 4.5 mg/m^3, respectively) for 1 year, followed by a 1-year postexposure period, did not increase tumor incidence in male or female Fischer 344 rats (N = 65/sex per group). Three lung tumors were observed in this study with one in a control group male, one in a mid-exposure group female, and one in a high-exposure group male.

Humans

No studies examining the carcinogenic potential of antimony trioxide in humans were identified in a review of the literature.

Genetic Toxicity

In bacterial mutagenicity assays, antimony trioxide (purity reported to be >99.9%) was negative in *Salmonella typhimurium* strains TA98, TA100, TA1535, and TA1537 and *Escherichia coli* strains WP2P and WP2P*uvrA* with or without induced rat liver S9 activation enzymes (S9 mix) at concentrations up to 5,000 µg/plate[36]. Antimony trioxide (purity >99.9%) was also reported to be negative in TA98 and TA100 with or without S9 mix at concentrations up to 1.71 µg/plate[2]. In the *Bacillus subtilis* rec assay, in which differential cytotoxicity between strains H17 (rec^+) and M45 (rec^-) is used as a measure of compound-induced DNA damage, antimony trioxide was positive at concentrations of 0.6 and 1.1 µg/disk[2]. In an earlier rec assay, antimony trioxide (purity not specified) was reported to be positive at a concentration of 50 mM[37]. Both of these rec assays were performed without S9 mix.

Antimony trioxide was also tested for genotoxicity in mammalian cell assays. Antimony trioxide induced sister chromatid exchanges (SCEs) in the absence of S9 at concentrations of 0.9, 0.17, and 0.34 µg/mL in cultured Chinese hamster ovary cells[2]. In a second study, antimony trioxide was reported to induce SCEs in cultured human lymphocytes at concentrations of 0.5, 1, and 2 µM in the absence of S9[38]. Significant increases in chromosomal aberrations were seen in cultured human lymphocytes exposed to 100 µg/mL antimony trioxide with or without S9 mix[36]; no increases in aberrations were seen at lower concentrations of antimony trioxide, and no alterations in mitotic index were seen at any of the concentrations used in this study. Antimony trioxide was negative in the L5178Y mouse lymphoma cell $Tk^{+/-}$ mutation assay with and without S9 mix at concentrations up to 50 µg/mL[36].

In vivo, no significant increases in micronucleated polychromatic erythrocytes (PCEs) were observed in bone marrow samples from male and female CD-1 mice given a single dose of 5,000 mg/kg antimony trioxide by oral gavage, and no significant increases in micronucleated PCEs were seen after repeated dosing with 400, 667, or 1,000 mg/kg per day by oral gavage for 8, 15, or 22 days[36]. No increases in chromosomal aberrations or micronucleated PCE frequencies were seen in bone marrow of a single cohort of male and female Sprague Dawley Crl:CD rats given antimony trioxide (purity >99.9%) at doses of 250, 500, or 1,000 mg/kg per day by oral gavage for 21 days[39]; inductively coupled plasma atomic emission spectroscopy was used to verify the concentration of solubilized antimony trioxide in the dosing solutions. Furthermore, these investigators used a toxicokinetic approach to confirm the presence of antimony trioxide in the bone marrow of exposed rats. Antimony trioxide was also negative in a liver DNA repair assay conducted using male Alderley Park Alpk:APfSD (Wistar-derived) rats exposed to a single dose of antimony trioxide (3,200 or 5,000 mg/kg) and assessed 2 or 16 hours after dosing[36].

The genotoxic effects of occupational exposure to antimony trioxide were studied in workers at a factory that produced fireproof textiles for car upholstery[40]. The study compared SCEs, micronuclei, and DNA damage levels (detected by the comet assay) in peripheral blood lymphocytes among 1) workers who prepared suspensions of antimony trioxide, 2) workers who had a different task at the factory, and 3) an unexposed control group. Biomonitoring equipment

showed only a small difference in antimony trioxide exposure levels between the two groups of workers and the levels of exposure recorded in this study were approximately 4,000 times lower than the occupational exposure limit. No differences in the three indicators of genotoxicity were observed among any of the three groups of workers that were evaluated in this study.

To summarize, antimony trioxide was not mutagenic in bacterial reverse mutation assays or in the mouse lymphoma assay, but results from the bacterial rec assay and mammalian cell SCE and chromosomal aberration assays suggest that antimony trioxide can damage DNA in vitro. However, results of chromosomal damage assays in laboratory animals and exposed workers were negative.

Study Rationale

Antimony trioxide was nominated by the Consumer Product Safety Commission and the National Institute of Environmental Health Sciences for National Toxicology Program testing due to the potential for substantial human exposure in occupational settings and the lack of adequate 2-year exposure carcinogenicity studies. Three 1-year inhalation exposure studies in rats are reported in the literature[14; 16; 35]; however, the methodologies and lung carcinogenicity results were inconsistent among the three studies. In response, NTP conducted 2-week and 2-year inhalation studies on antimony trioxide to determine if antimony trioxide poses a carcinogenic hazard in rats, to generate data in a second species, and to characterize the exposure-concentration responses in rats and mice. A 12-month interim evaluation was added as a means of comparison to previous inhalation studies. Inhalation exposure was selected because this is most common route of occupational exposure to antimony trioxide in humans. This Technical Report summarizes the results of the 2-week and 2-year toxicity and carcinogenicity studies conducted in male and female Wistar Han rats and B6C3F1/N mice.

Materials and Methods

Procurement and Characterization of Antimony Trioxide

Antimony trioxide was obtained from 3N International, Inc. (Akron, OH), in one lot (3N-06159) that was used in the 2-week and 2-year studies. Identity and purity analyses were conducted by the analytical chemistry laboratories at H&M Analytical Services, Inc. [Allentown, NJ; X-ray diffraction (XRD)], and Chemir Analytical Services, Inc. [Maryland Heights, MO; redox titration and ultraviolet (UV) spectrophotometry], and by the study laboratory at Battelle Toxicology Northwest [Richland, WA; inductively coupled plasma/atomic emission spectroscopy (ICP/AES)] (Appendix H). Reports on analyses performed in support of the antimony trioxide studies are on file at the National Institute of Environmental Health Sciences.

Lot 3N-06159 of the chemical, a finely divided white powder, was identified as antimony trioxide by XRD. The purity of lot 3N-06159 was determined using ICP/AES. In addition, redox titration and UV spectrophotometry of bulk chemical samples determined the oxidation state of antimony in the test article.

The ICP/AES analysis indicated a purity of 101.9% based on a theoretical content of 83.5% antimony in antimony trioxide. Of the 18 minor elements measured by ICP/AES, only arsenic (~0.019%) and lead (~0.016%) were detected above 0.01% relative to antimony trioxide. Redox titration and UV spectroscopy confirmed that antimony was present in the +3 oxidation state, consistent with antimony trioxide. The overall purity of lot 3N-06159 was determined to be greater than 99.9%.

To ensure stability, the bulk chemical was stored at room temperature in amber glass containers with Teflon®-lined lids. Periodic reanalyses of the bulk chemical were performed by the study laboratory using ICP/AES and the analytical chemistry laboratory using XRD, and no degradation of the bulk chemical was detected.

Aerosol Generation and Exposure System

For the 2-year studies, male and female rats were housed in separate chambers; female rat chambers also housed male and female mice from the concurrent study. For the 2-week and 2-year studies, the generation system used a linear feed device designed and built by Battelle to meter antimony trioxide into a Trost jet mill for aerosolization and particle size reduction. The linear feed device consisted of a slide bar, a body, a delivery tube, and a test article reservoir.

The compressed air driven slide bar slid back and forth during generation, and as the slide bar moved to the dispersing position, the metering port was aligned with a compressed air port in the body. A puff of air from the port dispersed the test article from the metering port. The output of the linear feeder was regulated by adjusting the shuttle bar cadence. Initial particle size reduction was accomplished within the Trost jet mill. From the jet mill, aerosol was directed to the main distribution line where it was diluted with humidified air then conveyed from the exposure control center to the exposure room where it passed through a cyclone separator to further reduce particle size. On exiting the cyclone, the aerosol-laden air was directed to either of two smaller branch lines. The distribution line pressure was continuously monitored and maintained slightly negative to the exposure room.

From the branch line, aerosol was delivered to each exposure chamber by a sampling tube. The aerosol then entered the chamber inlet duct where it was further diluted with conditioned chamber air to achieve the desired exposure concentration. During exposure periods, there was a small excess of aerosol in each branch line over that needed to maintain chamber concentrations. A high-efficiency particulate air (HEPA) filter was placed before the endline flow control assembly of each branch to remove aerosol from the airstream prior to exhausting from the room.

The study laboratory designed the inhalation exposure chambers so that uniform aerosol concentrations could be maintained throughout the chambers with the catch pans in place. The total volume of each chamber was 2.3 m^3 with an active mixing volume of 1.7 m^3. Tests showed that aerosol concentration could be reliably maintained homogenous within 8% throughout the chambers, provided the aerosol was uniformly mixed before passing through the chamber inlet and provided the test material did not react to a significant extent with animals, animal excrement, or the chamber interior[41].

Aerosol Concentration Monitoring

Summaries of the chamber aerosol concentrations are given in Table H-1 and Table H-2. The concentration of antimony trioxide in the exposure chambers and room air was monitored using three real-time aerosol monitors (RAMs) (MicroDust pro, Casella USA, Amherst, NH). The monitors were connected to the chambers by a sampling system designed by Battelle incorporating a valve that multiplexed each RAM to a 0 mg/m^3 chamber or the room, a HEPA-filtered air blank, and two exposure chambers. The output (voltage) of the RAM was recorded by a program designed by Battelle (Battelle Exposure Data Acquisition and Control) to select the correct sample stream and acquire a raw voltage signal from each RAM. Equations for the calibration curves resided within the program and were used to convert the measured RAM voltages to exposure chamber concentrations. Concentration control limits within the program were compared to each measured concentration and, if limits were exceeded, an audible alarm was triggered or, in extreme cases, exposure was terminated.

Each RAM was calibrated by constructing a response curve using the measured RAM voltages and antimony concentrations that were determined from filter samples that were collected daily from the exposure chambers, extracted with concentrated hydrochloric acid, sonicated, and analyzed using ICP/AES. The ICP/AES instrument was calibrated against serially diluted NIST traceable 10 mg/mL spectrometric standards of antimony trioxide and the internal standard yttrium. Quality control standards and a reagent blank were analyzed after calibration, after approximately every tenth sample, and at the end of the analysis to determine accuracy and calibration drift during analysis.

Chamber Atmosphere Characterization

Particle size distribution was determined once prior to the 2-week and 2-year studies (3.75 and 60 mg/m^3 chambers), once during the 2-week studies, and monthly during the 2-year studies. Cascade impactor samples were taken from each exposure chamber using a Mercer-style seven-stage impactor and the stages (coverslips lightly coated with silicone for stages 1 to 7 or filters for stage 8) were analyzed for antimony using ICP/AES after antimony trioxide was extracted from the slides or filters with concentrated hydrochloric acid and sonication. The mass of antimony trioxide collected was calculated based on the theoretical percent of antimony in

antimony trioxide (83.5%). The relative mass of test article collected on each stage was analyzed by the NEWCAS impactor analysis program developed at Battelle based on probit analysis[42]. The resulting estimates of the mass median aerodynamic particle diameter (MMAD) and the geometric standard deviation (GSD) of each set of samples are given in Table H-3, Table H-4, and Table H-5. Across exposure concentrations, MMAD ranged from 1.3 to 1.5 μm with GSD of 1.9 in the 2-week studies. MMAD ranged from 0.9 to 1.5 μm and GSD from 1.7 to 2.2 across exposure concentration and time in the 2-year studies. These data are consistent with NTP Specifications, which requires that particles have an MMAD of less than 3 μm with a GSD of less than 3. In addition, when feasible, NTP prefers to test particles with an MMAD of 1 to 2 μm and a GSD of less than 2 in order to maximize deposition in the lower respiratory tract[43]. This is particularly the case when mice are included in the studies.

Buildup and decay rates for chamber aerosol concentrations were determined with (all studies) and without (2-year studies) animals present in the chambers. At a chamber airflow rate of 15 air changes per hour, the theoretical value for the time to achieve 90% of the target concentration after the beginning of aerosol generation (T_{90}) was approximately 9.4 minutes. A T_{90} value of 12 minutes was selected for all studies.

The uniformity of aerosol concentration in the inhalation exposure chambers without animals present was evaluated before each of the studies began; in addition, concentration uniformity with animals present in the chambers was measured once during the 2-week studies, and every 2 to 3 months during the 2-year studies. Concentrations were measured at all 12 sample ports; one in front and one in back for each of six possible cage unit positions per chamber. Chamber concentration uniformity was maintained throughout the studies.

The persistence of antimony trioxide in the exposure chambers after aerosol delivery ended was determined by monitoring the aerosol concentration in the 60 mg/m^3 chambers in the 2-week studies with animals present and the 30 mg/m^3 chambers in the 2-year studies, with and without animals present. In the 2-week studies, the concentration decreased to 1% of the starting concentration within 17 minutes. In the 2-year study of male rats, the concentration decreased to 1% of the starting concentration within 23 minutes with animals present and within 18 minutes without animals. In the 2-year studies of female rats and male and female mice, the concentration decreased to 1% of the starting concentration within 16 minutes with animals present and within 15 minutes without animals.

Stability studies of antimony trioxide in the generation and exposure system were performed before (2-year studies only) and during the studies. In these studies, XRD analyses performed by the analytical chemistry laboratory consistently indicated that the samples contained antimony trioxide in the diamond cubic crystalline phase senarmontite at greater than 99% of the test sample; ICP/AES analyses conducted by the study laboratory detected levels of 18 minor elemental contaminants at generally less than 0.1% each. Taken together, these results demonstrated that the exposure atmosphere and generator reservoir samples were in good agreement with the bulk test article, the composition of antimony trioxide was stable in the exposure system, and contamination from metal materials in the exposure system did not occur.

Animal Source

For the 2-week and 2-year studies, male and female Wistar Han [Crl:WI(Han)] rats, referred to as Wistar Han rats in this report, were obtained from Charles River Laboratories, Inc. (Raleigh, NC), and male and female B6C3F1/N mice were obtained from the NTP colony maintained at Taconic Farms, Inc. (Germantown, NY). The rationale for change of rat strain from F344/N to F344/NTac was a programmatic decision. For many years NTP used the inbred F344/N rat for its toxicity and carcinogenicity studies. Over a period of time, the F344/N rat exhibited sporadic seizures and idiopathic chylothorax, and consistently high rates of mononuclear cell leukemia and testicular neoplasia. Because of these issues in the F344/N rat and NTP's desire to find a more fecund rat model that could be used in both reproductive and carcinogenesis studies for comparative purposes, a change in the rat model was explored. Following a workshop in 2005, the F344 rat from the Taconic commercial colony (F344/NTac) was used for a few NTP studies to allow NTP time to evaluate different rat models between 2005 and 2006[44]. The Wistar Han rat, an outbred rat stock, was then selected because it was projected to have a long lifespan, resistance to disease, large litter size, and low neonatal mortality.

Animal Welfare

Animal care and use are in accordance with the Public Health Service Policy on Humane Care and Use of Animals. All animal studies were conducted in an animal facility accredited by the Association for the Assessment and Accreditation of Laboratory Animal Care International. Studies were approved by the Battelle Toxicology Northwest Animal Care and Use Committee and conducted in accordance with all relevant NIH and NTP animal care and use policies and applicable federal, state, and local regulations and guidelines.

Two-week Studies

The 2-week toxicity and tissue burden studies in rats and mice were designed following a review of the existing inhalation study data from the literature; a 4-week postexposure hold followed the 2-week exposure in tissue burden study females. These studies were performed to generate short-term toxicity data in rats and mice under the conditions of an NTP inhalation study to aid in the design of the 2-year studies, including the selection of exposure concentrations and time points for pulmonary retention and clearance studies. Generation of short-term data was of particular importance for mice, as no inhalation toxicology studies have been reported in that species. The highest exposure concentration in the current 2-week studies (60 mg/m^3) was selected to be slightly higher than the highest exposure concentration (45 mg/m^3) used in the Groth et al.[35] study where no exposure-related decreases in survival or body weights greater than 10% were observed. Exposure concentrations were spaced by half to examine the exposure-concentration response relationship.

On receipt, the rats and mice were approximately 4 weeks old. Animals were quarantined for 12 or 13 days and were approximately 5 to 6 weeks old on the first day of the studies. Before the studies began, five male and five female rats and mice were randomly selected for parasite evaluation and gross observation for evidence of disease. The health of the animals was monitored during the studies according to the protocols of the NTP Sentinel Animal Program (Appendix J). All test results were negative.

Groups of five male and five female core study rats and mice were exposed by whole body inhalation to antimony trioxide aerosol at concentrations of 0, 3.75, 7.5, 15, 30, or 60 mg/m^3 for 6 hours plus T_{90} (12 minutes) per day, 5 days per week for 12 (rats) or 13 (mice) exposure days during a 16- (rats) or 17- (mice) day period. Additional groups of five female tissue burden study rats and mice were exposed to the same concentrations for 16 (rats) or 17 (mice) days then held for 28 days without exposure. Feed was available ad libitum except during exposure periods, and water was available ad libitum. Rats and mice were housed individually. Clinical findings were recorded twice daily and at terminal kill for core study rats and mice. The core study animals were weighed on days 1, 6, 13, and at the end of the studies. Details of the study design and animal maintenance are summarized in Table 1.

For tissue burden studies, blood was collected from the retroorbital plexus (rats) or retroorbital sinus (mice) of core study animals at terminal kill and tissue burden animals at the end of a 4-week recovery period. Animals were anesthetized by CO_2. Blood was placed in tubes containing potassium EDTA as the anticoagulant. After exsanguination the whole lung was collected and weighed; the right lung of core study animals and both lungs of tissue burden animals were trimmed from the mainstem bronchi and weighed. Blood and lung samples were stored at −70°C until analyses. Blood and lung samples were weighed, lung samples were homogenized, and all samples were placed into Teflon Xpress microwave digestion vessels (CEM Corporation, Matthews, NC) in a nitric acid and hydrochloric acid solution with an antimony spiking solution, predigested for at least 15 minutes at 200°C, digested in a CEM Corporation MARS5 Sample Preparation System, diluted with deionized water, centrifuged until clear or filtered with syringe filters (Acrodisc 0.45 µm PTFE filter, Pall Life Sciences, Ann Arbor, MI), and diluted again with a nitric acid and hydrochloric acid solution. Analyses of the blood for antimony concentrations were performed using an Agilent 7500ce inductively coupled plasma-mass spectrometer (Agilent Technologies, Palo Alto, CA). Analyses of the lung samples for antimony concentrations were performed using a Thermo Elemental IRIS Intrepid II inductively coupled plasma-atomic emission spectrometer (Thermo Electron Corporation, Waltham, MA).

Necropsies were performed on all core study rats and mice. The heart, right kidney, liver, lung, right testis, and thymus were weighed. Histopathologic examinations were performed on 0 and 60 mg/m^3 core study rats and mice. Table 1 lists the tissues and organs routinely examined.

Two-year Studies

Study Design

Groups of 60 male and 60 female core study rats and mice were exposed by whole body inhalation to antimony trioxide aerosol at concentrations of 0, 3, 10, or 30 mg/m^3 for 6 hours plus T_{90} (12 minutes) per day, 5 days per week for up to 105 weeks. Ten male and 10 female rats and mice from each core study exposure group were randomly selected for micronuclei evaluation, comet assay, organ weights, necropsy, and histopathology at 12 months. Additional groups of 25 tissue burden study female rats and mice were exposed to the same concentrations of antimony trioxide for up to 79 weeks.

Rats and mice were approximately 4 weeks old on receipt. The animals were quarantined for 12 days before the beginning of the studies. Five male and five female rats and mice were

randomly selected for parasite evaluation and gross observation of disease. Rats and mice were approximately 6 weeks old at the beginning of the studies. The health of the animals was monitored during the studies according to the protocols of the NTP Sentinel Animal Program (Appendix J). All test results were negative.

Rats and mice were housed individually. Feed and water were available ad libitum, except feed was withheld during exposure periods. Chambers and cages were rotated weekly. Further details of animal maintenance are given in Table 1. The feed was analyzed for contaminants and found acceptable. Information on feed composition and contaminants is provided in Appendix I.

Clinical Examinations and Pathology

All animals were observed twice daily. Core study animal body weights were recorded on day 1, weekly for the first 13 weeks, every 4 weeks through week 93, every 2 weeks thereafter, and at terminal kill. Clinical findings were recorded every 4 weeks through week 93, then every 2 weeks, and at terminal kill.

Complete necropsies and microscopic examinations were performed on all core study rats and mice. At the 12-month interim evaluations, the heart, right kidney, liver, lung, right testis, and thymus of rats and mice were weighed. At necropsy, all organs and tissues were examined for grossly visible lesions, and all major tissues were fixed and preserved in 10% neutral buffered formalin (except eyes were first fixed in Davidson's solution and testes were first fixed in modified Davidson's solution; lungs were perfused using a blunted needle and Marriott bottle apparatus until flow stopped due to equalization of pressures, ~25 cm water pressure), processed and trimmed, embedded in paraffin, sectioned to a thickness of 4 to 6 µm, and stained with hematoxylin and eosin for microscopic examination. For all paired organs (e.g., adrenal gland, kidney, ovary), samples from each organ were examined. Tissues examined microscopically are listed in Table 1.

Microscopic evaluations were completed by the study laboratory pathologist, and the pathology data were entered into the Toxicology Data Management System. The report, slides, paraffin blocks, residual wet tissues, and pathology data were sent to the NTP Archives for inventory, slide/block match, wet tissue audit, and storage. The slides, individual animal data records, and pathology tables were evaluated by an independent quality assessment (QA) laboratory. The individual animal records and tables were compared for accuracy, the slide and tissue counts were verified, and the histotechnique was evaluated. For the 2-year studies, a QA pathologist evaluated slides from all tumors and all potential target organs, which included the bone marrow, larynx, lung, bronchial lymph node, mediastinal lymph node, nose, and trachea of rats and mice; arteries and spleen of rats; and heart, liver, mandibular lymph node, and thymus of mice.

The QA report and the reviewed slides were submitted to the NTP Pathology Working Group (PWG) coordinator, who reviewed the selected tissues and addressed any inconsistencies in the diagnoses made by the laboratory and QA pathologists. Representative histopathology slides containing examples of lesions related to chemical administration, examples of disagreements in diagnoses between the laboratory and QA pathologists, or lesions of general interest were presented by the coordinator to the PWG for review. The PWG consisted of the QA pathologist and other pathologists experienced in rodent toxicologic pathology. This group examined the tissues without any knowledge of dose groups. When the PWG consensus differed from the

opinion of the laboratory pathologist, the diagnosis was changed. Final diagnoses for reviewed lesions represent a consensus between the laboratory pathologist, reviewing pathologist(s), and the PWG. Details of these review procedures have been described, in part, by Maronpot and Boorman[45] and Boorman et al.[46]. For subsequent analyses of the pathology data, the decision of whether to evaluate the diagnosed lesions for each tissue type separately or combined was generally based on the guidelines of McConnell et al.[47].

Tissue Burden Study

Up to five female tissue burden study rats and mice per group were randomly selected after exposure to antimony trioxide on days 61, 124, 271 for rats or 269 for mice, 369, and 551 (equivalent to 2, 4, 9, 12, and 18 months). At each time point, rats and mice were weighed and anesthetized by CO_2. Blood was collected from the retroorbital plexus (rats) or retroorbital sinus (mice), placed in tubes containing potassium EDTA as the anticoagulant, and stored at approximately −70°C until analyzed for antimony concentration as described for the 2-week studies. After exsanguination, the lungs with mainstem bronchi were removed and weighed and then both lung lobes were trimmed from the trachea and mainstem bronchi, weighed, and stored at approximately −70°C until analyzed for antimony concentration as described for the 2-week studies.

Mutation Analysis of Alveolar/Bronchiolar Adenomas and Carcinomas

After histopathology examination, formalin-fixed, paraffin-embedded (FFPE) tissue blocks from alveolar/bronchiolar adenomas and carcinomas that arose either spontaneously (in chamber controls) or due to antimony trioxide exposure were selected from rats and mice for mutation analysis of commonly altered genes in lung cancer (*Kras* and *Egfr*). DNA was extracted from the FFPE tissues and subjected to a seminested polymerase chain reaction (PCR) to amplify hot spot regions of *Kras* (exons 1 and 2) and *Egfr* (exons 18 to 21). The lyophilized PCR products were sequenced, and the resulting electropherograms were compared to identify mutations in alveolar/bronchiolar adenomas and carcinomas that arose spontaneously or were due to exposure to antimony trioxide. The results are presented in Appendix K.

Table 1. Experimental Design and Materials and Methods in the Inhalation Studies of Antimony Trioxide

Two-week Studies	Two-year Studies
Study Laboratory	
Battelle Toxicology Northwest (Richland, WA)	Battelle Toxicology Northwest (Richland, WA)
Strain and Species	
Wistar Han [Crl:WI(Han)] rats B6C3F1/N mice	Wistar Han [Crl:WI(Han)] rats B6C3F1/N mice
Animal Source	
Rats: Charles River Laboratories, Inc. (Raleigh, NC)	Rats: Charles River Laboratories, Inc. (Raleigh, NC)
Mice: Taconic Farms, Inc. (Germantown, NY)	Mice: Taconic Farms, Inc. (Germantown, NY)
Time Held Before Studies	
Rats: 13 days Mice: 12 days	12 days
Average Age When Studies Began	
Rats: 6 weeks Mice: 5 weeks	6 weeks
Date of First Exposure	
December 3, 2007	Rats: September 22, 2008 Mice: October 6, 2008
Duration of Exposure	
6 hours plus T_{90} (12 minutes) per day, 5 days per week, for 12 (rats) or 13 (mice) exposure days during a 16- (rats) or 17- (mice) day period	6 hours plus T_{90} (12 minutes) per day, 5 days per week, for up to 105 weeks
Date of Last Exposure	
Rats: December 18, 2007 Mice: December 19, 2007	Rats: September 22, 2010 Mice: October 6, 2010
Necropsy Dates	
Rats: December 18, 2007 (core study) Mice: December 19, 2007 (core study)	Rats: September 20-23, 2010 Mice: October 4-7, 2010
Average Age at Necropsy	
8 weeks	110 weeks
Size of Study Groups	
Five males and five females (core study) Five females (tissue burden study)	60 males and 60 females (core study; including 10 males and 10 females evaluated at 12 months) 25 females (tissue burden study)
Method of Distribution	
Animals were distributed randomly into groups of approximately equal initial mean body weights.	Same as 2-week studies

Two-week Studies	Two-year Studies
Animals per Cage	
1	1
Method of Animal Identification	
Tail tattoo	Tail tattoo
Diet	
Irradiated NTP-2000 wafer diet (Zeigler Brothers, Inc., Gardners, PA), available ad libitum, except during exposure periods, changed daily	Same as 2-week studies
Water	
Tap water (Richland, WA, municipal supply) via automatic watering system (Edstrom Industries, Waterford, WI), available ad libitum	Same as 2-week studies
Cages	
Stainless steel wire bottom (Lab Products, Inc., Seaford, DE), changed weekly with chambers, rotated daily in chambers	Same as 2-week studies, except changed and rotated weekly
Cageboard	
Untreated paper excreta pan liner (Techboard Ultra, Shepherd Specialty Papers, Watertown, TN), changed daily	Same as 2-week studies
Chamber Air Supply Filters	
Single HEPA (open stock), charcoal (RSE, Inc., New Baltimore, MI), Purafil (Environmental Systems, Lynnwood, WA), all new at study start	Same as 2-week studies, except HEPA filter changed annually
Chambers	
Stainless steel, excreta pan at each of six levels (Lab Products, Inc., Seaford, DE); chamber changed weekly; excreta pans changed daily	Same as 2-week studies
Chamber Environment	
Temperature: 75° ± 3°F Relative humidity: 55% ± 15% Room fluorescent light: 12 hours/day Chamber air changes: 15 ± 2/hour	Same as 2-week studies
Exposure Concentrations	
0, 3.75, 7.5, 15, 30, or 60 mg/m^3	0, 3, 10, or 30 mg/m^3
Type and Frequency of Observation	
Observed twice daily; core study animals were weighed on days 1, 6, 13, and at the end of the studies; clinical findings were recorded twice daily and at terminal kill.	Observed twice daily; core study animals were weighed initially, weekly for the first 13 weeks, every 4 weeks through week 93, every 2 weeks thereafter, and at terminal kill; clinical findings were recorded every 4 weeks through week 93, every 2 weeks thereafter, and at terminal kill.

Two-week Studies	Two-year Studies
Method of Kill	
Carbon dioxide asphyxiation	Same as 2-week studies
Necropsy	
Necropsies were performed on all core study rats and mice. Following blood collection, the heart, right kidney, liver, lung, right testis, and thymus were weighed. In addition, blood and the right lung plus the mainstem bronchi were weighed. For tissue burden study rats and mice, the lungs with mainstem bronchi were removed and weighed and the right and left lobes were collected and weighed together. Samples were stored in containers at approximately −70°C until analyzed for antimony concentration.	Necropsies were performed on all core study animals; organs weighed at the 12-month interim evaluations were heart, right kidney, liver, lung, right testis, and thymus.
Histopathology	
Histopathology was performed on 0 and 60 mg/m^3 core study rats and mice. In addition to gross lesions and tissue masses, the following tissues were examined to a no-effect level: larynx, lung, lymph nodes (mediastinal and tracheobronchial), nose, and trachea.	Complete histopathology was performed on all core study rats and mice. In addition to gross lesions and tissue masses, the following tissues were examined: adrenal gland, bone with marrow, brain, clitoral gland, esophagus, eyes, gallbladder (mice), harderian gland, heart, large intestine (cecum, colon, rectum), small intestine (duodenum, jejunum, ileum), kidney, larynx, liver, lung, lymph nodes (bronchial, mandibular, mesenteric, and mediastinal), mammary gland, nose, ovary, pancreas, parathyroid gland, pituitary gland, preputial gland, prostate gland, salivary gland, seminal vesicle, skin, spleen, stomach (forestomach and glandular), testis with epididymis, thymus, thyroid gland, trachea, urinary bladder, and uterus.
Tissue Burden Studies	
Blood was collected from the retroorbital plexus (rats) or retroorbital sinus (mice) of core study rats and mice at terminal kill and from tissue burden study female rats and female mice after a 4-week recovery period. The right lung with mainstem bronchi was collected (the whole lung with mainstem bronchi was weighed) from core study animals, and the whole lung with mainstem bronchi was collected and weighed from the tissue burden study animals. The blood and both lung lobes trimmed from the trachea and mainstem bronchi were weighed and analyzed for antimony concentrations.	On days 61, 124, 271 (rats) or 269 (mice), 369, and 551 (equivalent to 2, 4, 9, 12, and 18 months), blood was collected from the retroorbital plexus (rats) or retroorbital sinus (mice) from up to five female tissue burden study rats and mice per group. Lungs with mainstem bronchi were collected and weighed. The blood and both lung lobes trimmed from the trachea and mainstem bronchi were weighed and analyzed for antimony concentrations.

Two-week Studies	Two-year Studies
Mutation Analysis of Alveolar/Bronchiolar Adenomas and Carcinomas	
None	DNA was extracted from formalin-fixed, paraffin-embedded rat and mouse alveolar/bronchiolar adenomas and carcinomas. The samples were subjected to seminested polymerase chain reaction (PCR) to amplify hot spot regions of *Kras* and *Egfr* genes. The lyophilized PCR products were sequenced, and the resulting electropherograms were compared to identify mutations in alveolar/bronchiolar adenomas and carcinomas that either arose spontaneously or were due to exposure to antimony trioxide.

Statistical Methods

Survival Analyses

The probability of survival was estimated by the product-limit procedure of Kaplan and Meier[48] and is presented in the form of graphs. Animals found dead of other than natural causes were censored; animals dying from natural causes were not censored. Statistical analyses for possible dose-related effects on survival used Cox's[49] method for testing two groups for equality and Tarone's[50] life table test to identify dose-related trends. All reported P values for the survival analyses are two sided.

Calculation of Incidence

The incidences of neoplasms or nonneoplastic lesions are presented in Table A-1, Table A-5, Table B-1, Table B-5, Table C-1, Table C-7, Table D-1, and Table D-8 as the numbers of animals bearing such lesions at a specific anatomic site and the numbers of animals with that site examined microscopically. For calculation of statistical significance, the incidences of most neoplasms (Table A-2, Table B-2, Table C-2, and Table D-2) and all nonneoplastic lesions are given as the numbers of animals affected at each site examined microscopically. However, when macroscopic examination was required to detect neoplasms in certain tissues (e.g., mesentery, pleura, peripheral nerve, skeletal muscle, tongue, tooth, and Zymbal's gland) before microscopic evaluation, the denominators consist of the number of animals that had a gross abnormality. When neoplasms had multiple potential sites of occurrence (e.g., leukemia or lymphoma), the denominators consist of the number of animals on which a necropsy was performed. Table A-2, Table B-2, Table C-2, and Table D-2 also give the survival-adjusted neoplasm rate for each group and each site-specific neoplasm. This survival-adjusted rate (based on the Poly-3 method described below) accounts for differential mortality by assigning a reduced risk of neoplasm, proportional to the third power of the fraction of time on study, only to site-specific, lesion-free animals that do not reach terminal kill.

Analysis of Neoplasm and Nonneoplastic Lesion Incidences

The Poly-k test[51-53] was used to assess neoplasm and nonneoplastic lesion prevalence. This test is a survival-adjusted quantal-response procedure that modifies the Cochran-Armitage linear trend test to take survival differences into account. More specifically, this method modifies the denominator in the quantal estimate of lesion incidence to approximate more closely the total

number of animal years at risk. For analysis of a given site, each animal is assigned a risk weight. This value is one if the animal had a lesion at that site or if it survived until terminal kill; if the animal died prior to terminal kill and did not have a lesion at that site, its risk weight is the fraction of the entire study time that it survived, raised to the kth power.

This method yields a lesion prevalence rate that depends only upon the choice of a shape parameter for a Weibull hazard function describing cumulative lesion incidence over time[51]. Unless otherwise specified, a value of k = 3 was used in the analysis of site-specific lesions. This value was recommended by Bailer and Portier[51] following an evaluation of neoplasm onset time distributions for a variety of site-specific neoplasms in control F344/N rats and B6C3F1/N mice[54]. Bailer and Portier[51] showed that the Poly-3 test gave valid results if the true value of k was anywhere in the range from 1 to 5. A further advantage of the Poly-3 method is that it does not require lesion lethality assumptions. Variation introduced by the use of risk weights, which reflect differential mortality, was accommodated by adjusting the variance of the Poly-3 statistic as recommended by Bieler and Williams[55].

Tests of significance included pairwise comparisons of each dosed group with controls and a test for an overall dose-related trend. Continuity-corrected Poly-3 tests were used in the analysis of lesion incidence, and reported P values are one sided. The significance of lower incidences or decreasing trends in lesions is represented as 1 − P with the letter N added (e.g., P = 0.99 is presented as P = 0.01N). For neoplasms and nonneoplastic lesions detected at the interim evaluation, the Fisher exact test[56], a procedure based on the overall proportion of affected animals, was used.

Analysis of Continuous Variables

Organ and body weight data, which historically have approximately normal distributions, were analyzed with the parametric multiple comparison procedures of Dunnett[57] and Williams[58; 59]. Prior to statistical analysis, extreme values identified by the outlier test of Dixon and Massey[60] were examined by NTP personnel, and implausible values were eliminated from the analysis.

Historical Control Data

The concurrent control group represents the most valid comparison to the treated groups and is the only control group analyzed statistically in NTP bioassays. However, historical control data are often helpful in interpreting potential treatment-related effects, particularly for uncommon or rare neoplasm types. For meaningful comparisons, the conditions for studies in the historical control database must be generally similar. Significant factors affecting the background incidences of neoplasms at a variety of sites are diet, sex, strain/stock, and route of exposure. The NTP historical control database contains all 2-year studies for each species, sex, and strain/stock with histopathology findings in control animals completed within the most recent 5-year period[61-63]. In general, the historical control database for a given study includes studies using the same route of administration, and the overall incidences of neoplasms in controls for all routes of administration are included for comparison, including the current study.

Quality Assurance Methods

The 2-week and 2-year studies were conducted in compliance with Food and Drug Administration Good Laboratory Practice Regulations[64]. In addition, the 2-year study reports

were audited retrospectively by an independent QA contractor against study records submitted to the NTP Archives. Separate audits covered completeness and accuracy of the pathology data, pathology specimens, final pathology tables, and a draft of this NTP Technical Report. Audit procedures and findings are presented in the reports and are on file at NIEHS. The audit findings were reviewed and assessed by NTP staff, and all comments were resolved or otherwise addressed during the preparation of this Technical Report.

Genetic Toxicology

The genetic toxicity of antimony trioxide was assessed by testing the ability of the chemical to induce increases in the frequency of micronucleated erythrocytes in rat and mouse peripheral blood and DNA damage in blood and lung of rats and mice. Micronuclei (literally "small nuclei" or Howell-Jolly bodies) are biomarkers of induced structural or numerical chromosomal alterations and are formed when acentric fragments or whole chromosomes fail to incorporate into either of two daughter nuclei during cell division[65; 66]. The protocols for these studies and the results are given in Appendix E.

The genetic toxicity studies have evolved from an earlier effort by NTP to develop a comprehensive database permitting a critical anticipation of a chemical's carcinogenicity in experimental animals based on numerous considerations, including the molecular structure of the chemical and its observed effects in short-term in vitro and in vivo genetic toxicity tests (structure-activity relationships). The short-term tests were originally developed to clarify proposed mechanisms of chemical-induced DNA damage based on the relationship between electrophilicity and mutagenicity[67] and the somatic mutation theory of cancer[68; 69]. However, it should be noted that not all cancers arise through genotoxic mechanisms.

DNA reactivity carries the potential for carcinogenicity. In these studies with antimony, due to the insoluble nature of the compound and the exposure route employed in the 2-year studies, no bacterial mutagenicity studies were conducted. Instead, genotoxicity, in the form of chromosomal damage (micronuclei) and DNA damage (measured using the comet assay) was evaluated in an independent cohort of mice and rats after 12 months of inhalation exposure.

The predictivity for rodent carcinogenicity of clearly positive results in long-term peripheral blood micronucleus tests is high; a weak response in one sex only or negative results in both sexes of one species in this assay do not correlate well with either negative or positive results in rodent carcinogenicity studies[70]. NTP has not yet conducted an evaluation of the relationship between DNA damage assessed in the comet assay with rodent carcinogenicity, although others have demonstrated a correlation[71]. However, because of the theoretical and observed associations between induced genetic damage and adverse effects in somatic and germ cells, the determination of in vivo genetic effects is important to the overall understanding of the risks associated with exposure to a particular chemical.

Results

Data Availability

The National Toxicology Program (NTP) evaluated all study data. Data relevant for evaluating toxicological findings are presented here. All study data are available in the NTP Chemical Effects in Biological Systems (CEBS) database: https://doi.org/10.22427/NTP-DATA-TR-590.

Rats

Two-week Study

All rats survived to the end of the study (Table 2). The final mean body weights and body weight gains of exposed groups of males and females were similar to those of the chamber control groups. There were no clinical findings related to antimony trioxide exposure.

Relative lung weights of 30 mg/m^3 males and absolute and relative lung weights of 60 mg/m^3 males and 30 and 60 mg/m^3 females were significantly greater than those of the chamber controls (Table 3 and Table F-1). Relative liver weights of 7.5 and 15 mg/m^3 males were significantly decreased compared to the chamber controls, but the relationship to toxicity was uncertain. There were no gross observations associated with exposure to antimony trioxide noted at necropsy.

Table 2. Survival and Body Weights of Rats in the Two-week Inhalation Study of Antimony Trioxide[a]

Concentration (mg/m^3)	Survival[b]	Initial Body Weight (g)	Final Body Weight (g)	Change in Body Weight (g)	Final Weight Relative to Controls (%)
Male					
0	5/5	137 ± 2	227 ± 6	90 ± 4	
3.75	5/5	136 ± 2	217 ± 5	81 ± 3	95
7.5	5/5	138 ± 3	226 ± 5	88 ± 3	99
15	5/5	136 ± 1	220 ± 5	84 ± 6	97
30	5/5	135 ± 4	210 ± 7	75 ± 4	92
60	5/5	139 ± 5	224 ± 9	86 ± 5	99
Female					
0	5/5	123 ± 3	158 ± 3	34 ± 1	
3.75	5/5	120 ± 4	160 ± 3	40 ± 1	102
7.5	5/5	122 ± 2	160 ± 3	38 ± 2	102
15	5/5	121 ± 4	156 ± 5	35 ± 2	99
30	5/5	119 ± 3	156 ± 1	37 ± 2	99
60	5/5	120 ± 4	158 ± 7	38 ± 3	100

[a]Weights and weight changes are given as mean ± standard error.
[b]Number of animals surviving at 16 days/number initially in group.

Table 3. Selected Organ Weights and Organ-Weight-to-Body-Weight Ratios for Rats in the Two-week Inhalation Study of Antimony Trioxide[a]

	Chamber Control	3.75 mg/m^3	7.5 mg/m^3	15 mg/m^3	30 mg/m^3	60 mg/m^3
n	5	5	5	5	5	5
Male						
Necropsy body wt.	227 ± 6	217 ± 5	226 ± 5	220 ± 5	210 ± 7	224 ± 9
Liver						
Absolute	10.05 ± 0.25	8.53 ± 0.32	8.84 ± 0.39	8.55 ± 0.47	8.56 ± 0.56	9.40 ± 0.41
Relative	44.330 ± 1.402	39.406 ± 1.436	39.133 ± 1.363*	38.715 ± 1.306*	40.698 ± 1.534	41.859 ± 0.728
Lung						
Absolute	1.99 ± 0.11	1.93 ± 0.14	2.04 ± 0.15	2.08 ± 0.12	2.28 ± 0.19	2.56 ± 0.10**
Relative	8.758 ± 0.530	8.919 ± 0.592	9.038 ± 0.609	9.416 ± 0.402	10.871 ± 0.806*	11.423 ± 0.351**
Female						
Necropsy body wt.	158 ± 3	160 ± 3	160 ± 3	156 ± 5	156 ± 1	158 ± 7
Lung						
Absolute	1.39 ± 0.09	1.33 ± 0.08	1.52 ± 0.15	1.51 ± 0.11	1.70 ± 0.07*	1.71 ± 0.10*
Relative	8.849 ± 0.511	8.320 ± 0.391	9.508 ± 0.927	9.626 ± 0.445	10.911 ± 0.385*	10.865 ± 0.388*

*Significantly different ($P \leq 0.05$) from the chamber control group by Williams' or Dunnett's test.
**$P \leq 0.01$.
[a]Organ weights (absolute weights) and body weights are given in grams; organ-weight-to-body-weight ratios (relative weights) are given as mg organ weight/g body weight (mean ± standard error).

Incidences of minimal squamous metaplasia of the epithelium lining the base of the epiglottis in the larynx occurred in two male rats in each of the 30 and 60 mg/m^3 exposure groups, and were present in one or more female rats at each exposure level (Table 4). Significantly increased incidences of foreign body, presumed to be the test article, occurred in the lungs of all exposed groups of males and females compared to the chamber controls. The foreign bodies appeared as refractile gold to brown granules within the cytoplasm of alveolar macrophages and lying free within the alveolar spaces. Incidences of chronic active inflammation in the lungs were significantly increased in 30 and 60 mg/m^3 males and females compared to the chamber controls. Chronic active inflammation was characterized by increased numbers of alveolar macrophages and perivascular infiltrates of lymphocytes, monocytes, and neutrophils. In areas of more intense inflammation, the alveolar architecture was sometimes obscured by inflammatory cells, cell debris, and fibrin, and was accompanied by Type 2 alveolar epithelial cell hyperplasia.

Table 4. Incidences of Selected Nonneoplastic Lesions of the Respiratory System in Rats in the Two-week Inhalation Study of Antimony Trioxide

	Chamber Control	3.75 mg/m^3	7.5 mg/m^3	15 mg/m^3	30 mg/m^3	60 mg/m^3
Male						
Larynx[a]	5	0	0	5	5	5
Epiglottis, Metaplasia, Squamous[b]	0	–	–	0	2 (1.0)[c]	2 (1.0)
Lung	5	5	5	5	5	5
Foreign Body	0	5**	5**	5**	5**	5**
Inflammation, Chronic Active	0	0	0	0	5** (2.2)	5** (2.2)
Female						
Larynx	5	5	5	5	4	5
Epiglottis, Metaplasia, Squamous	0	1 (1.0)	1 (1.0)	1 (1.0)	2 (1.0)	3 (1.0)
Lung	5	5	5	5	5	5
Foreign Body	0	5**	5**	5**	5**	5**
Inflammation, Chronic Active	0	0	0	0	5** (2.4)	5** (2.6)

**Significantly different ($P \leq 0.01$) from the chamber control group by the Fisher exact test.
[a]Number of animals with tissue examined microscopically.
[b]Number of animals with lesion.
[c]Average severity grade of lesions in affected animals: 1 = minimal, 2 = mild, 3 = moderate, 4 = marked.

Exposure Concentration Selection Rationale: The 2-year rat inhalation study was designed following a review of the current 2-week study as well as the subchronic and chronic (1-year exposure duration) inhalation study data from the literature. These data were considered sufficient to design a 2-year study without conducting a 3-month NTP study. The highest exposure concentration selected for the 2-year study (30 mg/m^3) was selected based on similar toxicity observed in the 2-week rat study in the 30 and 60 mg/m^3 groups, and the lack of in-life toxicity that might be anticipated to limit survival in the previous chronic studies at exposure concentrations of up to 45 mg/m^3. Exposure concentrations were spaced in half-log intervals, such that the lowest exposure concentration of 3 mg/m^3 was slightly lower than the concentration that produced modest toxicity and was negative for carcinogenicity after 1 year of exposure (4.5 mg/m^3; Newton et al.[16]). A 12-month interim evaluation was included in the 2-year study to provide a means of comparison to the previous 1-year exposures.

Two-year Study

Survival

Estimates of 2-year survival probabilities for male and female rats are shown in Table 5 and in the Kaplan-Meier survival curves (Figure 2). Survival of 10 and 30 mg/m^3 females was significantly less than that of the chamber control group. The decrease in survival of females was attributed primarily to lung proteinosis. In males, the trend towards reduced survival was attributed primarily to lung inflammation and proteinosis.

Body Weights, Clinical Findings, and Organ Weights

Mean body weights of 30 mg/m^3 males were at least 10% less than those of the chamber control group after week 69 and 20% less than that of the chamber control group by the end of the study (Table 6 and Figure 3). Mean body weights of 3, 10, and 30 mg/m^3 females were at least 10% less than those of the chamber control group after weeks 99, 81, and 65, respectively, and those of 10 and 30 mg/m^3 females were 20% and 28% less, respectively, than that of the chamber controls by the end of the study (Table 7 and Figure 3).

Exposure-related clinical findings included abnormal breathing, cyanosis, and thinness in male and female rats. Increases over chamber controls were noted in exposed rats primarily in the 10 and 30 mg/m^3 groups. These findings generally appeared during the second year of the study. Appendage ulcer/abscesses were recorded in chamber control and exposed groups of males with equal incidences, apparently related to housing heavier male rats on wire caging.

Table 5. Survival of Rats in the Two-year Inhalation Study of Antimony Trioxide

	Chamber Control	3 mg/m^3	10 mg/m^3	30 mg/m^3
Male				
Animals initially in study	60	60	60	60
Twelve-month interim evaluation[a]	10	10	10	10
Moribund	15	19	22	29
Natural deaths	5	1	–	3
Animals surviving to study termination	30	30	28	18
Percent probability of survival at end of study[b]	60	60	56	36
Mean survival (days)[c]	672	669	673	668
Survival analysis[d]	P = 0.025	P = 1.000	P = 1.000	P = 0.084
Female				
Animals initially in study	60	60	60	60
Twelve-month interim evaluation[a]	10	10	10	10
Moribund	11	12	20	27
Natural deaths	–	–	2	3
Animals surviving to study termination	39	38	28[e]	20[e]
Percent probability of survival at end of study	78	76	56	40
Mean survival (days)	704	704	686	663
Survival analysis	P < 0.001	P = 0.968	P = 0.032	P < 0.001

[a]Excluded from survival analyses.
[b]Kaplan-Meier determinations.
[c]Mean of all deaths (uncensored, censored, and terminal kill).
[d]The result of the life table trend test[50] is in the chamber control column, and the results of the life table pairwise comparisons[49] with the chamber controls are in the exposed group columns.
[e]Includes one animal that died during the last week of the study.

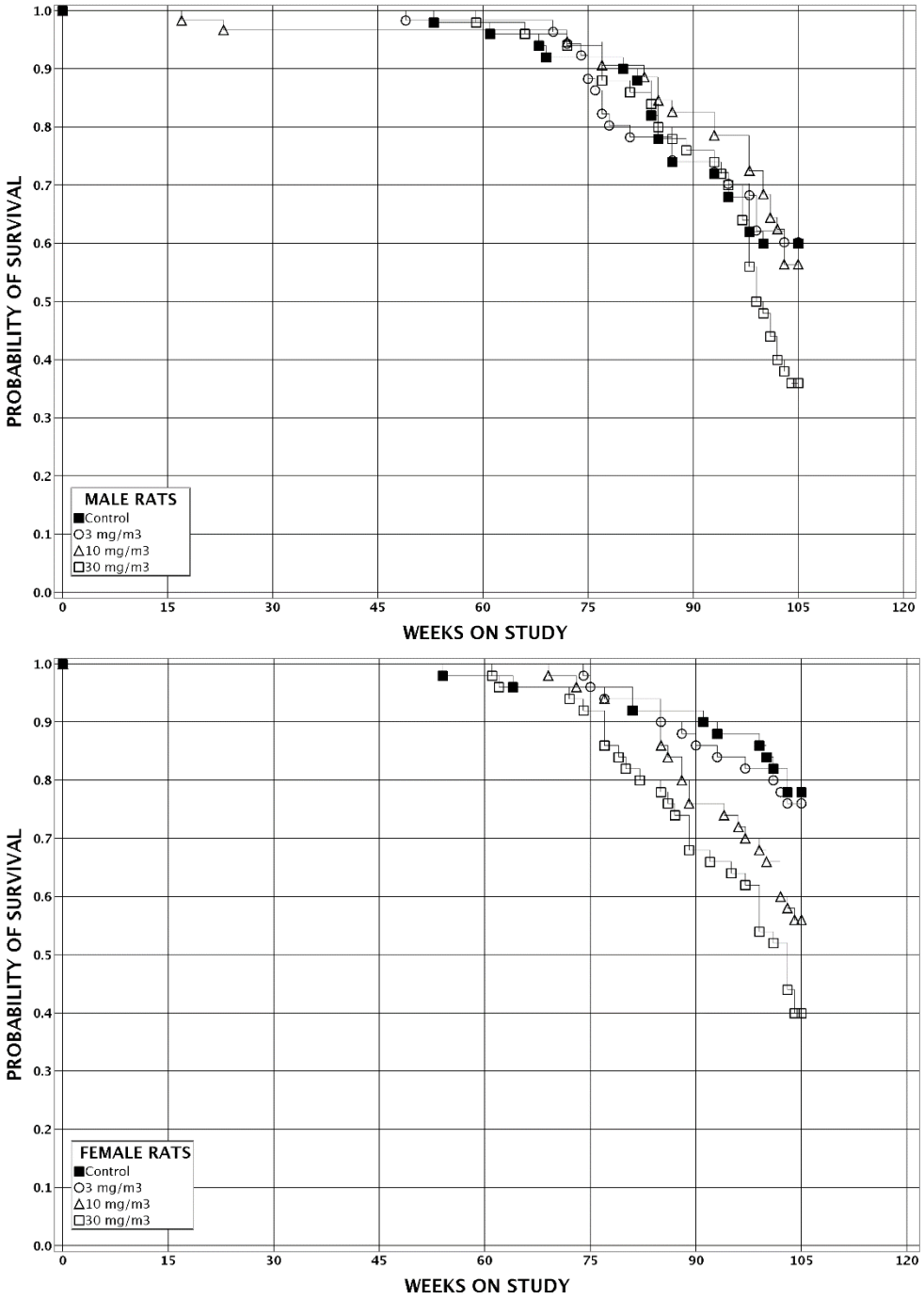

Figure 2. Kaplan-Meier Survival Curves for Rats Exposed to Antimony Trioxide by Inhalation for Two Years

Table 6. Mean Body Weights and Survival of Male Rats in the Two-year Inhalation Study of Antimony Trioxide

Day	Chamber Control		3 mg/m^3			10 mg/m^3			30 mg/m^3		
	Av. Wt. (g)	No. of Survivors	Av. Wt. (g)	Wt. (% of Controls)	No. of Survivors	Av. Wt. (g)	Wt. (% of Controls)	No. of Survivors	Av. Wt. (g)	Wt. (% of Controls)	No. of Survivors
1	120	60	119	99	60	119	100	60	118	99	60
8	163	60	160	98	60	162	100	60	158	97	60
16	209	60	205	98	60	209	100	60	203	97	60
22	242	60	238	99	60	241	100	60	234	97	60
29	272	60	269	99	60	272	100	60	265	98	60
36	297	60	294	99	60	296	100	60	289	97	60
43	317	60	314	99	60	317	100	60	309	97	60
50	337	60	332	98	60	336	100	60	327	97	60
57	351	60	346	99	60	350	100	60	340	97	60
64	364	60	358	99	60	362	99	60	352	97	60
71	374	60	368	98	60	370	99	60	361	96	60
78	383	60	378	99	60	379	99	60	369	97	60
85	390	60	384	99	60	387	99	60	377	97	60
113	418	60	412	99	60	415	99	59	402	96	60
141	436	60	428	98	60	432	99	59	419	96	60
169	451	60	444	99	60	449	100	58	434	96	60
197	466	60	459	99	60	465	100	58	447	96	60
225	477	60	470	98	60	478	100	58	458	96	60
253	491	60	482	98	60	490	100	58	470	96	60
281	502	60	493	98	60	501	100	58	480	96	60
309	516	60	503	98	60	515	100	58	489	95	60
337	526	60	511	97	60	522	99	58	497	95	60
365	535	60	519	97	59	531	99	58	503	94	60
393[a]	545	49	524	96	49	537	98	48	501	92	50
421	554	49	532	96	49	544	98	48	507	92	49
449	563	48	541	96	49	553	98	48	512	91	49
477	565	46	547	97	49	557	99	48	516	91	48
505	572	46	553	97	47	562	98	47	516	90	47
533	580	46	552	95	43	569	98	47	517	89	47
561	583	45	559	96	40	577	99	45	518	89	44
589	587	41	565	96	39	573	98	42	516	88	42
618	601	37	565	94	37	569	95	41	512	85	39
645	601	37	566	94	37	565	94	41	507	84	38
659	607	34	567	93	36	568	94	39	501	83	36
673	604	34	566	94	35	566	94	39	497	82	33
687	600	31	566	94	33	566	94	36	491	82	28
701	604	30	566	94	31	557	92	34	493	82	24
715	606	30	561	93	31	559	92	31	483	80	20
Mean for Weeks											
1–13	294		290	99		292	100		285	97	
14–52	476		467	98		474	100		455	96	
53–103	582		553	95		559	96		506	87	

[a]Interim evaluation occurred during week 53.

Table 7. Mean Body Weights and Survival of Female Rats in the Two-year Inhalation Study of Antimony Trioxide

Day	Chamber Control		3 mg/m^3			10 mg/m^3			30 mg/m^3		
	Av. Wt. (g)	No. of Survivors	Av. Wt. (g)	Wt. (% of Controls)	No. of Survivors	Av. Wt. (g)	Wt. (% of Controls)	No. of Survivors	Av. Wt. (g)	Wt. (% of Controls)	No. of Survivors
1	106	60	106	99	60	105	99	60	105	99	60
8	128	60	127	100	60	127	99	60	126	99	60
16	146	60	146	100	60	146	100	60	145	99	60
22	159	60	159	100	60	159	100	60	159	100	60
29	172	60	171	99	60	173	100	60	171	99	60
36	182	60	180	99	60	182	100	60	181	99	60
43	190	60	189	99	60	190	100	60	188	99	60
50	197	60	195	99	60	195	99	60	194	99	60
57	203	60	202	100	60	203	100	60	201	99	60
64	209	60	206	99	60	206	99	60	205	98	60
71	214	60	210	98	60	210	98	60	209	98	60
78	217	60	213	98	60	214	98	60	213	98	60
85	220	60	216	98	60	218	99	60	216	99	60
113	232	60	229	99	60	230	99	60	227	98	60
141	241	60	236	98	60	236	98	60	234	97	60
169	247	60	243	99	60	244	99	60	241	98	60
197	252	60	248	98	60	249	99	60	246	98	60
225	260	60	254	98	60	255	98	60	253	98	60
253	267	60	260	97	60	263	99	60	260	97	60
281	271	60	265	98	60	270	99	60	264	97	60
309	280	60	274	98	60	277	99	60	273	98	60
337	287	60	279	97	60	285	99	60	279	97	60
365	294	60	287	98	60	290	99	60	283	96	60
393[a]	304	49	292	96	50	299	98	50	289	95	50
421	316	49	298	94	50	310	98	50	294	93	50
449	325	48	303	94	50	311	96	50	298	92	48
477	332	48	312	94	50	317	96	50	299	90	48
505	342	48	321	94	50	322	94	48	301	88	47
533	352	48	330	94	48	324	92	48	301	86	46
561	362	47	339	94	47	328	91	47	303	84	41
589	371	46	345	93	45	327	88	45	303	82	40
618	378	46	347	92	44	332	88	38	298	79	36
645	383	44	351	92	43	329	86	38	293	77	33
659	384	44	353	92	42	325	85	37	288	75	32
673	387	44	353	91	42	321	83	36	285	74	32
687	388	44	353	91	41	320	82	35	284	73	31
701	392	41	353	90	41	319	81	33	286	73	27
715	396	40	355	90	39	315	80	30	286	72	25
Mean for Weeks											
1–13	180		178	99		179	99		178	99	
14–52	260		254	98		256	99		253	97	
53–103	356		331	93		318	90		293	83	

[a]Interim evaluation occurred during week 53.

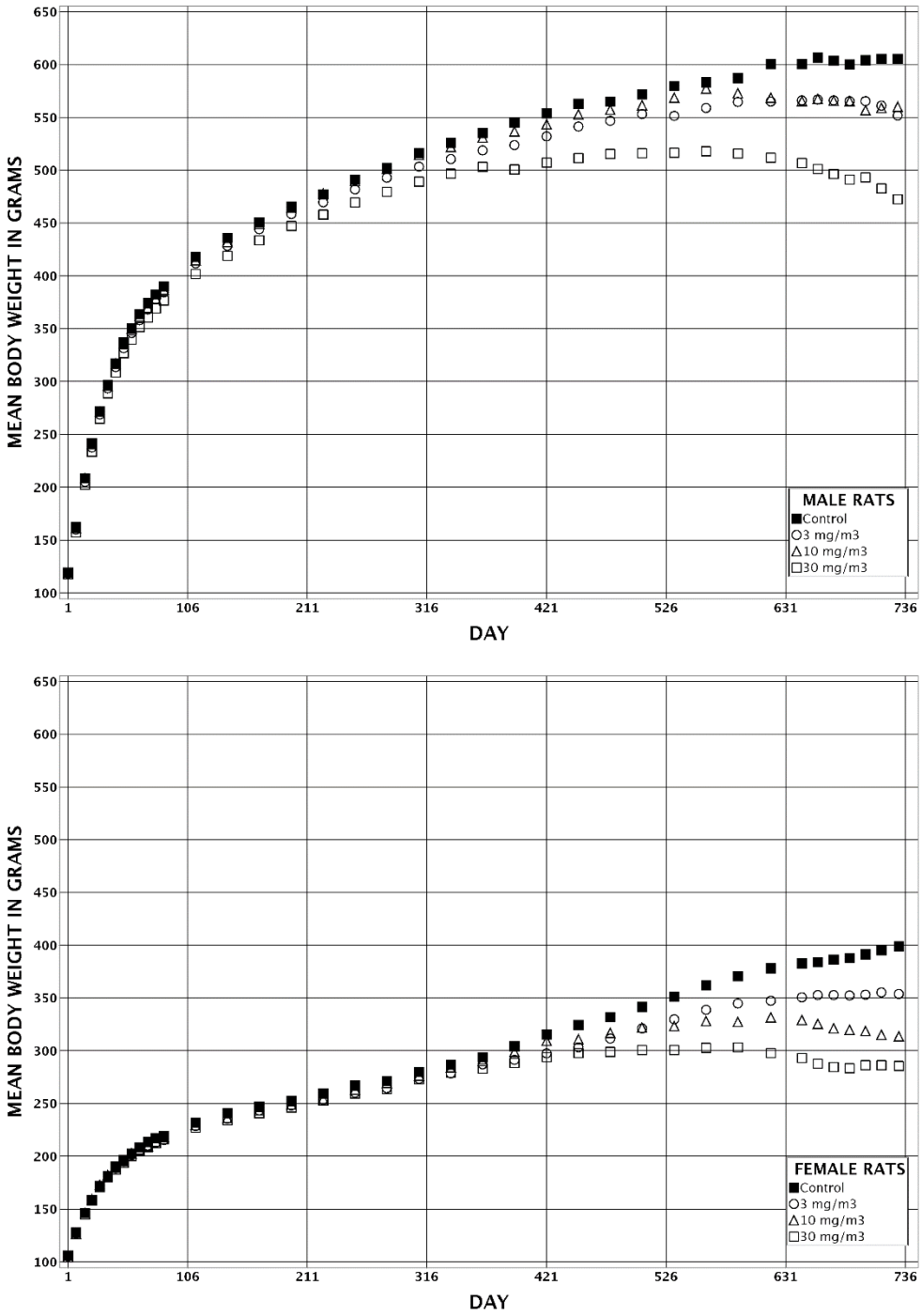

Figure 3. Growth Curves for Rats Exposed to Antimony Trioxide by Inhalation for Two Years

Absolute and relative lung weights were significantly increased in all exposed groups of males and females at the 12-month interim evaluation (Table 8 and Table F-2). Lung weights increased with exposure concentration in both males and females. Due at least in part to the decreases in body weight in females, group mean relative lung weights were much greater in exposed females than in males. Small, but statistically significant increases in relative liver weights were observed in the 10 and 30 mg/m^3 males; the increases were of uncertain toxicologic significance.

At necropsy, most of the exposed rats had lungs that were mottled or mottled pale, and many had lungs that were enlarged when compared to those of the chamber control groups. These gross changes corresponded to the proteinosis and/or chronic active inflammation seen microscopically.

Table 8. Selected Organ Weights and Organ-Weight-to-Body-Weight Ratios for Rats at the 12-month Interim Evaluation in the Two-year Inhalation Study of Antimony Trioxide[a]

	Chamber Control	3 mg/m^3	10 mg/m^3	30 mg/m^3
n	10	10	10	10
Male				
Necropsy body wt.	522 ± 16	531 ± 17	540 ± 20	534 ± 13
Liver				
Absolute	14.08 ± 0.64	14.78 ± 0.43	15.81 ± 0.61	15.75 ± 0.70
Relative	26.908 ± 0.582	27.910 ± 0.458	29.294 ± 0.508*	29.452 ± 0.886**
Lung				
Absolute	2.79 ± 0.18	3.65 ± 0.19*	4.32 ± 0.28**	6.57 ± 0.29**
Relative	5.368 ± 0.326	6.897 ± 0.312*	8.040 ± 0.490**	12.313 ± 0.484**
Female				
Necropsy body wt.	278 ± 10	293 ± 11	272 ± 7	278 ± 6
Lung				
Absolute	1.78 ± 0.09	2.89 ± 0.16**	4.20 ± 0.22**	5.48 ± 0.28**
Relative	6.451 ± 0.335	9.898 ± 0.448**	15.528 ± 0.975**	19.719 ± 0.901**

*Significantly different ($P \leq 0.05$) from the chamber control group by Williams' test.
**$P \leq 0.01$.
[a]Organ weights (absolute weights) and body weights are given in grams; organ-weight-to-body-weight ratios (relative weights) are given as mg organ weight/g body weight (mean ± standard error).

Pathology and Statistical Analyses

This section describes the statistically significant or biologically noteworthy changes in the incidences of neoplasms and/or nonneoplastic lesions of the lung, adrenal medulla, nose, larynx, trachea, bone marrow, lymph nodes (bronchial and mediastinal), arterial vessels (of the mediastinum, pancreas, mesentery, lung, and kidney), kidney, eye, prostate gland, skin, forestomach, thymus, uterus, pituitary gland, and mammary gland. Summaries of the incidences of neoplasms and/or nonneoplastic lesions, statistical analyses of primary neoplasms that occurred with an incidence of at least 5% in at least one animal group, and historical control incidences for the neoplasms mentioned in this section are presented in Appendix A for male rats and Appendix B for female rats.

Lung: At the 12-month interim evaluation, a single incidence of alveolar/bronchiolar adenoma occurred in a 30 mg/m^3 female (Table 9 and Table B-1).

In the 2-year study, the incidences of alveolar/bronchiolar adenoma were slightly increased without statistical significance in 10 and 30 mg/m^3 males (Table 9, Table A-1, and Table A-2).

Also, incidences of multiple alveolar/bronchiolar adenoma occurred in 3 and 30 mg/m^3 males, but not in chamber control males. Two alveolar/bronchiolar carcinomas occurred in 10 mg/m^3 male rats. In all exposed groups of male rats, the incidences of alveolar/bronchiolar adenoma and alveolar/bronchiolar adenoma or carcinoma (combined) exceeded the historical control ranges for inhalation studies and for all routes of administration (Table 9 and Table A-3). In female rats, incidences of alveolar/bronchiolar adenoma occurred with a positive trend (Table 9, Table B-1, and Table B-2). The incidences of alveolar/bronchiolar adenoma in 10 and 30 mg/m^3 females were significantly increased compared to that in the chamber controls. A single incidence of multiple alveolar/bronchiolar adenoma occurred in one 10 mg/m^3 female. No alveolar/bronchiolar carcinomas occurred in female rats. However, a single incidence of squamous cell carcinoma occurred in one 30 mg/m^3 female and cystic keratinizing epithelioma occurred in two 30 mg/m^3 females; neither of these neoplasms have occurred in historical control Wistar Han rats (Table 9 and Table B-3).

Microscopically, alveolar/bronchiolar adenomas were densely cellular, expansile masses, composed of closely spaced epithelial cells that primarily followed alveolar outlines, but also contained solid cellular clusters that extended into or obliterated alveolar spaces (Figure 6). The proliferative cells showed only minor atypia, and mitoses were few. Alveolar/bronchiolar carcinomas often contained several patterns within the same mass and exhibited more cellular pleomorphism than seen in adenomas. The squamous cell carcinoma present in one 30 mg/m^3 female rat was a solid mass composed of islands of pleomorphic squamous cells, sometimes with central keratin pearls, and separated by small to moderate amounts of fibrous stroma, infiltrating and obliterating the normal pulmonary architecture (Figure 6). On the other hand, the cystic keratinizing epitheliomas in female rats were cystic masses filled with keratin and lined by squamous epithelium that exhibited limited proliferation of mildly atypical squamous epithelium at the periphery (Figure 6).

A spectrum of nonneoplastic lung lesions occurred that was similar at the 12-month interim evaluation and in the 2-year study for exposed groups of male and female rats (Table 9, Table A-4, and Table B-4). Foreign body occurred in all exposed male and female rats and in none of the chamber controls. The foreign particles, presumed to be the test article, were present in alveolar macrophages, and often extracellularly in the proteinaceous fluid of the alveoli, of all exposed animals. The foreign particles were small, round to oval, refractile, nonpolarizing, golden brown material with central pallor, measuring approximately 1 micron in diameter (Figure 7). Occasionally, the foreign particles were noted within the cytoplasm of alveolar lining cells and/or within the interstitium of the alveolar walls. The response of the lung to the presence of this foreign material consisted of alveolar histiocytosis (macrophages), inflammation, alveolar proteinosis, alveolar and bronchiolar epithelial hyperplasia, and fibrosis (Figure 7, Figure 8, Figure 9, Figure 10, and Figure 11). The increased alveolar macrophages were often clustered in multifocal aggregates accompanied by smaller numbers of neutrophils and sometimes cellular debris, and were incorporated in the diagnosis of chronic active inflammation. Significantly increased incidences of mild to moderate chronic active inflammation occurred in all exposed groups of male and female rats, and incidences of minimal inflammation were observed in some chamber control rats. In addition, in some of the males and females, particularly the 10 and 30 mg/m^3 males, there were more concentrated intra-alveolar aggregates of intact and degenerate neutrophils and macrophages, associated with abundant karyorrhectic debris and foreign particles (presumed to be the test article), and these inflammatory aggregates were diagnosed as

alveolus, inflammation, suppurative. A third type of inflammation, characterized by minimal perivascular infiltrates of lymphocytes, was observed in exposed males and females. These incidences of perivascular, infiltration cellular, lymphocytes were significantly increased compared to those in the chamber control groups at the 12-month interim evaluation in 3 and 10 mg/m^3 males and females and in the 2-year study in 3 and 10 mg/m^3 males and all exposed groups of females.

Table 9. Incidences of Neoplasms and Nonneoplastic Lesions of the Lung in Rats in the Two-year Inhalation Study of Antimony Trioxide

	Chamber Control	3 mg/m^3	10 mg/m^3	30 mg/m^3
Male				
Twelve-month Interim Evaluation				
Number Examined Microscopically	10	10	10	10
Foreign Body[a]	0	10**	10**	10**
Inflammation, Chronic Active	1 (1.0)[b]	10** (2.1)	10** (2.9)	10** (3.0)
Alveolus, Inflammation, Suppurative	0	1 (1.0)	2 (1.0)	2 (1.5)
Perivascular, Infiltration Cellular, Lymphocyte	0	4* (1.0)	4* (1.0)	3 (1.0)
Proteinosis	0	9** (1.0)	10** (1.4)	10** (2.4)
Alveolar Epithelium, Hyperplasia	0	10** (1.2)	10** (1.9)	10** (2.2)
Bronchiole, Epithelium, Hyperplasia	0	5** (1.0)	5** (1.0)	6** (1.0)
Fibrosis	0	10** (1.1)	10** (1.8)	10** (1.8)
Two-year Study				
Number Examined Microscopically	50	50	50	50
Foreign Body	1	50**	50**	50**
Inflammation, Chronic Active	18 (1.0)	50** (2.5)	50** (2.7)	50** (2.8)
Alveolus, Inflammation, Suppurative	0	12** (1.2)	24** (1.4)	28** (1.7)
Perivascular, Infiltration Cellular, Lymphocyte	3 (1.7)	25** (1.1)	19** (1.2)	9 (1.1)
Proteinosis	0	47** (1.3)	50** (1.9)	50** (2.7)
Alveolar Epithelium, Hyperplasia	4 (1.3)	50** (1.8)	48** (2.1)	49** (2.2)
Bronchiole, Epithelium, Hyperplasia	3 (1.0)	34** (1.0)	36** (1.1)	33** (1.5)
Fibrosis	2 (1.0)	50** (1.4)	49** (1.6)	49** (1.7)
Alveolar/bronchiolar Adenoma, Multiple	0	1	0	3
Alveolar/bronchiolar Adenoma (includes multiple)[c]				
Overall rate[d]	3/50 (6%)	4/50 (8%)	6/50 (12%)	8/50 (16%)
Adjusted rate[e]	7.1%	9.8%	13.8%	19.7%
Terminal rate[f]	1/30 (3%)	4/30 (13%)	2/28 (7%)	4/18 (22%)
First incidence (days)	369	729 (T)	534	649
Poly-3 test[g]	P = 0.057	P = 0.478	P = 0.253	P = 0.083
Alveolar/bronchiolar Carcinoma[h]				

	Chamber Control	3 mg/m^3	10 mg/m^3	30 mg/m^3
Overall rate	0/50 (0%)	0/50 (0%)	2/50 (4%)	0/50 (0%)
Adjusted rate	0.0%	0.0%	4.7%	0.0%
Terminal rate	0/30 (0%)	0/30 (0%)	1/28 (4%)	0/18 (0%)
First incidence (days)	–[i]	–	719	–
Poly-3 test	P = 0.702N	–[j]	P = 0.245	–
Alveolar/bronchiolar Adenoma or Carcinoma[c]				
Overall rate	3/50 (6%)	4/50 (8%)	8/50 (16%)	8/50 (16%)
Adjusted rate	7.1%	9.8%	18.4%	19.7%
Terminal rate	1/30 (3%)	4/30 (13%)	3/28 (11%)	4/18 (22%)
First incidence (days)	369	729 (T)	534	649
Poly-3 test	P = 0.067	P = 0.478	P = 0.104	P = 0.083
Female				
Twelve-month Interim Evaluation				
Number Examined Microscopically	10	10	10	10
Foreign Body	0	10**	10**	10**
Inflammation, Chronic Active	2 (1.0)	10** (2.0)	10** (2.0)	10** (2.3)
Alveolus, Inflammation, Suppurative	0	1 (1.0)	0	3 (1.0)
Perivascular, Infiltration Cellular, Lymphocyte	0	4* (1.0)	5* (1.0)	3 (1.0)
Proteinosis	0	10** (1.7)	10** (2.8)	10** (3.0)
Alveolar Epithelium, Hyperplasia	0	10** (1.0)	10** (1.2)	10** (1.4)
Bronchiole, Epithelium, Hyperplasia	0	1 (1.0)	0	3 (1.0)
Fibrosis	0	10** (1.0)	10** (1.0)	10** (1.1)
Alveolar/bronchiolar Adenoma	0	0	0	1
Two-year Study				
Number Examined Microscopically	50	50	50	50
Foreign Body	0	50**	50**	50**
Inflammation, Chronic Active	21 (1.0)	50** (2.3)	50** (2.2)	50** (2.2)
Alveolus, Inflammation, Suppurative	0	5* (1.0)	6* (1.0)	5* (1.2)
Perivascular, Infiltration Cellular, Lymphocyte	0	18** (1.1)	11** (1.1)	8** (1.0)
Proteinosis	0	50** (2.4)	50** (2.9)	50** (3.1)
Alveolar Epithelium, Hyperplasia	5 (1.6)	50** (1.9)	49** (1.9)	50** (2.1)
Bronchiole, Epithelium, Hyperplasia	6 (1.0)	26** (1.1)	25** (1.0)	27** (1.1)
Alveolar Epithelium, Metaplasia, Squamous	0	5* (1.8)	3 (2.3)	1 (2.0)
Fibrosis	1 (1.0)	50** (1.5)	50** (1.5)	49** (1.4)
Alveolar/bronchiolar Adenoma, Multiple	0	0	1	0
Alveolar/bronchiolar Adenoma (includes multiple)[k]				
Overall rate	0/50 (0%)	2/50 (4%)	6/50 (12%)	5/50 (10%)

	Chamber Control	3 mg/m^3	10 mg/m^3	30 mg/m^3
Adjusted rate	0.0%	4.4%	13.8%	12.4%
Terminal rate	0/39 (0%)	2/38 (5%)	4/28 (14%)	2/20 (10%)
First incidence (days)	–	730 (T)	534	534
Poly-3 test	P = 0.029	P = 0.235	P = 0.012	P = 0.021
Cystic Keratinizing Epithelioma[k]	0	0	0	2
Squamous Cell Carcinoma[k]	0	0	0	1
Cystic Keratinizing Epithelioma or Squamous Cell Carcinoma[k]				
Overall rate	0/50 (0%)	0/50 (0%)	0/50 (0%)	3/50 (6%)
Adjusted rate	0.0%	0.0%	0.0%	7.4%
Terminal rate	0/39 (0%)	0/38 (0%)	0/28 (0%)	1/20 (5%)
First incidence (days)	–	–	–	554
Poly-3 test	P = 0.006	–	–	P = 0.096

*Significantly different ($P \leq 0.05$) from the chamber control group by the Fisher exact test (interim evaluation) or the Poly-3 test (2-year study).
**$P \leq 0.01$.
(T) = terminal kill.
[a]Number of animals with lesion.
[b]Average severity grade of lesions in affected animals: 1 = minimal, 2 = mild, 3 = moderate, 4 = marked.
[c]Historical incidence for 2-year inhalation studies with chamber control groups (mean ± standard deviation): 4/150 (2.7% ± 3.1%), range 0%–6%; all routes: 4/299 (1.3% ± 2.4%), range 0%–6%.
[d]Number of animals with neoplasm per number of animals with lung examined microscopically.
[e]Poly-3 estimated neoplasm incidence after adjustment for intercurrent mortality.
[f]Observed incidence at terminal kill.
[g]Beneath the chamber control incidence is the P value associated with the trend test. Beneath the exposed group incidence are the P values corresponding to pairwise comparisons between the chamber controls and that exposed group. The Poly-3 test accounts for differential mortality in animals that do not reach terminal kill. A negative trend is indicated by **N**.
[h]Historical incidence for inhalation studies: 0/150; all routes: 0/299.
[i]Not applicable; no neoplasms in animal group.
[j]Value of statistic cannot be computed.
[k]Historical incidence for inhalation studies: 0/150; all routes: 0/300.

Significantly increased incidences with increased exposure concentration-related severities of alveolar proteinosis occurred in all exposed groups of rats at the 12-month interim evaluation and in the 2-year study (Table 9, Table A-4, and Table B-4). The appearance of the proteinosis ranged from pale eosinophilic, wispy material in rare alveolar spaces to sheets of brightly eosinophilic, amorphous material filling numerous alveolar spaces. Immunohistochemical staining for surfactant A revealed strong staining of the proteinaceous material, Type 2 alveolar pneumocytes, and bronchiolar Clara cells for surfactant A. In contrast, immunohistochemical staining for surfactant C was limited to the Type 2 alveolar pneumocytes, and was not seen in the proteinotic material. The accumulation of surfactant A was probably related to both excessive production by the Type 2 alveolar epithelial cells due to the inflammation and to impaired clearance of the surfactant by the alveolar macrophages due to the foreign body.

The incidences of mild alveolar epithelium hyperplasia in all exposed groups of male and female rats at the 12-month interim evaluation and in the 2-year study were significantly increased compared to those in the chamber control groups (Table 9, Table A-4, and Table B-4). Hyperplasia was usually noted within areas of chronic active inflammation, and was characterized by hypertrophy and crowding of the Type 2 pneumocytes. In addition, relatively

circumscribed, typically circular foci of epithelial hyperplasia were occasionally noted in which all of the alveolar walls within a region were lined by enlarged, cuboidal epithelial cells (Figure 6A). Bronchiolar epithelium hyperplasia with minimal severity occurred in all exposed groups of rats (except 10 mg/m^3 females) at the 12-month interim evaluation and in the 2-year study, and the incidences were significantly increased in all exposed groups of males and females, except for females at the 12-month interim evaluation. Incidences of squamous metaplasia of alveolar epithelium occurred in all exposed female groups in the 2-year study, and the incidence of this lesion was significantly increased in the 3 mg/m^3 group.

The incidences of fibrosis were significantly increased in all exposed groups of males and females at the 12-month interim evaluation and in the 2-year study compared to those in the chamber control groups (Table 9, Table A-4, and Table B-4). These incidences of fibrosis were minimal to mild and occurred multifocally in the interstitium of the alveolar walls of almost all exposed 12-month interim evaluation and 2-year study rats. Fibrosis was usually manifested by slight thickening of the collagenous stroma within the alveolar walls, whereas some foci were characterized by nodular collagenous stromal thickening resulting in distortion of the normal lung architecture. Areas of subpleural fibrosis were sometimes noted. In areas of minimally increased collagen deposition within the alveolar walls, the fibrosis was highlighted by Masson trichrome staining in a subset of animals. Although the fibrosis was most often seen in areas of chronic active inflammation, there were some regions of fibrosis that had few to no inflammatory cells present.

Adrenal Medulla: No incidences of adrenal medullary hyperplasia or pheochromocytoma occurred in males or females at the 12-month interim evaluation (Table A-1, Table A-5, Table B-1, and Table B-5). In the 2-year study, the incidences of benign pheochromocytoma of the adrenal medulla were significantly increased in 30 mg/m^3 females and the incidence of benign or malignant pheochromocytoma (combined) was significantly increased in 30 mg/m^3 females compared to those in the chamber control groups and each exceeded the historical control ranges for inhalation studies and for all routes of administration (Table 10, Table B-1, Table B-2, and Table B-4). In addition, there were two occurrences of benign pheochromocytoma in each of the 3 and 10 mg/m^3 female groups. In male rats, the trend for increases in benign or complex pheochromocytomas was positive (Table 10 and Table A-2). Microscopically, the pheochromocytomas formed well-delineated masses of medullary cells, usually arranged in solid sheets but sometimes forming trabecular cords with intervening expanded blood-filled spaces (Figure 12). Compression of adjacent cortex and/or medulla was usually noted. One malignant pheochromocytoma, penetrating through the adrenal capsule, occurred in a 30 mg/m^3 female.

Incidences of adrenal medullary hyperplasia occurred with a positive trend in both males and females in the 2-year study, and the incidences were significantly increased in 30 mg/m^3 males and females compared to those of the chamber controls (Table 10, Table A-5, and Table B-5). Microscopically, hyperplasia of the adrenal medulla was characterized by noncompressive foci that were distinct from the adjacent parenchyma due to hypercellularity, decrease in cell size, and often a change in cytoplasmic coloration imparting a more basophilic appearance (Figure 12).

Table 10. Incidences of Neoplasms and Nonneoplastic Lesions of the Adrenal Medulla in Rats in the Two-year Inhalation Study of Antimony Trioxide

	Chamber Control	3 mg/m^3	10 mg/m^3	30 mg/m^3
Male				
Two-year Study				
Number Examined Microscopically	49	50	49	50
Hyperplasia[a]	1 (3.0)[b]	2 (3.5)	4 (1.5)	8* (1.5)
Benign Pheochromocytoma[c]	1	0	2	7*
Benign or Complex Pheochromocytoma[d]				
Overall rate[e]	2/49 (4%)	0/50 (0%)	2/49 (4%)	7/50 (14%)
Adjusted rate[f]	4.9%	0.0%	4.8%	17.2%
Terminal rate[g]	1/30 (3%)	0/30 (0%)	1/27 (4%)	3/18 (17%)
First incidence (days)	680	–[i]	537	590
Poly-3 test[h]	P = 0.003	P = 0.236N	P = 0.681N	P = 0.078
Female				
Two-year Study				
Number Examined Microscopically	49	49	49	50
Hyperplasia	0	0	3 (1.3)	5* (2.0)
Benign Pheochromocytoma[j]				
Overall rate	0/49 (0%)	2/49 (4%)	2/49 (4%)	6/50 (12%)
Adjusted rate	0.0%	4.5%	4.8%	15.2%
Terminal rate	0/38 (0%)	1/37 (3%)	1/27 (4%)	4/20 (20%)
First incidence (days)	–	719	698	705
Poly-3 test	P = 0.004	P = 0.235	P = 0.221	P = 0.009
Malignant Pheochromocytoma[k]	0	0	0	1
Benign or Malignant Pheochromocytoma[l]				
Overall rate	0/49 (0%)	2/49 (4%)	2/49 (4%)	7/50 (14%)
Adjusted rate	0.0%	4.5%	4.8%	17.6%
Terminal rate	0/38 (0%)	1/37 (3%)	1/27 (4%)	4/20 (20%)
First incidence (days)	–	719	698	621
Poly-3 test	P < 0.001	P = 0.235	P = 0.221	P = 0.004

*Significantly different ($P \leq 0.05$) from the chamber control group by the Poly-3 test.
(T) = terminal kill.
[a]Number of animals with lesion.
[b]Average severity grade of lesions in affected animals: 1 = minimal, 2 = mild, 3 = moderate, 4 = marked.
[c]Historical incidence for 2-year inhalation studies with chamber control groups (mean ± standard deviation): 5/149 (3.4% ± 4.2%), range 0%–8%; all routes: 6/297 (2.0% ± 3.1%), range 0%–8%.
[d]Historical incidence for inhalation studies: 6/149 (4.0% ± 4.0%), range 0%–8%; all routes 7/297 (2.4% ± 3.2%), range 0%–8%.
[e]Number of animals with neoplasm per number of animals with adrenal medulla examined microscopically.
[f]Poly-3 estimated neoplasm incidence after adjustment for intercurrent mortality.
[g]Observed incidence at terminal kill.
[h]Beneath the chamber control incidence is the P value associated with the trend test. Beneath the exposed group incidence are the P values corresponding to pairwise comparisons between the chamber controls and that exposed group. The Poly-3 test accounts for differential mortality in animals that do not reach terminal kill. A lower incidence in an exposure group is indicated by **N**.
[i]Not applicable; no neoplasms in animal group.
[j]Historical incidence for inhalation studies: 1/148 (0.7% ± 1.2%), range 0%–2%; all routes: 5/297 (1.7% ± 1.5%), range 0%–4%.
[k]Historical incidence for inhalation studies: 1/148 (0.7% ± 1.2%), range 0%–2%; all routes: 1/297 (0.3% ± 0.8%), range 0%–2%.
[l]Historical incidence for inhalation studies: 2/148 (1.4% ± 2.4%), range 0%–4%; all routes: 7/297 (2.4% ± 2.0%), range 0%–4% (includes one incidence of complex pheochromocytoma).

Nose: At the 12-month interim evaluation, foreign body, presumably the test article, occurred in a single 10 mg/m^3 male; incidences of this lesion were significantly increased in 30 mg/m^3 males and females compared to the chamber controls (Table 11, Table A-5, and Table B-5). In the 2-year study, significantly increased incidences of foreign body occurred in 10 and 30 mg/m^3 males and in all exposed groups of females. Foreign bodies occurred most commonly within macrophages adjacent to the nasal-associated lymphoid tissue along the nasopharyngeal duct of nasal Level III but were also commonly present within macrophages or entrapped within the mucous layer overlying the respiratory epithelium of the ventral-most portion of Level II.

Hyperplasia of the respiratory epithelium occurred in 10 and 30 mg/m^3 males and in 3 and 30 mg/m^3 females at the 12-month interim evaluation (Table 11, Table A-5, and Table B-5). In the 2-year study, incidences of hyperplasia of the respiratory epithelium occurred in both chamber control and exposed rats; the incidences were significantly increased in 3 and 30 mg/m^3 males and 30 mg/m^3 females compared to those in the chamber controls. The hyperplasia consisted of focal or multifocal hypercellularity of the epithelium along the lateral wall of Level I, the maxilloturbinates and, rarely, the nasoturbinates. The affected epithelium was composed of three or more layers of nonciliated, cuboidal to low columnar epithelium (Figure 13). A single incidence of respiratory epithelial adenoma was identified in a 30 mg/m^3 male rat (Table A-1); no adenomas were seen in the chamber controls, and none have been reported in the historical controls for inhalation studies (0/150) or for all routes of administration (0/299).

Squamous metaplasia of the respiratory epithelium occurred in a 30 mg/m^3 female at the 12-month interim evaluation, in males exposed to 10 and 30 mg/m^3 in the 2-year study, and in all exposed groups of females in the 2-year study (Table 11, Table A-5, and Table B-5). The incidences of this lesion in the 30 mg/m^3 males and females were significantly increased compared to those in the chamber control groups in the 2-year study.

Larynx: Incidences of foreign body, presumably the test article, occurred in all exposed males and females at the 12-month interim evaluation and in the 2-year study and the incidences were significantly increased compared to those in the chamber controls (Table 11, Table A-5, and Table B-5). The foreign bodies were predominantly located within the cytoplasm of macrophages in the lamina propria, but were also seen within the extracellular matrix, and were observed in all three Levels of the larynx. In the 2-year study, chronic active inflammation occurred in chamber control and all exposed groups of males and in 3 and 30 mg/m^3 females; the incidence of this lesion was significantly increased in 3 mg/m^3 females compared to that in the chamber control group.

Trachea: Significantly increased incidences of foreign body, presumably the test article, occurred in all exposed groups of males and females at the 12-month interim evaluation and in the 2-year study compared to those in the chamber control groups (Table 11, Table A-5, and Table B-5). Foreign bodies were located predominately within macrophages in the lamina propria, but were also seen within the extracellular matrix. Low incidences of minimal to mild squamous metaplasia occurred in the tracheal epithelium of the chamber control and exposed groups of males in the 2-year study.

Table 11. Incidences of Nonneoplastic Lesions of the Upper Respiratory Tract in Rats in the Two-year Inhalation Study of Antimony Trioxide

	Chamber Control	3 mg/m^3	10 mg/m^3	30 mg/m^3
Male				
Twelve-month Interim Evaluation				
Nose[a]	10	10	10	10
Foreign Body[b]	0	0	1	9**
Respiratory Epithelium, Hyperplasia	0	0	1 (1.0)[c]	2 (1.0)
Larynx	10	10	10	10
Foreign Body	0	10**	10**	10**
Trachea	10	10	10	10
Foreign Body	0	8**	9**	10**
Two-year Study				
Nose	50	49	50	50
Foreign Body	0	0	17**	40**
Respiratory Epithelium, Hyperplasia	6 (1.3)	15* (1.1)	13 (1.1)	25** (1.1)
Respiratory Epithelium, Metaplasia, Squamous	0	0	2 (1.0)	6* (1.7)
Larynx	50	50	50	50
Foreign Body	0	50**	50**	50**
Inflammation, Chronic Active	2 (1.5)	5 (1.4)	2 (2.0)	4 (2.0)
Metaplasia, Squamous	0	2 (1.0)	0	1 (1.0)
Trachea	50	50	50	50
Foreign Body	0	28**	43**	48**
Metaplasia, Squamous	1 (1.0)	1 (1.0)	4 (1.0)	3 (1.3)
Female				
Twelve-month Interim Evaluation				
Nose	10	10	10	10
Foreign Body	0	0	0	4*
Respiratory Epithelium, Hyperplasia	0	1 (1.0)	0	2 (1.0)
Respiratory Epithelium, Metaplasia, Squamous	0	0	0	1 (1.0)
Larynx	10	10	10	10
Foreign Body	0	10**	10**	10**
Trachea	10	10	10	10
Foreign Body	0	6**	10**	10**

	Chamber Control	3 mg/m^3	10 mg/m^3	30 mg/m^3
Two-year Study				
Nose	50	50	50	50
Foreign Body	0	5*	26**	45**
Respiratory Epithelium, Hyperplasia	4 (1.0)	6 (1.3)	7 (1.3)	16** (1.1)
Respiratory Epithelium, Metaplasia, Squamous	0	2 (1.5)	3 (2.0)	5* (1.2)
Larynx	50	50	50	50
Foreign Body	0	50**	50**	50**
Inflammation, Chronic Active	0	8** (1.1)	0	3 (1.3)
Trachea	50	50	50	50
Foreign Body	0	39**	47**	49**

*Significantly different ($P \leq 0.05$) from the chamber control group by the Fisher exact text (interim evaluation) or the Poly-3 test (2-year study).
**$P \leq 0.01$.
[a]Number of animals with tissue examined microscopically.
[b]Number of animals with lesion.
[c]Average severity grade of lesions in affected animals: 1 = minimal, 2 = mild, 3 = moderate, 4 = marked.

Bone Marrow: Hyperplasia of the hematopoietic elements of the marrow was not identified in male or female rats at the 12-month interim evaluation, but was observed in chamber control females and exposed groups of males and females in the 2-year study (Table 12, Table A-5, and Table B-5). The incidences of hyperplasia in the 2-year study were significantly increased in 30 mg/m^3 males and females compared to those in the chamber controls. The hyperplastic marrow in animals exposed to antimony trioxide often exhibited a shift in the myeloid/erythroid ratio, with a distinguishable increase in the erythroid precursors. In contrast, hyperplasia in chamber control rats often occurred with inflammatory lesions, in which the marrow generally maintained a normal myeloid to erythroid ratio, or tended towards an increase in myeloid precursors.

Lymph Nodes: The incidences of foreign body, presumed to be the test article, in the bronchial and mediastinal lymph nodes of all exposed groups of males and females at the 12-month interim evaluation and in the 2-year study were significantly increased compared to those in the chamber control groups (Table 12, Table A-5, and Table B-5). Foreign bodies were noted primarily within macrophages, which variably expanded the medullary and subcapsular sinuses.

Incidences of minimal to mild lymphoid hyperplasia occurred in the bronchial and mediastinal lymph nodes of most exposed groups of male and female rats at the 12-month interim evaluation and in all exposed groups of males and females in the 2-year study (Table 12, Table A-5, and Table B-5). The incidences of lymphoid hyperplasia in the bronchial and mediastinal lymph nodes were significantly increased in 10 mg/m^3 males and 3 mg/m^3 females at the 12-month interim evaluation and in all exposed groups of males and females in the 2-year study compared to those in the chamber controls. The lymphoid hyperplasia was characterized by expansion of the lymphocyte populations within the paracortical and medullary regions, resulting in a significant increase in lymph node size.

Golden brown pigment, resembling hemosiderin, was observed in the macrophages of the bronchial lymph nodes in male rats in the 2-year study; the incidence of pigmentation in 30 mg/m^3 males was significantly increased compared to that in the chamber control group (Table 12 and Table A-5).

Table 12. Incidences of Nonneoplastic Lesions of the Hematopoietic System in Rats in the Two-year Inhalation Study of Antimony Trioxide

	Chamber Control	3 mg/m^3	10 mg/m^3	30 mg/m^3
Male				
Twelve-month Interim Evaluation				
Lymph Node, Bronchial[a]	9	8	10	10
Foreign Body[b]	0	8**	10**	10**
Hyperplasia, Lymphoid	0	2 (1.5)[c]	5* (1.0)	2 (1.5)
Lymph Node, Mediastinal	10	8	10	9
Foreign Body	0	8**	6**	6**
Hyperplasia, Lymphoid	0	2 (1.0)	6** (1.3)	3 (1.7)
Two-year Study				
Bone Marrow	50	50	50	50
Hyperplasia	0	3 (1.0)	4 (1.0)	8** (1.0)
Lymph Node, Bronchial	41	40	48	47
Foreign Body	0	35**	45**	42**
Hyperplasia, Lymphoid	0	21** (1.0)	29** (1.3)	26** (1.3)
Pigmentation	1 (2.0)	4 (1.3)	5 (1.2)	10** (1.3)
Lymph Node, Mediastinal	42	45	49	49
Foreign Body	0	41**	41**	43**
Hyperplasia, Lymphoid	1 (1.0)	24** (1.3)	30** (1.4)	26** (1.3)
Female				
Twelve-month Interim Evaluation				
Lymph Node, Bronchial	7	8	9	5
Foreign Body	0	7**	9**	4**
Hyperplasia, Lymphoid	0	4* (1.0)	2 (1.0)	1 (1.0)
Lymph Node, Mediastinal	10	9	10	10
Foreign Body	0	9**	5**	6**
Hyperplasia, Lymphoid	0	8** (1.0)	0	3 (1.7)
Two-year Study				
Bone Marrow	50	50	50	50
Hyperplasia	8 (1.0)	5 (1.0)	11 (1.0)	20** (1.0)
Lymph Node, Bronchial	35	36	28	41

	Chamber Control	3 mg/m^3	10 mg/m^3	30 mg/m^3
Foreign Body	0	35**	23**	36**
Hyperplasia, Lymphoid	0	21** (1.0)	9** (1.6)	11** (1.0)
Lymph Node, Mediastinal	46	46	46	46
Foreign Body	0	27**	32**	33**
Hyperplasia, Lymphoid	0	14** (1.1)	10** (1.2)	15** (1.1)

*Significantly different ($P \leq 0.05$) from the chamber control group by the Fisher exact text (interim evaluation) or the Poly-3 test (2-year study).
**$P \leq 0.01$.
[a]Number of animals with tissue examined microscopically.
[b]Number of animals with lesion.
[c]Average severity grade of lesions in affected animals: 1 = minimal, 2 = mild, 3 = moderate, 4 = marked.

Arterial Vessels: No vascular lesions were noted at the 12-month interim evaluation (Table A-5 and Table B-5). In the 2-year study, incidences of chronic active inflammation of small to medium sized muscular arteries occurred mostly in a few 10 mg/m^3 males and females and many 30 mg/m^3 males and females; the vessels affected were located primarily within the mediastinum, pancreas, and mesentery, and were observed less frequently in the kidney and lung (Table 13, Table A-5, and Table B-5). The increased incidences of chronic active inflammation in the pancreas and mesentery of 30 mg/m^3 males and females were significant when compared to those in the chamber control groups. When the incidences of inflammatory vascular lesions in any tissue were combined, they were increased in 10 and 30 mg/m^3 males and females with the increased incidences being significant in 10 mg/m^3 females and in 30 mg/m^3 males and females compared to those in the chamber controls. The inflammatory infiltrate within affected vessels was predominantly composed of lymphocytes, with lesser numbers of macrophages and granulocytes (Figure 14). There were a small number of vessels with less advanced lesions that were composed primarily of neutrophils. In addition, affected vessels often had evidence of alterations to the media, variably characterized by cell swelling, vacuolation, or necrosis occasionally resulting in hemorrhage; all of these lesions were captured under the diagnosis of necrosis. In the 2-year study, the incidence of necrosis of the artery of the pancreas was significantly increased in 30 mg/m^3 females compared to that in the chamber controls. In two 30 mg/m^3 females, there were mediastinal arteries with marked proliferation of capillaries in the muscular walls of the vessels; this type of lesion has been referred to as plexiform vasculopathy in the literature[72], and is depicted in Figure 14D.

Table 13. Incidences of Nonneoplastic Lesions in the Arterial Vessels of Rats in the Two-year Inhalation Study of Antimony Trioxide

	Chamber Control	3 mg/m^3	10 mg/m^3	30 mg/m^3
Male				
Two-year Study				
Mediastinum[a]	0	1	2	10
Artery, Inflammation, Chronic Active[b]	−	1 (3.0)[c]	2 (2.5)	10 (2.3)
Artery, Necrosis	−	0	2 (3.0)	9 (1.8)

	Chamber Control	3 mg/m^3	10 mg/m^3	30 mg/m^3
Pancreas	50	50	50	50
Artery, Inflammation, Chronic Active	1 (2.0)	0	2 (2.5)	8* (3.1)
Artery, Necrosis	0	0	1 (2.0)	4 (2.0)
Mesentery	50	50	50	50
Artery, Inflammation, Chronic Active	0	0	0	6* (2.2)
Artery, Necrosis	0	0	0	3 (1.7)
Lung	50	50	50	50
Artery, Inflammation, Chronic Active	0	0	1 (1.0)	1 (2.0)
Kidney	50	50	50	50
Artery, Inflammation, Chronic Active	0	0	1 (1.0)	4 (1.3)
Artery, Necrosis	0	0	1 (2.0)	4 (1.3)
Artery (All Tissues Combined)	50	50	50	50
Artery, Inflammation, Chronic Active	1	1	5	16**
Female				
Two-year Study				
Mediastinum	0	0	2	9
Artery, Inflammation, Chronic Active	–	–	2 (1.5)	9 (2.3)
Artery, Necrosis	–	–	1 (1.0)	6 (2.2)
Pancreas	50	50	50	50
Artery, Inflammation, Chronic Active	0	0	3 (2.0)	8** (2.5)
Artery, Necrosis	0	0	0	4* (2.0)
Mesentery	50	50	50	50
Artery, Inflammation, Chronic Active	0	0	0	6** (2.5)
Artery, Necrosis	0	0	0	3 (1.7)
Lung	50	50	50	50
Artery, Inflammation, Chronic Active	0	0	1 (2.0)	2 (1.0)
Artery, Necrosis	0	0	0	2 (1.0)
Kidney	50	50	50	50
Artery, Inflammation, Chronic Active	0	0	0	2 (1.5)
Artery, Necrosis	0	0	1 (2.0)	2 (1.5)
Artery (All Tissues Combined)	50	50	50	50
Artery, Inflammation, Chronic Active	0	0	5*	15**

*Significantly different ($P \leq 0.05$) from the chamber control group by the Poly-3 test.
**$P \leq 0.01$.
[a]Number of animals with tissue examined microscopically.
[b]Number of animals with lesion.
[c]Average severity grade of lesions in affected animals: 1 = minimal, 2 = mild, 3 = moderate, 4 = marked.

Kidney: The incidences of hyaline droplet accumulation in the cytoplasm of renal tubule cells in 30 mg/m^3 males and 10 and 30 mg/m^3 females were significantly increased compared to those in the chamber controls in the 2-year study (Table 14, Table A-5, and Table B-5). The hyaline droplets were variably sized (2 to 5 microns), generally circular to ovoid, eosinophilic, and located primarily within the cytoplasm of proximal tubule epithelial cells. The possibility that the material in the renal tubule cells might be surfactant A was considered because of the accumulation of surfactant A in the lung, but immunohistochemical staining of representative animals with affected kidneys was negative for surfactant A. Hyaline droplet accumulation was not seen within the kidneys of males or females at the 12-month interim evaluation (Table A-5 and Table B-5).

In the 2-year study, the incidence of nephropathy in 30 mg/m^3 females was significantly increased compared to that in the chamber control group (Table 14 and Table B-5). Incidences of pelvis mineralization were significantly decreased in 30 mg/m^3 males and females compared to those in the chamber control groups (males: 16/50, 10/50, 11/50, 3/50; females: 31/50, 30/50, 24/50, 15/50; Table A-5, and Table B-5).

Eye: In the 2-year study, the incidences of retinal atrophy were significantly increased in all exposed groups of females compared to the chamber control group (Table 14 and Table B-5). The increased incidences of retinal atrophy were not exposure concentration-dependent, and there were no obvious differences between the chamber control group and exposed groups of females in either the appearance or the severity of the atrophy. The atrophy ranged from minimal focal loss of the photoreceptor layer and a portion of the outer nuclear layer to diffuse loss of all but the inner plexiform and nuclear layers and the ganglion cell layer.

In the 2-year study, incidences of minimal acute inflammation of the ciliary body occurred in males and females in the 10 and 30 mg/m^3 groups and the incidences were significantly increased in the 30 mg/m^3 groups of males and females compared to those in the chamber control groups (Table 14, Table A-5, and Table B-5). The lesion was characterized by infiltration of neutrophils predominantly within the ciliary processes, often accompanied by the accumulation of acellular eosinophilic material.

Prostate Gland: In the 2-year study, the incidences of epithelium hyperplasia were significantly increased in 3 and 10 mg/m^3 males compared to those in the chamber controls; and the severities were increased in all exposed groups (Table 14 and Table A-5). Microscopically, the hyperplastic foci presented as papillary or cribriform proliferations of the epithelial cells projecting into one or more adjacent prostatic acini, but without completely filling the lumens of the affected acini, and without distorting the acinar architecture or compressing the adjacent acini.

Table 14. Incidences of Selected Nonneoplastic Lesions in Rats in the Two-year Inhalation Study of Antimony Trioxide

	Chamber Control	3 mg/m^3	10 mg/m^3	30 mg/m^3
Male				
Two-year Study				
Kidney[a]	50	50	50	50
Renal Tubule, Accumulation, Hyaline Droplet[b]	0	1 (4.0)[c]	3 (2.0)	14** (1.3)
Eye	49	49	50	49
Ciliary Body, Inflammation, Acute	0	0	1 (1.0)	6* (1.2)
Prostate Gland	50	50	50	50
Epithelium, Hyperplasia	9 (1.3)	18* (2.1)	21* (1.5)	13 (1.7)
Female				
Two-year Study				
Kidney	50	50	50	50
Renal Tubule, Accumulation, Hyaline Droplet	0	0	5* (1.2)	11** (1.7)
Nephropathy	16 (1.4)	15 (1.0)	20 (1.4)	24* (1.6)
Eye	49	50	49	49
Retina, Atrophy	6 (2.5)	21** (2.0)	18** (2.1)	19** (1.9)
Ciliary Body, Inflammation, Acute	0	0	1 (1.0)	6** (1.0)

*Significantly different ($P \leq 0.05$) from the chamber control group by the Poly-3 test.
**$P \leq 0.01$.
[a]Number of animals with tissue examined microscopically.
[b]Number of animals with lesion.
[c]Average severity grade of lesions in affected animals: 1 = minimal, 2 = mild, 3 = moderate, 4 = marked.

Skin: In 2-year study males, increased incidences of chronic active inflammation (chamber control, 22/50; 3 mg/m^3, 30/50; 10 mg/m^3, 28/50; 30 mg/m^3, 32/50) and ulcer (17/50, 23/50, 23/50, 28/50) occurred in all exposed groups and were significantly increased in the 30 mg/m^3 group compared to those in the chamber control group (Table A-5). In 2-year study females, the incidences of ulcer (2/50, 5/49, 4/50, 8/50) in the chamber control and exposed groups were less than those in the males, but the incidence of this lesion was significantly increased in the 30 mg/m^3 group compared to that in the chamber control group (Table A-5 and Table B-5).

Other Organs: In the 2-year study, incidences of various nonneoplastic lesions of uncertain significance were increased in exposed groups compared to those in the chamber control groups. Incidences of squamous hyperplasia of the forestomach (chamber control, 2/50; 3 mg/m^3, 7/50; 10 mg/m^3, 4/50; 30 mg/m^3, 7/50) and cellular depletion of the thymus (5/41, 6/35, 6/47, 9/45) were slightly increased in exposed groups of males (Table A-5). In the uterus, increased incidences of cystic hyperplasia of the endometrium (9/50, 17/50, 6/50, 16/50) occurred in 3 and 30 mg/m^3 females, and the incidence of this lesion was significantly increased in the 30 mg/m^3 group compared to that in the chamber control group (Table B-5).

In the pituitary gland, the incidence of pars distalis adenoma was significantly decreased in 30 mg/m^3 males compared to that in the chamber controls (14/50, 15/50, 12/50, 5/50; Table A-1 and Table A-2); the incidence of this neoplasm was slightly decreased in 30 mg/m^3 females (19/50, 22/50, 19/50, 12/50; Table B-1 and Table B-2).

Mice

Two-week Study

All mice survived to the end of the study (Table 15). The final mean body weights and body weight gains of exposed groups of males and females were similar to the respective chamber control groups. There were no clinical findings related to antimony trioxide exposure.

Table 15. Survival and Body Weights of Mice in the Two-week Inhalation Study of Antimony Trioxide[a]

Concentration (mg/m^3)	Survival[b]	Initial Body Weight (g)	Final Body Weight (g)	Change in Body Weight (g)	Final Weight Relative to Controls (%)
Male					
0	5/5	24.0 ± 0.3	25.0 ± 0.2	1.0 ± 0.5	
3.75	5/5	24.2 ± 0.4	25.3 ± 0.1	1.1 ± 0.3	101
7.5	5/5	24.4 ± 0.2	26.4 ± 0.5	2.1 ± 0.5	106
15	5/5	24.7 ± 0.5	25.9 ± 0.6	1.2 ± 0.7	104
30	5/5	24.1 ± 0.4	25.5 ± 0.6	1.4 ± 0.4	102
60	5/5	24.5 ± 0.4	26.6 ± 0.8	2.1 ± 0.4	106
Female					
0	5/5	19.6 ± 0.2	21.2 ± 0.3	1.6 ± 0.4	
3.75	5/5	19.4 ± 0.3	20.9 ± 0.2	1.5 ± 0.2	98
7.5	5/5	18.7 ± 0.3	20.6 ± 0.4	1.9 ± 0.5	97
15	5/5	19.5 ± 0.2	20.9 ± 0.2	1.4 ± 0.4	99
30	5/5	19.8 ± 0.4	21.0 ± 0.3	1.2 ± 0.3	99
60	5/5	19.9 ± 0.4	21.1 ± 0.4	1.2 ± 0.6	100

[a]Weights and weight changes are given as mean ± standard error.
[b]Number of animals surviving at 17 days/number initially in group.

Absolute lung weights were significantly increased in 7.5 mg/m^3 or greater males and in females exposed to 15 mg/m^3 or greater compared to the chamber controls (Table 16 and Table F-3). Relative lung weights were significantly increased in 60 mg/m^3 males and in all exposed groups of females compared to the chamber control groups. There were no gross observations associated with exposure to antimony trioxide noted at necropsy.

Table 16. Lung Weights and Lung-Weight-to-Body-Weight Ratios for Mice in the Two-week Inhalation Study of Antimony Trioxide[a]

	Chamber Control	3.75 mg/m^3	7.5 mg/m^3	15 mg/m^3	30 mg/m^3	60 mg/m^3
n	5	5	5	5	5	5
Male						
Necropsy body wt.	25.0 ± 0.2	25.3 ± 0.1	26.4 ± 0.5	25.9 ± 0.6	25.5 ± 0.6	26.6 ± 0.8
Lung						
Absolute	0.17 ± 0.01	0.21 ± 0.02	0.22 ± 0.01*	0.21 ± 0.01*	0.21 ± 0.01*	0.23 ± 0.01**
Relative	6.939 ± 0.267	8.086 ± 0.835	8.184 ± 0.443	8.076 ± 0.321	8.147 ± 0.232	8.725 ± 0.209**
Female						
Necropsy body wt.	21.2 ± 0.3	20.9 ± 0.2	20.6 ± 0.4	20.9 ± 0.2	21.0 ± 0.3	21.1 ± 0.4
Lung						
Absolute	0.16 ± 0.00	0.18 ± 0.01	0.18 ± 0.00	0.20 ± 0.01**	0.20 ± 0.01**	0.22 ± 0.01**
Relative	7.656 ± 0.185	8.736 ± 0.336*	8.734 ± 0.131*	9.546 ± 0.308**	9.659 ± 0.229**	10.320 ± 0.397**

*Significantly different ($P \leq 0.05$) from the chamber control group by Williams' test.
**$P \leq 0.01$.
[a]Lung weights (absolute weights) and body weights are given in grams; lung-weight-to-body-weight ratios (relative weights) are given as mg lung weight/g body weight (mean ± standard error).

Minimal or mild squamous metaplasia of the epithelium lining the base of the epiglottis occurred in all male and female mice in the 30 and 60 mg/m^3 groups and the incidences were significantly increased compared to those of the chamber controls (Table 17). Also, minimal incidences of squamous metaplasia of the epiglottis occurred without statistical significance in one 15 mg/m^3 male and in several 3.75, 7.5, and 15 mg/m^3 females. Significantly increased incidences of foreign body, presumed to be the test article, occurred in the lung of all groups of mice exposed to antimony trioxide. The foreign bodies appeared as refractile gold to brown/black granules within the cytoplasm of alveolar macrophages and lying free within the alveolar spaces.

Exposure Concentration Selection Rationale: The 2-year mouse inhalation study was designed following a review of the current 2-week study as well as the subchronic and chronic (1-year exposure duration) inhalation study data for rats from the literature. These data were considered sufficient to design the 2-year study without conducting a 3-month NTP study. The highest exposure concentration selected for the 2-year study (30 mg/m^3) and half-log exposure concentration spacing intervals were selected to match the rat study. A 12-month interim evaluation was included in the 2-year study to provide a means of comparison to the previous 1-year rat exposures and the concurrent rat study.

Table 17. Incidences of Selected Nonneoplastic Lesions of the Respiratory System in Mice in the Two-week Inhalation Study of Antimony Trioxide

	Chamber Control	3.75 mg/m^3	7.5 mg/m^3	15 mg/m^3	30 mg/m^3	60 mg/m^3
Male						
Larynx[a]	5	0	5	4	5	5
Epiglottis, Metaplasia, Squamous[b]	0	–	0	1 (1.0)[c]	5** (1.0)	5** (1.8)
Lung	5	5	5	5	5	5
Foreign Body	0	5**	5**	5**	5**	5**
Female						
Larynx	5	5	5	5	5	5
Epiglottis, Metaplasia, Squamous	0	2 (1.0)	2 (1.0)	3 (1.0)	5** (1.0)	5** (2.0)
Lung	5	5	5	5	5	5
Foreign Body	0	5**	5**	5**	5**	5**

**Significantly different ($P \leq 0.01$) from the chamber control group by the Fisher exact test.
[a]Number of animals with tissue examined microscopically.
[b]Number of animals with lesion.
[c]Average severity grade of lesions in affected animals: 1 = minimal, 2 = mild, 3 = moderate, 4 = marked.

Two-year Study

Survival

Estimates of 2-year survival probabilities for male and female mice are shown in Table 18 and in the Kaplan-Meier survival curves (Figure 4). Survival of 10 and 30 mg/m^3 males and females was significantly less than that of the chamber control groups. Decreases in survival were attributed primarily to alveolar/bronchiolar carcinomas and inflammation of the lung in males and malignant lymphoma and lung inflammation in females.

Table 18. Survival of Mice in the Two-year Inhalation Study of Antimony Trioxide

	Chamber Control	3 mg/m^3	10 mg/m^3	30 mg/m^3
Male				
Animals initially in study	60	60	60	60
Twelve-month interim evaluation[a]	10	10	10	10
Accidental death	–	1		
Moribund	7	12	15	26
Natural deaths	5	7	8	7
Animals surviving to study termination	38	30	27	17
Percent probability of survival at end of study[b]	76	61	54	34
Mean survival (days)[c]	708	658	666	652
Survival analysis[d]	P < 0.001	P = 0.134	P = 0.027	P < 0.001
Female				
Animals initially in study	60	60	60	60
Twelve-month interim evaluation[a]	10	10	10	10
Accidental death	1	–	–	–
Moribund	10	11	16	27
Natural deaths	3	8	8	8
Animals surviving to study termination	36	31	26	15
Percent probability of survival at end of study	74	62	52	30
Mean survival (days)	692	693	666	642
Survival analysis	P < 0.001	P = 0.303	P = 0.032	P < 0.001

[a]Excluded from survival analyses.
[b]Kaplan-Meier determinations.
[c]Mean of all deaths (uncensored, censored, and terminal kill).
[d]The result of the life table trend test[50] is in the chamber control column, and the results of the life table pairwise comparisons[49] with the chamber controls are in the exposed group columns.

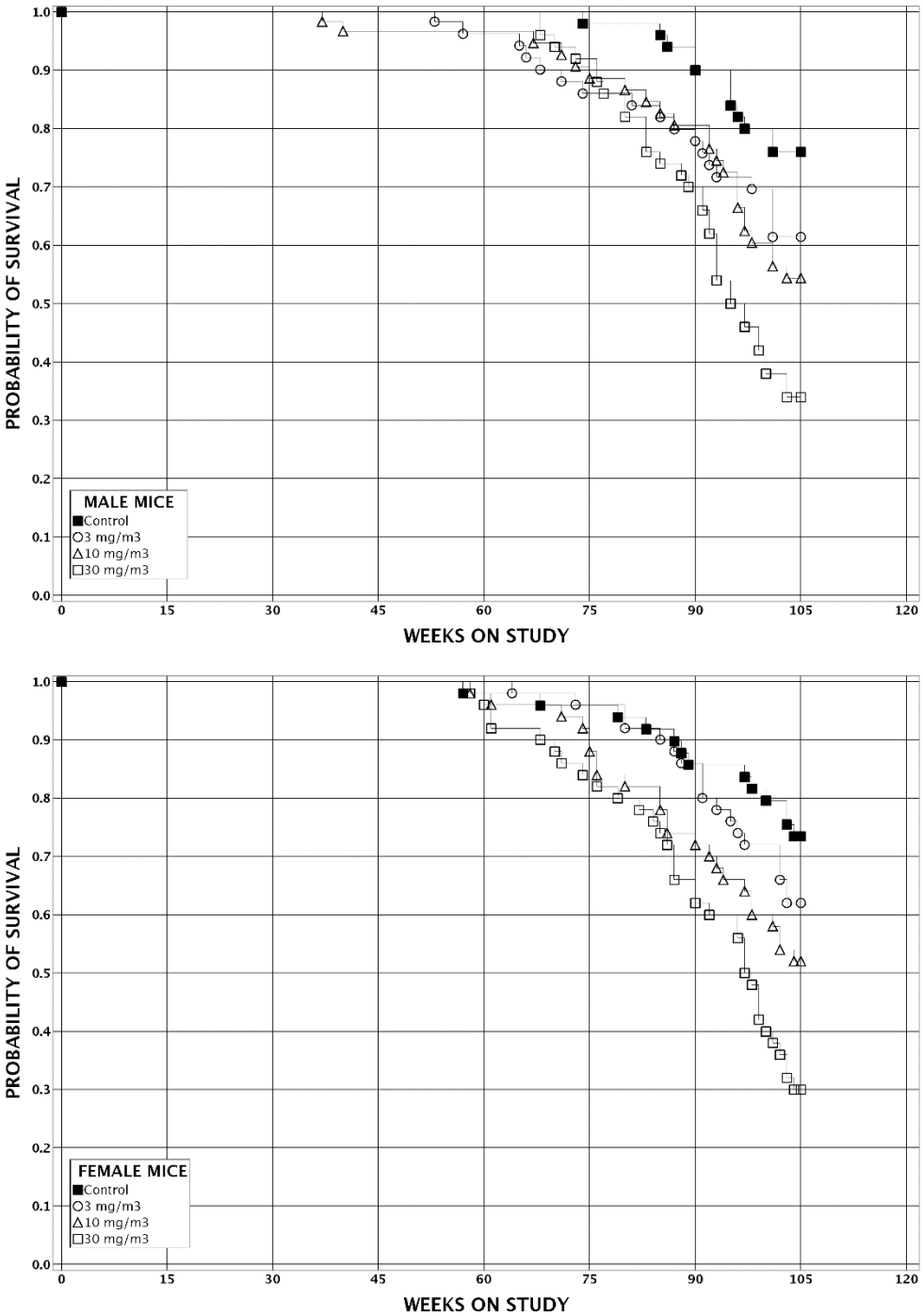

Figure 4. Kaplan-Meier Survival Curves for Mice Exposed to Antimony Trioxide by Inhalation for Two Years

Body Weights, Clinical Findings, and Organ Weights

The mean body weights of 30 mg/m^3 males were at least 10% less than those of the chamber controls after week 73 and 25% less than that of the chamber control group by the end of the study (Table 19 and Figure 5). Mean body weights of 30 mg/m^3 females were at least 10% less than those of the chamber controls after week 85 and 21% less than that of the chamber control group by the end of the study (Table 20 and Figure 5).

Exposure-related clinical findings in male and female mice included abnormal breathing and thinness, which were increased at all exposure concentrations. These findings generally appeared during the second year of the study.

At the 12-month interim evaluation, absolute and relative lung weights were significantly increased in all exposed groups of males and females (except relative lung weight in 3 mg/m^3 females) (Table 21 and Table F-4). In addition, absolute and relative thymus weights were significantly increased in 10 and 30 mg/m^3 males and females and absolute thymus weight was significantly increased in 3 mg/m^3 females. Significantly increased absolute heart and liver weights were observed in 30 mg/m^3 females, but the relative weights were not statistically increased, and the biologic significance was uncertain.

At the 12-month interim evaluation, almost all mice exposed to 10 or 30 mg/m^3, and occasional mice exposed to 3 mg/m^3, had lungs that were described as mottled or mottled pale. All terminal kill mice exposed to 30 mg/m^3, many mice exposed to 10 mg/m^3, and occasional mice exposed to 3 mg/m^3 had similar gross findings in the lungs. These gross lesions corresponded with the chronic inflammation seen microscopically. Many exposed mice from both sexes had liver and/or lung nodules or masses at terminal kill. Metastatic masses or systemic neoplasia resulting in splenomegaly, lymphadenopathy, or masses in various organs were present in several chamber control and exposed mice at terminal kill.

Table 19. Mean Body Weights and Survival of Male Mice in the Two-year Inhalation Study of Antimony Trioxide

Day	Chamber Control		3 mg/m^3			10 mg/m^3			30 mg/m^3		
	Av. Wt. (g)	No. of Survivors	Av. Wt. (g)	Wt. (% of Controls)	No. of Survivors	Av. Wt. (g)	Wt. (% of Controls)	No. of Survivors	Av. Wt. (g)	Wt. (% of Controls)	No. of Survivors
1	23.5	60	23.2	99	60	23.1	99	60	23.2	99	60
9	26.0	60	25.4	98	60	25.4	98	60	25.5	98	60
16	26.7	60	26.3	99	60	26.4	99	60	26.4	99	60
23	27.6	60	27.2	99	60	26.9	98	60	27.4	99	60
30	28.3	60	28.2	100	60	27.9	99	60	28.4	101	60
37	29.2	60	29.1	100	60	28.7	98	60	29.0	99	60
44	30.0	60	30.0	100	60	29.7	99	60	29.2	98	60
51	30.8	60	30.7	100	60	30.2	98	60	29.2	95	60
58	31.3	60	31.9	102	60	30.9	99	60	30.6	98	60
65	32.5	60	32.7	101	60	31.0	96	60	31.3	97	60
72	33.4	60	33.4	100	59	31.7	95	60	31.6	95	60
79	34.3	60	34.1	99	59	32.2	94	60	32.2	94	60
86	35.1	60	34.9	99	59	32.7	93	60	32.7	93	60
114	38.5	60	38.1	99	59	35.6	92	60	35.1	91	60
142	41.0	60	40.4	99	59	38.1	93	60	38.0	93	60
170	43.8	60	42.7	98	59	41.2	94	60	41.2	94	60
198	45.0	60	44.1	98	59	43.4	96	60	43.5	97	60
226	47.0	60	46.2	98	59	46.0	98	60	46.1	98	60
254	48.0	60	46.9	98	59	47.3	99	59	47.3	99	60
282	49.7	60	48.9	99	59	49.4	99	58	49.3	99	60
310	50.0	60	49.0	98	59	49.9	100	58	49.6	99	60
338	50.5	60	49.9	99	59	50.6	100	58	49.9	99	60
366	51.3	60	50.4	98	58	51.4	100	57	50.6	99	60
394[a]	51.8	50	51.1	99	47	52.0	100	47	50.5	98	50
422	51.7	50	51.2	99	47	51.7	100	47	49.6	96	50
450	52.1	50	51.1	98	46	51.9	100	47	49.2	94	50
478	51.4	50	51.1	99	44	51.2	99	46	48.1	93	48
506	51.8	50	51.3	99	43	51.0	98	45	47.0	91	47
534	52.0	49	51.3	99	42	51.3	99	43	46.1	89	44
562	51.5	49	50.7	98	42	50.8	99	42	45.3	88	41
590	51.9	48	50.8	98	40	50.0	96	41	44.8	86	38
618	51.0	47	48.7	96	39	49.7	97	39	42.6	84	36
646	50.8	45	47.3	93	36	48.3	95	36	41.8	82	27
660	50.0	45	46.8	94	35	47.2	94	35	40.2	80	27
674	51.2	41	46.9	92	35	46.0	90	32	40.8	80	23
688	50.6	40	46.4	92	34	46.0	91	29	38.6	76	23
702	51.4	38	46.1	90	34	46.7	91	28	39.9	78	19
716	51.2	38	47.1	92	30	45.5	89	28	38.4	75	18
Mean for Weeks											
1–13	29.9		29.8	100		29.0	97		29.0	97	
14–52	45.9		45.1	98		44.6	97		44.4	97	
53–103	51.4		49.3	96		49.4	96		44.6	87	

[a]Interim evaluation occurred during week 53.

Table 20. Mean Body Weights and Survival of Female Mice in the Two-year Inhalation Study of Antimony Trioxide

Day	Chamber Control		3 mg/m^3			10 mg/m^3			30 mg/m^3		
	Av. Wt. (g)	No. of Survivors	Av. Wt. (g)	Wt. (% of Controls)	No. of Survivors	Av. Wt. (g)	Wt. (% of Controls)	No. of Survivors	Av. Wt. (g)	Wt. (% of Controls)	No. of Survivors
1	18.6	60	18.4	99	60	18.5	100	60	18.3	98	60
9	20.7	60	20.7	100	60	20.7	100	60	20.4	98	60
16	21.2	60	21.2	100	60	21.4	101	60	21.4	101	60
23	22.1	60	22.7	103	60	22.4	101	60	22.6	102	60
30	23.1	60	23.9	104	60	23.8	103	60	23.9	103	60
37	23.8	60	24.5	103	60	24.3	102	60	24.5	103	60
44	24.5	60	25.2	103	60	25.0	102	60	25.1	103	60
51	25.1	60	26.1	104	60	26.0	104	60	25.9	103	60
58	24.9	60	26.6	107	60	26.5	106	60	26.5	106	60
65	26.1	60	27.2	104	60	26.8	103	60	27.3	105	60
72	26.4	60	27.5	104	60	26.9	102	60	27.5	104	60
79	27.2	60	28.2	104	60	27.5	101	60	27.9	102	60
86	27.5	60	29.5	107	60	28.0	102	60	27.9	102	60
114	29.8	60	31.8	107	60	29.8	100	60	30.6	103	60
142	32.3	60	34.6	107	60	32.7	101	60	32.6	101	60
170	35.8	60	38.1	107	60	36.7	103	60	36.3	101	60
198	37.3	60	40.5	109	60	39.2	105	60	38.2	102	60
226	39.8	60	43.9	110	60	42.4	107	60	40.4	102	60
254	41.6	60	45.5	109	60	44.1	106	60	41.7	100	60
282	43.9	59	48.9	111	60	46.8	107	60	44.4	101	60
310	45.6	59	50.6	111	60	48.4	106	60	46.5	102	60
338	47.0	59	52.3	111	60	50.3	107	60	48.0	102	60
366	48.9	59	54.3	111	60	53.0	108	60	49.6	101	60
394[a]	51.1	49	56.6	111	50	54.7	107	50	51.1	100	50
422	52.5	48	57.6	110	50	54.5	104	49	51.1	97	47
450	53.2	48	58.9	111	49	55.6	105	48	52.1	98	46
478	53.8	47	59.5	111	49	54.4	101	48	51.8	96	45
506	54.1	47	59.2	110	49	54.1	100	47	51.0	94	43
534	53.9	47	58.3	108	48	54.8	102	42	50.5	94	41
562	53.6	46	58.5	109	46	53.2	99	41	49.9	93	40
590	53.2	45	58.5	110	45	54.1	102	39	49.2	93	38
618	51.3	43	55.1	108	43	51.3	100	37	46.2	90	33
646	49.8	42	52.9	106	39	48.9	98	35	44.8	90	30
660	49.6	42	51.8	105	38	48.6	98	33	43.2	87	30
674	49.3	42	51.5	105	37	47.4	96	32	41.6	84	26
688	49.8	40	50.7	102	36	46.7	94	30	41.0	82	24
702	50.4	39	50.3	100	36	46.3	92	30	42.1	84	19
716	49.9	38	48.4	97	33	45.7	92	27	39.2	79	18
Mean for Weeks											
1–13	23.9		24.7	103		24.4	102		24.6	102	
14–52	39.2		42.9	109		41.2	105		39.9	102	
53–103	51.5		55.1	107		51.5	100		47.2	91	

[a]Interim evaluation occurred during week 53.

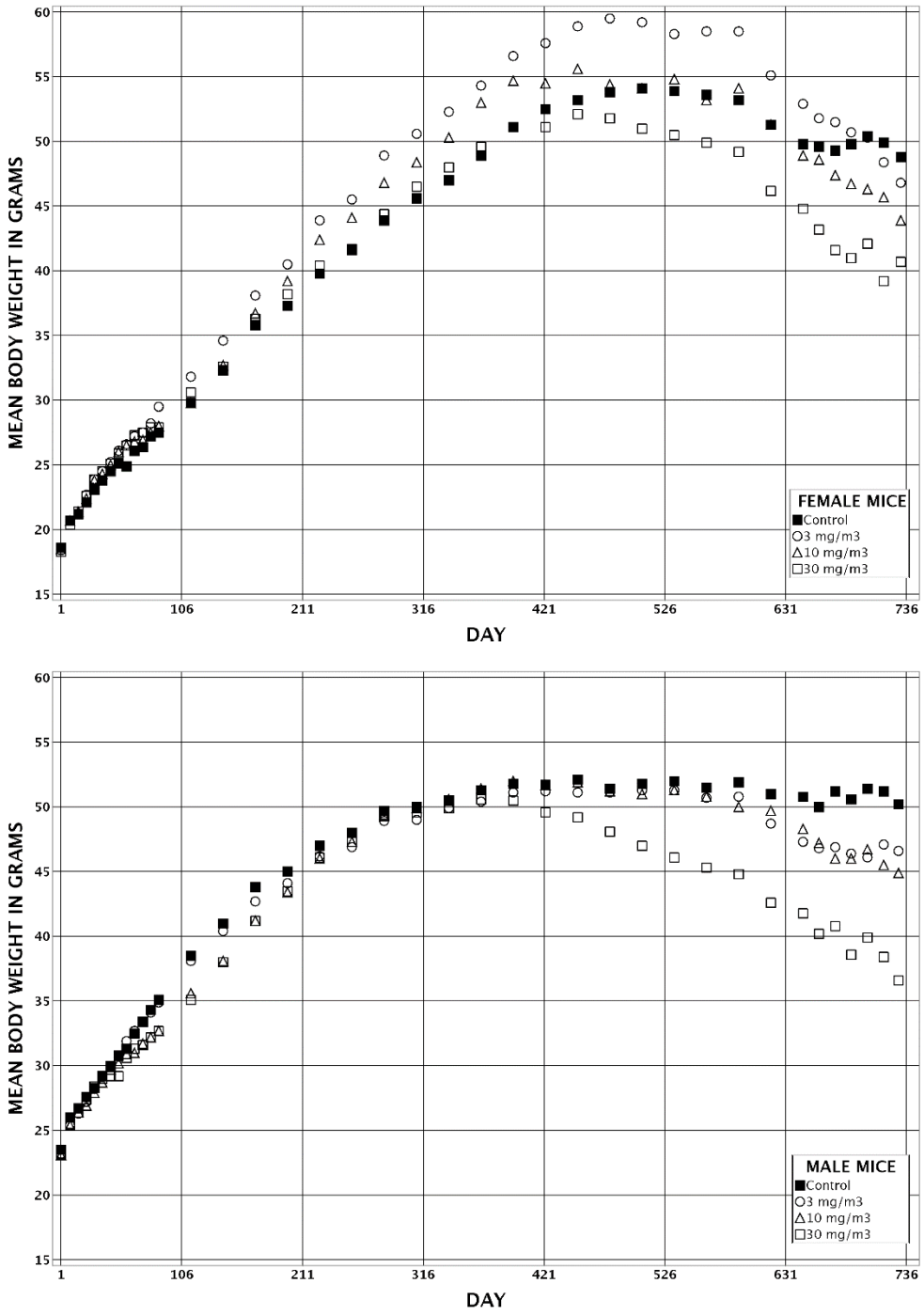

Figure 5. Growth Curves for Mice Exposed to Antimony Trioxide by Inhalation for Two Years

Table 21. Selected Organ Weights and Organ-Weight-to-Body-Weight Ratios for Mice at the 12 month Interim Evaluation in the Two-year Inhalation Study of Antimony Trioxide[a]

	Chamber Control	3 mg/m^3	10 mg/m^3	30 mg/m^3
n	10	10	10	10
Male				
Necropsy body wt.	51.4 ± 0.3	51.3 ± 0.9	51.5 ± 0.6	51.9 ± 0.8
Lung				
Absolute	0.24 ± 0.01	0.33 ± 0.01**	0.46 ± 0.01**	0.66 ± 0.04**
Relative	4.703 ± 0.113	6.396 ± 0.131*	8.862 ± 0.289**	12.857 ± 0.855**
Thymus				
Absolute	0.114 ± 0.005	0.126 ± 0.006	0.147 ± 0.008**	0.173 ± 0.011**
Relative	2.219 ± 0.102	2.450 ± 0.091	2.840 ± 0.151**	3.317 ± 0.170**
Female				
Necropsy body wt.	47.3 ± 2.1	55.4 ± 1.7*	50.5 ± 2.1	49.8 ± 1.7
Heart				
Absolute	0.17 ± 0.00	0.17 ± 0.00	0.17 ± 0.00	0.19 ± 0.01**
Relative	3.552 ± 0.129	3.120 ± 0.062*	3.423 ± 0.120	3.770 ± 0.119
Liver				
Absolute	1.73 ± 0.07	1.91 ± 0.06	1.83 ± 0.06	1.94 ± 0.06*
Relative	36.653 ± 0.588	34.465 ± 0.634	36.531 ± 1.129	39.158 ± 1.118
Lung				
Absolute	0.23 ± 0.01	0.33 ± 0.01**	0.42 ± 0.02**	0.79 ± 0.03**
Relative	4.799 ± 0.126	5.913 ± 0.169	8.331 ± 0.320**	16.000 ± 0.857**
Thymus				
Absolute	0.080 ± 0.005	0.116 ± 0.009*	0.112 ± 0.012*	0.129 ± 0.010**
Relative	1.681 ± 0.062	2.069 ± 0.126	2.216 ± 0.232*	2.554 ± 0.127**

*Significantly different ($P \leq 0.05$) from the chamber control group by Williams' or Dunnett's test.
**$P \leq 0.01$.
[a]Organ weights (absolute weights) and body weights are given in grams; organ-weight-to-body-weight ratios (relative weights) are given as mg organ weight/g body weight (mean ± standard error).

Pathology and Statistical Analyses

This section describes the statistically significant or biologically noteworthy changes in the incidences of malignant lymphoma and neoplasms and/or nonneoplastic lesions of the lung, skin, nose, larynx, trachea, hematopoietic system (bronchial, mediastinal, and mandibular lymph nodes; spleen; bone marrow; and thymus), heart, forestomach, adrenal medulla, liver, and eye. Summaries of the incidences of neoplasms and nonneoplastic lesions, statistical analyses of primary neoplasms that occurred with an incidence of at least 5% in at least one animal group, and historical control incidences for the neoplasms mentioned in this section are presented in Appendix C for male mice and Appendix D for female mice.

Lung: At the 12-month interim evaluation, alveolar/bronchiolar adenoma occurred in two 10 mg/m^3 males and in one 30 mg/m^3 female, and alveolar/bronchiolar carcinoma occurred in one 10 mg/m^3 male and two 30 mg/m^3 males (Table 22, Table C-1, and Table D-1). No lung neoplasms occurred in chamber controls at the 12-month interim evaluation.

In the 2-year study, significantly increased incidences of alveolar/bronchiolar carcinoma occurred in all exposed groups of males compared to that in the chamber controls; these incidences occurred in an exposure concentration-dependent manner and exceeded the historical control ranges for inhalation studies and for all routes of administration (Table 22, Table C-1, Table C-2, and Table C-3). Incidences of multiple alveolar/bronchiolar carcinoma occurred in approximately one-third of exposed males with carcinoma, whereas no incidences of multiple carcinoma occurred in the chamber control males. Slightly increased incidences of alveolar/bronchiolar adenoma in 3 and 30 mg/m^3 males exceeded the historical control ranges for inhalation studies and for all routes of administration. Combined incidences of alveolar/bronchiolar adenoma or carcinoma were significantly increased in all groups of exposed males compared to that in the chamber controls, and the incidences exceeded the historical control ranges for inhalation studies and for all routes of administration. In female mice, the incidences of alveolar/bronchiolar adenoma, alveolar/bronchiolar carcinoma, and alveolar/bronchiolar adenoma or carcinoma (combined) were significantly increased in all exposed groups compared to those in the chamber controls and exceeded the historical control ranges for inhalation studies and for all routes of administration (Table 22, Table D-1, Table D-2, and Table D-3). Incidences of multiple alveolar/bronchiolar adenoma occurred in a few females in each exposed group, and incidences of multiple alveolar/bronchiolar carcinoma occurred in almost half of females with carcinoma in each exposed group; neither multiple alveolar/bronchiolar adenoma nor carcinoma were observed in female chamber controls. Of the exposed mice with alveolar/bronchiolar carcinoma, 20% of the males and 19% of the females were found to have metastases, whereas metastases were not identified in any of the male or female chamber control mice. Bronchial and mediastinal lymph nodes were the most common sites of metastasis.

Microscopically, alveolar/bronchiolar adenomas and carcinomas in the exposed groups (Figure 15) were morphologically similar to those in the chamber control groups. Alveolar/bronchiolar adenomas were usually smaller than the carcinomas, well-differentiated cytologically, and often papillary or occasionally solid in pattern. Alveolar/bronchiolar carcinomas were expansile masses which typically exhibited several histologic patterns within the same tumor, and a greater degree of cytologic pleomorphism than seen in the adenomas.

A spectrum of nonneoplastic lesions occurred in the lung of mice that was similar at the 12-month interim evaluation and in the 2-year study (Table 22, Table C-7, and Table D-8). Incidences of peribronchial and perivascular lymphocytic cellular infiltrates, ranging from minimal to marked, occurred in all exposed groups of males and females, and often extended from the hilar to the peripheral portions of the lung. The incidences of this lesion were significantly increased compared to those in the chamber controls in all exposed groups of males and females at the 12-month interim evaluation and in the 2-year study. Generally, the extent and distribution of vessel and airway cuffing by the lymphoid cells were proportional to exposure concentration, as reflected in the severity grades. The lymphocytes in these infiltrates were mature in appearance, and were composed of a mixture of B and T lymphocytes, as demonstrated in immunohistochemical stained sections of representative animals (Figure 16).

Although the aggregates of B cells and the aggregates of T cells were contiguous and slightly intermingled, they often appeared to remain within relatively separate domains, as shown by staining of serial sections for B and T cells with antibodies to PAX5 and CD3, respectively. In some of the exposed mice at the 12-month interim evaluation, the lymphocytes in the infiltrates exhibited mild variation in size and shape, but with retention of nonneoplastic features such as follicle formation, admixture of plasma cells, and variable numbers of macrophages sometimes containing the presumed test article; however, in three 30 mg/m^3 females, the lymphocytic infiltrates exhibited more obvious cytologic atypicality, absence of follicle formation, and radial and longitudinal expansion of the perivascular and peribronchial lymphoid populations, indicative of malignant lymphoma. In the 2-year study, similarly and to a greater extent, some males and many females in the chamber control and exposed groups exhibited infiltration of malignant lymphoma in a predominantly perivascular and peribronchial distribution that often obscured or replaced the nonneoplastic lymphocytic infiltrates. In a few other exposed male and female mice, the nonneoplastic lymphocytic infiltrates were obscured or replaced by histiocytic sarcoma infiltrating in the same perivascular and peribronchial distribution.

Incidences of foreign body, presumed to be the test article, occurred in the cytoplasm of alveolar macrophages, as well as free in alveolar spaces, of all exposed groups of mice; incidences of this lesion were significantly increased compared to those in the chamber controls in all exposed groups of males and females at the 12-month interim evaluation and in the 2-year study (Table 22, Table C-7, and Table D-8). The foreign particles were round to oval, approximately one micron in diameter, dark brown at the periphery and light brown in the center, and refractile but not birefringent with polarizing lenses.

Mild to moderate chronic active inflammation that consisted of clusters of macrophages often containing the foreign body, lesser numbers of both viable and degenerate neutrophils, and cellular debris were noted primarily within the alveolar spaces of almost all exposed mice at the 12-month interim evaluation and in the 2-year study (Table 22, Table C-7, and Table D-8). The incidences of chronic active inflammation were significantly increased compared to those in the chamber control groups in exposed groups of males and females at the 12-month interim evaluation and in the 2-year study. The inflammation was variably associated with minimal to mild alveolus fibrosis in the majority of the 10 and 30 mg/m^3 males and females at the 12-month interim evaluation and in the 2-year study, and a minimal degree of alveolus fibrosis occurred in some of the 3 mg/m^3 males and females at the 12-month interim evaluation and in the 2-year study. The fibrosis was manifested by slight thickening of the alveolar walls by fine tendrils of collagen, imparting a more rigid appearance to the walls with hematoxylin and eosin (Figure 17), and accentuated by the Masson trichrome stain. Incidences of alveolus fibrosis were significantly increased at the 12-month interim evaluation in all exposed groups of males and in 10 and 30 mg/m^3 females; incidences of this lesion were significantly increased in all exposed groups of males and females in the 2-year study. Minimal to mild chronic inflammation and fibrosis of the visceral pleura of the lungs occurred in most exposed mice at the 12-month interim evaluation and in the 2-year study. Foreign body particles were sometimes seen individually within the fibrotic pleural matrix but were more frequently seen in aggregates within the cytoplasm of alveolar macrophages lying just beneath the fibrotic pleura. In addition, focal clusters of macrophages containing aggregates of foreign particles were seen randomly scattered within the fibrotic pleura, particularly in areas of lymphocytic and plasmacellular inflammation. Incidences

of pleural fibrosis and pleural inflammation were significantly increased in all exposed groups of males and females at the 12-month interim evaluation and in the 2-year study.

In the areas of chronic active inflammation, alveolar epithelium hyperplasia often occurred, ranging from minimal to mild, and this lesion occurred in most exposed male and female mice at the 12-month interim evaluation and in the 2-year study (Table 22, Table C-7, and Table D-8). Minimal to mild bronchiole epithelium hyperplasia occurred in the terminal bronchioles of most exposed mice at the 12-month interim evaluation and in the 2-year study, and was characterized either by crowding and piling up of the epithelium, and/or enlarged epithelial cells with karyomegaly and prominent nucleoli (Figure 17). The incidences of alveolar epithelium hyperplasia and bronchiole epithelium hyperplasia were significantly increased in all exposed groups of males and females compared to the chamber controls at the 12-month interim evaluation and in the 2-year study.

Table 22. Incidences of Neoplasms and Nonneoplastic Lesions of the Lung in Mice in the Two-year Inhalation Study of Antimony Trioxide

	Chamber Control	3 mg/m^3	10 mg/m^3	30 mg/m^3
Male				
Twelve-month Interim Evaluation				
Number Examined Microscopically	10	10	10	10
Infiltration Cellular, Lymphocyte[a]	0	10** (1.0)[b]	10** (1.9)	10** (2.5)
Foreign Body	0	10**	10**	10**
Inflammation, Chronic Active	0	10** (2.1)	10** (3.2)	10** (3.8)
Alveolus, Fibrosis	0	4* (1.0)	7** (1.9)	10** (1.8)
Pleura, Fibrosis	0	5** (1.0)	10** (1.2)	10** (1.8)
Pleura, Inflammation	0	7** (1.0)	10** (1.3)	10** (1.8)
Alveolar Epithelium, Hyperplasia	0	9** (1.0)	10** (1.7)	10** (1.9)
Bronchiole, Epithelium, Hyperplasia	0	9** (1.0)	9** (1.2)	9** (1.7)
Alveolar/bronchiolar Adenoma	0	0	2	0
Alveolar/bronchiolar Carcinoma	0	0	1	2
Two-year Study				
Number Examined Microscopically	50	50	50	50
Infiltration Cellular, Lymphocyte	13 (1.2)	47** (1.4)	48** (2.1)	45** (2.9)
Foreign Body	0	50**	50**	50**
Inflammation, Chronic Active	0	48** (2.3)	50** (3.1)	50** (3.7)
Alveolus, Fibrosis	0	12** (1.1)	30** (1.6)	37** (1.9)
Pleura, Fibrosis	0	36** (1.1)	46** (1.4)	50** (2.4)
Pleura, Inflammation	1 (1.0)	40** (1.0)	47** (1.3)	48** (1.8)
Alveolar Epithelium, Hyperplasia	6 (1.2)	39** (1.1)	45** (1.8)	49** (1.9)
Bronchiole, Epithelium, Hyperplasia	0	32** (1.2)	44** (1.3)	44** (1.6)
Alveolar/bronchiolar Adenoma, Multiple	3	3	2	4
Alveolar/bronchiolar Adenoma (includes multiple)[c]				

	Chamber Control	3 mg/m^3	10 mg/m^3	30 mg/m^3
Overall rate[d]	10/50 (20%)	14/50 (28%)	9/50 (18%)	14/50 (28%)
Adjusted rate[e]	21.5%	32.9%	21.8%	34.6%
Terminal rate[f]	9/38 (24%)	7/30 (23%)	6/27 (22%)	4/17 (24%)
First incidence (days)	702	449	646	530
Poly-3 test[g]	P = 0.190	P = 0.165	P = 0.592	P = 0.129
Alveolar/bronchiolar Carcinoma, Multiple	0	5*	6**	11**
Alveolar/bronchiolar Carcinoma (includes multiple)[h]				
Overall rate	4/50 (8%)	18/50 (36%)	20/50 (40%)	27/50 (54%)
Adjusted rate	8.5%	40.9%	46.2%	62.8%
Terminal rate	2/38 (5%)	9/30 (30%)	11/27 (41%)	12/17 (71%)
First incidence (days)	590	449	509	490
Poly-3 test	P < 0.001	P < 0.001	P < 0.001	P < 0.001
Alveolar/bronchiolar Adenoma or Carcinoma[i]				
Overall rate	13/50 (26%)	29/50 (58%)	28/50 (56%)	34/50 (68%)
Adjusted rate	27.5%	64.5%	63.6%	75.3%
Terminal rate	10/38 (26%)	16/30 (53%)	16/27 (59%)	12/17 (71%)
First incidence (days)	590	449	509	490
Poly-3 test	P < 0.001	P < 0.001	P < 0.001	P < 0.001
Female				
Twelve-month Interim Evaluation				
Number Examined Microscopically	10	10	10	10
Infiltration Cellular, Lymphocyte	3 (1.0)	10** (1.7)	10** (2.0)	9** (3.1)
Foreign Body	0	10**	10**	10**
Inflammation, Chronic Active	0	10** (1.9)	10** (2.8)	10** (4.0)
Alveolus, Fibrosis	0	2 (1.0)	6** (1.3)	10** (2.4)
Pleura, Fibrosis	0	6** (1.0)	9** (1.2)	10** (1.1)
Pleura, Inflammation	0	7** (1.1)	10** (1.3)	10** (1.8)
Alveolar Epithelium, Hyperplasia	0	8** (1.1)	10** (1.6)	10** (2.1)
Bronchiole, Epithelium, Hyperplasia	0	5** (1.0)	10** (1.4)	10** (1.5)
Alveolar/bronchiolar Adenoma	0	0	0	1
Two-year Study				
Number Examined Microscopically	50	50	50	50
Infiltration Cellular, Lymphocyte	7 (1.1)	37** (1.5)	37** (2.4)	26** (3.2)
Foreign Body	0	50**	50**	50**
Inflammation, Chronic Active	1 (1.0)	50** (2.2)	50** (3.2)	50** (3.5)
Alveolus, Fibrosis	0	13** (1.2)	30** (1.4)	38** (2.2)
Pleura, Fibrosis	1 (1.0)	39** (1.1)	50** (1.4)	50** (2.2)
Pleura, Inflammation	4 (1.3)	27** (1.4)	42** (1.6)	38** (2.2)
Alveolar Epithelium, Hyperplasia	1 (1.0)	36** (1.2)	49** (1.7)	48** (2.0)

	Chamber Control	3 mg/m^3	10 mg/m^3	30 mg/m^3
Bronchiole, Epithelium, Hyperplasia	1 (1.0)	34** (1.1)	48** (1.3)	45** (1.7)
Alveolar/bronchiolar Adenoma, Multiple	0	3	3	1
Alveolar/bronchiolar Adenoma (includes multiple)[j]				
Overall rate	1/50 (2%)	10/50 (20%)	19/50 (38%)	8/50 (16%)
Adjusted rate	2.3%	22.8%	44.9%	20.3%
Terminal rate	1/36 (3%)	7/31 (23%)	12/26 (46%)	1/15 (7%)
First incidence (days)	731 (T)	708	519	404
Poly-3 test	P = 0.137	P = 0.003	P < 0.001	P = 0.009
Alveolar/bronchiolar Carcinoma, Multiple	0	7**	6*	4*
Alveolar/bronchiolar Carcinoma (includes multiple)[k]				
Overall rate	2/50 (4%)	14/50 (28%)	11/50 (22%)	11/50 (22%)
Adjusted rate	4.4%	31.2%	26.8%	28.8%
Terminal rate	1/36 (3%)	9/31 (29%)	7/26 (27%)	5/15 (33%)
First incidence (days)	472	511	526	493
Poly-3 test	P = 0.065	P < 0.001	P = 0.003	P = 0.002
Alveolar/bronchiolar Adenoma or Carcinoma[l]				
Overall rate	3/50 (6%)	22/50 (44%)	27/50 (54%)	18/50 (36%)
Adjusted rate	6.6%	48.8%	62.6%	43.5%
Terminal rate	2/36 (6%)	15/31 (48%)	17/26 (65%)	5/15 (33%)
First incidence (days)	472	511	519	404
Poly-3 test	P = 0.019	P < 0.001	P < 0.001	P < 0.001

*Significantly different ($P \leq 0.05$) from the chamber control group by the Fisher exact test (interim evaluation) or the Poly-3 test (2-year study).
**$P \leq 0.01$.
(T) = terminal kill.
[a]Number of animals with lesion.
[b]Average severity grade of lesions in affected animals: 1 = minimal, 2 = mild, 3 = moderate, 4 = marked.
[c]Historical incidence for 2-year inhalation studies with chamber control groups (mean ± standard deviation): 35/250 (14.0% ± 3.7%), range 10%–20%; all routes: 83/550 (15.1% ± 5.9%), range 8%–26%.
[d]Number of animals with neoplasm per number of animals with lung examined microscopically.
[e]Poly-3 estimated neoplasm incidence after adjustment for intercurrent mortality.
[f]Observed incidence at terminal kill.
[g]Beneath the chamber control incidence is the P value associated with the trend test. Beneath the exposed group incidence are the P values corresponding to pairwise comparisons between the chamber controls and that exposed group. The Poly-3 test accounts for differential mortality in animals that do not reach terminal kill.
[h]Historical incidence for inhalation studies: 42/250 (16.8% ± 5.4%), range 8%–22%; all routes: 75/550 (13.6% ± 6.4%), range 4%–22%.
[i]Historical incidence for inhalation studies: 69/250 (27.6% ± 2.6%), range 26%–32%; all routes: 147/550 (26.7% ± 6.5%), range 16%–38%.
[j]Historical incidence for inhalation studies: 12/249 (4.8% ± 2.7%), range 2%–8%; all routes: 27/549 (4.9% ± 3.5%), range 0%–10%.
[k]Historical incidence for inhalation studies: 17/249 (6.8% ± 3.7%), range 2%–10%; all routes: 24/549 (4.4% ± 3.5%), range 0%–10%.
[l]Historical incidence for inhalation studies: 28/249 (11.3% ± 5.5%), range 6%–18%; all routes: 50/549 (9.1% ± 5.2%), range 2%–18%.

Malignant Lymphoma: At the 12-month interim evaluation, malignant lymphoma occurred in three 30 mg/m^3 females (Table 23 and Table D-1). In the 2-year study, incidences of malignant

lymphoma were significantly increased in exposed groups of females compared to those in the chamber control group and the incidences increased in an exposure concentration-related manner (Table 23, Table D-1, and Table D-2). In 10 and 30 mg/m^3 females, the incidences of malignant lymphoma exceeded the historical control ranges for inhalation studies and for all routes of administration; in 3 mg/m^3 females, incidences of this neoplasm were at the upper end of the historical control ranges for inhalation studies and for all routes of administration (Table 23 and Table D-4). Although the incidences of malignant lymphoma were not significantly increased in exposed groups of males compared to that in the chamber controls in the 2-year study (chamber control, 4/50; 3 mg/m^3, 4/50; 10 mg/m^3, 3/50; 30 mg/m^3, 6/50; Table C-1 and Table C-2), the incidence of malignant lymphoma in 30 mg/m^3 males was at the upper end of the historical control ranges for inhalation studies and for all routes of administration (Table C-4).

In most of the affected animals, lymphoma occurred in both the spleen and the lung, and in many animals the thymus, mediastinal lymph nodes, and/or bronchial lymph nodes were also involved. In the spleen, the lymphoma was usually manifested by marked expansion of the white pulp areas by a mixed population of small and large, irregularly shaped atypical lymphocytes, while in the lung the lymphomatous infiltrate was distributed in the same perivascular and peribronchial pattern that characterized the nonneoplastic lymphocytic infiltrates but with marked radial and longitudinal expansion, and sometimes with foci of pleural involvement (Figure 18). Most frequently, in the lung, thymus, and lymph nodes involved, the lymphomatous infiltrates were composed of a mixed small and large atypical lymphocyte population, similar to that noted in the spleen. In some mice, however, the lymphomatous cells were more uniform in size, appearing either moderate or large cytologically, and some of the large cell lymphomas exhibited prominent cytologic pleomorphism. Immunohistochemical stains for B and T cell markers (PAX5 and CD3, respectively) were performed in selected mice, and showed a predominance of B cells with a significant admixture of T cells in both the spleen and the lung.

Table 23. Incidences of Malignant Lymphoma in Female Mice in the Two-year Inhalation Study of Antimony Trioxide

	Chamber Control	3 mg/m^3	10 mg/m^3	30 mg/m^3
Twelve-month Interim Evaluation				
Number Necropsied	10	10	10	10
All Organs: Malignant Lymphoma[a]	0	0	0	3
Two-year Study				
All Organs: Malignant Lymphoma[b]				
Overall rate[c]	7/50 (14%)	17/50 (34%)	20/50 (40%)	27/50 (54%)
Adjusted rate[d]	15.6%	38.1%	47.5%	60.7%
Terminal rate[e]	5/36 (14%)	15/31 (48%)	12/26 (46%)	5/15 (33%)
First incidence (days)	677	558	512	404
Poly-3 test[f]	P < 0.001	P = 0.013	P < 0.001	P < 0.001

[a]Number of animals with neoplasm.
[b]Historical incidence for 2-year inhalation studies with chamber control groups (mean ± standard deviation): 63/250 (25.2% ± 8.4%), range 14%–36%; all routes: 109/550 (19.8% ± 7.9%), range 12%–36%.
[c]Number of animals with neoplasm per number of animals necropsied.
[d]Poly-3 estimated neoplasm incidence after adjustment for intercurrent mortality.
[e]Observed incidence at terminal kill.
[f]Beneath the chamber control incidence is the P value associated with the trend test. Beneath the exposed group incidence are the P values corresponding to pairwise comparisons between the chamber controls and that exposed group. The Poly-3 test accounts for differential mortality in animals that do not reach terminal kill.

Skin: Slight exposure concentration-related increases in the incidences of fibrous histiocytoma occurred in exposed groups of males in the 2-year study; the incidence of this neoplasm was significantly increased in 30 mg/m^3 males compared to that in the chamber control group and exceeded the historical control ranges for inhalation studies and for all routes of administration (Table 24, Table C-1, Table C-2, and Table C-5). In addition, two incidences of fibrosarcoma occurred in 10 mg/m^3 males, which exceeded the historical control ranges for inhalation studies and for all routes of administration (Table 24, Table C-1, and Table C-5). The combined incidences of fibrous histiocytoma or fibrosarcoma were also significantly increased in 30 mg/m^3 males compared to that in the chamber control group and exceeded the historical control ranges for inhalation studies and for all routes of administration (Table 24, Table C-1, Table C-2, and Table C-5). The fibrous histiocytomas were circumscribed dermal tumors composed of histiocyte-like cells and spindle cells, sometimes accompanied by multinucleated giant cells or hemosiderin containing macrophages, and occasionally exhibiting storiform patterns. Although showing some similarity to the fibrous histiocytomas, the fibrosarcomas differed in several respects, including the predominance of spindle cells, hypercellularity, pleomorphism, frequent mitotic figures, foci of necrosis, and often epidermal ulceration or invasion of fat or skeletal muscle. Two incidences of squamous cell carcinoma of the skin occurred in 30 mg/m^3 females, which exceeded the historical control ranges for inhalation studies and for all routes of administration (Table 24, Table D-1, and Table D-5).

Table 24. Incidences of Neoplasms of the Skin in Mice in the Two-year Inhalation Study of Antimony Trioxide

	Chamber Control	3 mg/m^3	10 mg/m^3	30 mg/m^3
Male				
Two-year Study				
Number of Animals Necropsied	50	50	50	50
Fibrous Histiocytoma[a]				
Overall rate[b]	0/50 (0%)	1/50 (2%)	1/50 (2%)	4/50 (8%)
Adjusted rate[c]	0.0%	2.5%	2.5%	10.6%
Terminal rate[d]	0/38 (0%)	1/30 (3%)	1/27 (4%)	2/17 (12%)
First incidence (days)	–[f]	729 (T)	729 (T)	612
Poly-3 test[e]	P = 0.012	P = 0.473	P = 0.474	P = 0.039
Fibrosarcoma[a]	0	0	2	0
Fibrous Histiocytoma or Fibrosarcoma (Combined)[g]				
Overall rate	0/50 (0%)	1/50 (2%)	3/50 (6%)	4/50 (8%)
Adjusted rate	0.0%	2.5%	7.3%	10.6%
Terminal rate	0/38 (0%)	1/30 (3%)	2/27 (7%)	2/17 (12%)
First incidence (days)	–	729 (T)	468	612
Poly-3 test	P = 0.023	P = 0.473	P = 0.100	P = 0.039
Female				
Two-year Study				
Number of Animals Necropsied	50	50	50	50
Squamous Cell Carcinoma[h]	0	0	0	2

(T) = terminal kill.
[a]Historical incidence for 2-year inhalation studies with chamber control groups (mean ± standard deviation): 1/250 (0.4% ± 0.9%), range 0%–2%; all routes: 2/550 (0.4% ± 0.8%), range 0%–2%.
[b]Number of animals with neoplasm per number of animals necropsied.
[c]Poly-3 estimated neoplasm incidence after adjustment for intercurrent mortality.
[d]Observed incidence at terminal kill.
[e]Beneath the chamber control incidence is the P value associated with the trend test. Beneath the exposed group incidence are the P values corresponding to pairwise comparisons between the chamber controls and that exposed group. The Poly-3 test accounts for differential mortality in animals that do not reach terminal kill.
[f]Not applicable; no neoplasms in animal group.
[g]Historical incidence for inhalation studies: 2/250 (0.8% ± 1.1%), range 0%–2%; all routes: 5/550 (0.9% ± 1.0%), range 0%–2% (includes one incidence of sarcoma).
[h]Historical incidence for inhalation studies: 0/250; all routes: 0/550.

Nose: Incidences of foreign body, presumably the test article, were significantly increased in all exposed groups of males and females at the 12-month interim evaluation and in the 2-year study compared to those in the chamber control groups (Table 25, Table C-7, and Table D-8). The foreign particles were most often seen in the nasal-associated lymphoid tissue of Level III, and less often in the subepithelial tissue of Levels I and II in association with small numbers of lymphocytes.

In the 2-year study, chronic active inflammation occurred in the respiratory epithelium of a few mice in every exposure group; the incidences of this lesion were significantly increased in 3 and 10 mg/m^3 males compared to those in the chamber control group (Table 25, Table C-7, and Table D-8). Low incidences of acute inflammation of the respiratory epithelium occurred in all exposure groups of females in the 2-year study. A few incidences of minimal to mild squamous metaplasia of the respiratory epithelium occurred in all exposed groups of females in the 2-year study, and the incidence of this lesion was significantly increased in the 30 mg/m^3 group.

Larynx: Incidences of foreign body, presumably the test article, occurred in many mice in all exposed groups at the 12-month interim evaluation and in the 2-year study (Table 25, Table C-7, and Table D-8). The incidences of foreign body were significantly increased in 10 and 30 mg/m^3 males and females at the 12-month interim evaluation and in all exposed groups of males and females in the 2-year study compared to those in the chamber control groups. The foreign body was most often recognized in the subepithelial tissue of Level I.

Incidences of minimal respiratory epithelium hyperplasia and/or squamous metaplasia occurred in the base of the epiglottis overlying the submucosal glands in some of the 10 and 30 mg/m^3 mice at the 12-month interim evaluation and in the 2-year study (Table 25, Table C-7, and Table D-8). The incidences of respiratory epithelium hyperplasia were significantly increased in 10 and 30 mg/m^3 males and in 10 mg/m^3 females at the 12-month interim evaluation and in 10 and 30 mg/m^3 males and females in the 2-year study compared to those in the chamber control groups. The incidences of respiratory epithelium squamous metaplasia were significantly increased in 30 mg/m^3 females at the 12-month interim evaluation and in 10 and 30 mg/m^3 males and 30 mg/m^3 females in the 2-year study (Figure 19). Both epithelial lesions presented repetitively in this location as minor degrees of increased cellularity, with the distinction between the two usually based upon flattening at the surface in squamous metaplasia. Incidences of minimal to mild hyperplasia of the squamous epithelium overlying the arytenoid cartilages in Level I were significantly increased in 30 mg/m^3 males and females compared to those in the chamber controls (Table 25, Table C-7, and Table D-8).

Trachea: Incidences of foreign body occurred at the 12-month interim evaluation in a few 10 and 30 mg/m^3 males and females and in the 2-year study in all exposed groups of males and females (Table 25, Table C-7, and Table D-8). The incidences of foreign body were significantly increased in 30 mg/m^3 males and females at the 12-month interim evaluation and in 30 mg/m^3 males and all exposed groups of females in the 2-year study compared to those in the chamber control groups.

Epithelium hyperplasia occurred in several 10 and 30 mg/m^3 males in the 2-year study; the incidence of this lesion was significantly increased in the 30 mg/m^3 group (Table 25 and Table C-7).

Table 25. Incidences of Nonneoplastic Lesions of the Upper Respiratory Tract in Mice in the Two-year Inhalation Study of Antimony Trioxide

	Chamber Control	3 mg/m^3	10 mg/m^3	30 mg/m^3
Male				
Twelve-month Interim Evaluation				
Nose[a]	10	10	10	10
Foreign Body[b]	0	8**	10**	9**
Larynx	10	10	10	10
Foreign Body	0	3	5**	10**
Respiratory Epithelium, Hyperplasia	0	1 (1.0)[c]	4* (1.0)	6** (1.2)
Respiratory Epithelium, Metaplasia, Squamous	0	0	2 (1.0)	3 (1.0)
Trachea	10	10	10	10
Foreign Body	0	0	2	4*
Two-year Study				
Nose	50	49	49	50
Foreign Body	0	48**	48**	49**
Respiratory Epithelium, Inflammation, Chronic Active	3 (2.3)	9* (1.2)	9* (1.1)	6 (1.5)
Larynx	50	50	50	50
Foreign Body	0	15**	29**	44**
Respiratory Epithelium, Hyperplasia	1 (1.0)	3 (1.3)	15** (1.1)	30** (1.2)
Respiratory Epithelium, Metaplasia, Squamous	0	0	8** (1.0)	18** (1.1)
Squamous Epithelium, Hyperplasia	2 (1.0)	0	4 (1.3)	13** (1.2)
Trachea	49	50	50	50
Foreign Body	0	3	1	20**
Epithelium, Hyperplasia	0	0	2 (1.5)	5* (1.2)
Female				
Twelve-month Interim Evaluation				
Nose	10	10	10	10
Foreign Body	0	6**	9**	10**
Larynx	10	9	10	10
Foreign Body	0	2	7**	7**
Respiratory Epithelium, Hyperplasia	0	1 (1.0)	4* (1.0)	0
Respiratory Epithelium, Metaplasia, Squamous	1 (2.0)	0	1 (1.0)	8** (1.5)
Trachea	10	10	10	10

	Chamber Control	3 mg/m^3	10 mg/m^3	30 mg/m^3
Foreign Body	0	0	2	4*
Two-year Study				
Nose	50	49	50	50
Foreign Body	1	44**	45**	48**
Respiratory Epithelium, Inflammation, Chronic Active	2 (1.5)	3 (1.3)	4 (1.0)	5 (1.0)
Respiratory Epithelium, Inflammation, Acute	2 (1.5)	7 (1.1)	7 (1.0)	5 (1.0)
Respiratory Epithelium, Metaplasia, Squamous	0	3 (1.3)	2 (1.0)	4* (1.3)
Larynx	50	50	50	50
Foreign Body	0	25**	39**	48**
Respiratory Epithelium, Hyperplasia	2 (1.0)	0	14** (1.1)	18** (1.1)
Respiratory Epithelium, Metaplasia, Squamous	1 (1.0)	0	5 (1.2)	24** (1.1)
Squamous Epithelium, Hyperplasia	4 (1.3)	1 (1.0)	1 (1.0)	12* (1.1)
Trachea	50	50	50	50
Foreign Body	0	7**	14**	20**

*Significantly different ($P \leq 0.05$) from the chamber control group by the Fisher exact text (interim evaluation) or the Poly-3 test (2-year study).
**$P \leq 0.01$.
[a]Number of animals with tissue examined microscopically.
[b]Number of animals with lesion.
[c]Average severity grade of lesions in affected animals: 1 = minimal, 2 = mild, 3 = moderate, 4 = marked.

Hematopoietic System [Lymph Nodes (Bronchial, Mediastinal, and Mandibular), Spleen, Bone Marrow, and Thymus]: Incidences of lymphoid hyperplasia of the bronchial lymph nodes were significantly increased in all exposed groups of male and female mice compared to those in the chamber controls at the 12-month interim evaluation and in the 2-year study (Table 26, Table C-7, and Table D-8). Incidences of lymphoid hyperplasia of the mediastinal lymph nodes were significantly increased in 30 mg/m^3 males at the 12-month interim evaluation and in 10 and 30 mg/m^3 males and females in the 2-year study. In females, the incidences of lymphoid hyperplasia of the spleen were significantly increased in all exposed groups at the 12-month interim evaluation but the incidence of this lesion was decreased in all exposed groups of females in the 2-year study and was significantly decreased in 3 mg/m^3 females (chamber control, 16/50; 3 mg/m^3, 6/50; 10 mg/m^3, 8/50; 30 mg/m^3, 7/50) in the 2-year study (Table 26 and Table D-8). The decreased incidence of hyperplasia at 2 years correlates with the increased incidence of malignant lymphoma, suggesting either neoplastic transformation of the hyperplastic cells, or overgrowth and replacement by the malignant cells. Lymphoid hyperplasia in the lymph nodes was characterized primarily by expansion of the paracortical areas, with occasional formation of lymphoid follicles with germinal centers.

Incidences of foreign body, presumably the test article, occurred in the bronchial, mediastinal, and mandibular lymph nodes of exposed groups of males and females (Table 26, Table C-7, and

Table D-8). The incidences of foreign body in the bronchial lymph node were significantly increased in all exposed groups of males and females compared to those in the chamber controls at the 12-month interim evaluation and in the 2-year study. The incidences of foreign body in the mediastinal lymph node were significantly increased in 10 and 30 mg/m^3 males and 30 mg/m^3 females at the 12-month interim evaluation and all exposed groups of males and females in the 2-year study. The incidences of foreign body in the mandibular lymph node were significantly increased in all exposed groups of males and in 3 and 10 mg/m^3 females in the 2-year study. Infiltrates of histiocytes occurred within the bronchial and mediastinal lymph nodes of most exposed groups of males and females at the 12-month interim evaluation and in the 2-year study. In the bronchial lymph node, the incidences of histiocytic cellular infiltration were significantly increased in 10 mg/m^3 females at the 12-month interim evaluation and in 30 mg/m^3 males and 10 and 30 mg/m^3 females in the 2-year study. In the mediastinal lymph nodes, the incidences of histiocytic cellular infiltration were significantly increased in 10 and 30 mg/m^3 males and in all exposed groups of females in the 2-year study.

In the 2-year study, the incidence of hematopoietic cell proliferation in the spleen was significantly increased in 30 mg/m^3 females compared to that in the chamber controls (Table 26 and Table D-8).

Incidences of bone marrow hyperplasia did not occur in mice at the 12-month interim evaluation, but in the 2-year study, the incidences of this lesion were significantly increased in all exposed groups of males and in 10 and 30 mg/m^3 females (Table 26, Table C-7, and Table D-8). Bone marrow hyperplasia was predominantly of myeloid cell type and may have been secondary to inflammation in the lung.

In the 2-year study, the incidences of cellular depletion of the thymus were significantly increased in 10 and 30 mg/m^3 males and in all exposed groups of females (Table 26, Table C-7, and Table D-8).

Table 26. Incidences of Nonneoplastic Lesions of the Hematopoietic System in Mice in the Two-year Inhalation Study of Antimony Trioxide

	Chamber Control	3 mg/m^3	10 mg/m^3	30 mg/m^3
Male				
Twelve-month Interim Evaluation				
Lymph Node, Bronchial[a]	8	10	10	10
Hyperplasia, Lymphoid[b]	0	7** (1.0)[c]	9** (1.8)	10** (2.7)
Foreign Body	0	10**	10**	10**
Lymph Node, Mediastinal	4	8	10	10
Hyperplasia, Lymphoid	0	1 (1.0)	4 (1.5)	9** (2.0)
Foreign Body	0	1	8*	10**
Two-year Study				
Lymph Node, Bronchial	30	43	47	41
Hyperplasia, Lymphoid	2 (2.0)	21** (1.5)	26** (1.8)	13** (1.8)
Foreign Body	0	34**	47**	38**
Infiltration Cellular, Histiocyte	0	2 (1.5)	4 (1.0)	6* (1.2)
Lymph Node, Mediastinal	37	45	48	49
Hyperplasia, Lymphoid	2 (1.5)	8 (1.6)	17** (1.6)	34** (1.9)
Foreign Body	0	32**	42**	48**
Infiltration Cellular, Histiocyte	0	4 (1.0)	13** (1.1)	34** (1.7)
Lymph Node, Mandibular	27	26	28	26
Foreign Body	0	7**	8**	16**
Bone Marrow	49	50	48	50
Hyperplasia	10 (1.0)	19* (1.0)	27** (1.0)	33** (1.1)
Thymus	41	38	43	39
Depletion Cellular	15 (2.5)	14 (2.6)	32** (2.9)	32** (3.5)
Female				
Twelve-month Interim Evaluation				
Lymph Node, Bronchial	5	10	9	10
Hyperplasia, Lymphoid	0	6* (1.7)	9** (1.9)	10** (2.1)
Foreign Body	0	10**	9**	10**
Infiltration Cellular, Histiocyte	0	1 (1.0)	6* (1.0)	4 (1.0)
Lymph Node, Mediastinal	4	7	8	10
Hyperplasia, Lymphoid	0	1 (2.0)	4 (1.5)	4 (2.0)
Foreign Body	0	2	2	9**

	Chamber Control	3 mg/m^3	10 mg/m^3	30 mg/m^3
Spleen	10	10	10	10
Hyperplasia, Lymphoid	0	4* (1.8)	6** (1.3)	5** (1.4)
Two-year Study				
Lymph Node, Bronchial	41	47	48	49
Hyperplasia, Lymphoid	2 (1.0)	15** (1.5)	17** (1.7)	11** (1.7)
Foreign Body	0	34**	46**	43**
Infiltration Cellular, Histiocyte	0	2 (1.0)	7** (1.0)	7** (1.1)
Lymph Node, Mediastinal	46	48	49	50
Hyperplasia, Lymphoid	0	3 (2.7)	16** (1.8)	18** (1.9)
Foreign Body	0	28**	45**	44**
Infiltration Cellular, Histiocyte	0	6* (1.3)	11** (1.5)	16** (1.1)
Lymph Node, Mandibular	41	28	38	39
Foreign Body	0	5**	9**	3
Spleen	50	50	50	50
Hematopoietic Cell Proliferation	17 (2.0)	19 (2.0)	20 (1.8)	35** (2.2)
Hyperplasia, Lymphoid	16 (1.6)	6 (1.3)	8 (1.4)	7 (1.6)
Bone Marrow	50	50	50	50
Hyperplasia	3 (1.0)	5 (1.0)	15** (1.0)	28** (1.2)
Thymus	47	49	49	49
Depletion Cellular	9 (1.9)	18* (2.9)	23** (2.8)	29** (2.3)

*Significantly different ($P \leq 0.05$) from the chamber control group by the Fisher exact text (interim evaluation) or the Poly-3 test (2-year study).
**$P \leq 0.01$.
[a]Number of animals with tissue examined microscopically.
[b]Number of animals with lesion.
[c]Average severity grade of lesions in affected animals: 1 = minimal, 2 = mild, 3 = moderate, 4 = marked.

Heart: Incidences of minimal to mild chronic active inflammation of the epicardium occurred in a few mice in all exposed groups in the 2-year study, and may have been secondary to inflammation in the pleura (Table 27, Table C-7, and Table D-8). The incidences of chronic active inflammation of the epicardium were significantly increased in 10 and 30 mg/m^3 males and females compared to those in the chamber control groups.

Forestomach: Exposure concentration-related increases in the incidences of chronic active inflammation occurred in exposed groups of males in the 2-year study; the incidence of this lesion in 30 mg/m^3 males was significantly increased compared to that in the chamber control group (Table 27 and Table C-7). Incidences of chronic active inflammation occurred in a single 3 mg/m^3 female and in three 30 mg/m^3 females in the 2-year study (Table 27 and Table D-8).

Table 27. Incidences of Selected Nonneoplastic Lesions in Mice in the Two-year Inhalation Study of Antimony Trioxide

	Chamber Control	3 mg/m^3	10 mg/m^3	30 mg/m^3
Male				
Two-year Study				
Heart[a]	50	50	50	50
Epicardium, Inflammation, Chronic Active[b]	0	2 (1.0)[c]	7** (1.4)	16** (1.3)
Stomach, Forestomach	50	50	49	50
Inflammation, Chronic Active	2 (1.0)	4 (1.0)	4 (1.3)	7* (1.3)
Female				
Two-year Study				
Heart	50	50	50	50
Epicardium, Inflammation, Chronic Active	0	2 (1.0)	7** (1.4)	7** (1.6)
Stomach, Forestomach	50	50	50	50
Inflammation, Chronic Active	0	1 (1.0)	0	3 (1.0)

*Significantly different ($P \leq 0.05$) from the chamber control group by the Poly-3 test.
**$P \leq 0.01$.
[a]Number of animals with tissue examined microscopically.
[b]Number of animals with lesion.
[c]Average severity grade of lesions in affected animals: 1 = minimal, 2 = mild, 3 = moderate, 4 = marked.

Adrenal Medulla: At the 12-month interim evaluation, an incidence of malignant pheochromocytoma was observed in one 30 mg/m^3 female (chamber control, 0/10; 3 mg/m^3, 0/10; 10 mg/m^3, 0/10; 30 mg/m^3, 1/10; Table D-1). In the 2-year study, benign pheochromocytomas occurred in one 10 mg/m^3 male, two 3 mg/m^3 females, and three 30 mg/m^3 females (males: 0/49, 0/50, 1/46, 0/49; females: 0/50, 2/50, 0/48, 3/49; Table C-1, Table D-1, and Table D-2); the incidence of this neoplasm in 30 mg/m^3 females exceeded the historical control ranges for inhalation studies and for all routes of administration (Table D-6).

Liver: In the 2-year study, the incidence of hepatocellular adenoma was significantly increased in 10 mg/m^3 males compared to that in the chamber control group (30/50; 31/50; 36/49; 33/50; Table C-1 and Table C-2), and it was at the upper end of the historical control range for inhalation studies (Table C-6). In addition, the incidence of hepatocellular carcinoma was significantly increased in 3 mg/m^3 males in the 2-year study (15/50, 23/50, 14/49, 20/50; Table C-1 and Table C-2). The incidence of hepatocellular adenoma or carcinoma (combined) was significantly increased in 10 mg/m^3 females in the 2-year study (14/50, 22/50, 22/50, 19/50; Table D-1 and Table D-2) but within the historical control ranges for inhalation studies and for all routes of study (Table D-7). Because there was no dose response and the increases were not outside of the historical control ranges, these increases were considered not related to treatment.

Eye: Slight increases in the incidences of cataract occurred in exposed groups of females in the 2-year study (1/49, 4/47, 2/49, 4/49; Table D-8).

Genetic Toxicology

In male and female Wistar Han rats, the reticulocyte population (polychromatic erythrocytes or PCEs), which is the only red blood cell population that can be accurately assessed for micronucleus frequency in peripheral blood of rats due to efficient splenic scavenging of damaged erythrocytes, did not show an increase in micronucleated cells following 12 months of inhalation exposure to antimony trioxide (0, 3, 10, or 30 mg/m^3) (Table E-1). In addition, no significant alterations in the percent reticulocytes in peripheral blood were observed in either male or female rats, suggesting no bone marrow toxicity or effect on erythropoiesis associated with exposure to antimony trioxide.

Micronucleus frequencies in mature erythrocytes (normochromatic erythrocytes or NCEs) of male and female B6C3F1/N mice exposed to antimony trioxide (0, 3, 10, or 30 mg/m^3) for 12 months via inhalation were significantly increased, based on significant trend tests and significantly elevated frequencies of micronucleated erythrocytes at the highest exposure concentration (Table E-2). Using flow cytometry, approximately 1 million erythrocytes were scored per animal for the presence of micronuclei, making this a highly sensitive method of scoring and allowing small increases in the endpoint to be detected. In mice, the micronucleus response in the reticulocyte population, indicative of damage induced in the bone marrow within the last 48 hours prior to sampling, was slightly increased with increasing exposure concentration, but the increase was not statistically significant. However, the trend toward increased frequencies of micronucleated reticulocytes in the mice is supportive of the observations in the mature erythrocyte population. In addition, significant increases in the percent reticulocytes were seen in both male and female mice, suggesting a stimulation of erythropoiesis in mice exposed to antimony trioxide. It should be noted that stimulation of erythropoiesis may, in some instances, result in elevated levels of micronucleated red blood cells due to an increase in mitotic errors associated with rapid cell division, although in in vivo micronucleus studies conducted by the National Toxicology Program, no consistent association between increases in percent reticulocytes and increases in micronuclei has been observed.

In addition to evaluating the potential for chromosomal damage, manifested as micronuclei resulting from exposure to antimony trioxide, the potential for DNA damage was assessed using the comet assay in the same animals in which micronucleus induction was evaluated. DNA damage was assessed in blood leukocytes and lung tissue samples. No increases in DNA damage were seen in blood leukocytes or lung cell samples in male or female Wistar Han rats exposed to antimony trioxide (Table E-3). In male and female B6C3F1/N mice, significant increases in DNA damage, measured as percent tail DNA, were seen in lung tissue samples; no increases in percent tail DNA were observed in leukocytes (Table E-4).

In summary, exposure to antimony trioxide for 12 months by inhalation resulted in increases in micronucleated erythrocytes and lung cell DNA damage in male and female mice, but not in male or female rats.

Tissue Burden

Tissue burden results are presented in Appendix G. In the 2-week studies, lung weights (g) and lung and blood antimony concentrations (μg Sb/g) were determined in male and female rats and mice following the end of exposures and in additional female rats and mice held for 4 weeks

after exposure ended. Lung burdens of antimony (µg Sb/lung) and antimony trioxide (µg Sb_2O_3/lung) and exposure concentration-normalized lung burdens (µg Sb_2O_3/lung per mg Sb_2O_3/m^3) and blood concentrations (µg Sb/g per mg Sb_2O_3/m^3) were calculated. In the 2-year studies, similar data were collected in female rats and mice following 61, 124, 269 (mice), 271 (rats), 369, or 551 days of exposure. In the 2-week and 2-year studies, lung weights generally increased with exposure concentration and duration (Table G-1, Table G-3, Table G-6, and Table G-8). Because of the increased lung weights in exposed rats and mice, lung burdens rather than concentrations were used for calculation of toxicokinetic parameters.

Two-week Tissue Burden Results in Rats and Mice

Total antimony trioxide lung burdens increased with increasing exposure concentration in male and female rats and mice (Table G-1 and Table G-6). In females held for 4 weeks postexposure, lung burdens decreased to approximately 77% to 85% (rats) or 66% to 73% (mice) of those found at terminal kill, with no relationship to exposure concentration in either species. Male and female rat lung antimony trioxide normalized lung burdens were generally similar among exposure groups, particularly at the lower concentrations ($\leq$15 mg/m^3) indicating proportionality with exposure concentration. Although normalized burdens appeared to be slightly less than proportional at 30 and 60 mg/m^3, the observed differences were small and became less apparent in females following the 4-week recovery period.

Blood antimony concentrations increased with exposure concentration in male and female rats and mice (Table G-1 and Table G-6). At 4 weeks postexposure in females, blood antimony concentrations increased to approximately 190%, 181%, 169%, 165%, and 162% (rats) or decreased to approximately 41%, 49%, 49%, 55%, and 49% (mice) of the concentrations at terminal kill for the 3.75, 7.5, 15, 30, and 60 mg/m^3 groups, respectively. In both rats and mice, normalized blood concentrations decreased with exposure concentration, particularly at higher exposure concentrations ($\geq$15 mg/m^3), indicating that increases in blood concentration were less than proportional with exposure concentration. This pattern persisted to the postexposure time point in females.

Kinetic parameters were determined in females using lung burden data generated at the end of exposure and 4 weeks postexposure. Because there were only two time points for kinetic estimates, variability was high and no statistical comparisons were made. Clearance half-lives ranged from 73 to 122 days in rats or 47 to 62 days in mice (Table G-2 and Table G-7). There was no clear exposure concentration-related trend in rats or mice, except that the shortest half-life was in the lowest exposure concentration group in mice. Deposition rates (µg Sb_2O_3/day) were approximately proportional to slightly less than proportional to exposure concentration, with a 16-fold increase in exposure concentration resulting in 15-fold (rats) or 13-fold (mice) increases in deposition rate. Steady-state lung burdens were proportional to exposure concentration in mice (16-fold increase in exposure concentration resulted in a 15-fold increase in steady-state lung burden) but less than proportional over the range of exposure concentrations in rats (16-fold increase in exposure concentration resulted in an 11-fold increase in steady-state lung burden). Based on estimated steady-state lung burdens, steady state was not reached during the postexposure period in rats or mice. Steady-state lung burdens are expected to be reached after about five clearance half-lives; the expected half-lives ranged from approximately 365 to 610 days in rats or approximately 235 to 310 days in mice without clear exposure concentration-related trends in either species.

In female rats, kinetic analysis (data not shown) of blood antimony concentration data (Table G-1) indicated negative clearance half-lives due to the continuing increase in antimony concentrations in the recovery rats. This was not unexpected because antimony trioxide lung burdens after 4 weeks of recovery were still approximately 77% to 85% of the lung burdens at terminal kill. Kinetic analysis of blood antimony concentration data from female mice indicated elimination half-lives from 22 to 32 days (Table G-7); the pattern of increases with exposure concentration was generally similar to that observed in the lung. Blood and lung mean antimony concentrations were compared at 30 mg/m^3; these comparisons were made for data at the end of the 2-week studies in males and females and at 4 weeks postexposure in females. In these comparisons, blood concentrations were 0.8% of lung concentrations in male and female rats at the end of exposure, and 2% of lung concentrations in female rats at 4 weeks postexposure (Table G-1). In male mice, the blood concentration was 0.004% of the lung concentration at the end of the study; in female mice, blood concentrations were 0.005% of lung concentrations at both time points (Table G-6).

Two-year Tissue Burden Results in Rats and Mice

Antimony trioxide lung burdens increased with exposure concentration and duration in rats and mice (Table G-3 and Table G-8). Lung burdens in 30 mg/m^3 rats and all exposed groups of mice failed to achieve or approach steady state and instead increased steadily over time, achieving mean values as high as approximately 35 mg Sb_2O_3/lung in rats and 6 mg Sb_2O_3/lung in mice, following 551 days of exposure to 30 mg/m^3. Normalized lung burdens were similar at each time point, indicating that lung burdens increased in a manner that was approximately proportional to exposure concentration and duration of exposure. However, a trend towards increased normalized lung burdens with exposure concentration was apparent at 551 days in rats. In mice, normalized burdens at 10 and 30 mg/m^3 were generally greater than those at 3 mg/m^3 and exposure durations greater than 124 days.

Figures presenting individual animal antimony trioxide lung burdens plotted versus days on study along with the fit of the lung burden model to the data are presented in Figure G-1, Figure G-2, Figure G-3, and Figure G-4. Rat deposition and clearance parameters calculated from antimony trioxide lung burden data for each exposure are presented in Table G-4. In mice, when all exposure durations were included, the model did not fit the data well for any exposure concentration as the day 551 lung burdens were considerably higher than the curves generated with the model fit; similarly poor model fits were obtained when the day 551 data were excluded. As a result, meaningful deposition and clearance parameters could not be calculated for any of the exposure concentrations in mice. In rats, the model-predicted deposition rates (D) of approximately 17, 44, and 119 µg Sb_2O_3/total lung per day were consistent with the measured lung burden data, indicating good proportionality with the exposure concentrations of 3, 10, and 30 mg/m^3. Based on these deposition rates and a literature value for the minute volume of adult male Sprague Dawley rats (0.33 L/min; Whalan et al.[73]), the calculated percent deposition efficiencies were approximately 3.3%, 3.7%, and 4.7% for the 3, 10, and 30 mg/m^3 groups, respectively. Model-estimated clearance half-lives ($t_{1/2}$) increased with exposure concentration with durations of 136, 203, and 262 days at 3, 10, and 30 mg/m^3, respectively.

In rats, the plots of lung burden over time superimposed with the model fits demonstrate that lung burdens in the 30 mg/m^3 group did not achieve steady state but increased steadily over time, showing little curvature over the course of the study, while the lung burdens in the 3 and

10 mg/m^3 exposure groups nearly reached steady state (Figure G-1). This pattern is also apparent when comparing the model-predicted steady-state lung burden data (Table G-4) to the day 551 measured lung burden data (Table G-3). Steady-state lung burdens (L_{ss}) were approximately proportional to increases in exposure concentration. Although steady-state lung burdens were not reached during this study, it should be recognized that these calculated steady-state lung burdens are only theoretical values that would certainly never be achieved in reality. It would take approximately five half-lives to reach these L_{ss} values, about 680, 1,015, and 1,310 days at 3, 10, and 30 mg/m^3, respectively, or longer than the normal life span of a Wistar Han rat for the two highest concentrations.

In rats and mice, blood antimony concentrations increased with exposure concentration (Table G-3 and Table G-8). While blood concentrations also increased with exposure duration in rats, they did not consistently increase over time in mice. These data indicate that in mice, blood antimony concentrations were at or near steady state throughout most of the study. Normalized concentrations decreased with exposure concentration at all time points, indicating that proportionately less antimony was present in the blood as exposure concentrations increased. In rats, this trend became more apparent over time, particularly between the 10 and 30 mg/m^3 groups. The normalized data suggest that as exposure concentrations (and lung burdens) increased, the rate or capacity of antimony trioxide dissolution and transport to the blood became progressively less, or that the rate of clearance from the blood increased. No attempts were made to model the blood concentration data to discern blood antimony deposition and clearance rates. However, this result, at least in rats, is consistent with the fact that clearance rates of antimony trioxide from the lungs also became progressively slower. In the 2-year studies, blood-to-lung mean antimony concentration comparisons were made using the day 551 data for 30 mg/m^3 females. In these comparisons, the rat blood concentration was 7% of the lung concentration and the mouse blood concentration was 0.002% of the lung concentration.

Based primarily on the relatively long clearance half-lives in the 10 and 30 mg/m^3 rats in the 2-year study as compared to the 3 mg/m^3 group in the present rat study and in the 2-week rat study and the unexpectedly high lung burdens in mice following 551 days of exposure, it was hypothesized that the reduced pulmonary clearance was associated with lung overload. Accordingly, calculations were performed to determine if lung overload occurred in either species, on the basis of particle volume or surface area[74-76]. The required assumptions and calculations are described in detail in Appendix G. Briefly, with volumetric overload, pulmonary clearance is thought to slow as the volume of particles in the lung reaches 6% of the alveolar macrophage (AM) volume (1X; 1.8×10^9 µm^3 in rats or 2.4×10^8 µm^3 in mice), with clearance ceasing when the particle volume reaches 60% of the AM volume (10X). Surface area-based overload is independent of the AM volume, and is thought to occur when the surface area of particles reaches 300 cm^2 in rats scaled to 40 cm^2 for mice (1X). These calculations demonstrated a graded onset of overload with similar results regardless of whether particle volume or surface area was used (Table G-5 and Table G-9). Overload was not reached at 3 mg/m^3 in either species, with lung burdens generally at 0.3X to 0.4X. At 10 mg/m^3, volumetric-based overload occurred in both species. In rats, overload was calculated to occur by day 418 of exposure, with a particle volume of 1.1X at 551 days; corresponding values in mice were day 369 and 1.8X at 551 days, respectively. In rats, the particle surface area required for overload was nearly reached (approximately 97% of the required surface area; data not shown). In mice, the surface-area results were similar to the volume-based overload results. At 30 mg/m^3,

volume-based overload was more apparent, occurring in rats by day 94 of exposure with a particle volume of 3.5X at 551 days; corresponding values in mice were day 124 and 4.7X at 551 days. Surface-area based overload results were similar to the volume-based results for rats and mice.

Molecular Pathology

In rats chronically exposed to antimony trioxide, point mutations in *Kras* [4% (1/26)] and *Egfr* [50% (13/26)] were noted in the alveolar/bronchiolar tumors, and none were found in spontaneously arising alveolar/bronchiolar adenomas in chamber control rats. The single *Kras* mutation that occurred (A to G transition) was present in exon 1, codon 16, a non-hot spot location for *Kras* mutations. The *Egfr* mutations were localized within exons 18 to 21 and all of them were transition mutations. The results for the molecular analyses are presented in Appendix K.

In mice chronically exposed to antimony trioxide, point mutations in *Kras* [43% (34/80)], and *Egfr* [46% (37/80)] were noted in the alveolar/bronchiolar tumors. *Kras* mutations [33% (3/9)] were also noted in the spontaneous alveolar/bronchiolar carcinomas in the chamber controls. However, the majority of the *Kras* mutations in alveolar/bronchiolar tumors in exposed and chamber control mice were located in codon 12 and were G to A transitions. *Egfr* mutations were found only in alveolar/bronchiolar tumors in exposed mice, were located primarily within exons 18 and 20, and were transition mutations. The results for the molecular analyses are presented in Appendix K.

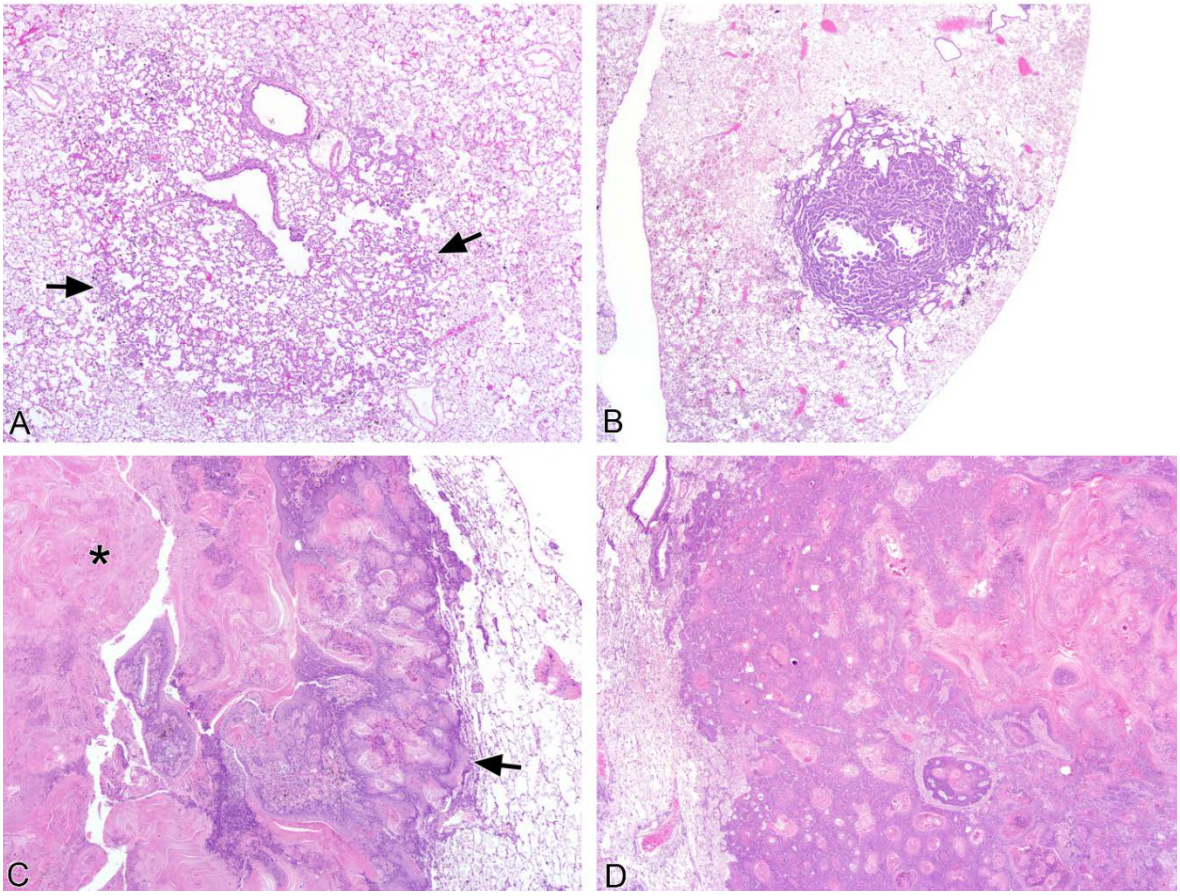

Figure 6. Epithelial Hyperplasia and Neoplasia in the Rat Lung (H&E)

A) A relatively circumscribed zone of alveolar epithelial hyperplasia (arrows) was noted in a female Wistar Han rat exposed to 10 mg antimony trioxide/m^3 by inhalation for 2 years. B) This alveolar/bronchiolar adenoma in a female Wistar Han rat exposed to 30 mg antimony trioxide/m^3 by inhalation for 2 years was compact, cellular, and displayed papillary projections into the alveolar lumens. C) Cystic keratinizing epithelioma found in the lung of a female Wistar Han rat exposed to 30 mg antimony trioxide/m^3 by inhalation for 2 years, characterized by a central, keratin-filled cavity (asterisk) with a thick, irregular outer wall of proliferating squamous epithelium (arrow). D) This squamous cell carcinoma in the lung of a female Wistar Han rat exposed to 30 mg antimony trioxide/m^3 by inhalation for 2 years formed a predominately solid mass, composed of coalescing nests of pleomorphic squamous cells infiltrating the pulmonary parenchyma.

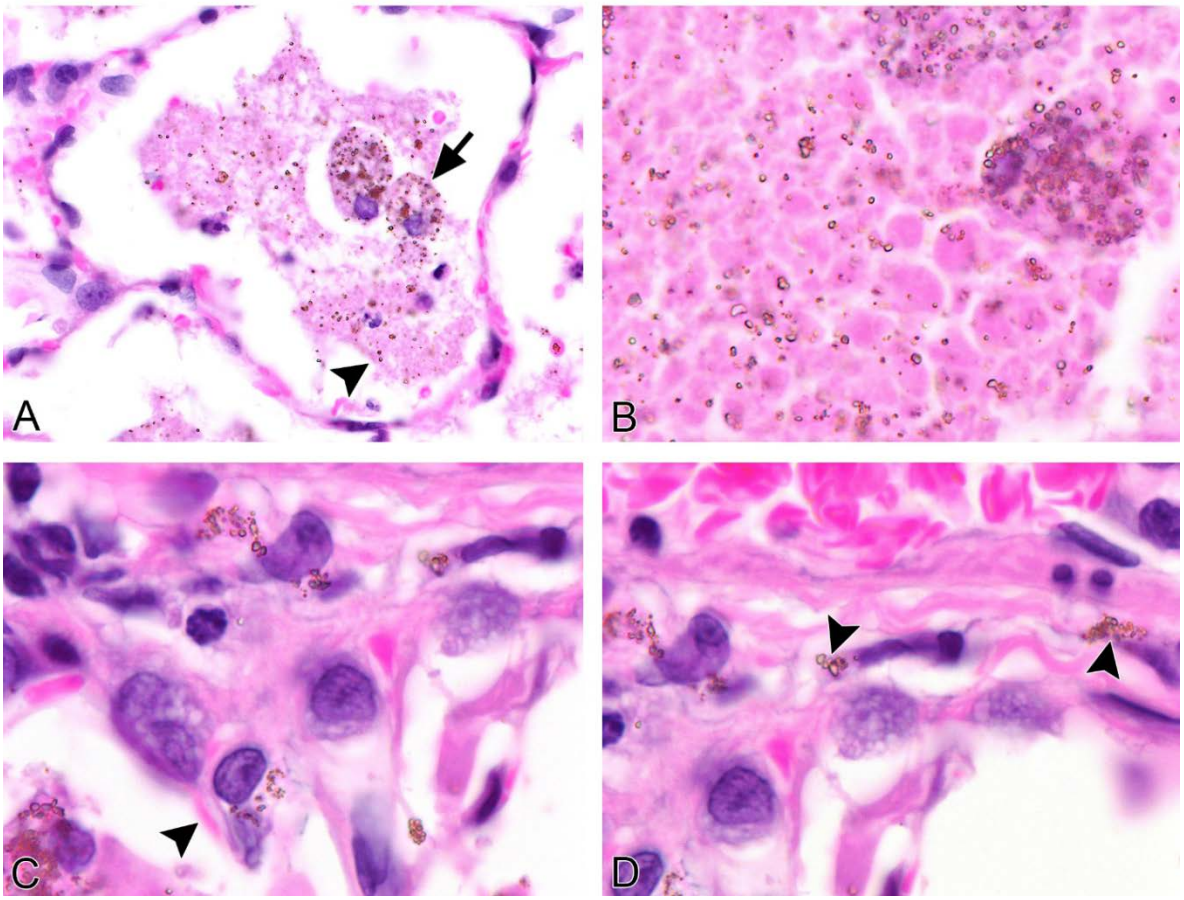

Figure 7. Foreign Body (Presumed Test Article) in the Lung of a Male Wistar Han Rat Exposed to 30 mg Antimony Trioxide/m^3 by Inhalation for Two Years (H&E)

A) The foreign particles were located within alveolar macrophages (arrow) as well as extracellularly in the alveolar proteinotic material (arrowhead). B) At higher magnification (100×), the particles were noted to be round to ovoid, golden brown, approximately 1 μm in diameter, and refractile. C) The foreign particles were sometimes seen within alveolar epithelial cells (arrowhead) and D) within interstitial macrophages (arrowheads).

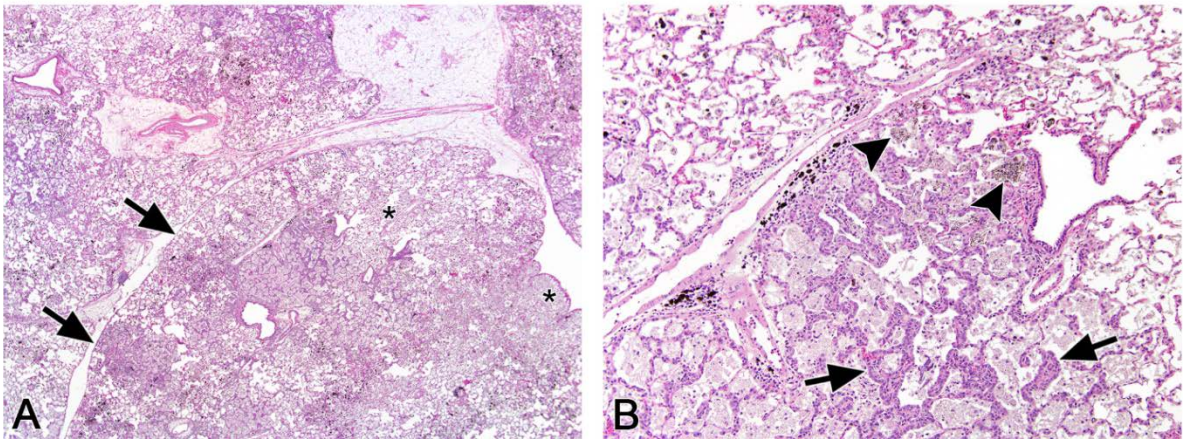

Figure 8. Nonneoplastic Changes in the Lung of a Male Wistar Han Rat Exposed to 30 mg Antimony Trioxide/m^3 by Inhalation for Two Years (H&E)

A) This low power view revealed extensive filling of alveolar spaces by alveolar proteinosis (asterisks) and inflammation (arrows). B) With higher magnification, two additional features of the reaction to the chemical were noted: alveolar epithelial hyperplasia (arrows) and increased alveolar macrophages containing foreign body particles (arrowheads).

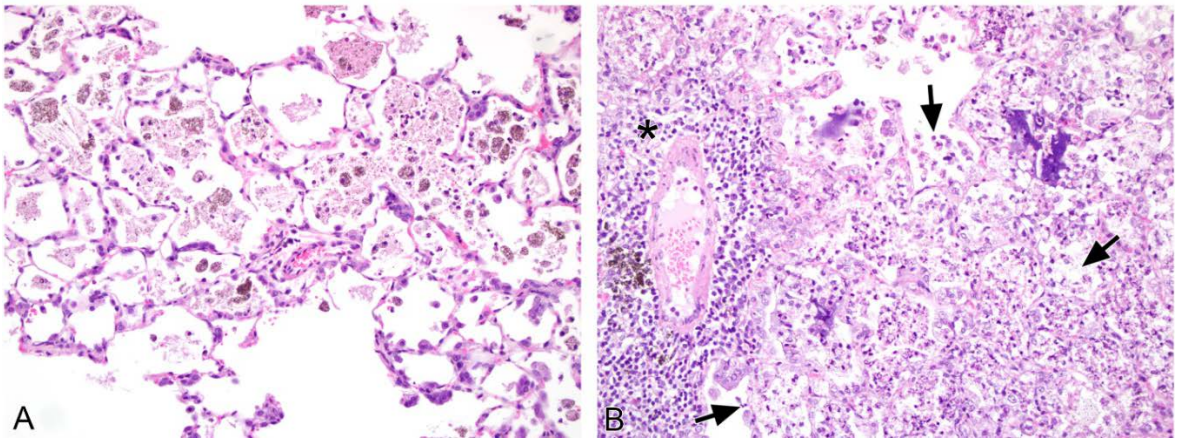

Figure 9. Inflammation in the Lung of a Male Wistar Han Rat Exposed to 30 mg Antimony Trioxide/m^3 by Inhalation for Two Years (H&E)

A) Chronic active inflammation was the predominant pattern, characterized by increased numbers of alveolar macrophages and lesser numbers of neutrophils. B) Two additional inflammatory patterns noted in this and other treated rats are depicted in this image: aggregates of alveolar neutrophils and karyorrhectic debris (arrows) and perivascular clusters of lymphocytes (asterisk).

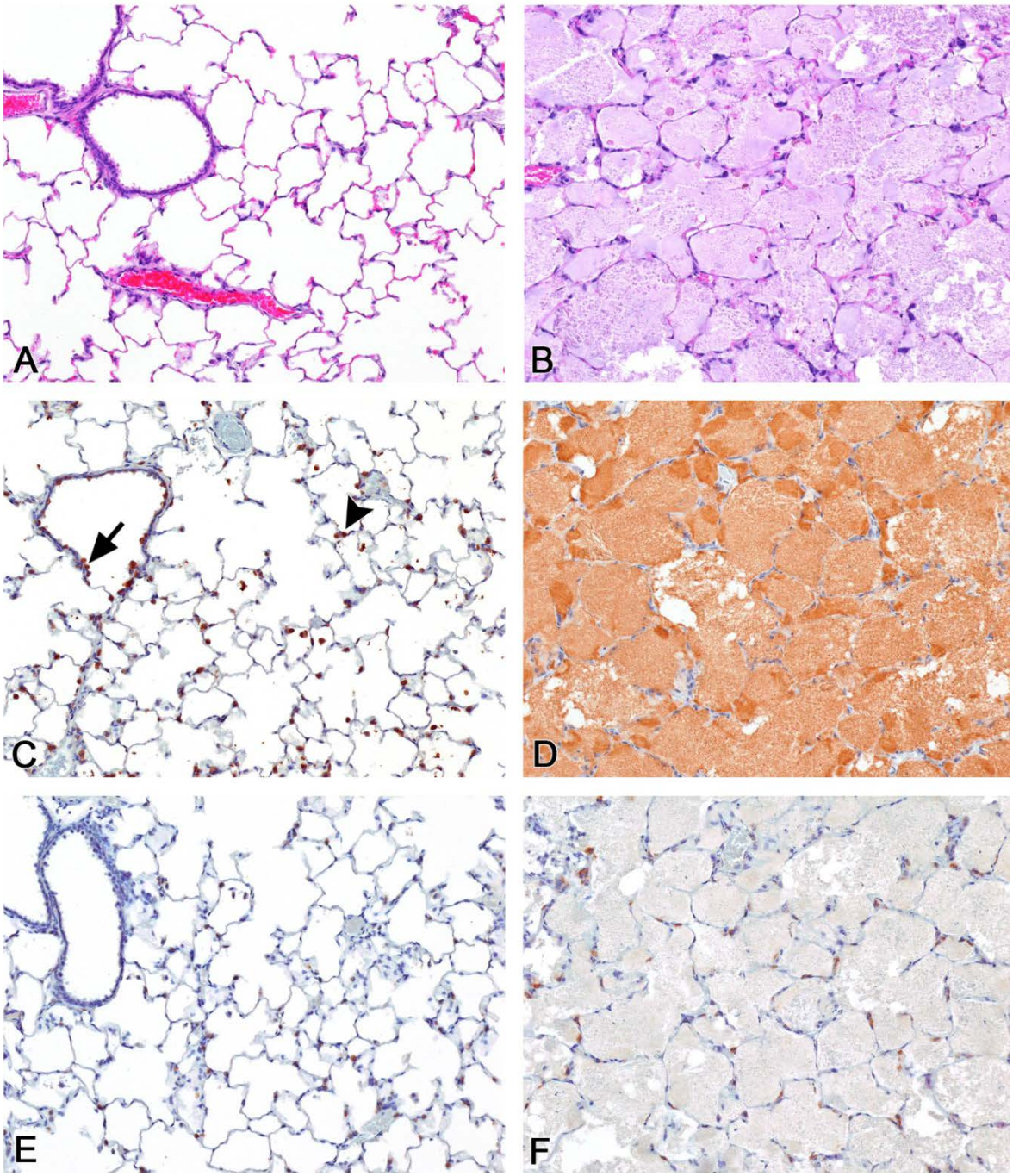

Figure 10. Alveolar Proteinosis in the Rat Lung

A) Normal lung of a chamber control female Wistar Han rat in the 2-year study of antimony trioxide by inhalation for comparison with the B) pulmonary alveolar proteinosis filling the alveolar spaces in the lung of a female Wistar Han rat exposed to 30 mg antimony trioxide/m^3 by inhalation for 2 years. (H&E) C) Immunohistochemical staining for surfactant A in the lung of a chamber control female Wistar Han rat showed staining of type II alveolar pneumocytes (arrowhead), bronchiolar Clara cells (arrow), and alveolar macrophages, but no staining of the alveolar spaces, whereas D) similar staining in the lung of the exposed female Wistar Han rat revealed strong, diffuse staining of the alveolar proteinotic material, indicating that accumulation of surfactant A was the cause of the proteinosis. Immunohistochemical staining for surfactant C in E) the lung of the same chamber control female Wistar Han rat, and in F) the lung of the same exposed female Wistar Han rat showed staining only of the type II alveolar pneumocytes with no staining of the alveolar spaces or of the proteinotic material.

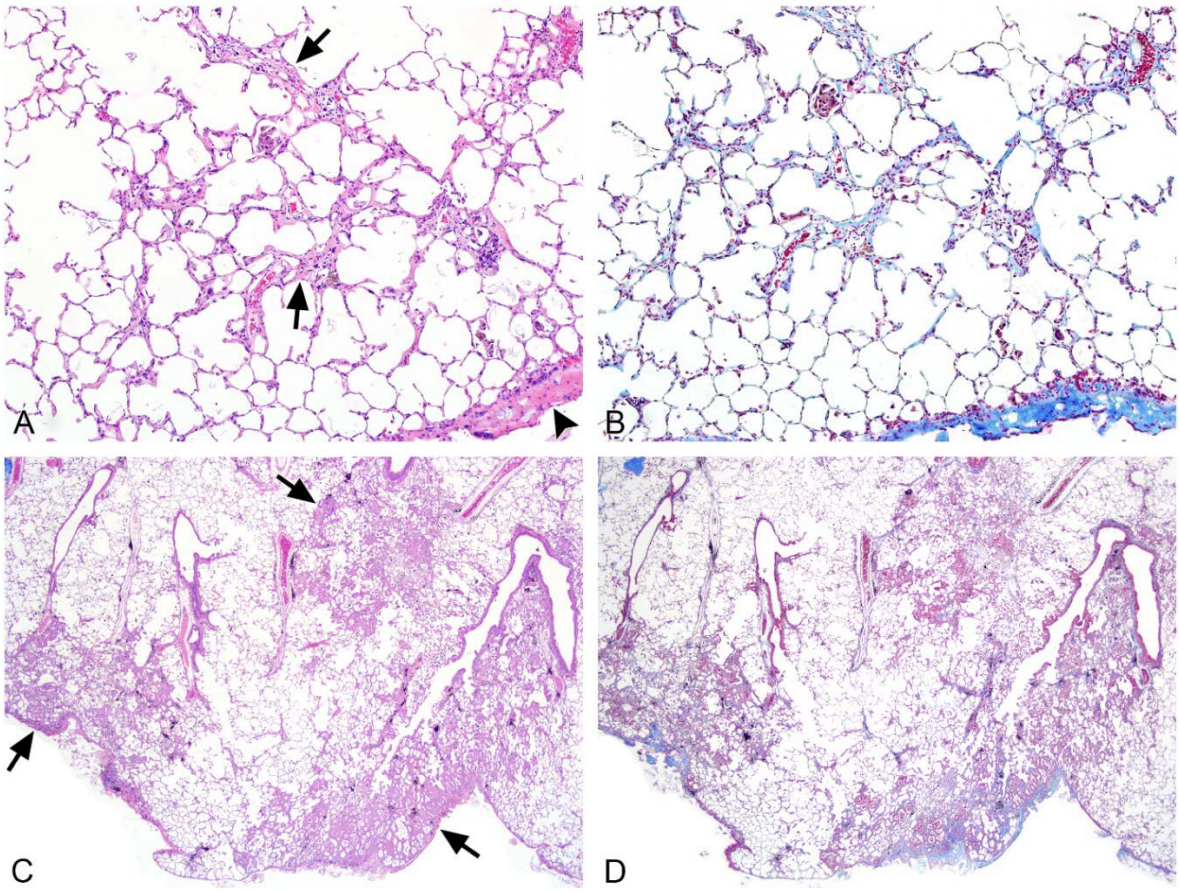

Figure 11. Fibrosis in the Lung

A) Many of the alveolar walls of this area were thickened by increased collagenous matrix (arrows) in a male Wistar Han rat exposed to 3 mg antimony trioxide/m^3 by inhalation for 2 years. The visceral pleura was also thickened (arrowhead). (H&E) B) Masson trichrome stain of the same area shown in A imparted a bluish cast to the increased collagen in the alveolar walls and the pleura. C) Zones of more extensive nodular fibrosis (arrows) were noted in a male Wistar Han rat exposed to 30 mg antimony trioxide/m^3 by inhalation for 2 years. (H&E) D) Masson trichrome stain of the same area shown in C highlighted the increase in blue staining collagen fibers within the parenchyma and the overlying pleura. Note that the foreign body, visible as black particulate material, was concentrated within the areas of fibrosis in both A and C.

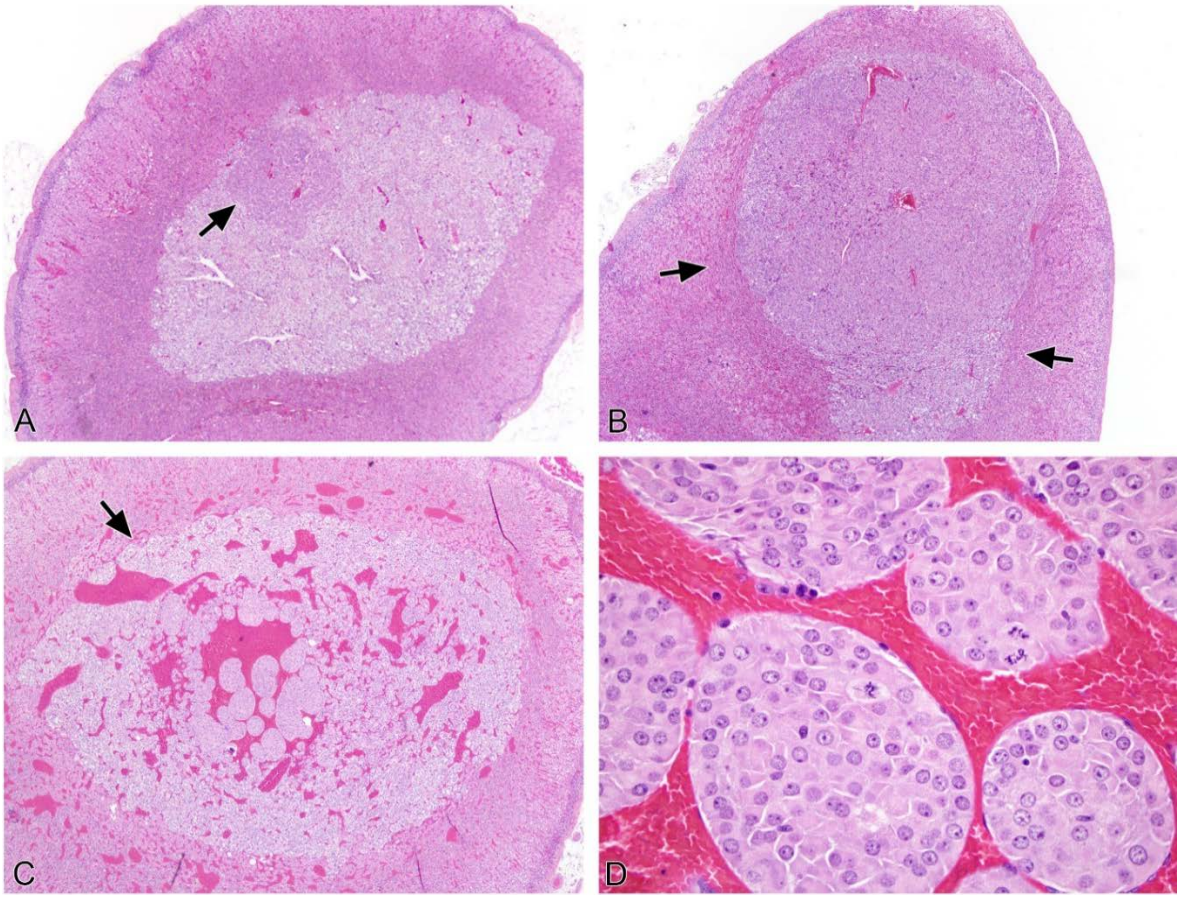

Figure 12. Hyperplasia and Neoplasia of the Adrenal Medulla (H&E)

A) The small focus of adrenal medullary hyperplasia (arrow) found in a male Wistar Han rat exposed to 30 mg antimony trioxide/m^3 by inhalation for 2 years displayed increased cellularity, without compression of the surrounding medulla. B) This benign pheochromocytoma in a male Wistar Han rat exposed to 30 mg antimony trioxide/m^3 by inhalation for 2 years exhibited a solid pattern, filled and expanded the adrenal medulla, and compressed the adjacent adrenal cortex (arrows). C) This benign pheochromocytoma in a female Wistar Han rat exposed to 30 mg antimony trioxide/m^3 by inhalation for 2 years formed a large, vascular nodule (arrow) with a trabecular pattern and frequent mitotic figures as seen at higher magnification in D).

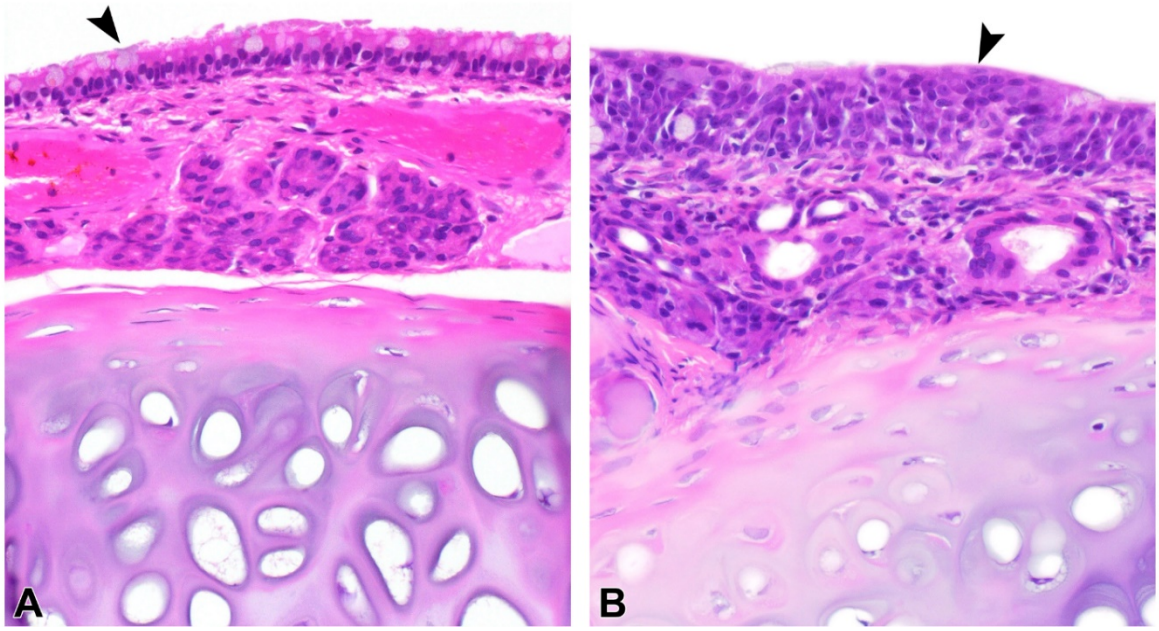

Figure 13. Respiratory Epithelial Hyperplasia of the Ventral Septum of the Nose (Level I) (H&E)

A) Normal columnar, ciliated epithelium (arrowhead) with scattered goblet cells in a chamber control, male Wistar Han rat in the 2-year study of antimony trioxide by inhalation. B) Respiratory epithelial hyperplasia (arrowhead) in a male Wistar Han rat exposed to 30 mg/m^3 antimony trioxide by inhalation for 2 years. The epithelium is thickened by proliferation of nonciliated, cuboidal epithelial cells with crowding of the nuclei; a reduction in the number of goblet cells is also noted. The underlying lamina propria is slightly inflamed.

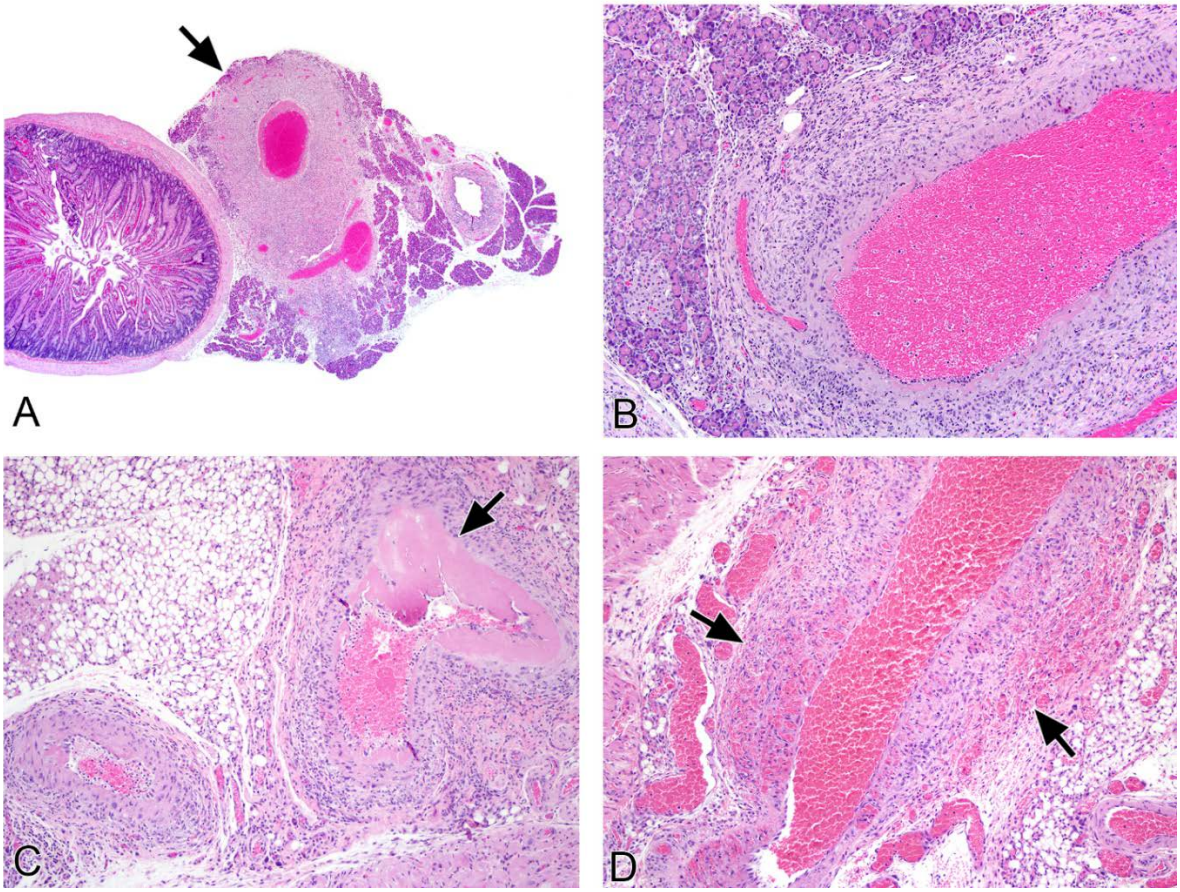

Figure 14. Arterial Inflammation (A, B, and C) and Plexiform Vasculopathy (D) (H&E)

A) The wall of this pancreatic artery in a female Wistar Han rat exposed to 30 mg antimony trioxide/m^3 by inhalation for 2 years was markedly thickened by chronic inflammatory changes (arrow). B) The pancreatic artery in a male Wistar Han rat exposed to 30 mg antimony trioxide/m^3 by inhalation for 2 years displayed a greatly thickened wall due to fibrosis and inflammatory infiltrate. C) This mediastinal artery in a male Wistar Han rat exposed to 30 mg antimony trioxide/m^3 by inhalation for 2 years exhibited chronic active inflammation throughout the wall and accumulation of eosinophilic material within the intima (arrow). D) Proliferation of numerous small, endothelial lined channels, accompanied by mild inflammatory infiltrate, was noted in the media and adventitia of this mediastinal artery in a female Wistar Han rat exposed to 30 mg antimony trioxide/m^3 by inhalation for 2 years (arrows). This type of change is sometimes referred to as plexiform or plexogenic vasculopathy.

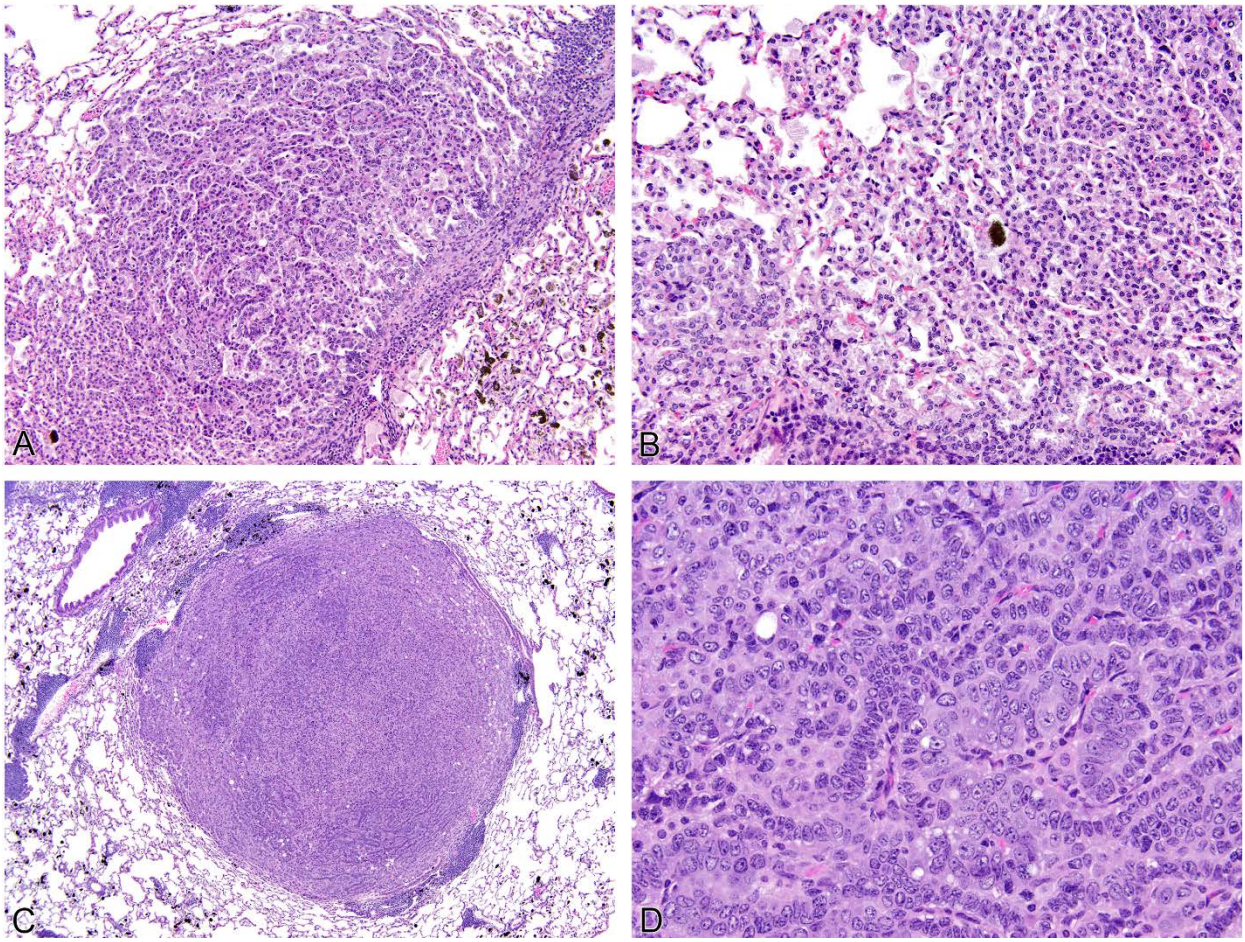

Figure 15. Epithelial Neoplasia in the Mouse Lung (H&E)

A) and B) Alveolar/bronchiolar adenoma, forming a relatively circumscribed proliferation of well-differentiated alveolar epithelial cells, focally replaced the normal lung parenchyma in a female B6C3F1/N mouse exposed to 30 mg antimony trioxide/m^3 by inhalation for 2 years. C) This alveolar/bronchiolar carcinoma presented as a solid, densely cellular mass in the lung of a female B6C3F1/N mouse exposed to 30 mg antimony trioxide/m^3 by inhalation for 2 years. D) Higher magnification of the tumor in C revealed cellular pleomorphism and a mixed growth pattern.

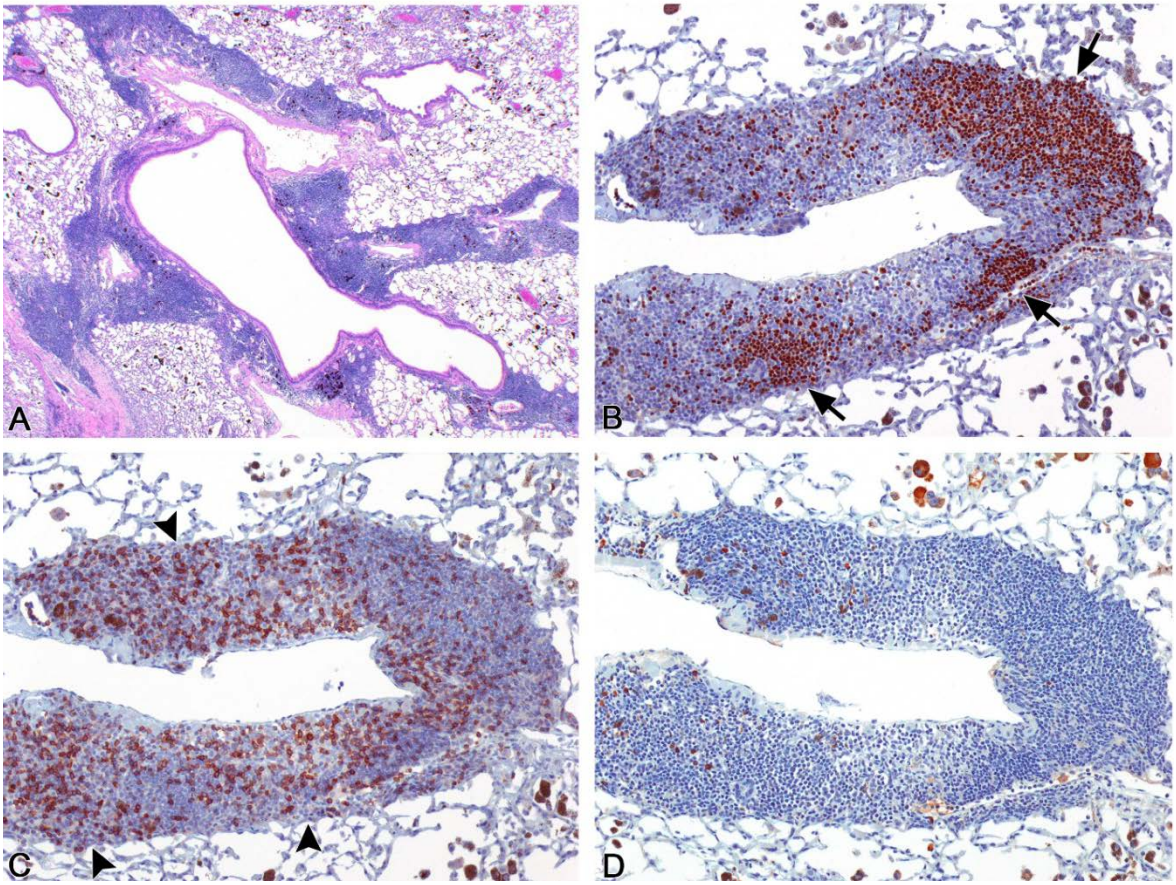

Figure 16. Lymphoid Hyperplasia in the Mouse Lung

A) Marked peribronchial and perivascular infiltration of small, well-differentiated lymphocytes in a male B6C3F1/N mouse exposed to 30 mg antimony trioxide/m^3 by inhalation for 2 years. (H&E) B) Immunohistochemical staining for B cells with anti-PAX5 revealed focal clusters of B cells within the infiltrates (arrows). C) Immunohistochemical staining for T cells with anti-CD3 demonstrated the presence of abundant T cells as well (arrowheads). Note that the B cells in B and the T cells in C occupy separate domains. D) Immunohistochemical staining for F4/80, a macrophage marker, showed a few scattered macrophages located primarily in the T cell regions.

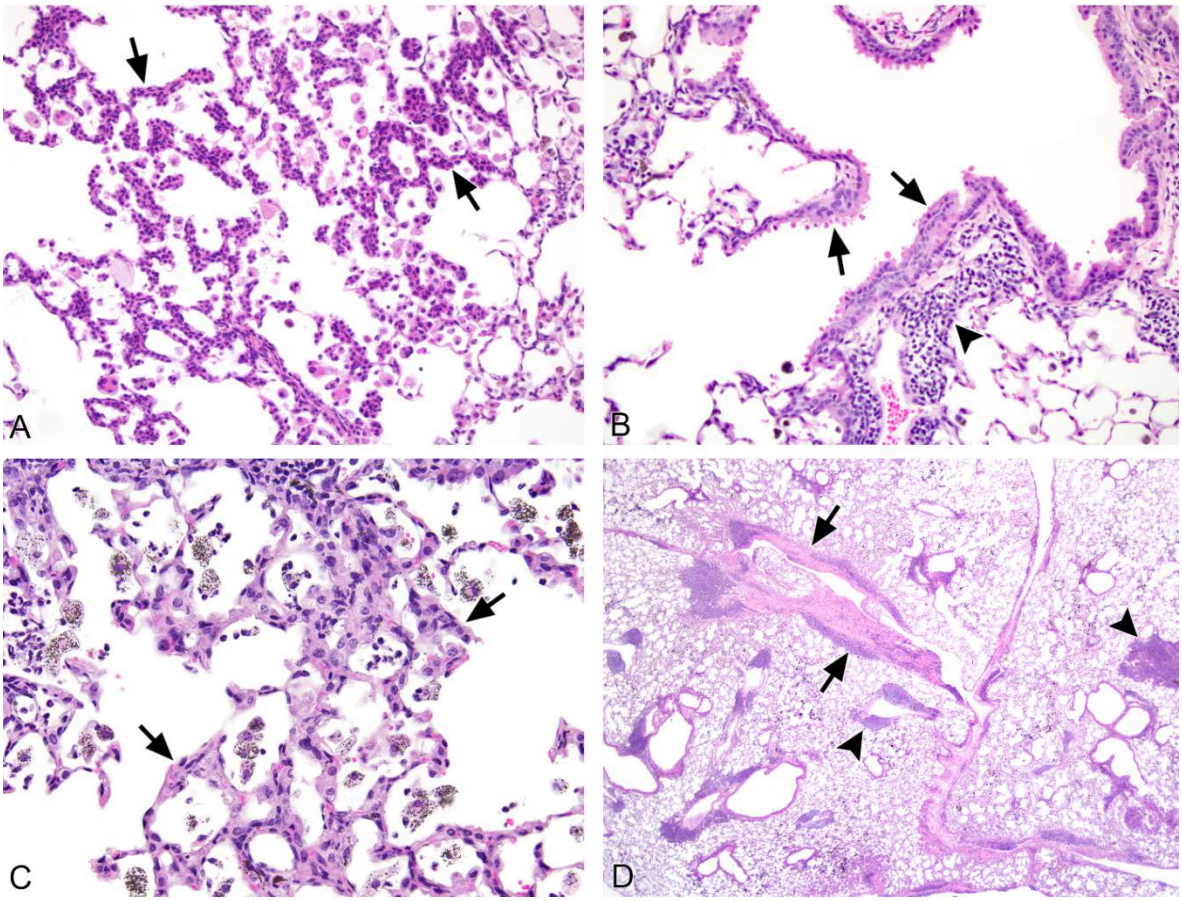

Figure 17. Epithelial Hyperplasia and Fibrosis in the Lung (H&E)

A) Prominent hyperplasia and hypertrophy of the alveolar epithelial cells (arrows) were noted in this section of lung from a female B6C3F1/N mouse exposed to 10 mg antimony trioxide/m^3 by inhalation for 2 years. Increased alveolar macrophages were also seen. B) Hyperplasia and hypertrophy of terminal bronchiolar epithelial cells (arrows) were sometimes observed, as seen in a female B6C3F1/N mouse exposed to 10 mg antimony trioxide/m^3 by inhalation for 2 years. Lymphocytic infiltrate was present in the adjacent lung (arrowhead). C) Interstitial fibrosis of alveolar walls, characterized by thickening of the walls by increased collagenous matrix (arrows), was present in this region of the lung from a female B6C3F1/N mouse exposed to 30 mg antimony trioxide/m^3 by inhalation for 2 years. Increased alveolar macrophages containing foreign particles, and a few neutrophils, were also present in the alveolar spaces. D) Fibrosis of the visceral pleura (arrows) was focally marked in this female B6C3F1/N mouse exposed to 10 mg antimony trioxide/m^3 by inhalation for 2 years. Perivascular and peribronchial lymphocytic infiltrates were also present (arrowheads).

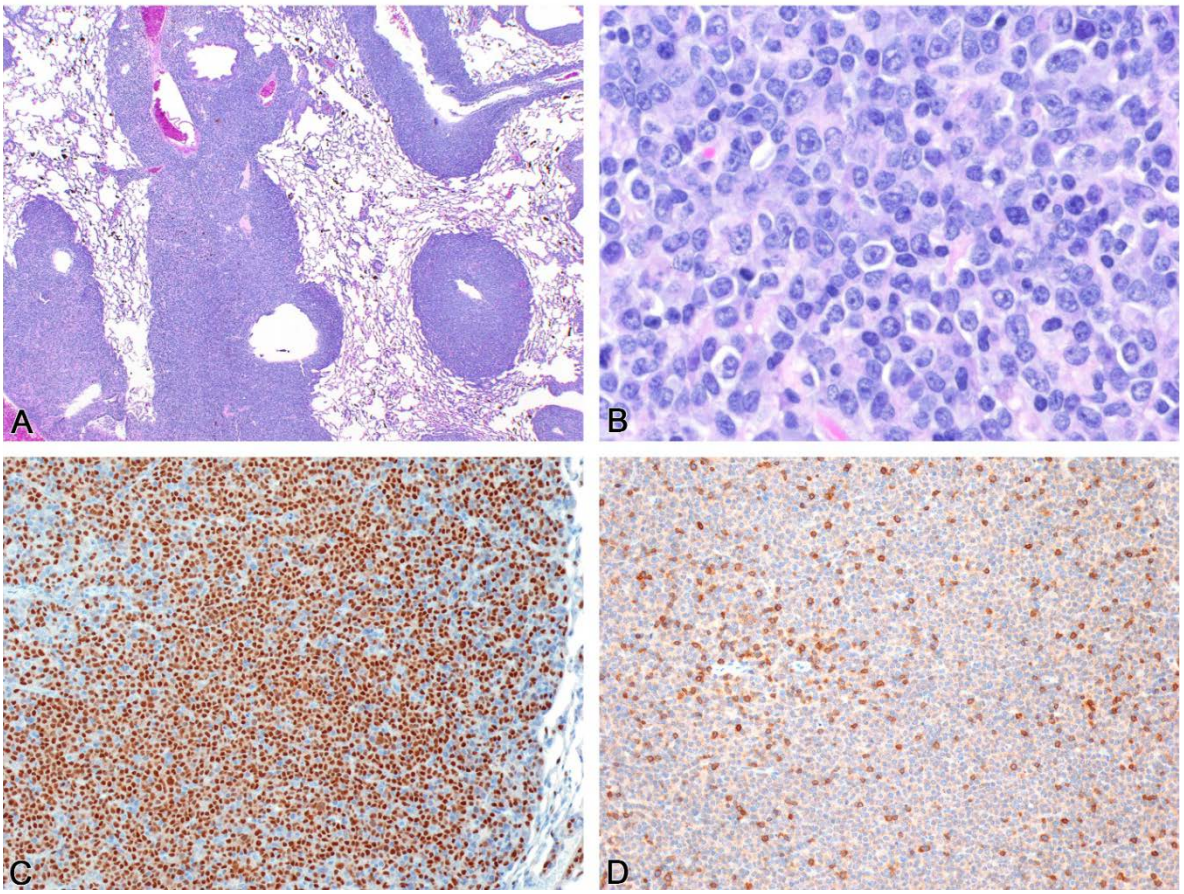

Figure 18. Malignant Lymphoma in the Mouse Lung

A) Malignant lymphoma, distributed primarily in peribronchial and perivascular regions, was found throughout the lung of a female B6C3F1/N mouse exposed to 30 mg antimony trioxide/m^3 by inhalation for 2 years. In comparison to lymphoid hyperplasia, such as that depicted in Figure 15, the lymphomatous infiltrates formed broader and more compact (densely cellular) cuffing of the bronchi and vessels and were distributed more widely throughout the lung. (H&E) B) Higher magnification of this infiltrate revealed a predominance of large lymphoid cells, along with lesser numbers of small lymphocytes. (H&E) C) Immunohistochemical staining for B cells with anti-PAX5 showed that most of the cells in the infiltrates were B cells. D) Immunohistochemical staining for T cells with anti-CD3 demonstrated a significant admixture of T cells in the infiltrates. Note that the B and T cells seem to be randomly admixed in this lymphomatous infiltrate, in contrast to the separate B and T cell domains seen with the lymphoid hyperplasia in Figure 15.

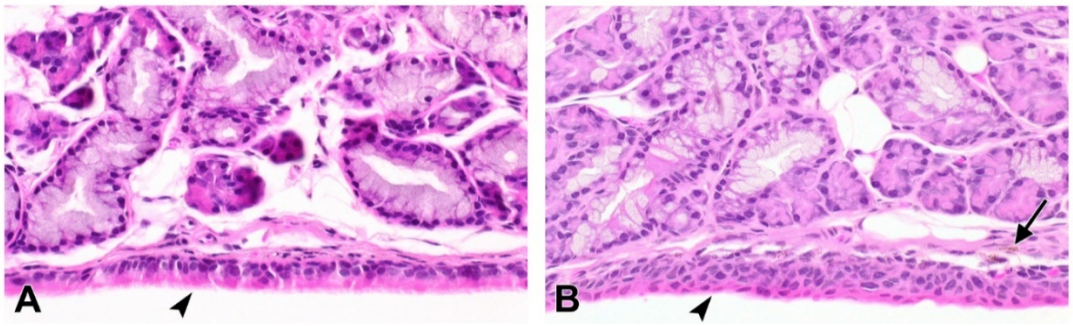

Figure 19. Squamous Metaplasia of the Base of the Epiglottis (H&E)

A) Normal columnar, ciliated epithelium (arrowhead) lining the base of the epiglottis of the larynx (Level 1) in a chamber control female B6C3F1/N mouse in the 2-year study of antimony trioxide by inhalation. B) A multilayered, squamous metaplastic epithelium has replaced the columnar epithelium in this female B6C3F1/N mouse exposed to 30 mg/m^3 antimony trioxide by inhalation for 2 years. Note the yellow-brown granular foreign body (presumed test article) within the stroma of the lamina propria (arrow) and within an adjacent subepithelial macrophage. Normal submucosal glands are noted in both A) and B).

Discussion

Antimony trioxide was nominated for National Toxicology Program testing by the Consumer Product Safety Commission and the National Institute of Environmental Health Sciences due to the potential for substantial human exposure in occupational settings and the lack of adequate 2-year exposure carcinogenicity studies. Three 1-year inhalation exposure studies in rats are reported in the literature[14; 16; 35]; however, the methodologies and lung carcinogenicity results were inconsistent among the three studies. In response, NTP conducted 2-week and 2-year inhalation studies to assess whether antimony trioxide poses a carcinogenic hazard in rats, to generate data in a second species, and to characterize the exposure-concentration responses in rats and mice. A 12-month interim evaluation was added as a means of comparison to previous inhalation studies. Inhalation exposure was selected because this is the most common route of occupational exposure to antimony trioxide in humans.

Due to the lack of overt toxicity in the current 2-week studies in rats and mice, the similar incidences and severities of chronic active lung inflammation in the 30 and 60 mg/m^3 groups in rats, and the effects observed in the previous 1-year studies in rats[14; 16; 35], 30 mg/m^3 was selected as the highest exposure concentration for the 2-year studies in rats and mice. Lower concentrations were spaced in half-log intervals, such that the lowest exposure concentration (3 mg/m^3) selected for the 2-year studies, was lower than the exposure concentration that resulted in modest increases in nonneoplastic lesions and no increases in neoplastic lesions following exposure of rats for 1 year[16]. There were several design differences between the current and previous chronic studies, notably, the exposure duration of 2 years, the inclusion of mice in the studies, and the antimony trioxide particle size in the exposure atmospheres. The mass median aerodynamic particle diameter and geometric standard deviation in the current studies were consistent with NTP specifications and were utilized to maximize deposition in the lower respiratory tract, particularly with the inclusion of mice in the studies[43]. The difference in particle size, increased alveolar deposition, and 2-year exposure duration likely explain, in part, the more apparent lung toxicity and carcinogenicity in the current studies in comparison to those reported in the literature.

In the 2-year studies, there were decreases in survival and body weight (greater than 10%) at the higher concentrations; these decreases were observed relatively late (approximately 18 months or later) in the studies. Decreases in survival were attributed primarily to nonneoplastic and/or neoplastic lung lesions (rats and mice) or malignant lymphoma (female mice). Consistent with the observed pulmonary toxicity and retention of particles, exposure-related clinical observations included abnormal breathing and thinness in male and female rats and mice and cyanosis in both sexes of rats. These observations were most prominent in the 10 and 30 mg/m^3 groups. These effects were not generally observed until the second year of exposure; there was no pattern observed when comparing day of onset with exposure concentration.

The lung was the major target of toxicity and carcinogenicity in rats and mice exposed to antimony trioxide for 2 years. Exposure-related increases in the incidences of lung neoplasms and in nonneoplastic lesions were observed in rats and mice of both sexes; increases in nonneoplastic lung lesions were observed at all exposure concentrations. Notably, the incidences of alveolar epithelium hyperplasia and bronchiole epithelium hyperplasia were increased in all exposed groups of rats and mice in the 2-year studies; these lesions are considered to be

preneoplastic. A 12-month interim evaluation was included in the current 2-year studies to compare to the previous 1-year exposure studies reported in the literature[14; 16; 35]. Overall, in comparison to studies reported in the literature, the toxicity of antimony trioxide to the lung was more pronounced and occurred at a lower concentration under a similar exposure paradigm.

In 2-year male rats, although not statistically significant, the incidences of alveolar/bronchiolar adenoma in the 10 and 30 mg/m^3 groups were higher than that of concurrent chamber controls and exceeded the historical control incidences for inhalation studies (4/150) and for all routes of administration (4/299). The concurrent chamber control incidence of alveolar/bronchiolar adenoma (3/50) was the highest observed incidence in the historical control database (consisting of six 2-year studies in Wistar Han rats). Multiple alveolar/bronchiolar adenomas were observed in 3 and 30 mg/m^3 male rats, and alveolar/bronchiolar carcinomas were observed in two 10 mg/m^3 male rats. In two of the male rats, alveolar/bronchiolar tumors were noted in the mediastinum as well as in the lung; although it is unusual for these tumors to be found in the mediastinum, this has been previously reported[77]. Alveolar/bronchiolar carcinomas have not been observed in the historical controls (inhalation studies: 0/150; all routes: 0/299). Finally, exposure-related increases in lung neoplasms occurred in female rats as well as male and female mice. Collectively, the higher combined incidences of adenoma or carcinoma were considered to be some evidence of carcinogenic activity in male rats.

In female rats at 2 years, incidences of alveolar/bronchiolar adenoma were higher than that in the concurrent chamber controls at all exposure concentrations, and these increases were statistically significant at 10 and 30 mg/m^3. Alveolar/bronchiolar adenomas were not observed in the historical control female rats (inhalation studies: 0/150; all routes: 0/300). Additionally, an alveolar/bronchiolar adenoma was observed in a 30 mg/m^3 female rat at the 12-month interim evaluation. These neoplasms are known to progress to carcinomas. However, the alveolar/bronchiolar adenoma response observed in this study was not marked and no alveolar/bronchiolar carcinomas were observed; alveolar/bronchiolar carcinomas were not observed in historical control female rats (inhalation studies: 0/150; all routes: 0/300). Collectively, these data were considered to be some evidence of carcinogenic activity in female rats.

Incidences of alveolar/bronchiolar carcinoma were significantly increased in all exposed groups of male and female mice compared to the chamber controls at 2 years. Additionally, the incidences of alveolar/bronchiolar adenoma were significantly increased in all exposed groups of female mice. These incidences exceeded the historical control ranges for inhalation studies and for all routes of administration in all exposed groups of males and females. The incidences of multiple alveolar/bronchiolar carcinomas were significantly increased in all groups of exposed males and females compared to the chamber controls. In addition, the incidence of metastases was elevated in all exposed groups of male and female mice; this response was exposure-concentration related in males. Finally, alveolar/bronchiolar neoplasms were observed at the 12-month interim evaluation in 10 and 30 mg/m^3 males and 30 mg/m^3 females. Collectively, these data were considered to be clear evidence of carcinogenic activity in male and female mice.

In addition to the alveolar/bronchiolar lung neoplasms, two occurrences of cystic keratinizing epithelioma and one occurrence of squamous cell carcinoma occurred in 30 mg/m^3 female rats; neither of these neoplasms has been observed in the historical controls. Squamous metaplasia of alveolar septa also occurred only in treated female rats. Cystic keratinizing epitheliomas are

considered part of a spectrum of lesions that form a morphologic continuum considered to progress from squamous metaplasia to keratin cysts to cystic keratinizing epithelioma to squamous cell carcinoma[78]. The occurrence of these lesions in female rats may have been related to treatment.

The overall pattern of nonneoplastic lung lesion incidences was similar between the sexes and between the 12-month and 2-year exposure durations within each species. In general, severities were similar or slightly higher in the 2-year studies, as compared to the 12-month interim evaluations. The incidences of a number of nonneoplastic lung lesions were increased in all exposed groups in most to all exposed animals. These included foreign body (presumed test article), chronic active inflammation, and alveolar fibrosis in addition to the hyperplasia discussed above. However, there were some notable differences between the species, including the presence of proteinosis exclusively in the lungs of rats, the presence of marked peribronchial and perivascular lymphoid hyperplasia in the lungs of mice, and the more prominent pleural inflammation and fibrosis in mice. Because pulmonary alveolar proteinosis in humans is usually associated with accumulation of surfactant, immunohistochemical stains for surfactants A and C were performed, resulting in strong, diffuse staining of the proteinosis for surfactant A. To our knowledge, this is the first demonstration of surfactant accumulation as a cause of proteinosis in rats.

In the upper respiratory tract, including the larynx, trachea, and nose of rats and mice, foreign body (presumed test article) was observed at both the 12-month interim evaluations and in the 2-year studies. Additional upper respiratory tract lesions occurred in both rats and mice, consisting primarily of respiratory epithelium hyperplasia and squamous metaplasia and occurred in the nose of rats and the larynx of mice.

The adrenal medulla was also a target tissue in the 2-year rat study. Exposure-related increases in the incidences of benign pheochromocytoma and of hyperplasia were observed in male and female rats and the incidences were significant at 30 mg/m^3 compared to the chamber controls. The incidences of benign pheochromocytoma in 30 mg/m^3 male and female rats exceeded the historical control ranges for inhalation studies and for all routes of administration. Malignant pheochromocytoma was observed in a single 30 mg/m^3 female rat. These increases were considered to be related to exposure in male and female rats. The results of several NTP inhalation studies with particulate compounds suggest that there may be an association between benign and malignant alveolar/bronchiolar neoplasms and variably extensive chronic pulmonary nonneoplastic lesions and significantly increased incidences of hyperplasias and benign and malignant pheochromocytomas of the adrenal medulla in rats[79-86]. With varying degrees of statistical significance, in some but not all studies, this relationship appeared to be associated with the severities of lung fibrosis and inflammation[87]. The mechanism(s) of this association between lung lesions and adrenal medulla pheochromocytoma in rats is not understood. However, reduced gas exchange induced by extensive space-occupying neoplasms and nonneoplastic lung lesions such as fibrosis, chronic inflammation, and alveolar proteinosis may lead to systemic hypoxemia that chronically stimulates catecholamine secretion from the adrenal medulla. This chronic hypersecretory activity may lead to medullary hyperplasia and subsequent neoplasia[87]. Clinically, the extensive lung disease was manifested by abnormal breathing (rats and mice) and cyanosis (rats only) during the second year of exposure in the current 2-year studies and considered to be related to exposure.

In 2-year female mice, the incidences of malignant lymphoma were increased in an exposure-concentration dependent manner, with significant increases in all exposed groups compared to the chamber controls; the incidences in the 10 and 30 mg/m^3 groups exceeded the historical control ranges for inhalation studies and for all routes of administration. The malignant lymphomas typically involved spleen, lung, bronchial and mediastinal lymph nodes, and sometimes the liver. Since almost all exposed mice exhibited prominent perivascular and peribronchial lymphoid hyperplasia, which was similar to the distribution of the lymphomatous infiltrates in the lung, the possibility of malignant transformation from the lymphoid hyperplasia in the lung to lymphoma was considered. However, almost all of the malignant lymphomas also involved the spleen, so the alternative possibility of splenic origin with secondary pulmonary involvement cannot be excluded. At the 12-month interim evaluation, three incidences of malignant lymphoma occurred in 30 mg/m^3 female mice and other 12-month interim evaluation female mice exhibited atypical lymphoid proliferations in the lung and spleen that were suggestive of preneoplastic proliferations or evolving lymphomas. Immunohistochemical stains for B and T cell markers in selected lymphomas from the 2-year study revealed a predominance of B cells with a significant admixture of T cells. The increased incidences of malignant lymphomas in female mice were considered to be clear evidence of carcinogenic activity.

The incidence of fibrous histiocytoma in the skin was significantly increased in 30 mg/m^3 male mice compared to the chamber controls at 2 years. In addition, fibrosarcoma was observed in two 10 mg/m^3 male mice. The increases in the combined incidences of fibrous histiocytoma and fibrosarcoma were considered to be related to exposure because the increases were exposure-related, a potential target after whole body exposure, and exceeded the historical control range. In 2-year female mice, squamous cell carcinoma of the skin occurred with a positive trend. This lesion has not been observed in historical control females in inhalation studies or all routes of administration. This occurrence in the 30 mg/m^3 females may have been related to exposure.

There were increased incidences of nonneoplastic lesions in the hematopoietic system. In the lung associated (bronchial and mediastinal) lymph nodes, foreign body (presumed test article) was present in most exposed rats and mice, while lymphoid hyperplasia was observed in exposed rats. Observed increases in bone marrow hyperplasia in rats and mice and hematopoietic cell proliferation of the spleen in female mice were probably secondary responses to hypoxia and pulmonary inflammation. The increased incidence and severity of cellular depletion of the thymus in both male and female mice in the 2-year study were probably related to stress. The decreased incidence of lymphoid hyperplasia in the spleen of exposed female mice at 2 years appeared to coincide with the concomitant transformation to malignant lymphoma.

In the eyes of rats, acute inflammation of the ciliary body was observed in some of the 10 and 30 mg/m^3 male and female rats. The ciliary body is part of the uveal tract, which is an important vascular region of the eye. Since the antimony trioxide entered the blood of exposed animals, the inflammatory reaction in the ciliary body may have been secondary to irritation from systemically derived test article. Incidences of retinal atrophy were significantly increased in all exposed groups of female rats compared to the chamber controls. In 2-year rodent bioassays, especially with albino rodents, phototoxic changes are seen fairly frequently as a background change, especially in females[88]. Although there appears to have been a test article-related exacerbation of the background incidence of retinal atrophy in the female rats, it is uncertain whether this was a direct effect of the chemical or a secondary compound-related effect on one of the pathways associated with phototoxicity, such as oxidative stress or apoptosis[88]. Although

the incidence of cataracts was slightly increased in female mice, the significance was uncertain because the incidence was low and without a dose response.

Arteritis was observed in multiple tissues in male and female rats. When all tissues were combined, incidences were significantly increased in an exposure concentration-dependent manner. Sites most commonly involved included mesentery, pancreas, and mediastinum. An increased incidence of arteritis has been previously described in rodents exposed to particulate matter by inhalation[89]. Although the cause of arteritis in these studies is unknown, it has been speculated that hypoxia may result in increased blood volume, creating shear stresses within arterial walls. The sites involved in this study offer some support for this hypothesis since these arteries are surrounded by less supporting tissue and might be more vulnerable to shear stresses from increased blood flow.

The incidences of renal tubule hyaline droplet accumulation were significantly increased in 30 mg/m^3 male and female rats and in 10 mg/m^3 female rats. The source and character of these droplets was not determined. The possibility that the droplets could be deposits of surfactant A originating from the pulmonary proteinosis was considered; however, immunohistochemical stains for surfactant A were negative. Several lines of evidence indicate that this lesion was not due to chemically bound alpha-2u globulin. The alpha-2u globulin syndrome, in which an accumulation of bound protein in the kidney leads to a cascade of events including cell death, sloughing off of cells, and finally nephropathy, only occurs in male rats. However, in the current 2-year studies, the lesion occurred in both males and females. In addition, in the alpha-2u globulin syndrome, increases in hyaline droplets typically occur following subchronic exposures and are not observed following chronic exposures as they were in the current studies. An increased incidence of nephropathy (chronic progressive nephropathy) was also noted in the 30 mg/m^3 female rats; chronic progressive nephropathy is a spontaneously occurring disease of rats, which can be exacerbated by many chemicals in chronic toxicity studies[90].

In the 2-year mouse study, incidences of chronic active inflammation of the epicardium in the heart were significantly increased in 10 and 30 mg/m^3 males and females; the lesion may have been secondary to inflammation of the pleura. In addition, absolute, but not relative, heart weights were increased in 30 mg/m^3 females at the 12-month interim evaluation. Based on reports in the literature[91; 92], the heart is one of the major target organs following exposure to soluble antimony compounds. However, no evidence of direct toxicity to the heart was observed in the current 2-year studies.

The chronic active inflammation and ulceration of the skin in male rats and ulceration of skin in female rats occurred predominately on the plantar surfaces of the feet of both the treated and control animals and were believed to be secondary to the large size of the rats walking on the wire cages; the increased incidences of these lesions in the treated animals may have been related to exacerbation by the test article.

In order to assess the potential for genotoxicity in rats and mice following exposure to antimony trioxide, the erythrocyte micronucleus assay, measuring chromosomal damage, was performed in blood, and the comet assay was performed to assess DNA damage in lung tissue and blood leukocytes. Significant increases in micronucleated mature erythrocytes (NCEs) and DNA damage in lung cells were observed in male and female mice. The increases in micronucleated NCEs were supported by a trend toward increased frequencies of micronucleated immature

erythrocytes (reticulocytes; PCEs). The increases in micronucleated erythrocytes occurred concomitantly with increases in percent reticulocytes in peripheral blood. The latter observation suggests a stimulation of erythropoiesis as a consequence of exposure to antimony trioxide, and increased cell turnover cannot be discounted as a factor in the small, but exposure concentration-related, increases in micro-nucleated NCEs observed in the mice. The increases in percent reticulocytes may have been a consequence of hypoxia that resulted from exposure to the higher concentrations of antimony trioxide, although hypoxia occurred in the rats as well (as indicated by the cyanosis), with no accompanying increases in percent reticulocytes or micronuclei. Results from the comet assay indicated that DNA damage occurred in lung cells of exposed male and female mice, as evidenced by increases in DNA migration measured as percent tail DNA. Antimony trioxide has previously been reported to be genotoxic in mammalian cells in vitro[2; 36; 38], but not in vivo[36; 39]; however, the in vivo studies reporting negative genotoxicity test results used gavage as the route of exposure, in contrast to the studies reported here, in which antimony trioxide was administered via inhalation. Due to its insoluble nature, absorption of antimony trioxide from the gastrointestinal tract following gavage administration is poor. The patterns of nonneoplastic and neoplastic lung lesions in rats and mice were compared to the genetic toxicology data. Genotoxicity was only observed in mice. While nonneoplastic lung lesions and lung neoplasms were observed in both species, the neoplastic observations were more striking in the mice than in the rats. Collectively, these data suggest multiple mechanisms of antimony trioxide-induced genetic toxicity and carcinogenicity.

Egfr and *Kras* genes were evaluated for mutation frequencies in lung tumors because mutations in these genes are frequently present in human lung tumors. In both rats and mice, chronic exposure to antimony trioxide resulted in mutations in the hot spot regions of the *Egfr* gene within alveolar/bronchiolar adenomas and carcinomas. These *Egfr* mutations were not observed in spontaneous alveolar/bronchiolar adenomas and/or carcinomas from chamber control rats or mice. However, in mice (but not in rats), *Kras* gene mutations were observed in alveolar/bronchiolar tumors of both chamber control and antimony trioxide exposed animals, and most of these mutations were G to A transitions. Mutations in *Kras* and *Egfr* are commonly observed in human nonsmall cell lung cancer and occur in a mutually exclusive manner. Both KRAS and EGFR are major components of the MAPK signaling pathway. In the rats, the antimony trioxide-induced alveolar/bronchiolar tumors preferentially harbored *Egfr* mutations, whereas the alveolar/bronchiolar tumors in mice contained roughly equal numbers of *Kras* and *Egfr* mutations. This association suggests that altered EGFR signaling may play an important role in the pulmonary carcinogenesis resulting from chronic antimony trioxide exposure in both rats and mice.

In the 2-week studies, antimony trioxide lung burdens increased with increasing exposure concentration in rats and mice. Deviations from dose proportionality were small with less than proportional increases occurring at the higher exposure concentrations, and were resolved to an extent in the 4-week postexposure females. Lung clearance half-lives were estimated in females using data generated immediately after the end of exposure and at 4 weeks postexposure and were approximately twice as long in female rats (approximately 4 months) compared to female mice (approximately 2 months); these half-lives were included as time points in the chronic tissue burden studies in rats and mice. Steady-state lung burdens were not reached during the 2-week studies and would have required exposure durations of at least 7 to 21 months of exposure by a similar regimen to be reached. In female rats, blood antimony concentrations

increased during the recovery period, indicating that antimony from the lung was entering the bloodstream. It is not clear whether this was the result of direct absorption or occurred following mucociliary clearance. In female mice, blood antimony concentrations decreased during the recovery period with half-lives of 22 to 32 days.

In the 2-year studies, only female rats and mice were evaluated for tissue burden because deposition patterns were similar between the sexes of both species in the 2-week studies. Lung burdens increased in proportion to exposure concentration and duration of exposure in rats and mice. In the 3 and 10 mg/m^3 rat groups, model-predicted lung steady-state burdens in rats were similar to those actually observed at 551 days, indicating that they approached steady-state. In contrast, predicted steady state burdens in the 30 mg/m^3 rat group were approximately 30% greater than observed burdens at 551 days, and thus did not approach steady state at this concentration. In rats, lung deposition rates were proportional to exposure concentration and were indicative of deposition efficiencies that approximately increased from 3% to 5% of the inhaled antimony trioxide. The calculated doses to the lung of rats after 551 days on study were 9.2, 24.4, and 65.6 mg/lung in the 3, 10, and 30 mg/m^3 groups, respectively. The lung clearance half-lives in rats doubled between the 3 and 30 mg/m^3 groups; the 3 mg/m^3 half-life was similar to that observed during the 2-week study. As a result, only approximately one-half of the antimony trioxide dose to the lung was cleared over the course of the study in the 10 and 30 mg/m^3 groups versus approximately two-thirds in the 3 mg/m^3 group over the course of the study. In all exposed groups of mice, lung burdens increased steadily throughout the studies, reaching unexpectedly high values by the end of the studies, indicating that mouse lung burdens did not approach steady state and precluding modeling of lung burden data in this species.

In the 2-year studies, blood antimony concentrations increased with increasing exposure concentration in both rats and mice. In rats, concentrations also increased with exposure duration. In contrast, mouse blood concentrations appeared to be at or near steady state over most of the study in all exposed groups. Normalized blood concentrations decreased with increasing exposure concentration in both species, suggesting that as exposure concentrations (and lung burdens) increased, the rate or capacity of antimony trioxide dissolution and transport to the blood became progressively less, or that the rate of clearance from the blood increased. Although the blood concentration data were not modeled to discern blood antimony deposition and clearance rates, the blood concentration results, at least in rats, were consistent with the fact that clearance rates of antimony trioxide from the lungs also became progressively slower in rats as exposure concentrations increased.

Based on the relatively long clearance half-lives at 10 and 30 mg/m^3 and high lung burdens at 30 mg/m^3 in rats, and the unexpectedly high lung burdens at 551 days in mice, which precluded the mouse data from being modeled, it was hypothesized that lung overload occurred in rats and mice[74-76]. Calculations were made to determine if volumetric- or surface area-based overload occurred in either species. These calculations yielded generally similar results for the two interpretations of overload. Notably, lung overload did not occur at 3 mg/m^3 in either species using either metric but did occur at 10 and 30 mg/m^3, with the degree of overload increasing with exposure concentration. These data are consistent with available guidance for chronic inhalation study exposure concentration selection and data interpretation for particles, which indicates that both concentrations predicted to induce and those predicted not to induce lung overload should be selected and that all data (both in presence and absence of overload) should be utilized in the interpretation of carcinogenicity data[93].

The lung overload hypothesis is considered to be applicable to poorly soluble particles of low intrinsic toxicity (e.g., carbon black, talc, coal dust, diesel soot, and titanium dioxide). In rats, lung overload is associated with pulmonary inflammation, fibrosis, epithelial hyperplasia, and lung tumors[93]. There is no similar association between exposure to these particles and occurrence of lung tumors in mice or hamsters. It is noteworthy that humans clear insoluble particles less readily than rodents, and with one such insoluble particle, coal dust, lung burdens similar to those that have been observed in rats with lung overload have been observed in humans. Both rats and humans develop fibrosis. While coal dust induces lung tumors in rats, the relationship is uncertain in humans[93]. Several lines of evidence from the current studies are in contrast with other particles that induce lung overload, as follows. In the current studies, the evidence for increases in lung tumors following antimony trioxide exposure was more apparent in mice than in rats with higher incidences and a predominance of malignant tumors in mice. In both species, there were increased incidences of lung neoplasms and/or nonneoplastic lesions at 3 mg/m^3, an exposure concentration that did not result in overload. In addition, there were no significant differences in the incidences or types of *Kras* or *Egfr* mutations in rat and mouse alveolar/bronchiolar adenomas and carcinomas from exposures that did and did not approach the threshold for pulmonary overload suggesting overload did not alter the mutation spectra of the observed neoplasms. Finally, antimony trioxide exposure resulted in genotoxicity in both the lung and blood of male and female mice. Collectively, these lines of evidence indicate that antimony trioxide displays at least some intrinsic toxicity, and that the observed lung tumors could not be explained only by the high lung burdens in the study animals. In addition, these studies demonstrated significantly increased toxicity and/or carcinogenicity at exposure concentrations as low as 3 mg/m^3, the lowest concentration tested.

Conclusions

Under the conditions of these 2-year inhalation studies, there was *some evidence of carcinogenic activity*[a] of antimony trioxide in male Wistar Han rats based on increased combined incidences of alveolar/bronchiolar adenoma or carcinoma in the lung and on increased incidences of benign pheochromocytoma of the adrenal medulla. There was *some evidence of carcinogenic activity* of antimony trioxide in female Wistar Han rats based on increased incidences of alveolar/bronchiolar adenoma in the lung and on increased combined incidences of benign or malignant pheochromocytoma of the adrenal medulla. The combined occurrence of cystic keratinizing epithelioma or squamous cell carcinoma in the lung may have been related to exposure. There was *clear evidence of carcinogenic activity* of antimony trioxide in male B6C3F1/N mice based on increased incidences of alveolar/bronchiolar carcinoma of the lung. Increases in the incidences of fibrous histiocytoma in the skin, as well as the combined incidences of fibrous histiocytoma or fibrosarcoma in the skin of male mice were also considered to be related to exposure. There was *clear evidence of carcinogenic activity* in female B6C3F1/N mice based on increases in the incidences of alveolar/bronchiolar adenoma and alveolar/bronchiolar carcinoma of the lung and on increased incidences of malignant lymphoma. The occurrence of squamous cell carcinoma of the skin may have been related to exposure.

Exposure to antimony trioxide resulted in increased incidences of nonneoplastic findings of the lung, nose, larynx, trachea, bronchial and mediastinal lymph nodes, and bone marrow of male and female rats and mice; the adrenal medulla, arteries of multiple tissues (mesentery, pancreas, mediastinum, kidney, and lung), kidney, and eye of male and female rats; the thymus and heart of male and female mice; the forestomach of male mice; and the spleen of female mice.

[a]See Explanation of Levels of Evidence of Carcinogenic Activity. See summary of the peer review panel comments and the public discussion on this Technical Report in Appendix L.

References

1. National Research Council (NRC). Toxicological Risk of Selected Flame-Retardant Chemicals. Washington, DC: National Academy Press; 2000.

2. Kuroda K, Endo G, Okamoto A, Yoo YS, Horiguchi S. Genotoxicity of beryllium, gallium and antimony in short-term assays. Mutat Res. 1991; 264(4):163-170. http://dx.doi.org/10.1016/0165-7992(91)90072-C

3. Agency for Toxic Substances and Disease Registry (ATSDR). Toxicological profile for antimony and compounds. Atlanta, GA: U.S. Public Health Service; 1992. http://www.atsdr.cdc.gov/toxprofiles/tp23.pdf

4. Antimony compounds. Environmental Defense: GoodGuide; 2005. [accessed June 29, 2015].

5. Anderson CG. The metallurgy of antimony. Chem Erde. 2012; 72:3-8. http://dx.doi.org/10.1016/j.chemer.2012.04.001

6. Hazardous Substances Data Bank (HSDB): Antimony trioxide database search. 2013. [accessed July 2, 2015] https://pubchem.ncbi.nlm.nih.gov/

7. High Density Packaging User Group International (HDPUGI). Environmental assessment of halogen-free printed circuit boards. Austin, TX: High Density Packaging User Group International Inc; 2005.

8. KEMI. Information on substances – Antimony trioxide. Sweden; 2015. https://web.archive.org/web/20140119053654/http://apps.kemi.se/flodessok/floden/kemamne_eng/antimon_eng.htm [Accessed May 21, 2015]

9. Murray HW, Berman JD, Davies CR, Saravia NG. Advances in leishmaniasis. Lancet. 2005; 366(9496):1561-1577. http://dx.doi.org/10.1016/S0140-6736(05)67629-5

10. Iyengar GV, Tanner JT, Wolf WR, Zeisler R. Preparation of a mixed human diet material for the determination of nutrient elements, selected toxic elements and organic nutrients: a preliminary report. Sci Total Environ. 1987; 61:235-252. http://dx.doi.org/10.1016/0048-9697(87)90371-8

11. Centers for Disease Control and Prevention (CDC). Third national report on human exposure to environmental chemicals. Atlanta, GA: Department of Health and Human Services, Centers for Disease Control and Prevention, National Center for Environmental Health; 2005. NCEH Publication No. 05 0570.

12. American Conference of Governmental Industrial Hygienist (ACGIH). 2015 TLVs® and BEIs® threshold limit values for chemical substances and physical agents and biological exposure indices. Cincinnati, OH: ACGIH; 2015.

13. National Institute for Occupational Safety and Health (NIOSH). NIOSH Pocket Guide to Chemical Hazards. Cincinnati, OH: U.S. Department of Health and Human Services, Public Health Service, Centers for Disease Control and Prevention; 2007.

14. United States Environmental Protection Agency (USEPA). Integrated Risk Information System (IRIS). United States Environmental Protection Agency (USEPA); 2014. http://www.epa.gov/iris/subst/0676.htm [Accessed June 29, 2015]

15. Leffler P, Gerhardsson L, Brune D, Nordberg GF. Lung retention of antimony and arsenic in hamsters after the intratracheal instillation of industrial dust. Scand J Work Environ Health. 1984; 10(4):245-251. http://dx.doi.org/10.5271/sjweh.2330

16. Newton PE, Bolte HF, Daly IW, Pillsbury BD, Terrill JB, Drew RT, Ben-Dyke R, Sheldon AW, Rubin LF. Subchronic and chronic inhalation toxicity of antimony trioxide in the rat. Fundam Appl Toxicol. 1994; 22(4):561-576. http://dx.doi.org/10.1006/faat.1994.1063

17. Felicetti SW, Thomas RG, McClellan RO. Retention of inhaled antimony-124 in the beagle dog as a function of temperature of aerosol formation. Health Phys. 1974; 26(6):515-531. http://dx.doi.org/10.1097/00004032-197406000-00006

18. Thomas RG, Felicetti SW, Lucchino RV, McClellan RO. Retention patterns of antimony in mice following inhalation of particles formed at different temperatures. Proc Soc Exp Biol Med. 1973; 144(2):544-550. http://dx.doi.org/10.3181/00379727-144-37632

19. Felicetti SA, Thomas RG, McClellan RO. Metabolism of two valence states of inhaled antimony in hamsters. Am Ind Hyg Assoc J. 1974; 35(5):292-300. http://dx.doi.org/10.1080/0002889748507037

20. Bailly R, Lauwerys R, Buchet JP, Mahieu P, Konings J. Experimental and human studies on antimony metabolism: Their relevance for the biological monitoring of workers exposed to inorganic antimony. Br J Ind Med. 1991; 48(2):93-97. http://dx.doi.org/10.1136/oem.48.2.93

21. Cooper DA, Pendergrass EP, Vorwald AJ, Mayock RL, Brieger H. Pneumoconiosis among workers in an antimony industry. Am J Roentgenol Radium Ther Nucl Med. 1968; 103(3):496-508. http://dx.doi.org/10.2214/ajr.103.3.495

22. Lüdersdorf R, Fuchs A, Mayer P, Skulsuksai G, Schacke G. Biological assessment of exposure to antimony and lead in the glass-producing industry. Int Arch Occup Environ Health. 1987; 59(5):469-474. http://dx.doi.org/10.1007/BF00377841

23. McCallum RI. The work of an occupational hygiene service in environmental control. Ann Occup Hyg. 1963; 6:55-64.

24. Gerhardsson L, Brune D, Nordberg GF, Wester PO. Antimony in lung, liver and kidney tissue from deceased smelter workers. Scand J Work Environ Health. 1982; 8(3):201-208. http://dx.doi.org/10.5271/sjweh.2475

25. Vanoeteren C, Cornelis R, Versieck J. Evaluation of trace elements in human lung tissue. I. Concentration and distribution. Sci Total Environ. 1986; 54:217-230. http://dx.doi.org/10.1016/0048-9697(86)90267-6

26. Vanoeteren C, Cornelis R, Dams R. Evaluation of trace elements in human lung tissue. II. Recovery and analysis of inhaled particulates. Sci Total Environ. 1986; 54:231-236. http://dx.doi.org/10.1016/0048-9697(86)90268-8

27. Vanoeteren C, Cornelis R, Verbeeck P. Evaluation of trace elements in human lung tissue. III. Correspondence analysis. Sci Total Environ. 1986; 54:237-245. http://dx.doi.org/10.1016/0048-9697(86)90269-X

28. Hext PM, Pinto PJ, Rimmel BA. Subchronic feeding study of antimony trioxide in rats. J Appl Toxicol. 1999; 19(3):205-209. https://doi.org/10.1002/(SICI)1099-1263(199905/06)19:3<205::AID-JAT567>3.0.CO;2-X

29. McCallum RI. Detection of antimony in process workers' lungs by x-radiation. Trans Soc Occup Med. 1967; 17(4):134-138. http://dx.doi.org/10.1093/occmed/17.4.134

30. Potkonjak V, Pavlovich M. Antimoniosis: A particular form of pneumoconiosis. I. Etiology, clinical and X-ray findings. Int Arch Occup Environ Health. 1983; 51(3):199-207. http://dx.doi.org/10.1007/BF00377752

31. McCallum RI, Day MJ, Underhill J, Aird EG. Measurement of antimony oxide dust in human lungs in vivo by X-ray spectrophotometry. Inhaled Part. 1970; 2:611-619.

32. Lauwers LF, Roelants A, Rosseel PM, Heyndrickx B, Baute L. Oral antimony intoxications in man. Crit Care Med. 1990; 18(3):324-326. http://dx.doi.org/10.1097/00003246-199003000-00017

33. Belyaeva AP. [The effect of antimony on reproduction (in Russian)]. Gig Truda Prof Zabol. 1967; 11:32-37.

34. Omura M, Tanaka A, Hirata M, Inoue N. Testicular toxicity evaluation of two antimony compounds, antimony trioxide and antimony potassium tartrate, in rats and mice. Environ Health Prev Med. 2002; 7:15-18. http://dx.doi.org/10.1007/BF02898061

35. Groth DH, Stettler LE, Burg JR, Busey WM, Grant GC, Wong L. Carcinogenic effects of antimony trioxide and antimony ore concentrate in rats. J Toxicol Environ Health. 1986; 18(4):607-626. http://dx.doi.org/10.1080/15287398609530898

36. Elliott BM, Mackay JM, Clay P, Ashby J. An assessment of the genetic toxicology of antimony trioxide. Mutat Res. 1998; 415(1-2):109-117. http://dx.doi.org/10.1016/S1383-5718(98)00065-5

37. Kanematsu N, Hara M, Kada T. Rec assay and mutagenicity studies on metal compounds. Mutat Res. 1980; 77(2):109-116. http://dx.doi.org/10.1016/0165-1218(80)90127-5

38. Gebel T, Christensen S, Dunkelberg H. Comparative and environmental genotoxicity of antimony and arsenic. Anticancer Res. 1997; 17(4a):2603-2607.

39. Kirkland D, Whitwell J, Deyo J, Serex T. Failure of antimony trioxide to induce micronuclei or chromosomal aberrations in rat bone-marrow after sub-chronic oral dosing. Mutat Res. 2007; 627(2):119-128. http://dx.doi.org/10.1016/j.mrgentox.2006.10.012

40. Cavallo D, Iavicoli I, Setini A, Marinaccio A, Perniconi B, Carelli G, Iavicoli S. Genotoxic risk and oxidative DNA damage in workers exposed to antimony trioxide. Environ Mol Mutag. 2002; 40(3):184-189. http://dx.doi.org/10.1002/em.10102

41. Griffis LC, Wolff RK, Beethe RL, Hobbs CH, McClellan RO. Evaluation of a multitiered inhalation exposure chamber. Fundam Appl Toxicol. 1981; 1(1):8-12. http://dx.doi.org/10.1093/toxsci/1.1.8

42. Hill MA, Watson CR, Moss OR. NEWCAS - An interactive computer program for particle size analysis. Richland, WA: Pacific Northwest Laboratory; 1977. PNL-2405, UC-32.

43. Lewis TR, Morrow PE, McClellan RO, Raabe OG, Kennedy GL, Schwetz BA, Goehl TJ, Roycroft JH, Chhabra RS. Establishing aerosol exposure concentrations for inhalation toxicity studies. Toxicol Appl Pharmacol. 1989; 99(3):377-383. http://dx.doi.org/10.1016/0041-008X(89)90147-6

44. King-Herbert A, Thayer K. NTP Workshop: Animal models for the NTP rodent cancer bioassay: Stocks and strains–Should we switch? Toxicol Pathol. 2006; 34(6):802-805. http://dx.doi.org/10.1080/01926230600935938

45. Maronpot RR, Boorman GA. Interpretation of rodent hepatocellular proliferative alterations and hepatocellular tumors in chemical safety assessment. Toxicol Pathol. 1982; 10(2):71-78. http://dx.doi.org/10.1177/019262338201000210

46. Boorman GA, Montgomery CA, Jr., Eustis SL, Wolfe MJ, McConnell EE, Hardisty JF. Quality assurance in pathology for rodent carcinogenicity studies In: Milman HA, Weisburger EK, editors. Handbook of Carcinogen Testing. Park Ridge, NJ: Noyes Publications; 1985. p. 345-357.

47. McConnell EE, Solleveld HA, Swenberg JA, Boorman GA. Guidelines for combining neoplasms for evaluation of rodent carcinogenesis studies. J Natl Cancer Inst. 1986; 76(2):283-289.

48. Kaplan EL, Meier P. Nonparametric estimation from incomplete observations. J Am Stat Assoc. 1958; 53(282):457-481. http://dx.doi.org/10.1080/01621459.1958.10501452

49. Cox DR. Regression models and life-tables. J R Stat Soc. 1972; B34(2):187-220.

50. Tarone RE. Tests for trend in life table analysis. Biometrika. 1975; 62(3):679-690. http://dx.doi.org/10.1093/biomet/62.3.679

51. Bailer AJ, Portier CJ. Effects of treatment-induced mortality and tumor-induced mortality on tests for carcinogenicity in small samples. Biometrics. 1988; 44(2):417-431. http://dx.doi.org/10.2307/2531856

52. Piegorsch WW, Bailer AJ. Statistics for Environmental Biology and Toxicology, Section 6.3.2. London, UK: Chapman and Hall; 1997.

53. Portier CJ, Bailer AJ. Testing for increased carcinogenicity using a survival-adjusted quantal response test. Fundam Appl Toxicol. 1989; 12(4):731-737. http://dx.doi.org/10.1016/0272-0590(89)90004-3

54. Portier CJ, Hedges JC, Hoel DG. Age-specific models of mortality and tumor onset for historical control animals in the National Toxicology Program's carcinogenicity experiments. Cancer Res. 1986; 46(9):4372-4378.

55. Bieler GS, Williams RL. Ratio estimates, the delta method, and quantal response tests for increased carcinogenicity. Biometrics. 1993; 49(3):793-801. http://dx.doi.org/10.2307/2532200

56. Gart JJ, Chu KC, Tarone RE. Statistical issues in interpretation of chronic bioassay tests for carcinogenicity. J Natl Cancer Inst. 1979; 62(4):957-974.

57. Dunnett CW. A multiple comparison procedure for comparing several treatments with a control. J American Stat Assoc. 1955; 50(272):1096-1121. http://dx.doi.org/10.1080/01621459.1955.10501294

58. Williams DA. The comparison of several dose levels with a zero dose control. Biometrics. 1972; 28(2):519-531. http://dx.doi.org/10.2307/2556164

59. Williams DA. A test for differences between treatment means when several dose levels are compared with a zero dose control. Biometrics. 1971; 27(1):103-117. http://dx.doi.org/10.2307/2528930

60. Dixon WJ, Massey FJ, Jr. Introduction to statistical analysis, 2nd ed. New York, NY: McGraw Hill Book Company Inc; 1957. http://dx.doi.org/10.2307/2332898

61. Haseman JK. Data analysis: Statistical analysis and use of historical control data. Regul Toxicol Pharmacol. 1995; 21(1):52-59; discussion 81-86. http://dx.doi.org/10.1006/rtph.1995.1009

62. Haseman JK, Rao GN. Effects of corn oil, time-related changes, and inter-laboratory variability on tumor occurrence in control Fischer 344 (F344/N) rats. Toxicol Pathol. 1992; 20(1):52-60. http://dx.doi.org/10.1177/019262339202000107

63. Haseman JK. Value of historical controls in the interpretation of rodent tumor data. Drug Inf J. 1992; 26(2):191-200. http://dx.doi.org/10.1177/009286159202600210

64. Code of Federal Regulations (CFR). 21:Part 58.

65. Heddle JA, Hite M, Kirkhart B, Mavournin K, MacGregor JT, Newell GW, Salamone MF. The induction of micronuclei as a measure of genotoxicity. A report of the U.S. Environmental Protection Agency Gene-Tox Program. Mutat Res. 1983; 123(1):61-118. http://dx.doi.org/10.1016/0165-1110(83)90047-7

66. Schmid W. The micronucleus test. Mutat Res. 1975; 31(1):9-15. http://dx.doi.org/10.1016/0165-1161(75)90058-8

67. Miller JA, Miller EC. Ultimate chemical carcinogens as reactive mutagenic electrophiles In: Hiatt HH, Watson JD, Winsten JA, editors. Origins of Human Cancer. Cold Spring Harbor, NY: Cold Spring Harbor Laboratory; 1977. p. 605-627.

68. Crawford BD. Perspectives on the somatic mutation model of carcinogenesis In: Mehlman MA, Flamm WG, Lorentzen RJ, editors. Advances in Modern Environmental Toxicology Mechanisms and Toxicity of Chemical Carcinogens and Mutagens. Princeton, NJ: Princton Scientific Publishing Co. Inc.; 1985. p. 13-59.

69. Straus DS. Somatic mutation, cellular differentiation, and cancer causation. J Natl Cancer Inst. 1981; 67(2):233-241.

70. Witt KL, Knapton A, Wehr CM, Hook GJ, Mirsalis J, Shelby MD, MacGregor JT. Micronucleated erythrocyte frequency in peripheral blood of B6C3F1 mice from short-term, prechronic, and chronic studies of the NTP carcinogenesis bioassay program. Environ Mol Mutag. 2000; 36(3):163-194. https://doi.org/10.1002/1098-2280(2000)36:3<163::AID-EM1>3.0.CO;2-P

71. Sasaki YF, Sekihashi K, Izumiyama F, Nishidate E, Saga A, Ishida K, Tsuda S. The comet assay with multiple mouse organs: comparison of comet assay results and carcinogenicity with 208 chemicals selected from the IARC monographs and U.S. NTP Carcinogenicity Database. Crit Rev Toxicol. 2000; 30(6):629-799. http://dx.doi.org/10.1080/10408440008951123

72. Greaves P. Histopathology of Preclinical Toxicity Studies, 4th ed. London, UK: Academic Press; 2012.

73. Whalen JE, Foureman GL, Vandenberg JJ. Inhalation Risk Assessment at the Environmental Protection Agency In: Salem H, Katz SA, editors. Inhalation Toxicology, 2nd ed. Boca Raton, FL: CRC Press Taylor and Francis Group; 2006. p. 3-38.

74. Morrow PE. Possible mechanisms to explain dust overloading of the lungs. Fundam Appl Toxicol. 1988; 10(3):369-384. http://dx.doi.org/10.1016/0272-0590(88)90284-9

75. Morrow PE. Dust overloading of the lungs: Update and appraisal. Toxicol Appl Pharmacol. 1992; 113(1):1-12. http://dx.doi.org/10.1016/0041-008X(92)90002-A

76. Tran CL, Buchanan D, Cullen RT, Searl A, Jones AD, Donaldson K. Inhalation of poorly soluble particles. II. Influence Of particle surface area on inflammation and clearance. Inhal Toxicol. 2000; 12(12):1113-1126. http://dx.doi.org/10.1080/08958370050166796

77. Howroyd P, Allison N, Foley JF, Hardisty J. Apparent alveolar bronchiolar tumors arising in the mediastinum of F344 rats. Toxicol Pathol. 2009; 37(3):351-358. http://dx.doi.org/10.1177/0192623309332988

78. Boorman GA, Brockmann M, Carlton WW, Davis JM, Dungworth DL, Hahn FF, Mohr U, Reichhelm HB, Turusov VS, Wagner BM. Classification of cystic keratinizing squamous lesions of the rat lung: report of a workshop. Toxicol Pathol. 1996; 24(5):564-572. http://dx.doi.org/10.1177/019262339602400505

79. National Toxicology Program (NTP). Toxicology and Carcinogenesis Studies of Talc (CAS No. 14807-96-6) in F344/N Rats and B6C3F1 Mice (Inhalation Studies). Research Triangle Park, NC: U.S. Department of Health and Human Services, Public Health Service, National Institutes of Health; 1993. Technical Report Series No. 421. NIH Publication No. 93-3152.

80. National Toxicology Program (NTP). Toxicology and Carcinogenesis Studies of Nickel Subsulfide (CAS No. 12035-72-2) in F344/N Rats and B6C3F1 Mice (Inhalation Studies). Research Triangle Park, NC: U.S. Department of Health and Human Services, Public Health Service, National Institutes of Health; 1996. Technical Report Series No. 453. NIH Publication No. 96-3369.

81. National Toxicology Program (NTP). Toxicology and Carcinogenesis Studies of Nickel Sulfate Hexahydrate (CAS No. 10101-97-0) in F344/N Rats and B6C3F1 Mice (Inhalation Studies). Research Triangle Park, NC: U.S. Department of Health and Human Services, Public Health Service, National Institutes of Health; 1996. Technical Report Series No. 454. NIH Publication No. 96-3370.

82. National Toxicology Program (NTP). Toxicology and Carcinogenesis Studies of Molybdenum Trioxide (CAS No. 1313-27-5) in F344/N Rats and B6C3F1 Mice (Inhalation Studies). Research Triangle Park, NC: U.S. Department of Health and Human Services, Public Health Service, National Institutes of Health; 1997. Technical Report Series No. 462. NIH Publication No. 97-3378.

83. National Toxicology Program (NTP). Toxicology and Carcinogenesis Studies of Cobalt Sulfate Heptahydrate (CAS No. 10026-24-1) in F344/N Rats and B6C3F1 Mice (Inhalation Studies). Research Triangle Park, NC: U.S. Department of Health and Human Services, Public Health Service, National Institutes of Health; 1998. Technical Report Series No. 471. NIH Publication No. 98-3961.

84. National Toxicology Program (NTP). Toxicology and Carcinogenesis Studies of Gallium Arsenide (CAS No. 1303-00-0) in F344/N Rats and B6C3F1 Mice (Inhalation Studies). Research Triangle Park, NC: U.S. Department of Health and Human Services, Public Health Service, National Institutes of Health; 2000. Technical Report Series No. 492. NIH Publication No. 00-3951.

85. National Toxicology Program (NTP). Toxicology and Carcinogenesis Studies of Indium Phosphide (CAS No. 22398-80-7) in F344/N Rats and B6C3F1 Mice (Inhalation Studies). Research Triangle Park, NC: U.S. Department of Health and Human Services, Public Health Service, National Institutes of Health; 2001. Technical Report Series No. 499. NIH Publication No. 01-4433.

86. National Toxicology Program (NTP). Toxicology Studies of Cobalt Metal (CAS No. 7440-48-4) in F344/N Rats and B6C3F1/N Mice and Toxicology and Carcinogenesis Studies of Cobalt Metal in F344/NTac Rats and B6C3F1/N Mice (Inhalation Studies). Research Triangle Park, NC: National Institutes of Health, Public Health Service, U.S. Department of Health and Human Services; 2014. Technical Report Series No. 581.

87. Ozaki K, Haseman JK, Hailey JR, Maronpot RR, Nyska A. Association of adrenal pheochromocytoma and lung pathology in inhalation studies with particulate compounds in the male F344 rat--the National Toxicology Program experience. Toxicol Pathol. 2002; 30(2):263-270. http://dx.doi.org/10.1080/019262302753559605

88. Teixeira L, Dubielzig RR. Chapter 53 - Eye. In: Haschek WM, Rousseaux CG, Wallig MA, editors. Haschek and Rosseaux's Handbook of Toxicologic Pathology, Volume 3, 3rd ed. Boston, MA: Elsevier; 2013. p. 2095-2185. http://dx.doi.org/10.1016/B978-0-12-415759-0.00053-4

89. Moyer CF, Kodavanti UP, Haseman JK, Costa DL, Nyska A. Systemic vascular disease in male B6C3F1 mice exposed to particulate matter by inhalation: Studies conducted by the

National Toxicology Program. Toxicol Pathol. 2002; 30(4):427-434. http://dx.doi.org/10.1080/01926230290105631

90. Frazier KS, Seely JC, Hard GC, Betton G, Burnett R, Nakatsuji S, Nishikawa A, Durchfeld-Meyer B, Bube A. Proliferative and nonproliferative lesions of the rat and mouse urinary system. Toxicol Pathol. 2012; 40(4 Suppl):14S-86S. http://dx.doi.org/10.1177/0192623312438736

91. Cooper RG, Harrison AP. The exposure to and health effects of antimony. Indian J Occup Environ Med. 2009; 13(1):3-10. http://dx.doi.org/10.4103/0019-5278.50716

92. Sundar S, Chakravarty J. Antimony toxicity. Int J Env Res Public Health. 2010; 7(12):4267-4277. http://dx.doi.org/10.3390/ijerph7124267

93. ILSI Risk Science Institute. The relevance of the rat lung response to particle overload for human risk assessment: A workshop consensus report. Inhal Toxicol. 2000; 12(1-2):1-17. http://dx.doi.org/10.1080/08958370050029725

94. Torous DK, Hall NE, Illi-Love AH, Diehl MS, Cederbrant K, Sandelin K, Ponten I, Bolcsfoldi G, Ferguson LR, Pearson A et al. Interlaboratory validation of a CD71-based flow cytometric method (Microflow) for the scoring of micronucleated reticulocytes in mouse peripheral blood. Environ Mol Mutag. 2005; 45(1):44-55. http://dx.doi.org/10.1002/em.20081

95. Witt KL, Livanos E, Kissling GE, Torous DK, Caspary W, Tice RR, Recio L. Comparison of flow cytometry- and microscopy-based methods for measuring micronucleated reticulocyte frequencies in rodents treated with nongenotoxic and genotoxic chemicals. Mutat Res. 2008; 649(1-2):101-113. http://dx.doi.org/10.1016/j.mrgentox.2007.08.004

96. Dertinger SD, Camphausen K, Macgregor JT, Bishop ME, Torous DK, Avlasevich S, Cairns S, Tometsko CR, Menard C, Muanza T et al. Three-color labeling method for flow cytometric measurement of cytogenetic damage in rodent and human blood. Environ Mol Mutag. 2004; 44(5):427-435. http://dx.doi.org/10.1002/em.20075

97. MacGregor JT, Bishop ME, McNamee JP, Hayashi M, Asano N, Wakata A, Nakajima M, Saito J, Aidoo A, Moore MM et al. Flow cytometric analysis of micronuclei in peripheral blood reticulocytes: II. An efficient method of monitoring chromosomal damage in the rat. Toxicol Sci. 2006; 94(1):92-107. http://dx.doi.org/10.1093/toxsci/kfl076

98. Kissling GE, Dertinger SD, Hayashi M, MacGregor JT. Sensitivity of the erythrocyte micronucleus assay: Dependence on number of cells scored and inter-animal variability. Mutat Res. 2007; 634(1-2):235-240. http://dx.doi.org/10.1016/j.mrgentox.2007.07.010

99. Recio L, Hobbs C, Caspary W, Witt KL. Dose-response assessment of four genotoxic chemicals in a combined mouse and rat micronucleus (MN) and Comet assay protocol. J Toxicol Sci. 2010; 35(2):149-162. http://dx.doi.org/10.2131/jts.35.149

100. Tice RR, Agurell E, Anderson D, Burlinson B, Hartmann A, Kobayashi H, Miyamae Y, Rojas E, Ryu J-C, Sasaki YF. Single cell gel/comet assay: guidelines for in vitro and in vivo genetic toxicology testing. Environ Mol Mutag. 2000; 35(3):206-221. http://dx.doi.org/10.1002/(SICI)1098-2280(2000)35:3<206::AID-EM8>3.0.CO;2-J

101. Ghanayem BI, Witt KL, Kissling GE, Tice RR, Recio L. Absence of acrylamide-induced genotoxicity in CYP2E1-null mice: Evidence consistent with a glycidamide-mediated effect. Mutat Res. 2005; 578(1-2):284-297. http://dx.doi.org/10.1016/j.mrfmmm.2005.05.004

102. Burlinson B, Tice RR, Speit G, Agurell E, Brendler-Schwaab SY, Collins AR, Escobar P, Honma M, Kumaravel TS, Nakajima M et al. Fourth International Workgroup on Genotoxicity testing: Results of the in vivo Comet assay workgroup. Mutat Res. 2007; 627(1):31-35. http://dx.doi.org/10.1016/j.mrgentox.2006.08.011

103. Mann HB, Whitney DR. On a test of whether one of two random variables is stochastically larger than the other. Ann Math Statist. 1947; 18(1):50-60. http://dx.doi.org/10.1214/aoms/1177730491

104. Kendall MG. A new measure of rank correlation. Biometrika. 1938; 30(1/2):81-93. http://dx.doi.org/10.2307/2332226

105. Bolton RE, Vincent JH, Jones AD, Addison J, Beckett ST. An overload hypothesis for pulmonary clearance of UICC amosite fibres inhaled by rats. Br J Ind Med. 1983; 40(3):264-272. http://dx.doi.org/10.1136/oem.40.3.264

106. Mauderly JL. Lung overload: The dilemma and opportunities for resolution In: Mauderly JL, McCuinney RJ, editors. Particle Overload in the Rat Lung and Lung Cancer: Implications for Human Risk Assessmen. Washington, DC: Taylor and Francis; 1995. p. 1-28.

107. Lehnert BE, Morrow PE. Characteristics of alveolar macrophages following the deposition of a low burden or iron oxide in the lung. J Toxicol Environ Health. 1985; 16(6):855-868. http://dx.doi.org/10.1080/15287398509530793

108. Lehnert BE, Morrow PE. Association of 59iron oxide with alveolar macrophages during alveolar clearance. Exp Lung Res. 1985; 9(1-2):1-16. http://dx.doi.org/10.3109/01902148509061524

109. Masse R, Fritsch P, Nolike D, LaFuma J, Chretien J. Cytokinetic study of alveolar macrophage renewal in rats In: Sanders CL, Snieder RP, Doyle GE, Ragan HA, editors. Pulmonary Macrophage and Epithelial Cells. Washington, DC: Energy Research and Development Administration, Technical Information Center; 1977. p. 106-114.

110. Crapo JD, Barry BE, Foscue HA, Shelburne J. Structural and biochemical changes in rat lungs occurring during exposures to lethal and adaptive doses of oxygen. Am Rev Respir Dis. 1980; 122(1):123-143.

111. Boch C, Kollmeier J, Roth A, Stephan-Falkenau S, Misch D, Gruning W, Bauer TT, Mairinger T. The frequency of EGFR and KRAS mutations in non-small cell lung cancer (NSCLC): Routine screening data for central Europe from a cohort study. BMJ Open. 2013; 3(4): e002560. http://dx.doi.org/10.1136/bmjopen-2013-002560

112. Ellis CA, Clark G. The importance of being K-Ras. Cell Signal. 2000; 12(7):425-434. http://dx.doi.org/10.1016/S0898-6568(00)00084-X

113. Roberts PJ, Der CJ. Targeting the Raf-MEK-ERK mitogen-activated protein kinase cascade for the treatment of cancer. Oncogene. 2007; 26(22):3291-3310. http://dx.doi.org/10.1038/sj.onc.1210422

114. Johnson BE, Janne PA. Epidermal growth factor receptor mutations in patients with non-small cell lung cancer. Cancer Res. 2005; 65(17):7525-7529. http://dx.doi.org/10.1158/0008-5472.CAN-05-1257

115. Baan RA. Carcinogenic hazards from inhaled carbon black, titanium dioxide, and talc not containing asbestos or asbestiform fibers: recent evaluations by an IARC Monographs Working Group. Inhal Toxicol. 2007; 19 Suppl 1:213-228. http://dx.doi.org/10.1080/08958370701497903

116. Hong H-HL, Ton T-VT, Kim Y, Wakamatsu N, Clayton NP, Chan P-C, Sills RC, Lahousse SA. Genetic alterations in K-ras and p53 cancer genes in lung neoplasms from B6C3F1 mice exposed to cumene. Toxicol Pathol. 2008; 36(5):720-726. http://dx.doi.org/10.1177/0192623308320280

117. Eberhard DA, Johnson BE, Amler LC, Goddard AD, Heldens SL, Herbst RS, Ince WL, Janne PA, Januario T, Johnson DH et al. Mutations in the epidermal growth factor receptor and in KRAS are predictive and prognostic indicators in patients with non-small-cell lung cancer treated with chemotherapy alone and in combination with erlotinib. J Clin Oncol. 2005; 23(25):5900-5909. http://dx.doi.org/10.1200/JCO.2005.02.857

118. Shigematsu H, Lin L, Takahashi T, Nomura M, Suzuki M, Wistuba, II, Fong KM, Lee H, Toyooka S, Shimizu N et al. Clinical and biological features associated with epidermal growth factor receptor gene mutations in lung cancers. J Natl Cancer Inst. 2005; 97(5):339-346. http://dx.doi.org/10.1093/jnci/dji055

119. Blons H, Cote JF, Le Corre D, Riquet M, Fabre-Guilevin E, Laurent-Puig P, Danel C. Epidermal growth factor receptor mutation in lung cancer are linked to bronchioloalveolar differentiation. Am J Surg Pathol. 2006; 30(10):1309-1315. http://dx.doi.org/10.1097/01.pas.0000213285.65907.31

Appendix A. Summary of Lesions in Male Rats in the Two-year Inhalation Study of Antimony Trioxide

Tables

Table A-1. Summary of the Incidence of Neoplasms in Male Rats in the Two-year Inhalation Study of Antimony Trioxide A-2
Table A-2. Statistical Analysis of Primary Neoplasms in Male Rats in the Two-year Inhalation Study of Antimony Trioxide A-9
Table A-3. Historical Incidence of Alveolar/Bronchiolar Neoplasms in Control Male Wistar Han Rats A-13
Table A-4. Historical Incidence of Pheochromocytoma of the Adrenal Medulla in Control Male Wistar Han Rats A-13
Table A-5. Summary of the Incidence of Nonneoplastic Lesions in Male Rats in the Two-year Inhalation Study of Antimony Trioxide A-14

Table A-1. Summary of the Incidence of Neoplasms in Male Rats in the Two-year Inhalation Study of Antimony Trioxide[a]

	Chamber Control	3 mg/m^3	10 mg/m^3	30 mg/m^3
Disposition Summary				
Animals initially in study	60	60	60	60
Twelve-month interim evaluation	10	10	10	10
Early deaths				
Moribund	15	19	22	29
Natural deaths	5	1	–	3
Survivors				
Terminal kill	30	30	28	18
Animals examined microscopically	60	60	60	60
Twelve-month Interim Evaluation				
Hematopoietic System				
Bone marrow	(10)	(10)	(10)	(10)
Lymph node, bronchial	(9)	(8)	(10)	(10)
Lymph node, mandibular	(10)	(9)	(9)	(8)
Lymph node, mediastinal	(10)	(8)	(10)	(9)
Lymph node, mesenteric	(10)	(10)	(10)	(10)
Hemangiosarcoma	–	–	–	1 (10%)
Spleen	(10)	(10)	(10)	(10)
Thymus	(10)	(10)	(10)	(10)
Systems Examined at 12 Months with No Neoplasms Observed				
Alimentary System				
Cardiovascular System				
Endocrine System				
General Body System				
Genital System				
Integumentary System				
Musculoskeletal System				
Nervous System				
Respiratory System				
Special Senses System				
Urinary System				
Two-year Study				
Alimentary System				
Esophagus	(50)	(50)	(50)	(50)

	Chamber Control	3 mg/m^3	10 mg/m^3	30 mg/m^3
Intestine large, cecum	(49)	(50)	(50)	(49)
Intestine large, colon	(50)	(50)	(50)	(50)
Intestine large, rectum	(44)	(49)	(48)	(48)
Carcinoma	–	–	1 (2%)	–
Intestine small, duodenum	(47)	(50)	(50)	(49)
Sarcoma, metastatic, tissue NOS	–	–	–	1 (2%)
Intestine small, ileum	(48)	(50)	(50)	(49)
Leiomyosarcoma	–	–	1 (2%)	–
Intestine small, jejunum	(46)	(49)	(50)	(48)
Liver	(50)	(50)	(50)	(50)
Hepatocellular adenoma		2 (4%)	1 (2%)	–
Leiomyosarcoma, metastatic, intestine small, ileum	–	–	1 (2%)	–
Mesentery	(50)	(50)	(50)	(50)
Hemangiosarcoma, metastatic, pancreas	–	–	–	1 (2%)
Leiomyosarcoma, metastatic, intestine small, ileum	–	–	1 (2%)	–
Sarcoma, metastatic, tissue NOS	–	–	–	1 (2%)
Pancreas	(50)	(50)	(50)	(50)
Hemangiosarcoma	–	–	–	1 (2%)
Sarcoma, metastatic, tissue NOS	–	–	–	1 (2%)
Salivary glands	(50)	(50)	(50)	(50)
Myoepithelioma	1 (2%)	–	–	–
Schwannoma malignant	–	–	–	1 (2%)
Stomach, forestomach	(50)	(50)	(50)	(50)
Sarcoma, metastatic, tissue NOS	–	–	–	1 (2%)
Stomach, glandular	(50)	(50)	(50)	(50)
Tongue	(1)	(1)	(0)	(1)
Squamous cell papilloma	–	1 (100%)	–	–
Tooth	(2)	(1)	(1)	(1)
Cardiovascular System				
Blood vessel	(50)	(50)	(50)	(49)
Heart	(50)	(50)	(50)	(50)
Schwannoma malignant	–	–	1 (2%)	–
Endocardium, schwannoma NOS	1 (2%)	–	–	–

	Chamber Control	3 mg/m^3	10 mg/m^3	30 mg/m^3
Endocrine System				
Adrenal cortex	(50)	(50)	(50)	(50)
Adenoma	3 (6%)	–	3 (6%)	–
Carcinoma	–	–	1 (2%)	–
Adrenal medulla	(49)	(50)	(49)	(50)
Ganglioneuroma	–	1 (2%)	–	–
Pheochromocytoma benign	1 (2%)	–	2 (4%)	7 (14%)
Pheochromocytoma complex	1 (2%)	–	–	–
Islets, pancreatic	(50)	(50)	(50)	(49)
Adenoma	–	1 (2%)	4 (8%)	1 (2%)
Carcinoma	–	–	–	1 (2%)
Parathyroid gland	(44)	(46)	(46)	(48)
Adenoma	–	–	1 (2%)	–
Pituitary gland	(50)	(50)	(50)	(50)
Pars distalis, adenoma	14 (28%)	15 (30%)	12 (24%)	5 (10%)
Pars intermedia, adenoma	1 (2%)	–	–	2 (4%)
Thyroid gland	(50)	(50)	(50)	(50)
Bilateral, c-cell, adenoma	–	–	–	1 (2%)
C-cell, adenoma	5 (10%)	9 (18%)	5 (10%)	3 (6%)
C-cell, adenoma, multiple	–	–	–	1 (2%)
C-cell, carcinoma	1 (2%)	1 (2%)	–	–
Follicular cell, adenoma	–	1 (2%)	2 (4%)	–
Follicular cell, carcinoma	–	1 (2%)	–	–
General Body System				
Tissue NOS	(0)	(1)	(0)	(1)
Sarcoma	–	–	–	1 (100%)
Mediastinum, carcinoma	–	1 (100%)	–	–
Genital System				
Coagulating gland	(0)	(0)	(0)	(1)
Epididymis	(50)	(50)	(50)	(50)
Sarcoma	–	–	–	1 (2%)
Preputial gland	(50)	(50)	(50)	(50)
Prostate	(50)	(50)	(50)	(50)
Adenoma	1 (2%)	1 (2%)	2 (4%)	2 (4%)
Carcinoma	–	1 (2%)	–	–

	Chamber Control	3 mg/m^3	10 mg/m^3	30 mg/m^3
Sarcoma, metastatic, tissue NOS	–	–	–	1 (2%)
Seminal vesicle	(50)	(50)	(50)	(50)
Adenoma	–	–	1 (2%)	–
Carcinoma, metastatic, prostate	–	1 (2%)	–	–
Hemangioma	–	1 (2%)	–	–
Testes	(50)	(50)	(50)	(50)
Hemangiosarcoma	1 (2%)	–	–	–
Interstitial cell, adenoma	6 (12%)	2 (4%)	1 (2%)	1 (2%)
Hematopoietic System				
Bone marrow	(50)	(50)	(50)	(50)
Lymph node	(2)	(4)	(7)	(7)
Lumbar, hemangiosarcoma	–	1 (25%)	–	–
Lymph node, bronchial	(41)	(40)	(48)	(47)
Lymph node, mandibular	(45)	(46)	(48)	(45)
Carcinoma, metastatic, thyroid gland	1 (2%)	–	–	–
Lymph node, mediastinal	(42)	(45)	(49)	(49)
Carcinoma, metastatic, thyroid gland	1 (2%)	–	–	–
Hemangioma	–	–	1 (2%)	–
Lymph node, mesenteric	(50)	(50)	(50)	(50)
Hemangioma	1 (2%)	–	2 (4%)	–
Hemangiosarcoma	2 (4%)	2 (4%)	4 (8%)	1 (2%)
Hemangiosarcoma, metastatic, pancreas	–	–	–	1 (2%)
Leiomyosarcoma, metastatic, intestine small, ileum	–	–	1 (2%)	–
Sarcoma, metastatic, epididymis	–	–	–	1 (2%)
Spleen	(50)	(50)	(50)	(50)
Hemangiosarcoma	–	–	–	1 (2%)
Thymus	(41)	(35)	(47)	(45)
Thymoma benign	3 (7%)	–	1 (2%)	4 (9%)
Thymoma malignant	–	1 (3%)	–	–
Integumentary System				
Mammary gland	(6)	(9)	(7)	(8)
Skin	(50)	(50)	(50)	(50)
Hemangioma	–	–	–	1 (2%)
Keratoacanthoma	1 (2%)	1 (2%)	–	–

	Chamber Control	3 mg/m^3	10 mg/m^3	30 mg/m^3
Trichoepithelioma	–	1 (2%)	–	–
Pinna, neural crest tumor, benign	–	–	1 (2%)	–
Sebaceous gland, adenoma	–	1 (2%)	–	–
Subcutaneous tissue, fibroma	2 (4%)	–	2 (4%)	–
Subcutaneous tissue, fibrosarcoma	–	–	–	1 (2%)
Subcutaneous tissue, hemangiosarcoma	–	1 (2%)	–	–
Subcutaneous tissue, schwannoma malignant	–	–	1 (2%)	1 (2%)
Musculoskeletal System				
Bone	(50)	(50)	(50)	(50)
Maxilla, osteosarcoma	–	–	1 (2%)	–
Skeletal muscle	(4)	(3)	(3)	(5)
Fibrosarcoma, metastatic, skin	–	–	–	1 (20%)
Sarcoma	–	–	–	1 (20%)
Sarcoma, metastatic, tissue NOS	–	–	–	1 (20%)
Nervous System				
Brain	(50)	(50)	(50)	(50)
Glioma malignant	–	–	1 (2%)	–
Glioma NOS	–	–	–	1 (2%)
Granular cell tumor benign	1 (2%)	1 (2%)	1 (2%)	1 (2%)
Neurocytoma	–	–	1 (2%)	–
Peripheral nerve	(3)	(3)	(2)	(0)
Spinal cord	(3)	(3)	(1)	(0)
Glioma NOS	–	1 (33%)	–	–
Respiratory System				
Larynx	(50)	(50)	(50)	(50)
Carcinoma, metastatic, thyroid gland	1 (2%)	–	–	–
Lung	(50)	(50)	(50)	(50)
Alveolar/bronchiolar adenoma	3 (6%)	3 (6%)	6 (12%)	5 (10%)
Alveolar/bronchiolar adenoma, multiple	–	1 (2%)	–	3 (6%)
Alveolar/bronchiolar carcinoma	–	–	1 (2%)	–
Carcinoma, metastatic, thyroid gland	1 (2%)	–	–	–
Fibrosarcoma, metastatic, skin	–	–	–	1 (2%)
Sarcoma, metastatic, skeletal muscle	–	–	–	1 (2%)
Mediastinum, alveolar/bronchiolar adenoma, multiple	–	–	–	1 (2%)

	Chamber Control	3 mg/m^3	10 mg/m^3	30 mg/m^3
Mediastinum, alveolar/bronchiolar carcinoma	–	–	1 (2%)	–
Mediastinum	(0)	(1)	(2)	(10)
Nose	(50)	(49)	(50)	(50)
Adenoma	–	–	–	1 (2%)
Osteosarcoma	–	–	1 (2%)	–
Turbinate, chondroma	1 (2%)	–	–	–
Trachea	(50)	(50)	(50)	(50)
Carcinoma, metastatic, thyroid gland	1 (2%)	–	–	–
Special Senses System				
Ear	(0)	(0)	(1)	(0)
Eye	(49)	(49)	(50)	(49)
Sarcoma	–	–	–	1 (2%)
Sarcoma, metastatic, Harderian gland	–	1 (2%)	–	–
Choroid, melanoma benign	–	1 (2%)	–	–
Harderian gland	(50)	(50)	(50)	(50)
Sarcoma	–	1 (2%)	–	–
Lacrimal gland	(1)	(0)	(1)	(0)
Urinary System				
Kidney	(50)	(50)	(50)	(50)
Carcinoma	–	–	–	1 (2%)
Sarcoma	–	–	1 (2%)	–
Ureter	(0)	(1)	(0)	(0)
Carcinoma, metastatic, prostate	–	1 (100%)	–	–
Urinary bladder	(50)	(50)	(50)	(50)
Serosa, carcinoma, metastatic, prostate	–	1 (2%)	–	–
Systemic Lesions				
Multiple organs[b]	(50)	(50)	(50)	(50)
Histiocytic sarcoma	–	–	–	1 (2%)
Leukemia mononuclear	1 (2%)	1 (2%)	1 (2%)	–
Lymphoma malignant	–	–	1 (2%)	–
Mesothelioma malignant	–	–	–	1 (2%)
Neoplasm Summary				
Total animals with primary neoplasms[c]				
Twelve-month interim evaluation	–	–	–	1

	Chamber Control	3 mg/m^3	10 mg/m^3	30 mg/m^3
Two-year study	36	34	40	35
Total primary neoplasms				
Twelve-month interim evaluation	–	–	–	1
Two-year study	51	55	66	54
Total animals with benign neoplasms				
Two-year study	34	31	32	26
Total benign neoplasms				
Two-year study	44	43	47	39
Total animals with malignant neoplasms				
Twelve-month interim evaluation	–	–	–	1
Two-year study	6	8	17	14
Total malignant neoplasms				
Twelve-month interim evaluation	–	–	–	1
Two-year study	6	11	18	14
Total animals with metastatic neoplasms				
Two-year study	1	2	1	5
Total metastatic neoplasms				
Two-year study	5	4	3	12
Total animals with uncertain neoplasms, benign or malignant				
Two-year study	1	1	1	1
Total uncertain neoplasms				
Two-year study	1	1	1	1

[a]Number of animals examined microscopically at the site and the number of animals with neoplasm.
[b]Number of animals with any tissue examined microscopically.
[c]Primary neoplasms: all neoplasms except metastatic neoplasms.

Table A-2. Statistical Analysis of Primary Neoplasms in Male Rats in the Two-year Inhalation Study of Antimony Trioxide

	Chamber Control	3 mg/m^3	10 mg/m^3	30 mg/m^3
Adrenal Cortex: Adenoma				
Overall rate[a]	3/50 (6%)	0/50 (0%)	3/50 (6%)	0/50 (0%)
Adjusted rate[b]	7.2%	0.0%	6.9%	0.0%
Terminal rate[c]	2/30 (7%)	0/30 (0%)	1/28 (4%)	0/18 (0%)
First incidence (days)	607	–[e]	589	–
Poly-3 test[d]	P = 0.205N	P = 0.121N	P = 0.642N	P = 0.125N
Adrenal Medulla: Benign Pheochromocytoma				
Overall rate	1/49 (2%)	0/50 (0%)	2/49 (4%)	7/50 (14%)
Adjusted rate	2.5%	0.0%	4.8%	17.2%
Terminal rate	1/30 (3%)	0/30 (0%)	1/27 (4%)	3/18 (17%)
First incidence (days)	729 (T)	–	537	590
Poly-3 test	P < 0.001	P = 0.498N	P = 0.515	P = 0.030
Adrenal Medulla: Benign or Complex Pheochromocytoma				
Overall rate	2/49 (4%)	0/50 (0%)	2/49 (4%)	7/50 (14%)
Adjusted rate	4.9%	0.0%	4.8%	17.2%
Terminal rate	1/30 (3%)	0/30 (0%)	1/27 (4%)	3/18 (17%)
First incidence (days)	680	–	537	590
Poly-3 test	P = 0.003	P = 0.236N	P = 0.681N	P = 0.078
Lung: Alveolar/Bronchiolar Adenoma				
Overall rate	3/50 (6%)	4/50 (8%)	6/50 (12%)	8/50 (16%)
Adjusted rate	7.1%	9.8%	13.8%	19.7%
Terminal rate	1/30 (3%)	4/30 (13%)	2/28 (7%)	4/18 (22%)
First incidence (days)	369	729 (T)	534	649
Poly-3 test	P = 0.057	P = 0.478	P = 0.253	P = 0.083
Lung: Alveolar/Bronchiolar Carcinoma				
Overall rate	0/50 (0%)	0/50 (0%)	2/50 (4%)	0/50 (0%)
Adjusted rate	0.0%	0.0%	4.7%	0.0%
Terminal rate	0/30 (0%)	0/30 (0%)	1/28 (4%)	0/18 (0%)
First incidence (days)	–	–	719	–
Poly-3 test	P = 0.702N	–[f]	P = 0.245	–
Lung: Alveolar/Bronchiolar Adenoma or Carcinoma				
Overall rate	3/50 (6%)	4/50 (8%)	8/50 (16%)	8/50 (16%)
Adjusted rate	7.1%	9.8%	18.4%	19.7%
Terminal rate	1/30 (3%)	4/30 (13%)	3/28 (11%)	4/18 (22%)

	Chamber Control	3 mg/m^3	10 mg/m^3	30 mg/m^3
First incidence (days)	369	729 (T)	534	649
Poly-3 test	P = 0.067	P = 0.478	P = 0.104	P = 0.083
Lymph Node (Mesenteric): Hemangiosarcoma				
Overall rate	2/50 (4%)	2/50 (4%)	4/50 (8%)	1/50 (2%)
Adjusted rate	4.8%	4.9%	9.3%	2.5%
Terminal rate	0/30 (0%)	2/30 (7%)	2/28 (7%)	0/18 (0%)
First incidence (days)	582	729 (T)	576	660
Poly-3 test	P = 0.391N	P = 0.684	P = 0.350	P = 0.515N
Pancreatic Islets: Adenoma				
Overall rate	0/50 (0%)	1/50 (2%)	4/50 (8%)	1/49 (2%)
Adjusted rate	0.0%	2.5%	9.2%	2.6%
Terminal rate	0/30 (0%)	1/30 (3%)	1/28 (4%)	0/17 (0%)
First incidence (days)	–	729 (T)	576	691
Poly-3 test	P = 0.509	P = 0.499	P = 0.067	P = 0.490
Pancreatic Islets: Adenoma or Carcinoma				
Overall rate	0/50 (0%)	1/50 (2%)	4/50 (8%)	2/49 (4%)
Adjusted rate	0.0%	2.5%	9.2%	5.1%
Terminal rate	0/30 (0%)	1/30 (3%)	1/28 (4%)	1/17 (6%)
First incidence (days)	–	729 (T)	576	691
Poly-3 test	P = 0.265	P = 0.499	P = 0.067	P = 0.226
Pituitary Gland (Pars Distalis): Adenoma				
Overall rate	14/50 (28%)	15/50 (30%)	12/50 (24%)	5/50 (10%)
Adjusted rate	31.4%	34.3%	26.8%	12.1%
Terminal rate	6/30 (20%)	8/30 (27%)	5/28 (18%)	1/18 (6%)
First incidence (days)	477	486	499	590
Poly-3 test	P = 0.010N	P = 0.474	P = 0.406N	P = 0.027N
Testes: Adenoma				
Overall rate	6/50 (12%)	2/50 (4%)	1/50 (2%)	1/50 (2%)
Adjusted rate	14.5%	4.9%	2.4%	2.5%
Terminal rate	4/30 (13%)	2/30 (7%)	1/28 (4%)	1/18 (6%)
First incidence (days)	659	729 (T)	729 (T)	729 (T)
Poly-3 test	P = 0.083N	P = 0.137N	P = 0.051N	P = 0.060N

	Chamber Control	3 mg/m^3	10 mg/m^3	30 mg/m^3
Thymus: Benign Thymoma				
Overall rate	3/41 (7%)	0/35 (0%)	1/47 (2%)	4/45 (9%)
Adjusted rate	8.8%	0.0%	2.5%	11.0%
Terminal rate	1/25 (4%)	0/21 (0%)	1/27 (4%)	2/16 (13%)
First incidence (days)	680	–	729 (T)	607
Poly-3 test	P = 0.174	P = 0.147N	P = 0.249N	P = 0.536
Thymus: Benign or Malignant Thymoma				
Overall rate	3/41 (7%)	1/35 (3%)	1/47 (2%)	4/45 (9%)
Adjusted rate	8.8%	3.5%	2.5%	11.0%
Terminal rate	1/25 (4%)	1/21 (5%)	1/27 (4%)	2/16 (13%)
First incidence (days)	680	729 (T)	729 (T)	607
Poly-3 test	P = 0.264	P = 0.365N	P = 0.249N	P = 0.536
Thyroid Gland (C-Cell): Adenoma				
Overall rate	5/50 (10%)	9/50 (18%)	5/50 (10%)	5/50 (10%)
Adjusted rate	12.2%	21.4%	11.8%	12.4%
Terminal rate	5/30 (17%)	7/30 (23%)	4/28 (14%)	3/18 (17%)
First incidence (days)	729 (T)	499	719	649
Poly-3 test	P = 0.358N	P = 0.201	P = 0.609N	P = 0.620
Thyroid Gland (C-Cell): Adenoma or Carcinoma				
Overall rate	6/50 (12%)	10/50 (20%)	5/50 (10%)	5/50 (10%)
Adjusted rate	14.5%	23.8%	11.8%	12.4%
Terminal rate	5/30 (17%)	8/30 (27%)	4/28 (14%)	3/18 (17%)
First incidence (days)	659	499	719	649
Poly-3 test	P = 0.248N	P = 0.210	P = 0.480N	P = 0.517N
All Organs: Hemangiosarcoma				
Overall rate	3/50 (6%)	4/50 (8%)	4/50 (8%)	3/50 (6%)
Adjusted rate	7.0%	9.8%	9.3%	7.2%
Terminal rate	0/30 (0%)	3/30 (10%)	2/28 (7%)	0/18 (0%)
First incidence (days)	369	691	576	459
Poly-3 test	P = 0.522N	P = 0.475	P = 0.504	P = 0.648

	Chamber Control	3 mg/m^3	10 mg/m^3	30 mg/m^3
All Organs: Hemangioma or Hemangiosarcoma				
Overall rate	4/50 (8%)	5/50 (10%)	6/50 (12%)	4/50 (8%)
Adjusted rate	9.2%	12.2%	13.9%	9.6%
Terminal rate	0/30 (0%)	4/30 (13%)	3/28 (11%)	0/18 (0%)
First incidence (days)	369	691	576	459
Poly-3 test	P = 0.523N	P = 0.460	P = 0.363	P = 0.617
All Organs: Benign Neoplasms				
Overall rate	34/50 (68%)	31/50 (62%)	32/50 (64%)	26/50 (52%)
Adjusted rate	72.4%	68.7%	67.6%	59.6%
Terminal rate	20/30 (67%)	22/30 (73%)	16/28 (57%)	10/18 (56%)
First incidence (days)	369	486	499	562
Poly-3 test	P = 0.115N	P = 0.433N	P = 0.387N	P = 0.131N
All Organs: Malignant Neoplasms				
Overall rate	6/50 (12%)	8/50 (16%)	17/50 (34%)	14/50 (28%)
Adjusted rate	13.7%	18.7%	37.4%	32.6%
Terminal rate	0/30 (0%)	4/30 (13%)	6/28 (21%)	7/18 (39%)
First incidence (days)	369	339	159	409
Poly-3 test	P = 0.033	P = 0.369	P = 0.008	P = 0.030
All Organs: Benign or Malignant Neoplasms				
Overall rate	36/50 (72%)	34/50 (68%)	40/50 (80%)	35/50 (70%)
Adjusted rate	75.5%	72.3%	80.6%	74.3%
Terminal rate	20/30 (67%)	22/30 (73%)	20/28 (71%)	12/18 (67%)
First incidence (days)	369	339	113	409
Poly-3 test	P = 0.554N	P = 0.449N	P = 0.358	P = 0.542N

(T) = terminal kill.
[a]Number of neoplasm-bearing animals/number of animals examined. Denominator is number of animals examined microscopically for adrenal gland, lung, pancreatic islets, pituitary gland, testes, thymus, and thyroid gland; for other tissues, denominator is number of animals necropsied.
[b]Poly-3 estimated neoplasm incidence after adjustment for intercurrent mortality.
[c]Observed incidence at terminal kill.
[d]Beneath the chamber control incidence is the P value associated with the trend test. Beneath the exposed group incidence are the P values corresponding to pairwise comparisons between the chamber controls and that exposed group. The Poly-3 test accounts for differential mortality in animals that do not reach terminal kill. A negative trend or a lower incidence in an exposure group is indicated by **N**.
[e]Not applicable; no neoplasms in animal group.
[f]Value of statistic cannot be computed.

Table A-3. Historical Incidence of Alveolar/Bronchiolar Neoplasms in Control Male Wistar Han Rats[a]

Study (Study Start)	Adenoma	Carcinoma	Adenoma or Carcinoma
Historical Incidence: Inhalation Studies			
Antimony trioxide (September 2008)	3/50	0/50	3/50
CIMSTAR 3800 (April 2008)	1/50	0/50	1/50
Trim VX (July 2009)	0/50	0/50	0/50
Total (%)	4/150 (2.7%)	0/150	4/150 (2.7%)
Mean ± standard deviation	2.7% ± 3.1%	–	2.7% ± 3.1%
Range	0%–6%	–	0%–6%
Overall Historical Incidence: All Routes			
Total (%)	4/299 (1.3%)	0/299	4/299 (1.3%)
Mean ± standard deviation	1.3% ± 2.4%	–	1.3% ± 2.4%
Range	0%–6%	–	0%–6%

[a]Data as of November 2014.

Table A-4. Historical Incidence of Pheochromocytoma of the Adrenal Medulla in Control Male Wistar Han Rats[a]

Study (Study Start)	Benign	Benign or Complex
Historical Incidence: Inhalation Studies		
Antimony trioxide (September 2008)	1/49	2/49
CIMSTAR 3800 (April 2008)	4/50	4/50
Trim VX (July 2009)	0/50	0/50
Total (%)	5/149 (3.4%)	6/149 (4.0%)
Mean ± standard deviation	3.4% ± 4.2%	4.0% ± 4.0%
Range	0%–8%	0%–8%
Overall Historical Incidence: All Routes		
Total (%)	6/297 (2.0%)	7/297 (2.4%)
Mean ± standard deviation	2.0% ± 3.1%	2.4% ± 3.2%
Range	0%–8%	0%–8%

[a]Data as of November 2014.

Table A-5. Summary of the Incidence of Nonneoplastic Lesions in Male Rats in the Two-year Inhalation Study of Antimony Trioxide[a]

	Chamber Control	3 mg/m^3	10 mg/m^3	30 mg/m^3
Disposition Summary				
Animals initially in study	60	60	60	60
Twelve-month interim evaluation	10	10	10	10
Early deaths				
Moribund	15	19	22	29
Natural deaths	5	1	–	3
Survivors				
Terminal kill	30	30	28	18
Animals examined microscopically	60	60	60	60
Twelve-month Interim Evaluation				
Alimentary System				
Esophagus	(10)	(10)	(10)	(10)
Intestine large, cecum	(10)	(10)	(10)	(10)
Intestine large, colon	(10)	(10)	(10)	(10)
Intestine large, rectum	(10)	(9)	(10)	(10)
Intestine small, duodenum	(10)	(10)	(10)	(10)
Intestine small, ileum	(10)	(10)	(10)	(10)
Intestine small, jejunum	(10)	(10)	(10)	(10)
Liver	(10)	(10)	(10)	(10)
Congestion	–	1 (10%)	–	–
Pancreas	(10)	(10)	(10)	(10)
Atrophy	3 (30%)	2 (20%)	2 (20%)	–
Inflammation, chronic active	3 (30%)	1 (10%)	1 (10%)	–
Arteriole, inflammation, chronic active	–	–	1 (10%)	–
Salivary glands	(10)	(10)	(10)	(10)
Stomach, forestomach	(10)	(10)	(10)	(10)
Ulcer	1 (10%)	–	–	–
Stomach, glandular	(10)	(10)	(10)	(10)
Inflammation, chronic active	1 (10%)	–	–	2 (20%)
Cardiovascular System				
Blood vessel	(10)	(10)	(10)	(10)
Heart	(10)	(10)	(10)	(10)
Cardiomyopathy	3 (30%)	2 (20%)	5 (50%)	2 (20%)

	Chamber Control	3 mg/m^3	10 mg/m^3	30 mg/m^3
Endocrine System				
Adrenal cortex	(10)	(10)	(10)	(10)
Hyperplasia	1 (10%)	3 (30%)	2 (20%)	3 (30%)
Adrenal medulla	(10)	(10)	(9)	(10)
Hypertrophy	1 (10%)	–	–	–
Islets, pancreatic	(10)	(10)	(10)	(10)
Parathyroid gland	(10)	(10)	(9)	(8)
Pituitary gland	(10)	(10)	(10)	(10)
Pars distalis, hyperplasia	1 (10%)	–	–	–
Thyroid gland	(10)	(10)	(10)	(10)
Hyperplasia, squamous	–	1 (10%)	–	–
Genital System				
Epididymis	(10)	(10)	(10)	(10)
Preputial gland	(10)	(10)	(10)	(9)
Inflammation, chronic active	4 (40%)	2 (20%)	6 (60%)	3 (33%)
Prostate	(10)	(10)	(10)	(10)
Inflammation, suppurative	3 (30%)	–	–	1 (10%)
Epithelium, hyperplasia	–	1 (10%)	–	–
Seminal vesicle	(10)	(10)	(10)	(10)
Testes	(10)	(10)	(10)	(10)
Germinal epithelium, degeneration	2 (20%)	2 (20%)	–	–
Hematopoietic System				
Bone marrow	(10)	(10)	(10)	(10)
Lymph node, bronchial	(9)	(8)	(10)	(10)
Foreign body	–	8 (100%)	10 (100%)	10 (100%)
Hyperplasia, lymphoid	–	2 (25%)	5 (50%)	2 (20%)
Lymph node, mandibular	(10)	(9)	(9)	(8)
Lymph node, mediastinal	(10)	(8)	(10)	(9)
Foreign body	–	8 (100%)	6 (60%)	6 (67%)
Hyperplasia, lymphoid	–	2 (25%)	6 (60%)	3 (33%)
Pigmentation	5 (50%)	5 (63%)	8 (80%)	5 (56%)
Lymph node, mesenteric	(10)	(10)	(10)	(10)
Spleen	(10)	(10)	(10)	(10)
Hematopoietic cell proliferation	2 (20%)	5 (50%)	2 (20%)	4 (40%)
Thymus	(10)	(10)	(10)	(10)

	Chamber Control	3 mg/m^3	10 mg/m^3	30 mg/m^3
Integumentary System				
Mammary gland	(4)	(1)	(1)	(3)
Skin	(10)	(10)	(10)	(10)
Fibrosis	–	–	1 (10%)	–
Respiratory System				
Larynx	(10)	(10)	(10)	(10)
Foreign body	–	10 (100%)	10 (100%)	10 (100%)
Infiltration cellular, lymphocyte	1 (10%)	–	–	–
Lung	(10)	(10)	(10)	(10)
Fibrosis	–	10 (100%)	10 (100%)	10 (100%)
Foreign body	–	10 (100%)	10 (100%)	10 (100%)
Inflammation, chronic active	1 (10%)	10 (100%)	10 (100%)	10 (100%)
Metaplasia, osseous	–	–	1 (10%)	–
Proteinosis	–	9 (90%)	10 (100%)	10 (100%)
Alveolar epithelium, hyperplasia	–	10 (100%)	10 (100%)	10 (100%)
Alveolus, inflammation, suppurative	–	1 (10%)	2 (20%)	2 (20%)
Bronchiole, epithelium, hyperplasia	–	5 (50%)	5 (50%)	6 (60%)
Perivascular, infiltration cellular, lymphocyte	–	4 (40%)	4 (40%)	3 (30%)
Nose	(10)	(10)	(10)	(10)
Foreign body	–	–	1 (10%)	9 (90%)
Inflammation, suppurative	–	1 (10%)	–	1 (10%)
Glands, respiratory epithelium, cyst	–	–	1 (10%)	–
Olfactory epithelium, accumulation, hyaline droplet	3 (30%)	1 (10%)	4 (40%)	2 (20%)
Respiratory epithelium, accumulation, hyaline droplet	2 (20%)	–	–	–
Respiratory epithelium, hyperplasia	–	–	1 (10%)	2 (20%)
Trachea	(10)	(10)	(10)	(10)
Foreign body	–	8 (80%)	9 (90%)	10 (100%)
Infiltration cellular, polymorphonuclear	–	–	–	1 (10%)
Special Senses System				
Eye	(10)	(10)	(10)	(10)
Lens, degeneration	–	–	1 (10%)	–
Retina, atrophy	2 (20%)	1 (10%)	–	–
Harderian gland	(10)	(10)	(10)	(10)

	Chamber Control	3 mg/m^3	10 mg/m^3	30 mg/m^3
Urinary System				
Kidney	(10)	(10)	(10)	(10)
Nephropathy	6 (60%)	3 (30%)	4 (40%)	5 (50%)
Pelvis, dilatation	1 (10%)	–	–	–
Pelvis, inflammation, chronic active	–	1 (10%)	–	–
Urinary bladder	(10)	(10)	(10)	(10)
Calculus gross observation	–	–	3 (30%)	2 (20%)
Systems Examined at 12 Months with No Lesions Observed				
General Body System				
Musculoskeletal System				
Nervous System				
Two-year Study				
Alimentary System				
Esophagus	(50)	(50)	(50)	(50)
Intestine large, cecum	(49)	(50)	(50)	(49)
Necrosis	–	–	–	1 (2%)
Intestine large, colon	(50)	(50)	(50)	(50)
Edema	1 (2%)	–	–	–
Inflammation, chronic active	1 (2%)	–	–	–
Intestine large, rectum	(44)	(49)	(48)	(48)
Inflammation, chronic active	–	–	1 (2%)	1 (2%)
Intestine small, duodenum	(47)	(50)	(50)	(49)
Fibrosis	–	–	1 (2%)	–
Inflammation, chronic active	–	1 (2%)	–	–
Intestine small, ileum	(48)	(50)	(50)	(49)
Hemorrhage	–	–	–	1 (2%)
Inflammation, suppurative	–	–	–	1 (2%)
Inflammation, chronic active	–	–	1 (2%)	–
Necrosis	–	–	1 (2%)	–
Epithelium, atrophy	–	–	–	1 (2%)
Intestine small, jejunum	(46)	(49)	(50)	(48)
Fibrosis	1 (2%)	–	–	–
Inflammation, chronic active	1 (2%)	–	–	–
Liver	(50)	(50)	(50)	(50)
Angiectasis	1 (2%)	3 (6%)	4 (8%)	1 (2%)

	Chamber Control	3 mg/m^3	10 mg/m^3	30 mg/m^3
Basophilic focus	3 (6%)	5 (10%)	5 (10%)	1 (2%)
Clear cell focus	18 (36%)	14 (28%)	15 (30%)	8 (16%)
Congestion	3 (6%)	8 (16%)	6 (12%)	6 (12%)
Cyst	2 (4%)	4 (8%)	2 (4%)	1 (2%)
Eosinophilic focus	–	1 (2%)	1 (2%)	2 (4%)
Fatty change	4 (8%)	8 (16%)	4 (8%)	3 (6%)
Fibrosis	–	1 (2%)	–	1 (2%)
Hematopoietic cell proliferation	–	–	–	1 (2%)
Hepatodiaphragmatic nodule	–	2 (4%)	3 (6%)	1 (2%)
Inflammation, chronic active	2 (4%)	–	1 (2%)	1 (2%)
Mineralization	–	1 (2%)	–	–
Mixed cell focus	–	1 (2%)	–	–
Necrosis	–	1 (2%)	1 (2%)	2 (4%)
Bile duct, cyst, multiple	–	–	–	1 (2%)
Bile duct, dilatation	–	–	1 (2%)	–
Bile duct, hyperplasia	–	–	–	3 (6%)
Sinusoid, dilatation	1 (2%)	–	–	–
Vein, dilatation	–	1 (2%)	–	–
Mesentery	(50)	(50)	(50)	(50)
Arteriole, inflammation, chronic active	1 (2%)	–	–	–
Artery, inflammation, chronic active	–	–	–	6 (12%)
Artery, necrosis	–	–	–	3 (6%)
Fat, necrosis	1 (2%)	4 (8%)	3 (6%)	2 (4%)
Pancreas	(50)	(50)	(50)	(50)
Atrophy	15 (30%)	12 (24%)	14 (28%)	20 (40%)
Basophilic focus	3 (6%)	4 (8%)	–	–
Inflammation, chronic active	1 (2%)	–	2 (4%)	2 (4%)
Arteriole, inflammation, chronic active	–	–	1 (2%)	1 (2%)
Artery, hemorrhage	–	–	1 (2%)	–
Artery, inflammation, chronic active	1 (2%)	–	2 (4%)	8 (16%)
Artery, necrosis	–	–	1 (2%)	4 (8%)
Salivary glands	(50)	(50)	(50)	(50)
Atrophy	–	2 (4%)	–	2 (4%)
Basophilic focus	–	1 (2%)	–	–
Inflammation, suppurative	–	1 (2%)	–	–

	Chamber Control	3 mg/m^3	10 mg/m^3	30 mg/m^3
Stomach, forestomach	(50)	(50)	(50)	(50)
Cyst, squamous	1 (2%)	–	–	–
Edema	–	–	–	2 (4%)
Hyperplasia, squamous	2 (4%)	7 (14%)	4 (8%)	7 (14%)
Inflammation, suppurative	–	1 (2%)	–	–
Inflammation, chronic active	–	–	1 (2%)	–
Ulcer	1 (2%)	–	–	1 (2%)
Stomach, glandular	(50)	(50)	(50)	(50)
Edema	–	–	–	1 (2%)
Erosion	–	–	–	1 (2%)
Fibrosis	–	1 (2%)	–	–
Hemorrhage	–	–	–	1 (2%)
Inflammation, chronic active	1 (2%)	–	1 (2%)	3 (6%)
Metaplasia, squamous	–	–	1 (2%)	–
Mineralization	1 (2%)	–	1 (2%)	1 (2%)
Ulcer	–	1 (2%)	–	–
Arteriole, mineralization	–	1 (2%)	–	–
Capillary, hyperplasia	–	–	–	1 (2%)
Tongue	(1)	(1)	(0)	(1)
Epithelium, hyperplasia	1 (100%)	–	–	1 (100%)
Tooth	(2)	(1)	(1)	(1)
Inflammation, suppurative	–	1 (100%)	–	–
Inflammation, chronic active	–	–	1 (100%)	1 (100%)
Malformation	2 (100%)	–	–	–
Cardiovascular System				
Blood vessel	(50)	(50)	(50)	(49)
Angiomatous hyperplasia	–	–	1 (2%)	–
Mineralization	1 (2%)	–	1 (2%)	–
Heart	(50)	(50)	(50)	(50)
Angiectasis	–	–	–	1 (2%)
Cardiomyopathy	41 (82%)	44 (88%)	42 (84%)	40 (80%)
Hemorrhage	–	–	1 (2%)	–
Inflammation, chronic active	–	–	–	1 (2%)
Thrombosis	–	–	–	2 (4%)
Artery, inflammation, chronic active	–	–	–	1 (2%)

	Chamber Control	3 mg/m^3	10 mg/m^3	30 mg/m^3
Valve, fibrosis	–	–	1 (2%)	–
Valve, inflammation, suppurative	–	–	–	1 (2%)
Valve, thrombosis	–	–	–	2 (4%)
Endocrine System				
Adrenal cortex	(50)	(50)	(50)	(50)
Accessory adrenal cortical nodule	–	1 (2%)	1 (2%)	–
Angiectasis	–	2 (4%)	–	3 (6%)
Atrophy	1 (2%)	–	2 (4%)	–
Degeneration, cystic	3 (6%)	–	1 (2%)	3 (6%)
Hematopoietic cell proliferation	–	–	–	1 (2%)
Hemorrhage	1 (2%)	–	–	–
Hyperplasia	30 (60%)	32 (64%)	33 (66%)	32 (64%)
Vacuolization cytoplasmic	1 (2%)	–	–	–
Adrenal medulla	(49)	(50)	(49)	(50)
Degeneration, fatty	–	–	–	1 (2%)
Hyperplasia	1 (2%)	2 (4%)	4 (8%)	8 (16%)
Thrombosis	–	–	–	1 (2%)
Islets, pancreatic	(50)	(50)	(50)	(49)
Parathyroid gland	(44)	(46)	(46)	(48)
Fibrosis	–	–	1 (2%)	–
Hyperplasia	4 (9%)	–	1 (2%)	1 (2%)
Pituitary gland	(50)	(50)	(50)	(50)
Angiectasis	1 (2%)	–	–	–
Cyst	–	1 (2%)	–	–
Hemorrhage	1 (2%)	–	–	–
Pars distalis, hyperplasia	11 (22%)	11 (22%)	14 (28%)	15 (30%)
Pars intermedia, angiectasis	1 (2%)	–	–	–
Pars intermedia, hyperplasia	1 (2%)	4 (8%)	–	1 (2%)
Thyroid gland	(50)	(50)	(50)	(50)
C-cell, hyperplasia	9 (18%)	11 (22%)	13 (26%)	6 (12%)
Follicle, cyst	1 (2%)	1 (2%)	–	–
Follicular cell, hyperplasia	1 (2%)	2 (4%)	–	2 (4%)
General Body System				
Tissue NOS	(0)	(1)	(0)	(1)

	Chamber Control	3 mg/m^3	10 mg/m^3	30 mg/m^3
Genital System				
Coagulating gland	(0)	(0)	(0)	(1)
Inflammation, chronic active	–	–	–	1 (100%)
Epididymis	(50)	(50)	(50)	(50)
Epithelium, cytoplasmic alteration	1 (2%)	–	–	–
Preputial gland	(50)	(50)	(50)	(50)
Ectasia	1 (2%)	1 (2%)	4 (8%)	–
Fibrosis	–	1 (2%)	–	–
Inflammation, chronic active	7 (14%)	5 (10%)	4 (8%)	4 (8%)
Prostate	(50)	(50)	(50)	(50)
Inflammation, suppurative	1 (2%)	6 (12%)	5 (10%)	4 (8%)
Inflammation, chronic active	8 (16%)	3 (6%)	5 (10%)	3 (6%)
Epithelium, hyperplasia	9 (18%)	18 (36%)	21 (42%)	13 (26%)
Seminal vesicle	(50)	(50)	(50)	(50)
Congestion	–	–	–	1 (2%)
Hyperplasia	–	1 (2%)	–	–
Inflammation, suppurative	–	1 (2%)	–	–
Inflammation, chronic active	2 (4%)	–	–	1 (2%)
Epithelium, hyperplasia	1 (2%)	–	–	–
Testes	(50)	(50)	(50)	(50)
Cyst	1 (2%)	–	–	–
Edema	30 (60%)	37 (74%)	31 (62%)	26 (52%)
Fibrosis	–	1 (2%)	–	–
Hemorrhage	–	–	1 (2%)	–
Inflammation, chronic active	–	1 (2%)	1 (2%)	–
Arteriole, inflammation, chronic active	1 (2%)	–	–	–
Germinal epithelium, degeneration	3 (6%)	6 (12%)	6 (12%)	4 (8%)
Interstitial cell, hyperplasia	1 (2%)	–	–	–
Hematopoietic System				
Bone marrow	(50)	(50)	(50)	(50)
Depletion cellular	–	1 (2%)	–	–
Fibrosis	–	1 (2%)	–	–
Hyperplasia	–	3 (6%)	4 (8%)	8 (16%)
Lymph node	(2)	(4)	(7)	(7)
Hyperplasia, plasma cell	–	–	1 (14%)	–

	Chamber Control	3 mg/m^3	10 mg/m^3	30 mg/m^3
Axillary, hyperplasia, plasma cell	–	1 (25%)	–	–
Axillary, infiltration cellular, histiocyte	–	–	–	1 (14%)
Iliac, ectasia	–	–	2 (29%)	–
Iliac, hyperplasia, plasma cell	–	–	1 (14%)	1 (14%)
Lumbar, ectasia	–	–	–	1 (14%)
Lumbar, hyperplasia, plasma cell		2 (50%)	2 (29%)	3 (43%)
Lumbar, infiltration cellular, histiocyte	–	–	–	1 (14%)
Lumbar, renal, hyperplasia, plasma cell	1 (50%)	–	–	–
Pancreatic, congestion	–	–	1 (14%)	–
Renal, ectasia	1 (50%)	–	–	2 (29%)
Renal, infiltration cellular, histiocyte	–	–	–	1 (14%)
Lymph node, bronchial	(41)	(40)	(48)	(47)
Ectasia	–	–	1 (2%)	–
Foreign body	–	35 (88%)	45 (94%)	42 (89%)
Hyperplasia, lymphoid	–	21 (52%)	29 (60%)	26 (55%)
Pigmentation	1 (2%)	4 (10%)	5 (10%)	10 (21%)
Lymph node, mandibular	(45)	(46)	(48)	(45)
Hyperplasia, plasma cell	–	1 (2%)	2 (4%)	–
Lymph node, mediastinal	(42)	(45)	(49)	(49)
Congestion	–	–	–	1 (2%)
Foreign body	–	41 (91%)	41 (84%)	43 (88%)
Hyperplasia	–	–	–	1 (2%)
Hyperplasia, lymphoid	1 (2%)	24 (53%)	30 (61%)	26 (53%)
Pigmentation	24 (57%)	23 (51%)	29 (59%)	26 (53%)
Lymph node, mesenteric	(50)	(50)	(50)	(50)
Angiomatous hyperplasia	–	1 (2%)	–	3 (6%)
Ectasia	–	–	–	2 (4%)
Fibrosis	–	–	1 (2%)	1 (2%)
Hemorrhage	–	–	–	1 (2%)
Artery, inflammation, chronic active	–	–	–	1 (2%)
Spleen	(50)	(50)	(50)	(50)
Accessory spleen	1 (2%)	–	–	–
Cyst		1 (2%)	–	–
Depletion cellular	1 (2%)	–	1 (2%)	1 (2%)
Depletion cellular, focal	–	–	1 (2%)	–

	Chamber Control	3 mg/m^3	10 mg/m^3	30 mg/m^3
Fibrosis	–	–	1 (2%)	–
Hematopoietic cell proliferation	41 (82%)	45 (90%)	43 (86%)	46 (92%)
Hemorrhage	–	1 (2%)	–	–
Mineralization	–	–	–	1 (2%)
Necrosis	–	1 (2%)	–	–
Thymus	(41)	(35)	(47)	(45)
Cyst	–	–	1 (2%)	–
Depletion cellular	5 (12%)	6 (17%)	6 (13%)	9 (20%)
Hemorrhage	1 (2%)	–	–	–
Epithelial cell, hyperplasia	–	–	1 (2%)	–
Integumentary System				
Mammary gland	(6)	(9)	(7)	(8)
Galactocele	–	1 (11%)	1 (14%)	–
Skin	(50)	(50)	(50)	(50)
Cyst, squamous	2 (4%)	–	–	–
Dysplasia	1 (2%)	–	–	–
Foreign body	–	1 (2%)	–	–
Inflammation, chronic active	22 (44%)	30 (60%)	28 (56%)	32 (64%)
Ulcer	17 (34%)	23 (46%)	23 (46%)	28 (56%)
Epidermis, hyperplasia	–	1 (2%)	–	–
Hair follicle, hyperplasia	–	–	–	1 (2%)
Subcutaneous tissue, hemorrhage	1 (2%)	–	–	–
Subcutaneous tissue, inflammation, granulomatous	1 (2%)	–	1 (2%)	–
Subcutaneous tissue, inflammation, chronic active	–	–	1 (2%)	1 (2%)
Musculoskeletal System				
Bone	(50)	(50)	(50)	(50)
Inflammation, chronic active	–	–	1 (2%)	–
Epiphysis, femur, cyst	–	–	1 (2%)	–
Femur, hyperostosis	–	1 (2%)	–	–
Mandible, cyst, squamous	–	–	1 (2%)	–
Maxilla, cyst, squamous	–	1 (2%)	–	–
Maxilla, inflammation, chronic active	3 (6%)	4 (8%)	2 (4%)	1 (2%)
Vertebra, fibrosis	–	1 (2%)	–	–
Skeletal muscle	(4)	(3)	(3)	(5)

	Chamber Control	3 mg/m^3	10 mg/m^3	30 mg/m^3
Atrophy	–	1 (33%)	–	–
Cyst	–	–	–	1 (20%)
Hemorrhage	1 (25%)	–	–	–
Inflammation, chronic active	–	–	–	1 (20%)
Necrosis	–	–	1 (33%)	–
Nervous System				
Brain	(50)	(50)	(50)	(50)
Compression	7 (14%)	11 (22%)	8 (16%)	2 (4%)
Hemorrhage	1 (2%)	–	–	–
Meninges, hyperplasia	–	–	1 (2%)	1 (2%)
Peripheral nerve	(3)	(3)	(2)	(0)
Degeneration	–	1 (33%)	1 (50%)	–
Spinal cord	(3)	(3)	(1)	(0)
Respiratory System				
Larynx	(50)	(50)	(50)	(50)
Foreign body		50 (100%)	50 (100%)	50 (100%)
Hyperplasia, squamous	–	–	–	2 (4%)
Inflammation, chronic active	2 (4%)	5 (10%)	2 (4%)	4 (8%)
Metaplasia, squamous	–	2 (4%)	–	1 (2%)
Mineralization	–	–	1 (2%)	–
Necrosis	1 (2%)	–	–	1 (2%)
Respiratory epithelium, hyperplasia	2 (4%)	4 (8%)	1 (2%)	–
Lung	(50)	(50)	(50)	(50)
Congestion	–	1 (2%)	–	–
Fibrosis	2 (4%)	50 (100%)	49 (98%)	49 (98%)
Foreign body	1 (2%)	50 (100%)	50 (100%)	50 (100%)
Hemorrhage	2 (4%)	2 (4%)	1 (2%)	3 (6%)
Inflammation, chronic active	18 (36%)	50 (100%)	50 (100%)	50 (100%)
Metaplasia, osseous	1 (2%)	2 (4%)	2 (4%)	9 (18%)
Proteinosis	–	47 (94%)	50 (100%)	50 (100%)
Alveolar epithelium, hyperplasia	4 (8%)	50 (100%)	48 (96%)	49 (98%)
Alveolar epithelium, metaplasia, squamous	–	–	1 (2%)	–
Alveolus, inflammation, suppurative	–	12 (24%)	24 (48%)	28 (56%)
Artery, inflammation, chronic active	–	–	1 (2%)	1 (2%)
Bronchiole, epithelium, hyperplasia	3 (6%)	34 (68%)	36 (72%)	33 (66%)

	Chamber Control	3 mg/m^3	10 mg/m^3	30 mg/m^3
Bronchus, hyperplasia	–	–	–	1 (2%)
Bronchus, inflammation, chronic active	–	1 (2%)	–	–
Bronchus, metaplasia, squamous	–	1 (2%)	–	–
Perivascular, infiltration cellular, lymphocyte	3 (6%)	25 (50%)	19 (38%)	9 (18%)
Perivascular, infiltration cellular, lymphoid	–	–	–	1 (2%)
Mediastinum	(0)	(1)	(2)	(10)
Artery, inflammation, chronic active	–	1 (100%)	2 (100%)	10 (100%)
Artery, necrosis	–	–	2 (100%)	9 (90%)
Nose	(50)	(49)	(50)	(50)
Foreign body	–	–	17 (34%)	40 (80%)
Hyperplasia, squamous	1 (2%)	–	–	–
Inflammation, suppurative	4 (8%)	4 (8%)	6 (12%)	7 (14%)
Inflammation, acute	–	–	–	1 (2%)
Inflammation, chronic active	–	–	1 (2%)	1 (2%)
Mineralization	1 (2%)	–	–	–
Glands, cyst	–	1 (2%)	–	–
Glands, respiratory epithelium, cyst	1 (2%)	–	–	2 (4%)
Olfactory epithelium, accumulation, hyaline droplet	16 (32%)	15 (31%)	15 (30%)	18 (36%)
Olfactory epithelium, atrophy	–	–	1 (2%)	–
Olfactory epithelium, hyperplasia	–	–	1 (2%)	–
Olfactory epithelium, metaplasia, respiratory	–	1 (2%)	–	1 (2%)
Respiratory epithelium, hyperplasia	6 (12%)	15 (31%)	13 (26%)	25 (50%)
Respiratory epithelium, metaplasia, squamous	–	–	2 (4%)	6 (12%)
Respiratory epithelium, necrosis	1 (2%)	–	3 (6%)	1 (2%)
Respiratory epithelium, regeneration	–	–	–	2 (4%)
Turbinate, hyperostosis	–	–	1 (2%)	1 (2%)
Trachea	(50)	(50)	(50)	(50)
Foreign body	–	28 (56%)	43 (86%)	48 (96%)
Inflammation, suppurative	–	3 (6%)	1 (2%)	–
Inflammation, chronic active	–	–	–	1 (2%)
Metaplasia, squamous	1 (2%)	1 (2%)	4 (8%)	3 (6%)

	Chamber Control	3 mg/m^3	10 mg/m^3	30 mg/m^3
Mineralization	–	–	1 (2%)	1 (2%)
Necrosis	–	–	–	1 (2%)
Epithelium, hyperplasia	–	1 (2%)	–	–
Epithelium, regeneration	–	–	–	1 (2%)
Special Senses System				
Ear	(0)	(0)	(1)	(0)
Eye	(49)	(49)	(50)	(49)
Ciliary body, inflammation, acute	–	–	1 (2%)	6 (12%)
Cornea, inflammation, chronic active	–	–	–	2 (4%)
Iris, infiltration cellular, histiocyte	–	–	1 (2%)	–
Lens, degeneration	2 (4%)	5 (10%)	3 (6%)	4 (8%)
Retina, atrophy	8 (16%)	11 (22%)	9 (18%)	6 (12%)
Harderian gland	(50)	(50)	(50)	(50)
Hyperplasia	2 (4%)	1 (2%)	–	3 (6%)
Inflammation, chronic active	–	–	1 (2%)	1 (2%)
Lacrimal gland	(1)	(0)	(1)	(0)
Atrophy	–	–	1 (100%)	–
Hypertrophy	1 (100%)	–	–	–
Urinary System				
Kidney	(50)	(50)	(50)	(50)
Accumulation, hyaline droplet	–	–	1 (2%)	–
Amyloid deposition	–	1 (2%)	–	–
Cyst	1 (2%)	2 (4%)	3 (6%)	1 (2%)
Fibrosis	–	–	–	1 (2%)
Infarct	–	1 (2%)	2 (4%)	1 (2%)
Inflammation, suppurative	1 (2%)	–	–	1 (2%)
Inflammation, chronic active	1 (2%)	–	–	2 (4%)
Metaplasia, osseous	–	–	–	1 (2%)
Nephropathy	41 (82%)	41 (82%)	40 (80%)	38 (76%)
Thrombosis	–	1 (2%)	–	–
Artery, inflammation, chronic active	–	–	1 (2%)	4 (8%)
Artery, necrosis	–	–	1 (2%)	4 (8%)
Papilla, necrosis	–	–	–	2 (4%)
Pelvis, dilatation	2 (4%)	2 (4%)	1 (2%)	3 (6%)
Pelvis, inflammation, suppurative	2 (4%)	3 (6%)	5 (10%)	2 (4%)

	Chamber Control	3 mg/m^3	10 mg/m^3	30 mg/m^3
Pelvis, inflammation, chronic active	4 (8%)	–	1 (2%)	1 (2%)
Pelvis, mineralization	16 (32%)	10 (20%)	11 (22%)	3 (6%)
Renal tubule, accumulation, hyaline droplet	–	1 (2%)	3 (6%)	14 (28%)
Renal tubule, hyperplasia	1 (2%)	–	–	1 (2%)
Renal tubule, mineralization	1 (2%)	–	–	2 (4%)
Vein, thrombosis	–	1 (2%)	–	–
Ureter	(0)	(1)	(0)	(0)
Urinary bladder	(50)	(50)	(50)	(50)
Calculus gross observation	–	–	–	1 (2%)
Hemorrhage	–	–	–	1 (2%)
Inflammation, suppurative	1 (2%)	–	–	–
Necrosis	1 (2%)	–	–	–
Serosa, inflammation, chronic active	–	–	–	1 (2%)
Transitional epithelium, hyperplasia	–	–	–	1 (2%)

[a]Number of animals examined microscopically at the site and the number of animals with lesion.

Appendix B. Summary of Lesions in Female Rats in the Two-year Inhalation Study of Antimony Trioxide

Tables

Table B-1. Summary of the Incidence of Neoplasms in Female Rats in the Two-year Inhalation Study of Antimony Trioxide B-2
Table B-2. Statistical Analysis of Primary Neoplasms in Female Rats in the Two-year Inhalation Study of Antimony Trioxide B-9
Table B-3. Historical Incidence of Lung Neoplasms in Control Female Wistar Han Rats B-13
Table B-4. Historical Incidence of Pheochromocytoma of the Adrenal Medulla in Control Female Wistar Han Rats B-13
Table B-5. Summary of the Incidence of Nonneoplastic Lesions in Female Rats in the Two-year Inhalation Study of Antimony Trioxide B-14

Table B-1. Summary of the Incidence of Neoplasms in Female Rats in the Two-year Inhalation Study of Antimony Trioxide[a]

	Chamber Control	3 mg/m^3	10 mg/m^3	30 mg/m^3
Disposition Summary				
Animals initially in study	60	60	60	60
Twelve-month interim evaluation	10	10	10	10
Early deaths				
Moribund	11	12	20	27
Natural deaths	–	–	2	3
Survivors				
Died last week of study	–	–	1	1
Terminal kill	39	38	27	19
Animals examined microscopically	60	60	60	60
Twelve-month Interim Evaluation				
Alimentary System				
Esophagus	(10)	(10)	(9)	(10)
Intestine large, cecum	(10)	(10)	(10)	(10)
Intestine large, colon	(10)	(10)	(10)	(10)
Intestine large, rectum	(10)	(10)	(10)	(10)
Intestine small, duodenum	(10)	(10)	(10)	(10)
Intestine small, ileum	(10)	(10)	(10)	(10)
Intestine small, jejunum	(10)	(10)	(10)	(10)
Liver	(10)	(10)	(10)	(10)
Pancreas	(10)	(10)	(10)	(10)
Salivary glands	(10)	(10)	(10)	(10)
Stomach, forestomach	(10)	(10)	(10)	(10)
Squamous cell papilloma	1 (10%)	–	–	–
Stomach, glandular	(10)	(10)	(10)	(10)
Endocrine System				
Adrenal cortex	(10)	(10)	(10)	(10)
Adrenal medulla	(10)	(10)	(10)	(10)
Islets, pancreatic	(10)	(10)	(10)	(10)
Parathyroid gland	(10)	(8)	(8)	(10)
Pituitary gland	(10)	(10)	(10)	(10)
Pars distalis, adenoma	–	–	–	1 (10%)
Thyroid gland	(10)	(10)	(10)	(10)

	Chamber Control	3 mg/m^3	10 mg/m^3	30 mg/m^3
Genital System				
Clitoral gland	(10)	(10)	(10)	(10)
Ovary	(10)	(10)	(10)	(10)
Uterus	(10)	(10)	(10)	(10)
Polyp stromal	1 (10%)	1 (10%)	2 (20%)	1 (10%)
Integumentary System				
Mammary gland	(10)	(10)	(10)	(10)
Fibroadenoma	–	–	–	1 (10%)
Skin	(10)	(10)	(10)	(10)
Respiratory System				
Larynx	(10)	(10)	(10)	(10)
Lung	(10)	(10)	(10)	(10)
Alveolar/bronchiolar adenoma	–	–	–	1 (10%)
Nose	(10)	(10)	(10)	(10)
Trachea	(10)	(10)	(10)	(10)
Systemic Lesions				
Multiple organs[b]	(10)	(10)	(10)	(10)
Lymphoma malignant	1 (10%)	–	–	–
Systems Examined at 12 Months with No Neoplasms Observed				
Cardiovascular System				
General Body System				
Hematopoietic System				
Musculoskeletal System				
Nervous System				
Special Senses System				
Urinary System				
Two-year Study				
Alimentary System				
Esophagus	(50)	(50)	(50)	(50)
Intestine large, cecum	(50)	(50)	(49)	(50)
Intestine large, colon	(50)	(50)	(50)	(50)
Leiomyoma	–	1 (2%)	–	–
Intestine large, rectum	(48)	(47)	(50)	(49)
Leiomyosarcoma, metastatic, uterus	–	–	–	1 (2%)
Intestine small, duodenum	(50)	(50)	(50)	(50)

	Chamber Control	3 mg/m^3	10 mg/m^3	30 mg/m^3
Intestine small, ileum	(50)	(50)	(49)	(50)
Intestine small, jejunum	(50)	(50)	(49)	(49)
Leiomyoma	1 (2%)	–	–	–
Leiomyosarcoma	–	1 (2%)	1 (2%)	–
Liver	(50)	(50)	(50)	(50)
Hepatocellular adenoma	1 (2%)	2 (4%)	–	–
Sarcoma	–	1 (2%)	–	–
Squamous cell carcinoma, metastatic, uterus	1 (2%)	–	–	–
Mesentery	(50)	(50)	(50)	(50)
Leiomyosarcoma, metastatic, uterus	–	–	–	1 (2%)
Sarcoma, metastatic, liver	–	1 (2%)	–	–
Sarcoma, metastatic, uterus	–	–	1 (2%)	–
Squamous cell carcinoma, metastatic, uterus	1 (2%)	–	–	–
Pancreas	(50)	(50)	(50)	(50)
Sarcoma, metastatic, liver	–	1 (2%)	–	–
Sarcoma, metastatic, uterus	–	–	1 (2%)	–
Salivary glands	(50)	(50)	(50)	(50)
Adenoma	–	1 (2%)	–	–
Stomach, forestomach	(50)	(50)	(50)	(50)
Leiomyoma	1 (2%)	–	–	–
Squamous cell carcinoma	–	–	1 (2%)	
Squamous cell papilloma	–	–	–	1 (2%)
Stomach, glandular	(50)	(50)	(50)	(50)
Squamous cell carcinoma, metastatic, stomach, forestomach	–	–	1 (2%)	–
Tooth	(1)	(1)	(0)	(1)
Cardiovascular System				
Blood vessel	(49)	(50)	(50)	(49)
Heart	(50)	(50)	(50)	(50)
Schwannoma malignant	–	–	–	1 (2%)
Endocrine System				
Adrenal cortex	(50)	(50)	(50)	(50)
Adenoma	–	1 (2%)	–	–

	Chamber Control	3 mg/m^3	10 mg/m^3	30 mg/m^3
Adrenal medulla	(49)	(49)	(49)	(50)
Pheochromocytoma benign	–	2 (4%)	2 (4%)	6 (12%)
Pheochromocytoma malignant	–	–	–	1 (2%)
Islets, pancreatic	(50)	(50)	(50)	(50)
Parathyroid gland	(39)	(41)	(43)	(46)
Adenoma	–	–	1 (2%)	–
Pituitary gland	(50)	(50)	(50)	(50)
Schwannoma malignant	–	1 (2%)	–	–
Pars distalis, adenoma	19 (38%)	22 (44%)	19 (38%)	12 (24%)
Pars distalis, carcinoma	1 (2%)	–	–	–
Thyroid gland	(50)	(50)	(50)	(50)
Carcinoma	1 (2%)	–	–	–
C-cell, adenoma	4 (8%)	3 (6%)	5 (10%)	2 (4%)
C-cell, adenoma, multiple	–	1 (2%)	–	–
C-cell, carcinoma	1 (2%)	–	–	–
Follicular cell, adenoma	1 (2%)	–	2 (4%)	2 (4%)
Follicular cell, carcinoma	1 (2%)	–	1 (2%)	–
General Body System				
None	–	–	–	–
Genital System				
Clitoral gland	(50)	(49)	(47)	(49)
Carcinoma	–	1 (2%)	1 (2%)	–
Ovary	(50)	(49)	(50)	(50)
Adenoma	2 (4%)	–	–	1 (2%)
Cystadenoma	–	–	–	3 (6%)
Granulosa cell tumor benign	–	2 (4%)	–	–
Granulosa cell tumor malignant	–	–	–	1 (2%)
Leiomyosarcoma, metastatic, uterus	–	–	–	1 (2%)
Luteoma	–	–	–	1 (2%)
Tubulostromal adenoma	2 (4%)	–	1 (2%)	–
Bilateral, cystadenoma	1 (2%)	–	–	–

	Chamber Control	3 mg/m^3	10 mg/m^3	30 mg/m^3
Uterus	(50)	(50)	(50)	(50)
Adenocarcinoma	3 (6%)	–	–	2 (4%)
Adenoma	–	–	–	1 (2%)
Fibroma	–	–	–	1 (2%)
Hemangiosarcoma	1 (2%)	–	–	–
Leiomyosarcoma	1 (2%)	–	1 (2%)	1 (2%)
Polyp stromal	2 (4%)	9 (18%)	2 (4%)	4 (8%)
Sarcoma	–	–	1 (2%)	–
Sarcoma stromal	1 (2%)	–	–	–
Squamous cell carcinoma, metastatic, uncertain primary site	1 (2%)	–	–	–
Cervix, carcinoma	–	–	–	1 (2%)
Endometrium, adenoma	–	–	1 (2%)	–
Vagina	(0)	(0)	(1)	(0)
Sarcoma, metastatic, uterus	–	–	1 (100%)	–
Hematopoietic System				
Bone marrow	(50)	(50)	(50)	(50)
Lymph node	(2)	(3)	(3)	(3)
Iliac, leiomyosarcoma, metastatic, uterus	–	–	–	1 (33%)
Pancreatic, sarcoma, metastatic, liver	–	1 (33%)	–	–
Lymph node, bronchial	(35)	(36)	(28)	(41)
Lymph node, mandibular	(42)	(46)	(44)	(48)
Lymph node, mediastinal	(46)	(46)	(46)	(46)
Lymph node, mesenteric	(50)	(50)	(50)	(50)
Hemangioma	–	–	1 (2%)	1 (2%)
Spleen	(50)	(50)	(50)	(50)
Thymus	(46)	(41)	(37)	(48)
Thymoma benign	6 (13%)	6 (15%)	6 (16%)	8 (17%)
Integumentary System				
Mammary gland	(50)	(50)	(50)	(50)
Adenoma	–	2 (4%)	2 (4%)	1 (2%)
Carcinoma	5 (10%)	1 (2%)	4 (8%)	2 (4%)
Fibroadenoma	7 (14%)	4 (8%)	8 (16%)	4 (8%)
Fibroma	–	1 (2%)	–	–

	Chamber Control	3 mg/m^3	10 mg/m^3	30 mg/m^3
Skin	(50)	(49)	(50)	(50)
Squamous cell carcinoma	–	1 (2%)	–	–
Subcutaneous tissue, fibroma	2 (4%)	–	–	–
Subcutaneous tissue, schwannoma malignant	–	–	–	1 (2%)
Musculoskeletal System				
Bone	(50)	(50)	(50)	(50)
Mandible, squamous cell carcinoma, metastatic, skin	–	1 (2%)	–	–
Skeletal muscle	(2)	(1)	(2)	(7)
Leiomyosarcoma, metastatic, uterus	–	–	–	1 (14%)
Schwannoma malignant, metastatic, skin	–	–	–	1 (14%)
Nervous System				
Brain	(50)	(50)	(50)	(50)
Granular cell tumor benign	1 (2%)	1 (2%)	1 (2%)	–
Granular cell tumor malignant	1 (2%)	–	–	–
Peripheral nerve	(2)	(1)	(2)	(2)
Spinal cord	(2)	(1)	(2)	(2)
Respiratory System				
Larynx	(50)	(50)	(50)	(50)
Lung	(50)	(50)	(50)	(50)
Alveolar/bronchiolar adenoma	–	2 (4%)	5 (10%)	5 (10%)
Alveolar/bronchiolar adenoma, multiple	–	–	1 (2%)	–
Cystic keratinizing epithelioma	–	–	–	2 (4%)
Granular cell tumor malignant, metastatic, brain	1 (2%)	–	–	–
Leiomyosarcoma, metastatic, uterus	–	–	–	1 (2%)
Schwannoma malignant, metastatic, heart	–	–	–	1 (2%)
Squamous cell carcinoma	–	–	–	1 (2%)
Mediastinum	(0)	(0)	(2)	(9)
Nose	(50)	(50)	(50)	(50)
Nerve, granular cell tumor benign	–	–	1 (2%)	–
Trachea	(50)	(50)	(50)	(50)
Special Senses System				
Eye	(49)	(50)	(49)	(49)
Harderian gland	(50)	(50)	(50)	(50)

	Chamber Control	3 mg/m^3	10 mg/m^3	30 mg/m^3
Urinary System				
Kidney	(50)	(50)	(50)	(50)
Urinary bladder	(50)	(50)	(50)	(50)
Leiomyosarcoma, metastatic, uterus	–	–	–	1 (2%)
Systemic Lesions				
None	–	–	–	–
Neoplasm Summary				
Total animals with primary neoplasms[c]				
Twelve-month interim evaluation	3	1	2	4
Two-year study	39	41	38	35
Total primary neoplasms				
Twelve-month interim evaluation	3	1	2	4
Two-year study	66	66	68	66
Total animals with benign neoplasms				
Twelve-month interim evaluation	2	1	2	4
Two-year study	33	39	35	33
Total benign neoplasms				
Twelve-month interim evaluation	2	1	2	4
Two-year study	50	60	58	55
Total animals with malignant neoplasms				
Twelve-month interim evaluation	1			
Two-year study	16	6	9	10
Total malignant neoplasms				
Twelve-month interim evaluation	1	–	–	–
Two-year study	16	6	10	11
Total animals with metastatic neoplasms				
Two-year study	2	2	2	3
Total metastatic neoplasms				
Two-year study	4	4	4	9
Total animals with malignant neoplasms of uncertain primary site				
Two-year study	1	–	–	–

[a]Number of animals examined microscopically at the site and the number of animals with neoplasm.
[b]Number of animals with any tissue examined microscopically.
[c]Primary neoplasms: all neoplasms except metastatic neoplasms.

Table B-2. Statistical Analysis of Primary Neoplasms in Female Rats in the Two-year Inhalation Study of Antimony Trioxide

	Chamber Control	3 mg/m^3	10 mg/m^3	30 mg/m^3
Adrenal Medulla: Benign Pheochromocytoma				
Overall rate[a]	0/49 (0%)	2/49 (4%)	2/49 (4%)	6/50 (12%)
Adjusted rate[b]	0.0%	4.5%	4.8%	15.2%
Terminal rate[c]	0/38 (0%)	1/37 (3%)	1/27 (4%)	4/20 (20%)
First incidence (days)	–[e]	719	698	705
Poly-3 test[d]	P = 0.004	P = 0.235	P = 0.221	P = 0.009
Adrenal Medulla: Benign or Malignant Pheochromocytoma				
Overall rate	0/49 (0%)	2/49 (4%)	2/49 (4%)	7/50 (14%)
Adjusted rate	0.0%	4.5%	4.8%	17.6%
Terminal rate	0/38 (0%)	1/37 (3%)	1/27 (4%)	4/20 (20%)
First incidence (days)	–	719	698	621
Poly-3 test	P < 0.001	P = 0.235	P = 0.221	P = 0.004
Lung: Alveolar/Bronchiolar Adenoma				
Overall rate	0/50 (0%)	2/50 (4%)	6/50 (12%)	5/50 (10%)
Adjusted rate	0.0%	4.4%	13.8%	12.4%
Terminal rate	0/39 (0%)	2/38 (5%)	4/28 (14%)	2/20 (10%)
First incidence (days)	–	730 (T)	534	534
Poly-3 test	P = 0.029	P = 0.235	P = 0.012	P = 0.021
Lung: Cystic Keratinizing Epithelioma or Squamous Cell Carcinoma				
Overall rate	0/50 (0%)	0/50 (0%)	0/50 (0%)	3/50 (6%)
Adjusted rate	0.0%	0.0%	0.0%	7.4%
Terminal rate	0/39 (0%)	0/38 (0%)	0/28 (0%)	1/20 (5%)
First incidence (days)	–	–	–	554
Poly-3 test	P = 0.006	–[f]	–	P = 0.096
Mammary Gland: Fibroadenoma				
Overall rate	7/50 (14%)	4/50 (8%)	8/50 (16%)	4/50 (8%)
Adjusted rate	14.9%	8.7%	18.1%	9.7%
Terminal rate	5/39 (13%)	3/38 (8%)	5/28 (18%)	0/20 (0%)
First incidence (days)	561	589	505	498
Poly-3 test	P = 0.421N	P = 0.272N	P = 0.450	P = 0.342N

	Chamber Control	3 mg/m^3	10 mg/m^3	30 mg/m^3
Mammary Gland: Fibroma, Fibroadenoma, or Adenoma				
Overall rate	7/50 (14%)	6/50 (12%)	10/50 (20%)	5/50 (10%)
Adjusted rate	14.9%	12.8%	22.5%	12.1%
Terminal rate	5/39 (13%)	3/38 (8%)	6/28 (21%)	0/20 (0%)
First incidence (days)	561	589	505	498
Poly-3 test	P = 0.462N	P = 0.503N	P = 0.252	P = 0.469N
Mammary Gland: Carcinoma				
Overall rate	5/50 (10%)	1/50 (2%)	4/50 (8%)	2/50 (4%)
Adjusted rate	10.8%	2.2%	9.3%	5.0%
Terminal rate	3/39 (8%)	1/38 (3%)	2/28 (7%)	0/20 (0%)
First incidence (days)	635	730 (T)	654	618
Poly-3 test	P = 0.429N	P = 0.106N	P = 0.548N	P = 0.284N
Mammary Gland: Adenoma or Carcinoma				
Overall rate	5/50 (10%)	3/50 (6%)	5/50 (10%)	2/50 (4%)
Adjusted rate	10.8%	6.5%	11.6%	5.0%
Terminal rate	3/39 (8%)	2/38 (5%)	2/28 (7%)	0/20 (0%)
First incidence (days)	635	589	654	618
Poly-3 test	P = 0.316N	P = 0.361N	P = 0.583	P = 0.284N
Mammary Gland: Fibroma, Fibroadenoma, Adenoma, or Carcinoma				
Overall rate	10/50 (20%)	7/50 (14%)	12/50 (24%)	6/50 (12%)
Adjusted rate	21.3%	15.0%	26.8%	14.4%
Terminal rate	7/39 (18%)	4/38 (11%)	6/28 (21%)	0/20 (0%)
First incidence (days)	561	589	505	498
Poly-3 test	P = 0.353N	P = 0.301N	P = 0.352	P = 0.290N
Ovary: Cystadenoma				
Overall rate	1/50 (2%)	0/49 (0%)	0/50 (0%)	3/50 (6%)
Adjusted rate	2.2%	0.0%	0.0%	7.6%
Terminal rate	1/39 (3%)	0/38 (0%)	0/28 (0%)	3/20 (15%)
First incidence (days)	730 (T)	–	–	730 (T)
Poly-3 test	P = 0.043	P = 0.504N	P = 0.515N	P = 0.251
Pituitary Gland (Pars Distalis): Adenoma				
Overall rate	19/50 (38%)	22/50 (44%)	19/50 (38%)	12/50 (24%)
Adjusted rate	39.3%	45.5%	41.9%	27.9%
Terminal rate	12/39 (31%)	13/38 (34%)	10/28 (36%)	4/20 (20%)
First incidence (days)	443	513	534	423
Poly-3 test	P = 0.077N	P = 0.343	P = 0.482	P = 0.175N

	Chamber Control	3 mg/m^3	10 mg/m^3	30 mg/m^3
Pituitary Gland (Pars Distalis): Adenoma or Carcinoma				
Overall rate	20/50 (40%)	22/50 (44%)	19/50 (38%)	12/50 (24%)
Adjusted rate	41.3%	45.5%	41.9%	27.9%
Terminal rate	12/39 (31%)	13/38 (34%)	10/28 (36%)	4/20 (20%)
First incidence (days)	443	513	534	423
Poly-3 test	P = 0.061N	P = 0.418	P = 0.558	P = 0.129N
Thymus: Benign Thymoma				
Overall rate	6/46 (13%)	6/41 (15%)	6/37 (16%)	8/48 (17%)
Adjusted rate	14.1%	16.2%	19.2%	21.1%
Terminal rate	6/36 (17%)	6/32 (19%)	5/20 (25%)	3/19 (16%)
First incidence (days)	730 (T)	730 (T)	534	691
Poly-3 test	P = 0.263	P = 0.523	P = 0.399	P = 0.298
Thyroid Gland (C-Cell): Adenoma				
Overall rate	4/50 (8%)	4/50 (8%)	5/50 (10%)	2/50 (4%)
Adjusted rate	8.7%	8.7%	11.5%	5.1%
Terminal rate	4/39 (10%)	2/38 (5%)	3/28 (11%)	1/20 (5%)
First incidence (days)	730 (T)	610	562	719
Poly-3 test	P = 0.342N	P = 0.641N	P = 0.462	P = 0.412N
Thyroid Gland (C-Cell): Adenoma or Carcinoma				
Overall rate	5/50 (10%)	4/50 (8%)	5/50 (10%)	2/50 (4%)
Adjusted rate	10.9%	8.7%	11.5%	5.1%
Terminal rate	5/39 (13%)	2/38 (5%)	3/28 (11%)	1/20 (5%)
First incidence (days)	730 (T)	610	562	719
Poly-3 test	P = 0.268N	P = 0.498N	P = 0.592	P = 0.284N
Thyroid Gland (Follicular Cell): Adenoma or Carcinoma				
Overall rate	2/50 (4%)	0/50 (0%)	3/50 (6%)	2/50 (4%)
Adjusted rate	4.3%	0.0%	7%	5.1%
Terminal rate	1/39 (3%)	0/38 (0%)	3/28 (11%)	0/20 (0%)
First incidence (days)	645	–	730 (T)	719
Poly-3 test	P = 0.354	P = 0.241N	P = 0.462	P = 0.634
Uterus: Stromal Polyp				
Overall rate	2/50 (4%)	9/50 (18%)	2/50 (4%)	4/50 (8%)
Adjusted rate	4.3%	19.6%	4.6%	10.1%
Terminal rate	1/39 (3%)	7/38 (18%)	1/28 (4%)	2/20 (10%)
First incidence (days)	561	705	599	691
Poly-3 test	P = 0.534N	P = 0.023	P = 0.666	P = 0.265

	Chamber Control	3 mg/m^3	10 mg/m^3	30 mg/m^3
Uterus: Stromal Polyp or Stromal Sarcoma				
Overall rate	3/50 (6%)	9/50 (18%)	2/50 (4%)	4/50 (8%)
Adjusted rate	6.4%	19.6%	4.6%	10.1%
Terminal rate	2/39 (5%)	7/38 (18%)	1/28 (4%)	2/20 (10%)
First incidence (days)	561	705	599	691
Poly-3 test	P = 0.446N	P = 0.055	P = 0.535N	P = 0.412
Uterus: Carcinoma				
Overall rate	3/50 (6%)	0/50 (0%)	0/50 (0%)	3/50 (6%)
Adjusted rate	6.5%	0.0%	0.0%	7.6%
Terminal rate	3/39 (8%)	0/38 (0%)	0/28 (0%)	2/20 (10%)
First incidence (days)	730 (T)	–	–	726
Poly-3 test	P = 0.243	P = 0.120N	P = 0.133N	P = 0.587
All Organs: Benign Neoplasms				
Overall rate	33/50 (66%)	39/50 (78%)	35/50 (70%)	33/50 (66%)
Adjusted rate	67.5%	79.0%	73.0%	71.9%
Terminal rate	25/39 (64%)	28/38 (74%)	19/28 (68%)	14/20 (70%)
First incidence (days)	443	513	505	423
Poly-3 test	P = 0.527N	P = 0.143	P = 0.354	P = 0.401
All Organs: Malignant Neoplasms				
Overall rate	17/50 (34%)	6/50 (12%)	9/50 (18%)	10/50 (20%)
Adjusted rate	36.2%	13.0%	20.4%	24.1%
Terminal rate	13/39 (33%)	5/38 (13%)	4/28 (14%)	4/20 (20%)
First incidence (days)	635	519	478	423
Poly-3 test	P = 0.437N	P = 0.007N	P = 0.073N	P = 0.155N
All Organs: Benign or Malignant Neoplasms				
Overall rate	40/50 (80%)	41/50 (82%)	38/50 (76%)	35/50 (70%)
Adjusted rate	81.6%	82.0%	77.7%	75.4%
Terminal rate	31/39 (80%)	29/38 (76%)	20/28 (71%)	15/20 (75%)
First incidence (days)	443	513	478	423
Poly-3 test	P = 0.230N	P = 0.584	P = 0.409N	P = 0.303N

(T) = terminal kill.
[a]Number of neoplasm-bearing animals/number of animals examined. Denominator is number of animals examined microscopically for adrenal gland, lung, ovary, pituitary gland, thymus, and thyroid gland; for other tissues, denominator is number of animals necropsied.
[b]Poly-3 estimated neoplasm incidence after adjustment for intercurrent mortality.
[c]Observed incidence at terminal kill.
[d]Beneath the chamber control incidence is the P value associated with the trend test. Beneath the exposed group incidence are the P values corresponding to pairwise comparisons between the chamber controls and that exposed group. The Poly-3 test accounts for differential mortality in animals that do not reach terminal kill. A negative trend or a lower incidence in an exposure group is indicated by **N**.

[e]Not applicable; no neoplasms in animal group.
[f]Value of statistic cannot be computed.

Table B-3. Historical Incidence of Lung Neoplasms in Control Female Wistar Han Rats[a]

Study (Study Start)	Alveolar/Bronchiolar Adenoma	Cystic Keratinizing Epithelioma	Squamous Cell Carcinoma	Cystic Keratinizing Epithelioma or Squamous Cell Carcinoma
Historical Incidence: Inhalation Studies				
Antimony trioxide (September 2008)	0/50	0/50	0/50	0/50
CIMSTAR 3800 (April 2008)	0/50	0/50	0/50	0/50
Trim VX (July 2009)	0/50	0/50	0/50	0/50
Total	0/150	0/150	0/150	0/150
Overall Historical Incidence: All Routes				
Total	0/300	0/300	0/300	0/300

[a]Data as of November 2014.

Table B-4. Historical Incidence of Pheochromocytoma of the Adrenal Medulla in Control Female Wistar Han Rats[a]

Study (Study Start)	Benign	Malignant	Benign or Malignant
Historical Incidence: Inhalation Studies			
Antimony trioxide (September 2008)	0/49	0/49	0/49
CIMSTAR 3800 (April 2008)	1/49	1/49	2/49
Trim VX (July 2009)	0/50	0/50	0/50
Total (%)	1/148 (0.7%)	1/148 (0.7%)	2/148 (1.4%)
Mean ± standard deviation	0.7% ± 1.2%	0.7% ± 1.2%	1.4% ± 2.4%
Range	0%–2%	0%–2%	0%–4%
Overall Historical Incidence: All Routes			
Total (%)	5/297 (1.7%)	1/297 (0.3%)	7/297 (2.4%)[b]
Mean ± standard deviation	1.7% ± 1.5%	0.3% ± 0.8%	2.4% ± 2.0%
Range	0%–4%	0%–2%	0%–4%

[a]Data as of November 2014.
[b]Includes one incidence of complex pheochromocytoma.

Table B-5. Summary of the Incidence of Nonneoplastic Lesions in Female Rats in the Two-year Inhalation Study of Antimony Trioxide[a]

	Chamber Control	3 mg/m^3	10 mg/m^3	30 mg/m^3
Disposition Summary				
Animals initially in study	60	60	60	60
Twelve-month interim evaluation	10	10	10	10
Early deaths				
Moribund	11	12	20	27
Natural deaths	–	–	2	3
Survivors				
Died last week of study	–	–	1	1
Terminal kill	39	38	27	19
Animals examined microscopically	60	60	60	60
Twelve-month Interim Evaluation				
Alimentary System				
Esophagus	(10)	(10)	(9)	(10)
Intestine large, cecum	(10)	(10)	(10)	(10)
Intestine large, colon	(10)	(10)	(10)	(10)
Intestine large, rectum	(10)	(10)	(10)	(10)
Intestine small, duodenum	(10)	(10)	(10)	(10)
Intestine small, ileum	(10)	(10)	(10)	(10)
Intestine small, jejunum	(10)	(10)	(10)	(10)
Liver	(10)	(10)	(10)	(10)
Basophilic focus	1 (10%)	–	–	–
Hematopoietic cell proliferation	1 (10%)	–	–	–
Hepatodiaphragmatic nodule	1 (10%)	–	–	–
Infiltration cellular, histiocyte	–	–	1 (10%)	–
Pigmentation, hemosiderin	–	–	1 (10%)	–
Pancreas	(10)	(10)	(10)	(10)
Atrophy	–	–	1 (10%)	2 (20%)
Basophilic focus		1 (10%)	–	–
Inflammation, chronic active	–	–	1 (10%)	1 (10%)
Artery, fibrosis		1 (10%)	–	–
Salivary glands	(10)	(10)	(10)	(10)
Stomach, forestomach	(10)	(10)	(10)	(10)
Stomach, glandular	(10)	(10)	(10)	(10)

	Chamber Control	3 mg/m^3	10 mg/m^3	30 mg/m^3
Cardiovascular System				
Blood vessel	(10)	(10)	(10)	(10)
Heart	(10)	(10)	(10)	(10)
Cardiomyopathy	–	3 (30%)	–	1 (10%)
Mineralization	1 (10%)	–	–	–
Endocrine System				
Adrenal cortex	(10)	(10)	(10)	(10)
Hyperplasia	–	1 (10%)	1 (10%)	1 (10%)
Adrenal medulla	(10)	(10)	(10)	(10)
Islets, pancreatic	(10)	(10)	(10)	(10)
Parathyroid gland	(10)	(8)	(8)	(10)
Pituitary gland	(10)	(10)	(10)	(10)
Pars distalis, hyperplasia	2 (20%)	2 (20%)	–	1 (10%)
Thyroid gland	(10)	(10)	(10)	(10)
C-cell, hyperplasia	–	–	–	1 (10%)
Genital System				
Clitoral gland	(10)	(10)	(10)	(10)
Inflammation, chronic active	4 (40%)	3 (30%)	3 (30%)	1 (10%)
Ovary	(10)	(10)	(10)	(10)
Cyst	2 (20%)	1 (10%)	4 (40%)	–
Uterus	(10)	(10)	(10)	(10)
Dilatation	–	1 (10%)	–	–
Endometrial glands, metaplasia, squamous	–	–	1 (10%)	1 (10%)
Hematopoietic System				
Bone marrow	(10)	(10)	(10)	(10)
Hyperplasia	1 (10%)	1 (10%)	3 (30%)	–
Lymph node, bronchial	(7)	(8)	(9)	(5)
Foreign body	–	7 (88%)	9 (100%)	4 (80%)
Hyperplasia, lymphoid	–	4 (50%)	2 (22%)	1 (20%)
Pigmentation	–	–	–	1 (20%)
Lymph node, mandibular	(10)	(10)	(10)	(8)
Lymph node, mediastinal	(10)	(9)	(10)	(10)
Foreign body	–	9 (100%)	5 (50%)	6 (60%)
Hyperplasia, lymphoid	–	8 (89%)	–	3 (30%)
Pigmentation	8 (80%)	8 (89%)	8 (80%)	8 (80%)

	Chamber Control	3 mg/m^3	10 mg/m^3	30 mg/m^3
Lymph node, mesenteric	(10)	(10)	(10)	(10)
Spleen	(10)	(10)	(10)	(10)
Hematopoietic cell proliferation	4 (40%)	6 (60%)	6 (60%)	7 (70%)
Thymus	(10)	(10)	(10)	(10)
Cyst	1 (10%)	–	2 (20%)	–
Hyperplasia, squamous	–	1 (10%)	–	1 (10%)
Integumentary System				
Mammary gland	(10)	(10)	(10)	(10)
Skin	(10)	(10)	(10)	(10)
Cyst, squamous	1 (10%)	–	–	–
Respiratory System				
Larynx	(10)	(10)	(10)	(10)
Foreign body	–	10 (100%)	10 (100%)	10 (100%)
Lung	(10)	(10)	(10)	(10)
Fibrosis	–	10 (100%)	10 (100%)	10 (100%)
Foreign body	–	10 (100%)	10 (100%)	10 (100%)
Hemorrhage	–	–	1 (10%)	1 (10%)
Inflammation, chronic active	2 (20%)	10 (100%)	10 (100%)	10 (100%)
Proteinosis	–	10 (100%)	10 (100%)	10 (100%)
Alveolar epithelium, hyperplasia	–	10 (100%)	10 (100%)	10 (100%)
Alveolus, inflammation, suppurative	–	1 (10%)	–	3 (30%)
Bronchiole, epithelium, hyperplasia	–	1 (10%)	–	3 (30%)
Perivascular, infiltration cellular, lymphocyte	–	4 (40%)	5 (50%)	3 (30%)
Nose	(10)	(10)	(10)	(10)
Foreign body	–	–	–	4 (40%)
Metaplasia, mucous	–	–	–	1 (10%)
Olfactory epithelium, accumulation, hyaline droplet	2 (20%)	2 (20%)	1 (10%)	2 (20%)
Respiratory epithelium, accumulation, hyaline droplet	–	1 (10%)	–	1 (10%)
Respiratory epithelium, hyperplasia	–	1 (10%)	–	2 (20%)
Respiratory epithelium, metaplasia, squamous	–	–	–	1 (10%)
Trachea	(10)	(10)	(10)	(10)
Foreign body	–	6 (60%)	10 (100%)	10 (100%)

	Chamber Control	3 mg/m^3	10 mg/m^3	30 mg/m^3
Special Senses System				
Eye	(10)	(10)	(10)	(10)
Lens, degeneration	–	1 (10%)	–	–
Retina, atrophy	1 (10%)	–	1 (10%)	1 (10%)
Harderian gland	(10)	(10)	(10)	(10)
Urinary System				
Kidney	(10)	(10)	(10)	(10)
Calculus microscopic observation only	–	1 (10%)	1 (10%)	–
Nephropathy	–	2 (20%)	1 (10%)	2 (20%)
Cortex, vein, dilatation	–	–	–	1 (10%)
Urinary bladder	(10)	(10)	(10)	(10)
Systems Examined at 12 Months with No Lesions Observed				
General Body System				
Musculoskeletal System				
Nervous System				
Two-year Study				
Alimentary System				
Esophagus	(50)	(50)	(50)	(50)
Intestine large, cecum	(50)	(50)	(49)	(50)
Intestine large, colon	(50)	(50)	(50)	(50)
Hemorrhage	–	–	–	1 (2%)
Necrosis	–	–	–	1 (2%)
Intestine large, rectum	(48)	(47)	(50)	(49)
Edema	–	1 (2%)	–	–
Inflammation, chronic active	–	1 (2%)	–	–
Intestine small, duodenum	(50)	(50)	(50)	(50)
Inflammation, chronic active	–	–	–	1 (2%)
Intestine small, ileum	(50)	(50)	(49)	(50)
Inflammation, suppurative	–	–	1 (2%)	–
Intestine small, jejunum	(50)	(50)	(49)	(49)
Liver	(50)	(50)	(50)	(50)
Angiectasis	3 (6%)	2 (4%)	1 (2%)	2 (4%)
Basophilic focus	12 (24%)	7 (14%)	11 (22%)	6 (12%)
Clear cell focus	4 (8%)	5 (10%)	1 (2%)	2 (4%)
Congestion	2 (4%)	4 (8%)	1 (2%)	1 (2%)

	Chamber Control	3 mg/m^3	10 mg/m^3	30 mg/m^3
Cyst	2 (4%)	4 (8%)	3 (6%)	1 (2%)
Degeneration	–	–	1 (2%)	–
Eosinophilic focus	3 (6%)	1 (2%)	1 (2%)	1 (2%)
Fatty change	6 (12%)	1 (2%)	1 (2%)	–
Fibrosis	–	–	4 (8%)	2 (4%)
Hepatodiaphragmatic nodule	2 (4%)	2 (4%)	4 (8%)	4 (8%)
Hyperplasia	–	1 (2%)	–	–
Infiltration cellular, histiocyte	–	1 (2%)	–	–
Infiltration cellular, lymphocyte	–	–	1 (2%)	–
Inflammation, chronic active	–	–	3 (6%)	4 (8%)
Mixed cell focus	–	1 (2%)	1 (2%)	2 (4%)
Necrosis	–	–	–	2 (4%)
Pigmentation, hemosiderin	–	1 (2%)	–	–
Bile duct, hyperplasia	3 (6%)	2 (4%)	–	1 (2%)
Bile duct, hypertrophy	–	–	1 (2%)	–
Bile duct, inflammation, chronic active	1 (2%)	–	–	–
Hepatocyte, hypertrophy, focal	–	–	1 (2%)	–
Serosa, fibrosis	–	1 (2%)	–	–
Mesentery	(50)	(50)	(50)	(50)
Necrosis	–	–	–	1 (2%)
Artery, inflammation, chronic active	–	–	–	6 (12%)
Artery, necrosis	–	–	–	3 (6%)
Fat, necrosis	5 (10%)	3 (6%)	3 (6%)	6 (12%)
Pancreas	(50)	(50)	(50)	(50)
Atrophy	11 (22%)	14 (28%)	9 (18%)	16 (32%)
Basophilic focus	2 (4%)	–	–	1 (2%)
Inflammation, chronic active	–	2 (4%)	1 (2%)	–
Artery, hemorrhage	–	–	–	2 (4%)
Artery, inflammation, chronic active	–	–	3 (6%)	8 (16%)
Artery, necrosis	–	–	–	4 (8%)
Artery, thrombosis	–	–	–	1 (2%)
Salivary glands	(50)	(50)	(50)	(50)
Atrophy	–	1 (2%)	–	2 (4%)
Duct, hyperplasia	–	–	–	1 (2%)
Stomach, forestomach	(50)	(50)	(50)	(50)

	Chamber Control	3 mg/m^3	10 mg/m^3	30 mg/m^3
Cyst, squamous	1 (2%)	–	–	–
Fibrosis	–	1 (2%)	–	–
Hyperplasia, squamous	4 (8%)	5 (10%)	4 (8%)	6 (12%)
Inflammation, acute	–	1 (2%)	–	–
Inflammation, chronic active	–	–	–	1 (2%)
Mineralization	–	–	1 (2%)	1 (2%)
Ulcer	2 (4%)	1 (2%)	–	–
Stomach, glandular	(50)	(50)	(50)	(50)
Hemorrhage	–	–	1 (2%)	1 (2%)
Inflammation, chronic active	–	–	–	1 (2%)
Mineralization	–	–	–	1 (2%)
Ulcer	–	–	1 (2%)	–
Tooth	(1)	(1)	(0)	(1)
Inflammation, chronic active	1 (100%)	–	–	–
Malformation	–	1 (100%)	–	1 (100%)
Cardiovascular System				
Blood vessel	(49)	(50)	(50)	(49)
Heart	(50)	(50)	(50)	(50)
Cardiomyopathy	29 (58%)	19 (38%)	29 (58%)	29 (58%)
Inflammation, suppurative	–	–	1 (2%)	–
Valve, fibrosis	–	–	–	1 (2%)
Valve, inflammation, chronic active	–	–	1 (2%)	–
Endocrine System				
Adrenal cortex	(50)	(50)	(50)	(50)
Accessory adrenal cortical nodule	1 (2%)	–	–	–
Angiectasis	–	–	–	1 (2%)
Degeneration	–	–	–	1 (2%)
Degeneration, cystic	37 (74%)	44 (88%)	39 (78%)	31 (62%)
Degeneration, fatty	–	–	–	1 (2%)
Fibrosis	–	1 (2%)	1 (2%)	–
Hematopoietic cell proliferation	1 (2%)	–	1 (2%)	–
Hyperplasia	27 (54%)	23 (46%)	30 (60%)	23 (46%)
Hypertrophy	2 (4%)	2 (4%)	–	1 (2%)
Vacuolization cytoplasmic	1 (2%)	–	–	–
Adrenal medulla	(49)	(49)	(49)	(50)

	Chamber Control	3 mg/m^3	10 mg/m^3	30 mg/m^3
Atrophy	–	1 (2%)	–	–
Hyperplasia	–	–	3 (6%)	5 (10%)
Islets, pancreatic	(50)	(50)	(50)	(50)
Hyperplasia	1 (2%)	–	1 (2%)	–
Parathyroid gland	(39)	(41)	(43)	(46)
Pituitary gland	(50)	(50)	(50)	(50)
Angiectasis	–	–	–	2 (4%)
Necrosis	–	–	1 (2%)	–
Vacuolization cytoplasmic	–	1 (2%)	–	–
Pars distalis, hyperplasia	22 (44%)	16 (32%)	17 (34%)	21 (42%)
Pars intermedia, hyperplasia	1 (2%)	2 (4%)	2 (4%)	2 (4%)
Thyroid gland	(50)	(50)	(50)	(50)
C-cell, hyperplasia	21 (42%)	16 (32%)	15 (30%)	8 (16%)
Follicle, cyst	–	–	–	1 (2%)
Follicular cell, hyperplasia	3 (6%)	3 (6%)	1 (2%)	–
General Body System				
None	–	–	–	–
Genital System				
Clitoral gland	(50)	(49)	(47)	(49)
Cyst	–	–	4 (9%)	–
Fibrosis	–	–	–	1 (2%)
Inflammation, chronic active	2 (4%)	1 (2%)	2 (4%)	5 (10%)
Ovary	(50)	(49)	(50)	(50)
Congestion	–	–	2 (4%)	5 (10%)
Cyst	11 (22%)	10 (20%)	14 (28%)	15 (30%)
Fibrosis	–	–	2 (4%)	3 (6%)
Hemorrhage	–	1 (2%)	–	3 (6%)
Inflammation, chronic active	–	–	–	1 (2%)
Mineralization	–	–	–	1 (2%)
Necrosis	–	–	–	1 (2%)
Thrombosis	–	–	1 (2%)	1 (2%)
Granulosa cell, hyperplasia	1 (2%)	1 (2%)	2 (4%)	–
Interstitial cell, hyperplasia	2 (4%)	1 (2%)	1 (2%)	–
Uterus	(50)	(50)	(50)	(50)
Cyst	1 (2%)	–	–	–

	Chamber Control	3 mg/m^3	10 mg/m^3	30 mg/m^3
Dilatation	2 (4%)	3 (6%)	1 (2%)	2 (4%)
Hemorrhage	–	–	–	1 (2%)
Inflammation, suppurative	1 (2%)	–	1 (2%)	2 (4%)
Inflammation, chronic active	1 (2%)	1 (2%)	–	–
Necrosis	1 (2%)	–	–	–
Thrombosis	–	–	1 (2%)	–
Endometrial glands, hyperplasia	2 (4%)	–	3 (6%)	–
Endometrial glands, metaplasia, squamous	–	4 (8%)	2 (4%)	1 (2%)
Endometrium, cyst	–	–	–	1 (2%)
Endometrium, hyperplasia	–	1 (2%)	2 (4%)	–
Endometrium, hyperplasia, cystic	9 (18%)	17 (34%)	7 (14%)	16 (32%)
Endometrium, metaplasia, squamous	1 (2%)	–	–	–
Vagina	(0)	(0)	(1)	(0)
Hematopoietic System				
Bone marrow	(50)	(50)	(50)	(50)
Hemorrhage	–	–	1 (2%)	–
Hyperplasia	8 (16%)	5 (10%)	11 (22%)	20 (40%)
Myelofibrosis	–	–	–	1 (2%)
Lymph node	(2)	(3)	(3)	(3)
Pigmentation	1 (50%)	1 (33%)	–	–
Axillary, ectasia	–	–	1 (33%)	–
Iliac, congestion	–	–	–	1 (33%)
Iliac, hyperplasia, plasma cell	–	–	1 (33%)	–
Lumbar, ectasia	–	–	1 (33%)	–
Lumbar, foreign body	1 (50%)	–	–	–
Lumbar, hyperplasia	–	1 (33%)	–	–
Renal, congestion	–	–	1 (33%)	–
Renal, hemorrhage	–	–	1 (33%)	–
Thoracic, foreign body	–	–	–	1 (33%)
Lymph node, bronchial	(35)	(36)	(28)	(41)
Foreign body	–	35 (97%)	23 (82%)	36 (88%)
Hyperplasia, lymphoid	–	21 (58%)	9 (32%)	11 (27%)
Pigmentation	14 (40%)	12 (33%)	8 (29%)	18 (44%)
Lymph node, mandibular	(42)	(46)	(44)	(48)
Ectasia	–	–	1 (2%)	–

	Chamber Control	3 mg/m^3	10 mg/m^3	30 mg/m^3
Foreign body	–	1 (2%)	–	5 (10%)
Lymph node, mediastinal	(46)	(46)	(46)	(46)
Congestion	–	–	–	1 (2%)
Fibrosis	–	1 (2%)	–	–
Foreign body	–	27 (59%)	32 (70%)	33 (72%)
Hyperplasia, lymphoid	–	14 (30%)	10 (22%)	15 (33%)
Pigmentation	39 (85%)	42 (91%)	41 (89%)	41 (89%)
Lymph node, mesenteric	(50)	(50)	(50)	(50)
Spleen	(50)	(50)	(50)	(50)
Congestion	–	1 (2%)	1 (2%)	–
Depletion cellular	1 (2%)	–	–	–
Fibrosis	–	1 (2%)	1 (2%)	–
Hematopoietic cell proliferation	44 (88%)	43 (86%)	46 (92%)	48 (96%)
Hemorrhage	–	–	1 (2%)	1 (2%)
Pigmentation	–	–	1 (2%)	1 (2%)
Artery, inflammation, chronic active	–	–	1 (2%)	–
Artery, necrosis	–	–	1 (2%)	1 (2%)
Lymphoid follicle, atrophy	1 (2%)	–	–	–
Thymus	(46)	(41)	(37)	(48)
Cyst	–	1 (2%)	1 (3%)	1 (2%)
Depletion cellular	3 (7%)	1 (2%)	2 (5%)	3 (6%)
Hemorrhage	–	4 (10%)	2 (5%)	–
Hyperplasia	–	1 (2%)	–	–
Inflammation, chronic active	–	–	–	1 (2%)
Vacuolization cytoplasmic	1 (2%)	–	–	–
Integumentary System				
Mammary gland	(50)	(50)	(50)	(50)
Cyst	–	–	–	1 (2%)
Fibrosis	–	–	1 (2%)	1 (2%)
Galactocele	7 (14%)	9 (18%)	13 (26%)	10 (20%)
Granuloma, lipomatous	–	–	–	2 (4%)
Hyperplasia	6 (12%)	3 (6%)	8 (16%)	3 (6%)
Infiltration cellular, histiocyte	1 (2%)	–	–	–
Skin	(50)	(49)	(50)	(50)
Angiectasis	1 (2%)	–	–	1 (2%)

	Chamber Control	3 mg/m^3	10 mg/m^3	30 mg/m^3
Cyst, squamous	–	4 (8%)	–	1 (2%)
Fibrosis	1 (2%)	–	–	–
Hyperplasia	1 (2%)	–	–	–
Inflammation, suppurative	–	–	–	1 (2%)
Inflammation, chronic active	8 (16%)	5 (10%)	9 (18%)	9 (18%)
Ulcer	2 (4%)	5 (10%)	4 (8%)	8 (16%)
Epidermis, hyperplasia	–	–	–	1 (2%)
Epidermis, necrosis	–	–	2 (4%)	–
Subcutaneous tissue, inflammation, chronic active	–	1 (2%)	–	–
Musculoskeletal System	–	–	–	–
Bone	(50)	(50)	(50)	(50)
Femur, degeneration	–	–	–	1 (2%)
Femur, hyperostosis	–	–	–	2 (4%)
Femur, osteomalacia	–	–	–	1 (2%)
Maxilla, inflammation, chronic active	–	1 (2%)	2 (4%)	–
Skeletal muscle	(2)	(1)	(2)	(7)
Atrophy	–	–	–	1 (14%)
Inflammation, suppurative	–	–	–	1 (14%)
Inflammation, chronic active	–	–	–	1 (14%)
Necrosis	–	–	–	1 (14%)
Nervous System				
Brain	(50)	(50)	(50)	(50)
Compression	10 (20%)	12 (24%)	12 (24%)	5 (10%)
Edema	–	–	1 (2%)	–
Hemorrhage	–	–	2 (4%)	2 (4%)
Infiltration cellular, mixed cell	–	1 (2%)	–	–
Meninges, hyperplasia	–	–	1 (2%)	–
Peripheral nerve	(2)	(1)	(2)	(2)
Spinal cord	(2)	(1)	(2)	(2)
Respiratory System				
Larynx	(50)	(50)	(50)	(50)
Foreign body	–	50 (100%)	50 (100%)	50 (100%)
Inflammation, chronic active	–	8 (16%)	–	3 (6%)
Metaplasia, squamous	–	–	–	1 (2%)

	Chamber Control	3 mg/m^3	10 mg/m^3	30 mg/m^3
Arteriole, necrosis	–	–	–	1 (2%)
Respiratory epithelium, hyperplasia	5 (10%)	6 (12%)	2 (4%)	3 (6%)
Lung	(50)	(50)	(50)	(50)
Fibrosis	1 (2%)	50 (100%)	50 (100%)	49 (98%)
Foreign body	–	50 (100%)	50 (100%)	50 (100%)
Hemorrhage	–	5 (10%)	3 (6%)	–
Hyperplasia, lymphoid	–	1 (2%)	–	–
Inflammation, suppurative	1 (2%)	–	–	–
Inflammation, chronic active	21 (42%)	50 (100%)	50 (100%)	50 (100%)
Mineralization	1 (2%)	–	–	–
Proteinosis	–	50 (100%)	50 (100%)	50 (100%)
Thrombosis	–	–	–	1 (2%)
Alveolar epithelium, hyperplasia	5 (10%)	50 (100%)	49 (98%)	50 (100%)
Alveolar epithelium, metaplasia, squamous	–	5 (10%)	3 (6%)	1 (2%)
Alveolus, inflammation, suppurative	–	5 (10%)	6 (12%)	5 (10%)
Artery, inflammation, chronic active	–	–	1 (2%)	2 (4%)
Artery, necrosis	–	–	–	2 (4%)
Bronchiole, epithelium, hyperplasia	6 (12%)	26 (52%)	25 (50%)	27 (54%)
Perivascular, infiltration cellular, lymphocyte	–	18 (36%)	11 (22%)	8 (16%)
Mediastinum	(0)	(0)	(2)	(9)
Artery, inflammation, chronic active	–	–	2 (100%)	9 (100%)
Artery, necrosis	–	–	1 (50%)	6 (67%)
Nose	(50)	(50)	(50)	(50)
Foreign body	–	5 (10%)	26 (52%)	45 (90%)
Hyperplasia, squamous	–	–	1 (2%)	–
Inflammation, suppurative	2 (4%)	6 (12%)	5 (10%)	4 (8%)
Necrosis	–	–	–	2 (4%)
Glands, respiratory epithelium, hyperplasia	–	–	1 (2%)	–
Olfactory epithelium, accumulation, hyaline droplet	9 (18%)	14 (28%)	13 (26%)	13 (26%)
Olfactory epithelium, atrophy	–	–	–	2 (4%)
Olfactory epithelium, degeneration	–	–	–	1 (2%)
Olfactory epithelium, metaplasia, respiratory	–	1 (2%)	–	–

	Chamber Control	3 mg/m^3	10 mg/m^3	30 mg/m^3
Olfactory epithelium, necrosis	–	–	–	1 (2%)
Olfactory epithelium, vacuolization cytoplasmic	–	–	1 (2%)	–
Respiratory epithelium, accumulation, hyaline droplet	–	2 (4%)	2 (4%)	1 (2%)
Respiratory epithelium, degeneration	–	1 (2%)	–	–
Respiratory epithelium, hyperplasia	4 (8%)	6 (12%)	7 (14%)	16 (32%)
Respiratory epithelium, metaplasia, squamous	–	2 (4%)	3 (6%)	5 (10%)
Respiratory epithelium, necrosis	1 (2%)	1 (2%)	2 (4%)	1 (2%)
Respiratory epithelium, regeneration	–	–	1 (2%)	–
Squamous epithelium, hyperplasia	–	–	–	1 (2%)
Squamous epithelium, necrosis	–	–	1 (2%)	1 (2%)
Trachea	(50)	(50)	(50)	(50)
Fibrosis	–	–	1 (2%)	1 (2%)
Foreign body	–	39 (78%)	47 (94%)	49 (98%)
Inflammation, suppurative	–	–	–	1 (2%)
Metaplasia, squamous	1 (2%)	–	–	–
Epithelium, hyperplasia	–	–	–	2 (4%)
Epithelium, metaplasia, squamous	–	–	1 (2%)	–
Epithelium, regeneration	1 (2%)	–	2 (4%)	1 (2%)
Special Senses System				
Eye	(49)	(50)	(49)	(49)
Ciliary body, inflammation, acute	–	–	1 (2%)	6 (12%)
Lens, degeneration	–	2 (4%)	2 (4%)	–
Posterior chamber, exudate	–	–	1 (2%)	–
Retina, atrophy	6 (12%)	21 (42%)	18 (37%)	19 (39%)
Retina, infiltration cellular, polymorphonuclear	–	–	1 (2%)	–
Harderian gland	(50)	(50)	(50)	(50)
Hyperplasia	1 (2%)	–	–	–
Urinary System				
Kidney	(50)	(50)	(50)	(50)
Cyst	1 (2%)	2 (4%)	–	–
Infarct	–	3 (6%)	2 (4%)	1 (2%)
Nephropathy	16 (32%)	15 (30%)	20 (40%)	24 (48%)
Arteriole, inflammation, chronic active	–	–	–	1 (2%)

	Chamber Control	3 mg/m^3	10 mg/m^3	30 mg/m^3
Artery, fibrosis	–	–	–	1 (2%)
Artery, inflammation, chronic active	–	–	–	2 (4%)
Artery, necrosis	–	–	1 (2%)	2 (4%)
Papilla, necrosis	1 (2%)	–	–	–
Pelvis, dilatation	1 (2%)	–	–	1 (2%)
Pelvis, inflammation, suppurative	–	–	–	2 (4%)
Pelvis, inflammation, chronic active	2 (4%)	3 (6%)	–	1 (2%)
Pelvis, mineralization	31 (62%)	30 (60%)	24 (48%)	15 (30%)
Renal tubule, accumulation, hyaline droplet	–	–	5 (10%)	11 (22%)
Renal tubule, hyperplasia	1 (2%)	–	–	1 (2%)
Renal tubule, infiltration cellular, polymorphonuclear	–	–	1 (2%)	–
Urinary bladder	(50)	(50)	(50)	(50)
Angiectasis	–	–	–	1 (2%)

[a]Number of animals examined microscopically at the site and the number of animals with lesion.

Appendix C. Summary of Lesions in Male Mice in the Two-year Inhalation Study of Antimony Trioxide

Tables

Table C-1. Summary of the Incidence of Neoplasms in Male Mice in the Two-year Inhalation Study of Antimony Trioxide C-2
Table C-2. Statistical Analysis of Primary Neoplasms in Male Mice in the Two-year Inhalation Study of Antimony Trioxide C-10
Table C-3. Historical Incidence of Alveolar/Bronchiolar Neoplasms in Control Male B6C3F1/N Mice C-14
Table C-4. Historical Incidence of Malignant Lymphoma in Control Male B6C3F1/N Mice C-14
Table C-5. Historical Incidence of Skin Neoplasms in Control Male B6C3F1/N Mice C-15
Table C-6. Historical Incidence of Hepatocellular Neoplasms in Control Male B6C3F1/N Mice C-15
Table C-7. Summary of the Incidence of Nonneoplastic Lesions in Male Mice in the Two-year Inhalation Study of Antimony Trioxide C-16

Table C-1. Summary of the Incidence of Neoplasms in Male Mice in the Two-year Inhalation Study of Antimony Trioxide[a]

	Chamber Control	3 mg/m^3	10 mg/m^3	30 mg/m^3
Disposition Summary				
Animals initially in study	60	60	60	60
Twelve-month interim evaluation	10	10	10	10
Early deaths				
Accidental death	–	1	–	–
Moribund	7	12	15	26
Natural deaths	5	7	8	7
Survivors				
Terminal kill	38	30	27	17
Animals examined microscopically	60	60	60	60
Twelve-month Interim Evaluation				
Alimentary System				
Esophagus	(10)	(10)	(10)	(10)
Gallbladder	(8)	(10)	(9)	(9)
Intestine large, cecum	(10)	(10)	(10)	(10)
Intestine large, colon	(10)	(10)	(10)	(10)
Intestine large, rectum	(10)	(10)	(10)	(10)
Intestine small, duodenum	(10)	(10)	(10)	(10)
Intestine small, ileum	(10)	(10)	(10)	(10)
Intestine small, jejunum	(10)	(10)	(10)	(10)
Liver	(10)	(10)	(10)	(10)
Hepatocellular adenoma	2 (20%)	2 (20%)	1 (10%)	3 (30%)
Hepatocellular adenoma, multiple	1 (10%)	–	2 (20%)	2 (20%)
Hepatocellular carcinoma	1 (10%)	1 (10%)	1 (10%)	2 (20%)
Mesentery	(0)	(0)	(0)	(1)
Pancreas	(10)	(10)	(10)	(10)
Salivary glands	(10)	(10)	(10)	(10)
Stomach, forestomach	(10)	(10)	(10)	(10)
Stomach, glandular	(10)	(9)	(10)	(10)
Tooth	(1)	(0)	(0)	(0)
Respiratory System				
Larynx	(10)	(10)	(10)	(10)
Lung	(10)	(10)	(10)	(10)
Alveolar/bronchiolar adenoma	–	–	2 (20%)	–

	Chamber Control	3 mg/m^3	10 mg/m^3	30 mg/m^3
Alveolar/bronchiolar carcinoma	–	–	1 (10%)	2 (20%)
Nose	(10)	(10)	(10)	(10)
Trachea	(10)	(10)	(10)	(10)
Systems Examined at 12 Months with No Neoplasms Observed				
Cardiovascular System				
Endocrine System				
General Body System				
Genital System				
Hematopoietic System				
Integumentary System				
Musculoskeletal System				
Nervous System				
Special Senses System				
Urinary System				
Two-year Study				
Alimentary System				
Esophagus	(50)	(50)	(50)	(50)
Hepatocholangiocarcinoma, metastatic, liver	1 (2%)	–	–	–
Gallbladder	(44)	(41)	(38)	(40)
Intestine large, cecum	(46)	(45)	(45)	(47)
Adenoma	–	2 (4%)	–	–
Intestine large, colon	(48)	(45)	(47)	(48)
Intestine large, rectum	(47)	(42)	(45)	(48)
Intestine small, duodenum	(45)	(45)	(42)	(46)
Adenoma	2 (4%)	–	–	–
Intestine small, ileum	(46)	(44)	(43)	(48)
Adenoma	–	–	1 (2%)	–
Intestine small, jejunum	(46)	(44)	(42)	(48)
Carcinoma	1 (2%)	1 (2%)	–	1 (2%)
Liver	(50)	(50)	(49)	(50)
Alveolar/bronchiolar carcinoma, metastatic, lung	–	–	–	1 (2%)
Cholangiocarcinoma	1 (2%)	–	–	–
Cholangioma	–	–	–	1 (2%)
Hemangiosarcoma	–	–	–	1 (2%)
Hemangiosarcoma, metastatic, spleen	–	–	1 (2%)	–

	Chamber Control	3 mg/m^3	10 mg/m^3	30 mg/m^3
Hepatoblastoma	2 (4%)	1 (2%)	–	4 (8%)
Hepatocellular adenoma	12 (24%)	15 (30%)	22 (45%)	15 (30%)
Hepatocellular adenoma, multiple	18 (36%)	16 (32%)	14 (29%)	18 (36%)
Hepatocellular carcinoma	13 (26%)	17 (34%)	7 (14%)	15 (30%)
Hepatocellular carcinoma, multiple	2 (4%)	6 (12%)	7 (14%)	5 (10%)
Hepatocholangiocarcinoma	1 (2%)	–	–	–
Plasma cell tumor malignant, metastatic spleen	–	1 (2%)	–	–
Rhabdomyosarcoma, metastatic, skeletal muscle	–	1 (2%)	–	–
Mesentery	(7)	(4)	(4)	(5)
Alveolar/bronchiolar carcinoma, metastatic, lung	–	1 (25%)	–	–
Hepatocholangiocarcinoma, metastatic, liver	1 (14%)	–	–	–
Rhabdomyosarcoma, metastatic, skeletal muscle	–	1 (25%)	–	–
Oral mucosa	(1)	(0)	(0)	(0)
Pancreas	(49)	(49)	(49)	(50)
Hepatocellular carcinoma, metastatic, liver	–	–	–	1 (2%)
Plasma cell tumor malignant, metastatic, spleen	–	1 (2%)	–	–
Rhabdomyosarcoma, metastatic, skeletal muscle	–	1 (2%)	–	–
Salivary glands	(50)	(50)	(50)	(50)
Stomach, forestomach	(50)	(50)	(49)	(50)
Squamous cell papilloma	1 (2%)	–	–	–
Stomach, glandular	(48)	(49)	(49)	(50)
Rhabdomyosarcoma, metastatic, skeletal muscle	–	1 (2%)	–	–
Tooth	(14)	(14)	(14)	(6)
Blood vessel	(50)	(49)	(48)	(44)
Alveolar/bronchiolar carcinoma, metastatic, lung	–	–	–	1 (2%)
Sarcoma, metastatic, uncertain primary site	–	–	1 (2%)	–
Heart	(50)	(50)	(50)	(50)
Alveolar/bronchiolar carcinoma, metastatic, lung	–	–	1 (2%)	2 (4%)
Hemangioma	–	1 (2%)	–	–
Hemangiosarcoma	–	–	2 (4%)	–
Rhabdomyosarcoma, metastatic, skeletal muscle	–	1 (2%)	–	–
Sarcoma, metastatic, uncertain primary site	–	–	1 (2%)	–
Epicardium, carcinoma, metastatic, uncertain primary site	–	1 (2%)	1 (2%)	–
Endocrine System				
Adrenal cortex	(49)	(50)	(49)	(49)

	Chamber Control	3 mg/m^3	10 mg/m^3	30 mg/m^3
Adenoma	–	1 (2%)	–	–
Rhabdomyosarcoma, metastatic, skeletal muscle	–	1 (2%)	–	–
Capsule, hepatocholangiocarcinoma, metastatic, liver	1 (2%)	–	–	–
Subcapsular, adenoma	4 (8%)	–	2 (4%)	–
Zona fasciculata, adenoma	–	–	1 (2%)	–
Adrenal medulla	(49)	(50)	(46)	(49)
Pheochromocytoma benign	–	–	1 (2%)	–
Islets, pancreatic	(49)	(49)	(49)	(50)
Adenoma	–	–	1 (2%)	–
Parathyroid gland	(27)	(32)	(26)	(33)
Pituitary gland	(49)	(49)	(48)	(50)
Pars distalis, adenoma	–	–	2 (4%)	–
Thyroid gland	(49)	(49)	(48)	(49)
C-cell, carcinoma	–	1 (2%)	–	–
Follicular cell, adenoma	–	–	1 (2%)	–
Follicular cell, carcinoma	–	–	1 (2%)	–
General Body System				
Peritoneum	(0)	(0)	(0)	(1)
Alveolar/bronchiolar carcinoma, metastatic, lung	–	–	–	1 (100%)
Genital System				
Epididymis	(50)	(50)	(50)	(50)
Fibrosarcoma	–	–	1 (2%)	–
Hepatocholangiocarcinoma, metastatic, liver	1 (2%)	–	–	–
Preputial gland	(50)	(50)	(49)	(50)
Prostate	(49)	(50)	(49)	(50)
Rhabdomyosarcoma, metastatic, skeletal muscle	–	1 (2%)	–	–
Seminal vesicle	(49)	(50)	(49)	(50)
Adenoma	1 (2%)	–	–	–
Rhabdomyosarcoma, metastatic, skeletal muscle	–	1 (2%)	–	–
Testes	(49)	(49)	(50)	(50)
Rhabdomyosarcoma, metastatic, skeletal muscle	–	1 (2%)	–	–
Hematopoietic System				
Bone marrow	(49)	(50)	(48)	(50)
Hemangiosarcoma, metastatic, lymph node	–	1 (2%)	–	–

	Chamber Control	3 mg/m^3	10 mg/m^3	30 mg/m^3
Hemangiosarcoma, metastatic, spleen	1 (2%)	–	–	–
Rhabdomyosarcoma, metastatic, skeletal muscle	–	1 (2%)	–	–
Lymph node	(2)	(2)	(2)	(2)
Hemangiosarcoma	–	1 (50%)	–	–
Iliac, hemangiosarcoma	–	–	1 (50%)	–
Pancreatic, alveolar/bronchiolar carcinoma, metastatic, lung	–	–	–	1 (50%)
Lymph node, bronchial	(30)	(43)	(47)	(41)
Alveolar/bronchiolar carcinoma, metastatic, lung	–	3 (7%)	1 (2%)	5 (12%)
Hemangiosarcoma, metastatic, heart	–	–	1 (2%)	–
Hepatocellular carcinoma, metastatic, liver	1 (3%)	–	–	1 (2%)
Hepatocholangiocarcinoma, metastatic, liver	1 (3%)	–	–	–
Plasma cell tumor malignant, metastatic, spleen	–	1 (2%)	–	–
Rhabdomyosarcoma, metastatic, skeletal muscle	–	1 (2%)	–	–
Sarcoma, metastatic, uncertain primary site	–	–	1 (2%)	–
Lymph node, mandibular	(27)	(26)	(28)	(26)
Lymph node, mediastinal	(37)	(45)	(48)	(49)
Alveolar/bronchiolar carcinoma, metastatic, lung	–	2 (4%)	3 (6%)	4 (8%)
Carcinoma, metastatic, uncertain primary site	–	–	1 (2%)	–
Hemangiosarcoma, metastatic, heart	–	–	1 (2%)	–
Hemangiosarcoma, metastatic, spleen	–	–	1 (2%)	–
Hepatocellular carcinoma, metastatic, liver	1 (3%)	–	–	2 (4%)
Hepatocholangiocarcinoma, metastatic, liver	1 (3%)	–	–	–
Plasma cell tumor malignant, metastatic, spleen	–	1 (2%)	–	–
Rhabdomyosarcoma, metastatic, skeletal muscle	–	1 (2%)	–	–
Sarcoma, metastatic, uncertain primary site	–	–	1 (2%)	–
Lymph node, mesenteric	(48)	(47)	(47)	(50)
Fibrous histiocytoma, metastatic, skin	–	–	–	1 (2%)
Hepatocellular carcinoma, metastatic, liver	–	–	1 (2%)	–
Hepatocholangiocarcinoma, metastatic, liver	1 (2%)	–	–	–
Plasma cell tumor malignant, metastatic, spleen	–	1 (2%)	–	–
Rhabdomyosarcoma, metastatic, skeletal muscle	–	1 (2%)	–	–
Spleen	(49)	(50)	(50)	(50)
Hemangiosarcoma	2 (4%)	–	1 (2%)	–
Hepatocellular carcinoma, metastatic, liver	1 (2%)	–	–	–
Plasma cell tumor malignant	–	1 (2%)	–	–

	Chamber Control	3 mg/m^3	10 mg/m^3	30 mg/m^3
Thymus	(41)	(38)	(43)	(39)
Alveolar/bronchiolar carcinoma, metastatic, lung	–	2 (5%)	–	3 (8%)
Hemangiosarcoma, metastatic, heart	–	–	1 (2%)	–
Hepatocellular carcinoma, metastatic, liver	1 (2%)	–	–	–
Rhabdomyosarcoma, metastatic, skeletal muscle	–	1 (3%)	–	–
Sarcoma, metastatic, uncertain primary site	–	–	1 (2%)	–
Integumentary System				
Mammary gland	(0)	(2)	(4)	(1)
Skin	(50)	(50)	(50)	(50)
Alveolar/bronchiolar carcinoma, metastatic, lung	–	–	–	1 (2%)
Fibrosarcoma	–	–	2 (4%)	–
Fibrous histiocytoma	–	1 (2%)	1 (2%)	4 (8%)
Hemangioma	–	1 (2%)	–	–
Sebaceous gland, carcinoma	–	–	1 (2%)	–
Subcutaneous tissue, alveolar/bronchiolar carcinoma, metastatic, lung	–	–	–	1 (2%)
Musculoskeletal System				
Bone	(50)	(50)	(49)	(50)
Hemangiosarcoma, metastatic, spleen	–	–	1 (2%)	–
Rhabdomyosarcoma, metastatic, skeletal muscle	–	1 (2%)	–	–
Skeletal muscle	(2)	(3)	(1)	(1)
Alveolar/bronchiolar carcinoma, metastatic, lung	–	–	–	1 (100%)
Hepatocholangiocarcinoma, metastatic, liver	1 (50%)	–	–	–
Rhabdomyosarcoma	–	1 (33%)	–	–
Nervous System				
Brain	(50)	(50)	(50)	(50)
Rhabdomyosarcoma, metastatic, skeletal muscle	–	1 (2%)	–	–
Peripheral nerve	(1)	(1)	(0)	(0)
Spinal cord	(1)	(2)	(0)	(0)
Respiratory System				
Larynx	(50)	(50)	(50)	(50)
Lung	(50)	(50)	(50)	(50)
Alveolar/bronchiolar adenoma	7 (14%)	11 (22%)	7 (14%)	10 (20%)
Alveolar/bronchiolar adenoma, multiple	3 (6%)	3 (6%)	2 (4%)	4 (8%)
Alveolar/bronchiolar carcinoma	4 (8%)	13 (26%)	14 (28%)	16 (32%)

	Chamber Control	3 mg/m^3	10 mg/m^3	30 mg/m^3
Alveolar/bronchiolar carcinoma, multiple	–	5 (10%)	6 (12%)	11 (22%)
Hepatoblastoma, metastatic, liver	1 (2%)	–	–	–
Hepatocellular carcinoma, metastatic, liver	1 (2%)	3 (6%)	2 (4%)	5 (10%)
Hepatocholangiocarcinoma, metastatic, liver	1 (2%)	–	–	–
Plasma cell tumor malignant, metastatic, spleen	–	1 (2%)	–	–
Rhabdomyosarcoma, metastatic, skeletal muscle	–	1 (2%)	–	–
Sarcoma, metastatic, uncertain primary site	–	–	1 (2%)	–
Nose	(50)	(49)	(49)	(50)
Alveolar/bronchiolar carcinoma, metastatic, lung	–	–	–	1 (2%)
Pleura	(0)	(0)	(0)	(2)
Alveolar/bronchiolar carcinoma, metastatic, lung	–	–	–	1 (50%)
Trachea	(49)	(50)	(50)	(50)
Special Senses System				
Eye	(48)	(49)	(47)	(50)
Hepatocellular carcinoma, metastatic, liver	1 (2%)	–	–	–
Retrobulbar, alveolar/bronchiolar carcinoma, metastatic, lung	–	–	–	1 (2%)
Harderian gland	(49)	(50)	(50)	(50)
Adenoma	5 (10%)	5 (10%)	4 (8%)	3 (6%)
Adenoma, multiple	1 (2%)	1 (2%)	–	–
Carcinoma	1 (2%)	1 (2%)	1 (2%)	1 (2%)
Hemangioma	–	–	–	1 (2%)
Urinary System				
Kidney	(50)	(50)	(49)	(50)
Alveolar/bronchiolar carcinoma, metastatic, lung	–	–	–	1 (2%)
Hepatocellular carcinoma, metastatic, liver	1 (2%)	–	1 (2%)	1 (2%)
Plasma cell tumor malignant	–	1 (2%)	–	–
Rhabdomyosarcoma, metastatic, skeletal muscle	–	1 (2%)	–	–
Ureter	(1)	(0)	(0)	(0)
Urinary bladder	(50)	(50)	(48)	(50)
Rhabdomyosarcoma, metastatic, skeletal muscle	–	1 (2%)	–	–
Systemic Lesions				
Multiple organs[b]	(50)	(50)	(50)	(50)
Histiocytic sarcoma	1 (2%)	1 (2%)	3 (6%)	1 (2%)
Lymphoma malignant	4 (8%)	4 (8%)	3 (6%)	6 (12%)

	Chamber Control	3 mg/m^3	10 mg/m^3	30 mg/m^3
Mesothelioma malignant	–	–	–	1 (2%)
Neoplasm Summary				
Total animals with primary neoplasms[c]				
Twelve-month interim evaluation	3	3	7	6
Two-year study	45	45	46	46
Total primary neoplasms				
Twelve-month interim evaluation	4	3	7	9
Two-year study	86	111	109	119
Total animals with benign neoplasms				
Twelve-month interim evaluation	3	2	5	5
Two-year study	37	38	38	37
Total benign neoplasms				
Twelve-month interim evaluation	3	2	5	5
Two-year study	54	56	58	52
Total animals with malignant neoplasms				
Twelve-month interim evaluation	1	1	2	4
Two-year study	25	40	36	40
Total malignant neoplasms				
Twelve-month interim evaluation	1	1	2	4
Two-year study	32	55	51	67
Total animals with metastatic neoplasms				
Two-year study	5	9	11	14
Total metastatic neoplasms				
Two-year study	20	38	24	36
Total animals with malignant neoplasms of uncertain primary site				
Two-year study	–	1	3	–

[a]Number of animals examined microscopically at the site and the number of animals with neoplasm.
[b]Number of animals with any tissue examined microscopically.
[c]Primary neoplasms: all neoplasms except metastatic neoplasms.

Table C-2. Statistical Analysis of Primary Neoplasms in Male Mice in the Two-year Inhalation Study of Antimony Trioxide

	Chamber Control	3 mg/m^3	10 mg/m^3	30 mg/m^3
Adrenal Cortex: Adenoma				
Overall rate[a]	4/49 (8%)	1/50 (2%)	3/49 (6%)	0/49 (0%)
Adjusted rate[b]	8.7%	2.5%	7.3%	0.0%
Terminal rate[c]	3/38 (8%)	1/30 (3%)	2/27 (7%)	0/17 (0%)
First incidence (days)	702	729 (T)	666	–[e]
Poly-3 test[d]	P = 0.123N	P = 0.221N	P = 0.565N	P = 0.095N
Harderian Gland: Adenoma				
Overall rate	6/50 (12%)	6/50 (12%)	4/50 (8%)	3/50 (6%)
Adjusted rate	12.9%	14.6%	9.8%	7.9%
Terminal rate	5/38 (13%)	4/30 (13%)	4/27 (15%)	1/17 (6%)
First incidence (days)	663	514	729 (T)	536
Poly-3 test	P = 0.242N	P = 0.532	P = 0.457N	P = 0.349N
Harderian Gland: Adenoma or Carcinoma				
Overall rate	7/50 (14%)	7/50 (14%)	5/50 (10%)	4/50 (8%)
Adjusted rate	15.0%	17.0%	12.2%	10.5%
Terminal rate	5/38 (13%)	5/30 (17%)	4/27 (15%)	2/17 (12%)
First incidence (days)	663	514	576	536
Poly-3 test	P = 0.279N	P = 0.512	P = 0.471N	P = 0.388N
Liver: Hepatocellular Adenoma				
Overall rate	30/50 (60%)	31/50 (62%)	36/49 (73%)	33/50 (66%)
Adjusted rate	62.8%	68.8%	80.2%	76.5%
Terminal rate	25/38 (66%)	21/30 (70%)	24/27 (89%)	14/17 (82%)
First incidence (days)	626	365	279	474
Poly-3 test	P = 0.105	P = 0.344	P = 0.043	P = 0.106
Liver: Hepatocellular Carcinoma				
Overall rate	15/50 (30%)	23/50 (46%)	14/49 (29%)	20/50 (40%)
Adjusted rate	30.8%	50.5%	33.2%	46.6%
Terminal rate	9/38 (24%)	12/30 (40%)	7/27 (26%)	7/17 (41%)
First incidence (days)	512	365	554	474
Poly-3 test	P = 0.220	P = 0.039	P = 0.492	P = 0.086
Liver: Hepatocellular Adenoma or Carcinoma				
Overall rate	39/50 (78%)	38/50 (76%)	40/49 (82%)	39/50 (78%)
Adjusted rate	78.7%	81.5%	87.7%	85.4%
Terminal rate	30/38 (79%)	23/30 (77%)	25/27 (93%)	14/17 (82%)

	Chamber Control	3 mg/m^3	10 mg/m^3	30 mg/m^3
First incidence (days)	512	365	279	474
Poly-3 test	P = 0.249	P = 0.464	P = 0.174	P = 0.271
Liver: Hepatoblastoma				
Overall rate	2/50 (4%)	1/50 (2%)	0/49 (0%)	4/50 (8%)
Adjusted rate	4.3%	2.5%	0.0%	10.3%
Terminal rate	2/38 (5%)	0/30 (0%)	0/27 (0%)	1/17 (6%)
First incidence (days)	729 (T)	604	–	554
Poly-3 test	P = 0.088	P = 0.544N	P = 0.268N	P = 0.261
Liver: Hepatocellular Carcinoma or Hepatoblastoma				
Overall rate	16/50 (32%)	24/50 (48%)	14/49 (29%)	21/50 (42%)
Adjusted rate	32.8%	52.2%	33.2%	49%
Terminal rate	10/38 (26%)	12/30 (40%)	7/27 (26%)	8/17 (47%)
First incidence (days)	512	365	554	474
Poly-3 test	P = 0.211	P = 0.042	P = 0.574	P = 0.084
Liver: Hepatocellular Adenoma, Hepatocellular Carcinoma, or Hepatoblastoma				
Overall rate	39/50 (78%)	39/50 (78%)	40/49 (82%)	39/50 (78%)
Adjusted rate	78.7%	82.8%	87.7%	85.4%
Terminal rate	30/38 (79%)	23/30 (77%)	25/27 (93%)	14/17 (82%)
First incidence (days)	512	365	279	474
Poly-3 test	P = 0.276	P = 0.395	P = 0.174	P = 0.271
Lung: Alveolar/Bronchiolar Adenoma				
Overall rate	10/50 (20%)	14/50 (28%)	9/50 (18%)	14/50 (28%)
Adjusted rate	21.5%	32.9%	21.8%	34.6%
Terminal rate	9/38 (24%)	7/30 (23%)	6/27 (22%)	4/17 (24%)
First incidence (days)	702	449	646	530
Poly-3 test	P = 0.190	P = 0.165	P = 0.592	P = 0.129
Lung: Alveolar/Bronchiolar Carcinoma				
Overall rate	4/50 (8%)	18/50 (36%)	20/50 (40%)	27/50 (54%)
Adjusted rate	8.5%	40.9%	46.2%	62.8%
Terminal rate	2/38 (5%)	9/30 (30%)	11/27 (41%)	12/17 (71%)
First incidence (days)	590	449	509	490
Poly-3 test	P < 0.001	P < 0.001	P < 0.001	P < 0.001
Lung: Alveolar/Bronchiolar Adenoma or Carcinoma				
Overall rate	13/50 (26%)	29/50 (58%)	28/50 (56%)	34/50 (68%)
Adjusted rate	27.5%	64.5%	63.6%	75.3%

	Chamber Control	3 mg/m^3	10 mg/m^3	30 mg/m^3
Terminal rate	10/38 (26%)	16/30 (53%)	16/27 (59%)	12/17 (71%)
First incidence (days)	590	449	509	490
Poly-3 test	P < 0.001	P < 0.001	P < 0.001	P < 0.001
Skin: Fibrous Histiocytoma				
Overall rate	0/50 (0%)	1/50 (2%)	1/50 (2%)	4/50 (8%)
Adjusted rate	0.0%	2.5%	2.5%	10.6%
Terminal rate	0/38 (0%)	1/30 (3%)	1/27 (4%)	2/17 (12%)
First incidence (days)	–	729 (T)	729 (T)	612
Poly-3 test	P = 0.012	P = 0.473	P = 0.474	P = 0.039
Skin: Fibrous Histiocytoma or Fibrosarcoma				
Overall rate	0/50 (0%)	1/50 (2%)	3/50 (6%)	4/50 (8%)
Adjusted rate	0.0%	2.5%	7.3%	10.6%
Terminal rate	0/38 (0%)	1/30 (3%)	2/27 (7%)	2/17 (12%)
First incidence (days)	–	729 (T)	468	612
Poly-3 test	P = 0.023	P = 0.473	P = 0.100	P = 0.039
Small Intestine (Site Unspecified): Adenoma or Carcinoma				
Overall rate	3/50 (6%)	1/50 (2%)	1/50 (2%)	1/50 (2%)
Adjusted rate	6.5%	2.4%	2.5%	2.7%
Terminal rate	2/38 (5%)	0/30 (0%)	1/27 (4%)	1/17 (6%)
First incidence (days)	702	365	729 (T)	729 (T)
Poly-3 test	P = 0.386N	P = 0.349N	P = 0.354N	P = 0.387N
All Organs: Hemangiosarcoma				
Overall rate	2/50 (4%)	1/50 (2%)	3/50 (6%)	1/50 (2%)
Adjusted rate	4.3%	2.5%	7.2%	2.7%
Terminal rate	2/38 (5%)	1/30 (3%)	1/27 (4%)	1/17 (6%)
First incidence (days)	729 (T)	729 (T)	509	729 (T)
Poly-3 test	P = 0.542N	P = 0.547N	P = 0.450	P = 0.574N
All Organs: Hemangioma or Hemangiosarcoma				
Overall rate	2/50 (4%)	3/50 (6%)	3/50 (6%)	2/50 (4%)
Adjusted rate	4.3%	7.4%	7.2%	5.3%
Terminal rate	2/38 (5%)	2/30 (7%)	1/27 (4%)	1/17 (6%)
First incidence (days)	729 (T)	651	509	490
Poly-3 test	P = 0.595N	P = 0.441	P = 0.450	P = 0.621
All Organs: Histiocytic Sarcoma				
Overall rate	1/50 (2%)	1/50 (2%)	3/50 (6%)	1/50 (2%)

	Chamber Control	3 mg/m^3	10 mg/m^3	30 mg/m^3
Adjusted rate	2.2%	2.5%	7.3%	2.7%
Terminal rate	0/38 (0%)	1/30 (3%)	1/27 (4%)	1/17 (6%)
First incidence (days)	663	729 (T)	639	729 (T)
Poly-3 test	P = 0.574	P = 0.728	P = 0.263	P = 0.709
All Organs: Malignant Lymphoma				
Overall rate	4/50 (8%)	4/50 (8%)	3/50 (6%)	6/50 (12%)
Adjusted rate	8.6%	9.8%	7.4%	15.7%
Terminal rate	3/38 (8%)	2/30 (7%)	3/27 (11%)	2/17 (12%)
First incidence (days)	670	590	729 (T)	639
Poly-3 test	P = 0.189	P = 0.571	P = 0.573N	P = 0.254
All Organs: Benign Neoplasms				
Overall rate	37/50 (74%)	38/50 (76%)	38/50 (76%)	37/50 (74%)
Adjusted rate	76.7%	82.1%	84.6%	81.5%
Terminal rate	29/38 (76%)	24/30 (80%)	26/27 (96%)	14/17 (82%)
First incidence (days)	626	365	279	474
Poly-3 test	P = 0.425	P = 0.343	P = 0.228	P = 0.372
All Organs: Malignant Neoplasms				
Overall rate	25/50 (50%)	40/50 (80%)	38/50 (76%)	40/50 (80%)
Adjusted rate	50.7%	83.1%	81.0%	84.4%
Terminal rate	16/38 (42%)	22/30 (73%)	20/27 (74%)	14/17 (82%)
First incidence (days)	512	365	468	474
Poly-3 test	P = 0.005	P < 0.001	P < 0.001	P < 0.001
All Organs: Benign or Malignant Neoplasms				
Overall rate	45/50 (90%)	45/50 (90%)	47/50 (94%)	46/50 (92%)
Adjusted rate	90.0%	93.4%	97.8%	95.6%
Terminal rate	33/38 (87%)	27/30 (90%)	27/27 (100%)	16/17 (94%)
First incidence (days)	512	365	279	474
Poly-3 test	P = 0.229	P = 0.401	P = 0.110	P = 0.239

(T) = terminal kill.
[a]Number of neoplasm-bearing animals/number of animals examined. Denominator is number of animals examined microscopically for adrenal gland, liver, and lung; for other tissues, denominator is number of animals necropsied.
[b]Poly-3 estimated neoplasm incidence after adjustment for intercurrent mortality.
[c]Observed incidence at terminal kill.
[d]Beneath the chamber control incidence is the P value associated with the trend test. Beneath the exposed group incidence are the P values corresponding to pairwise comparisons between the chamber controls and that exposed group. The Poly-3 test accounts for differential mortality in animals that do not reach terminal kill. A negative trend or a lower incidence in an exposure group is indicated by **N**.
[e]Not applicable; no neoplasms in animal group.

Table C-3. Historical Incidence of Alveolar/Bronchiolar Neoplasms in Control Male B6C3F1/N Mice[a]

Study (Study Start)	Adenoma	Carcinoma	Adenoma or Carcinoma
Historical Incidence: Inhalation Studies			
Antimony trioxide (October 2008)	10/50	4/50	13/50
CIMSTAR 3800 (May 2008)	5/50	8/50	13/50
Cobalt metal (May 2006)	7/50	11/50	16/50
Vinylidene chloride (June 2005)	7/50	9/50	13/50
Trim VX (August 2009)	6/50	10/50	14/50
Total (%)	35/250 (14.0%)	42/250 (16.8%)	69/250 (27.6%)
Mean ± standard deviation	14.0% ± 3.7%	16.8% ± 5.4%	27.6% ± 2.6%
Range	10%–20%	8%–22%	26%–32%
Overall Historical Incidence: All Routes			
Total (%)	83/550 (15.1%)	75/550 (13.6%)	147/550 (26.7%)
Mean ± standard deviation	15.1% ± 5.9%	13.6% ± 6.4%	26.7% ± 6.5%
Range	8%–26%	4%–22%	16%–38%

[a]Data as of June 2015.

Table C-4. Historical Incidence of Malignant Lymphoma in Control Male B6C3F1/N Mice[a]

Study (Study Start)	Incidence in Controls
Historical Incidence: Inhalation Studies	
Antimony trioxide (October 2008)	4/50
CIMSTAR 3800 (May 2008)	3/50
Cobalt metal (May 2006)	4/50
Vinylidene chloride (June 2005)	2/50
Trim VX (August 2009)	6/50
Total (%)	19/250 (7.6%)
Mean ± standard deviation	7.6% ± 3.0%
Range	4%–12%
Overall Historical Incidence: All Routes	
Total (%)	35/550 (6.4%)
Mean ± standard deviation	6.4% ± 3.4%
Range	0%–12%

[a]Data as of June 2015; may include data for histiocytic, lymphocytic, mixed, unspecified, or undifferentiated cell types.

Table C-5. Historical Incidence of Skin Neoplasms in Control Male B6C3F1/N Mice[a]

Study (Study Start)	Fibrous Histiocytoma	Fibrosarcoma	Fibrous Histiocytoma or Fibrosarcoma
Historical Incidence: Inhalation Studies			
Antimony trioxide (October 2008)	0/50	0/50	0/50
CIMSTAR 3800 (May 2008)	0/50	0/50	0/50
Cobalt metal (May 2006)	0/50	0/50	0/50
Vinylidene chloride (June 2005)	1/50	0/50	1/50
Trim VX (August 2009)	0/50	1/50	1/50
Total (%)	1/250 (0.4%)	1/250 (0.4%)	2/250 (0.8%)
Mean ± standard deviation	0.4% ± 0.9%	0.4% ± 0.9%	0.8% ± 1.1%
Range	0%–2%	0%–2%	0%–2%
Overall Historical Incidence: All Routes			
Total (%)	2/550 (0.4%)	2/550 (0.4%)	5/550 (0.9%)[b]
Mean ± standard deviation	0.4% ± 0.8%	0.4% ± 0.8%	0.9% ± 1.0%
Range	0%–2%	0%–2%	0%–2%

[a]Data as of June 2015.
[b]Includes one incidence of sarcoma.

Table C-6. Historical Incidence of Hepatocellular Neoplasms in Control Male B6C3F1/N Mice[a]

Study (Study Start)	Adenoma	Carcinoma
Historical Incidence: Inhalation Studies		
Antimony trioxide (October 2008)	30/50	15/50
CIMSTAR 3800 (May 2008)	24/50	11/50
Cobalt metal (May 2006)	28/50	25/50
Vinylidene chloride (June 2005)	37/50	26/50
Trim VX (August 2009)	23/50	21/50
Total (%)	142/250 (56.8%)	98/250 (39.2%)
Mean ± standard deviation	56.8% ± 11.2%	39.2% ± 12.9%
Range	46%–74%	22%–52%
Overall Historical Incidence: All Routes		
Total (%)	328/550 (59.6%)	188/550 (34.2%)
Mean ± standard deviation	59.6% ± 11.2%	34.2% ± 11.3%
Range	46%–78%	22%–52%

[a]Data as of June 2015.

Table C-7. Summary of the Incidence of Nonneoplastic Lesions in Male Mice in the Two-year Inhalation Study of Antimony Trioxide[a]

	Chamber Control	3 mg/m^3	10 mg/m^3	30 mg/m^3
Disposition Summary				
Animals initially in study	60	60	60	60
Twelve-month interim evaluation	10	10	10	10
Early deaths				
Accidental death	–	1	–	–
Moribund	7	12	15	26
Natural deaths	5	7	8	7
Survivors				
Terminal kill	38	30	27	17
Animals examined microscopically	60	60	60	60
Twelve-month Interim Evaluation				
Alimentary System				
Esophagus	(10)	(10)	(10)	(10)
Gallbladder	(8)	(10)	(9)	(9)
Intestine large, cecum	(10)	(10)	(10)	(10)
Intestine large, colon	(10)	(10)	(10)	(10)
Intestine large, rectum	(10)	(10)	(10)	(10)
Intestine small, duodenum	(10)	(10)	(10)	(10)
Intestine small, ileum	(10)	(10)	(10)	(10)
Intestine small, jejunum	(10)	(10)	(10)	(10)
Liver	(10)	(10)	(10)	(10)
Basophilic focus	–	1 (10%)	–	–
Clear cell focus	2 (20%)	2 (20%)	2 (20%)	–
Mesentery	(0)	(0)	(0)	(1)
Necrosis, fatty	–	–	–	1 (100%)
Pancreas	(10)	(10)	(10)	(10)
Salivary glands	(10)	(10)	(10)	(10)
Stomach, forestomach	(10)	(10)	(10)	(10)
Stomach, glandular	(10)	(9)	(10)	(10)
Tooth	(1)	(0)	(0)	(0)
Malformation	1 (100%)	–	–	–
Cardiovascular System				
Blood vessel	(10)	(10)	(10)	(10)
Heart	(10)	(10)	(10)	(10)

	Chamber Control	3 mg/m^3	10 mg/m^3	30 mg/m^3
Cardiomyopathy	–	–	–	1 (10%)
Endocrine System				
Adrenal cortex	(10)	(10)	(10)	(10)
Zona fasciculata, hypertrophy	3 (30%)	1 (10%)	–	1 (10%)
Adrenal medulla	(10)	(10)	(10)	(10)
Islets, pancreatic	(10)	(10)	(10)	(10)
Parathyroid gland	(6)	(7)	(5)	(8)
Pituitary gland	(10)	(10)	(10)	(9)
Thyroid gland	(10)	(10)	(10)	(10)
Genital System				
Epididymis	(10)	(10)	(10)	(10)
Preputial gland	(10)	(10)	(10)	(10)
Inflammation, chronic active	1 (10%)	–	–	–
Prostate	(10)	(10)	(10)	(10)
Seminal vesicle	(10)	(10)	(10)	(10)
Testes	(10)	(10)	(10)	(10)
Hematopoietic System				
Bone marrow	(10)	(10)	(10)	(10)
Lymph node, bronchial	(8)	(10)	(10)	(10)
Foreign body	–	10 (100%)	10 (100%)	10 (100%)
Hyperplasia, lymphoid	–	7 (70%)	9 (90%)	10 (100%)
Infiltration cellular, histiocyte	–	4 (40%)	4 (40%)	1 (10%)
Lymph node, mandibular	(5)	(4)	(4)	(4)
Infiltration cellular, histiocyte	–	–	–	2 (50%)
Lymph node, mediastinal	(4)	(8)	(10)	(10)
Foreign body	–	1 (13%)	8 (80%)	10 (100%)
Hyperplasia, lymphoid	–	1 (13%)	4 (40%)	9 (90%)
Infiltration cellular, histiocyte	–	1 (13%)	3 (30%)	4 (40%)
Lymph node, mesenteric	(10)	(10)	(10)	(10)
Spleen	(10)	(10)	(10)	(10)
Thymus	(10)	(10)	(10)	(10)
Inflammation, chronic active	–	–	–	1 (10%)
Medulla, hyperplasia, lymphoid	–	1 (10%)	1 (10%)	–
Respiratory System				
Larynx	(10)	(10)	(10)	(10)

	Chamber Control	3 mg/m^3	10 mg/m^3	30 mg/m^3
Foreign body	–	3 (30%)	5 (50%)	10 (100%)
Respiratory epithelium, degeneration	–	–	1 (10%)	–
Respiratory epithelium, hyperplasia	–	1 (10%)	4 (40%)	6 (60%)
Respiratory epithelium, metaplasia, squamous	–	–	2 (20%)	3 (30%)
Lung	(10)	(10)	(10)	(10)
Foreign body	–	10 (100%)	10 (100%)	10 (100%)
Infiltration cellular, lymphocyte	–	10 (100%)	10 (100%)	10 (100%)
Inflammation, chronic active	–	10 (100%)	10 (100%)	10 (100%)
Alveolar epithelium, hyperplasia	–	9 (90%)	10 (100%)	10 (100%)
Alveolar epithelium, metaplasia, squamous	–	–	–	1 (10%)
Alveolus, fibrosis	–	4 (40%)	7 (70%)	10 (100%)
Bronchiole, epithelium, hyperplasia	–	9 (90%)	9 (90%)	9 (90%)
Pleura, fibrosis	–	5 (50%)	10 (100%)	10 (100%)
Pleura, inflammation	–	7 (70%)	10 (100%)	10 (100%)
Nose	(10)	(10)	(10)	(10)
Foreign body	–	8 (80%)	10 (100%)	9 (90%)
Inflammation, acute	–	–	1 (10%)	–
Respiratory epithelium, accumulation, hyaline droplet	1 (10%)	–	–	1 (10%)
Respiratory epithelium, inflammation, chronic active	1 (10%)	–	–	–
Trachea	(10)	(10)	(10)	(10)
Foreign body	–	–	2 (20%)	4 (40%)
Epithelium, hyperplasia	–	–	1 (10%)	–
Epithelium, metaplasia, squamous	–	1 (10%)	–	1 (10%)
Special Senses System				
Eye	(10)	(10)	(10)	(10)
Harderian gland	(10)	(10)	(10)	(10)
Hyperplasia	–	–	–	1 (10%)
Urinary System				
Kidney	(10)	(10)	(10)	(10)
Nephropathy	2 (20%)	3 (30%)	4 (40%)	2 (20%)
Glomerulus, hyalinization	–	–	–	1 (10%)
Papilla, necrosis	1 (10%)	–	–	–
Urinary bladder	(10)	(10)	(10)	(10)

	Chamber Control	3 mg/m^3	10 mg/m^3	30 mg/m^3
Systems Examined at 12 Months with No Lesions Observed				
General Body System				
Integumentary System				
Musculoskeletal System				
Nervous System				
Two-year Study				
Alimentary System				
Esophagus	(50)	(50)	(50)	(50)
Inflammation, chronic active	1 (2%)	–	–	–
Gallbladder	(44)	(41)	(38)	(40)
Inflammation, chronic	2 (5%)	1 (2%)	–	2 (5%)
Intestine large, cecum	(46)	(45)	(45)	(47)
Inflammation, chronic active	–	3 (7%)	–	1 (2%)
Intestine large, colon	(48)	(45)	(47)	(48)
Lymphoid tissue, hyperplasia	1 (2%)	–	–	–
Intestine large, rectum	(47)	(42)	(45)	(48)
Intestine small, duodenum	(45)	(45)	(42)	(46)
Intestine small, ileum	(46)	(44)	(43)	(48)
Atrophy	–	1 (2%)	–	–
Inflammation, chronic active	–	3 (7%)	–	1 (2%)
Peyer’s patch, hyperplasia, lymphoid	2 (4%)	–	–	2 (4%)
Intestine small, jejunum	(46)	(44)	(42)	(48)
Atrophy	–	1 (2%)	–	–
Inflammation	1 (2%)	–	1 (2%)	2 (4%)
Mineralization	–	–	–	1 (2%)
Necrosis	–	–	1 (2%)	–
Peyer’s patch, hyperplasia, lymphoid	1 (2%)	–	–	2 (4%)
Liver	(50)	(50)	(49)	(50)
Angiectasis	1 (2%)	–	1 (2%)	–
Basophilic focus	4 (8%)	3 (6%)	2 (4%)	5 (10%)
Clear cell focus	14 (28%)	9 (18%)	10 (20%)	6 (12%)
Eosinophilic focus	4 (8%)	5 (10%)	7 (14%)	7 (14%)
Eosinophilic focus, multiple	–	–	–	1 (2%)
Fatty change	–	–	1 (2%)	–
Hepatodiaphragmatic nodule	–	–	–	1 (2%)

	Chamber Control	3 mg/m^3	10 mg/m^3	30 mg/m^3
Inflammation, chronic active	1 (2%)	1 (2%)	–	3 (6%)
Mineralization	1 (2%)	–	–	–
Mixed cell focus	1 (2%)	2 (4%)	3 (6%)	1 (2%)
Necrosis	3 (6%)	2 (4%)	1 (2%)	6 (12%)
Pigmentation	–	–	–	1 (2%)
Syncytial alteration	–	1 (2%)	1 (2%)	–
Thrombosis	1 (2%)	–	–	1 (2%)
Centrilobular, atrophy	1 (2%)	–	–	–
Centrilobular, atrophy, chronic	–	1 (2%)	–	–
Mesentery	(7)	(4)	(4)	(5)
Cyst, squamous	–	–	–	1 (20%)
Hemorrhage	–	–	1 (25%)	–
Inflammation, chronic active	–	–	1 (25%)	–
Necrosis, fatty	3 (43%)	2 (50%)	2 (50%)	1 (20%)
Thrombosis	1 (14%)	–	1 (25%)	–
Artery, inflammation, chronic active	1 (14%)	–	–	2 (40%)
Artery, necrosis, chronic active	–	–	–	1 (20%)
Oral mucosa	(1)	(0)	(0)	(0)
Pharyngeal, inflammation, chronic active	1 (100%)	–	–	–
Pancreas	(49)	(49)	(49)	(50)
Inflammation	1 (2%)	–	–	1 (2%)
Salivary glands	(50)	(50)	(50)	(50)
Artery, inflammation, chronic active	1 (2%)	–	–	–
Stomach, forestomach	(50)	(50)	(49)	(50)
Hyperkeratosis	–	2 (4%)	1 (2%)	3 (6%)
Hyperplasia, squamous	1 (2%)	–	–	3 (6%)
Inflammation, chronic active	2 (4%)	4 (8%)	4 (8%)	7 (14%)
Mineralization	–	–	1 (2%)	–
Ulcer	–	–	–	2 (4%)
Stomach, glandular	(48)	(49)	(49)	(50)
Atrophy	–	1 (2%)	–	–
Dysplasia, focal	1 (2%)	–	–	–
Inflammation, chronic active	2 (4%)	4 (8%)	–	1 (2%)
Mineralization	3 (6%)	2 (4%)	1 (2%)	1 (2%)
Necrosis	1 (2%)	–	1 (2%)	–

	Chamber Control	3 mg/m^3	10 mg/m^3	30 mg/m^3
Thrombosis	–	–	1 (2%)	–
Artery, inflammation, chronic active	–	1 (2%)	–	–
Tooth	(14)	(14)	(14)	(6)
Dysplasia	12 (86%)	13 (93%)	12 (86%)	6 (100%)
Inflammation, chronic active	11 (79%)	5 (36%)	6 (43%)	3 (50%)
Cardiovascular System				
Blood vessel	(50)	(49)	(48)	(44)
Adventitia, inflammation, chronic active	–	–	–	1 (2%)
Media, inflammation, chronic active	1 (2%)	–	1 (2%)	1 (2%)
Thoracic, thrombosis	–	1 (2%)	–	–
Heart	(50)	(50)	(50)	(50)
Cardiomyopathy	14 (28%)	13 (26%)	14 (28%)	19 (38%)
Necrosis	–	–	1 (2%)	–
Thrombosis	–	–	2 (4%)	–
Arteriole, degeneration	–	–	1 (2%)	–
Artery, inflammation, chronic active	6 (12%)	10 (20%)	8 (16%)	9 (18%)
Artery, mineralization	–	–	1 (2%)	–
Atrium, inflammation, acute	–	–	–	1 (2%)
Epicardium, fibrosis	–	–	–	1 (2%)
Epicardium, inflammation, chronic active	–	2 (4%)	7 (14%)	16 (32%)
Valve, inflammation, chronic	–	–	1 (2%)	–
Valve, inflammation, chronic active	–	1 (2%)	2 (4%)	–
Valve, thrombosis	–	1 (2%)	–	–
Endocrine System				
Adrenal cortex	(49)	(50)	(49)	(49)
Necrosis	–	–	1 (2%)	–
Subcapsular, hypertrophy	–	1 (2%)	–	–
Zona fasciculata, hypertrophy	26 (53%)	20 (40%)	15 (31%)	8 (16%)
Zona glomerulosa, necrosis	–	–	–	1 (2%)
Adrenal medulla	(49)	(50)	(46)	(49)
Hyperplasia	5 (10%)	8 (16%)	9 (20%)	7 (14%)
Necrosis	–	–	1 (2%)	–
Islets, pancreatic	(49)	(49)	(49)	(50)
Angiectasis	–	–	1 (2%)	–
Hyperplasia	4 (8%)	3 (6%)	–	2 (4%)

	Chamber Control	3 mg/m^3	10 mg/m^3	30 mg/m^3
Parathyroid gland	(27)	(32)	(26)	(33)
Pituitary gland	(49)	(49)	(48)	(50)
Pars distalis, cyst	3 (6%)	3 (6%)	–	6 (12%)
Pars distalis, hyperplasia	4 (8%)	9 (18%)	8 (17%)	3 (6%)
Pars intermedia, hyperplasia	–	1 (2%)	–	–
Thyroid gland	(49)	(49)	(48)	(49)
Artery, inflammation, chronic active	–	1 (2%)	–	–
General Body System				
Peritoneum	(0)	(0)	(0)	(1)
Genital System				
Epididymis	(50)	(50)	(50)	(50)
Inflammation, chronic active	1 (2%)	–	1 (2%)	–
Arteriole, inflammation, chronic active	1 (2%)	1 (2%)	–	1 (2%)
Epithelium, hypertrophy	1 (2%)	–	–	–
Preputial gland	(50)	(50)	(49)	(50)
Ectasia	12 (24%)	7 (14%)	15 (31%)	18 (36%)
Hyperplasia	1 (2%)	–	–	–
Inflammation, chronic active	3 (6%)	4 (8%)	4 (8%)	2 (4%)
Prostate	(49)	(50)	(49)	(50)
Inflammation, chronic active	–	1 (2%)	1 (2%)	–
Artery, inflammation, chronic active	1 (2%)	1 (2%)	–	–
Seminal vesicle	(49)	(50)	(49)	(50)
Hyperplasia, adenomatous	1 (2%)	–	–	–
Inflammation, chronic	–	1 (2%)	–	–
Testes	(49)	(49)	(50)	(50)
Degeneration	29 (59%)	28 (57%)	26 (52%)	22 (44%)
Mineralization	1 (2%)	1 (2%)	–	1 (2%)
Necrosis	–	1 (2%)	–	–
Hematopoietic System				
Bone marrow	(49)	(50)	(48)	(50)
Hemorrhage	–	–	–	1 (2%)
Hyperplasia	10 (20%)	19 (38%)	27 (56%)	33 (66%)
Myelofibrosis	1 (2%)	–	–	–
Necrosis	1 (2%)	1 (2%)	–	1 (2%)
Thrombosis	–	–	1 (2%)	1 (2%)

	Chamber Control	3 mg/m^3	10 mg/m^3	30 mg/m^3
Lymph node	(2)	(2)	(2)	(2)
Hyperplasia, plasma cell	1 (50%)	–	–	–
Lymph node, bronchial	(30)	(43)	(47)	(41)
Ectasia	–	1 (2%)	–	–
Foreign body	–	34 (79%)	47 (100%)	38 (93%)
Hyperplasia, lymphoid	2 (7%)	21 (49%)	26 (55%)	13 (32%)
Infiltration cellular, histiocyte	–	2 (5%)	4 (9%)	6 (15%)
Lymph node, mandibular	(27)	(26)	(28)	(26)
Foreign body	–	7 (27%)	8 (29%)	16 (62%)
Hyperplasia, lymphoid	4 (15%)	8 (31%)	6 (21%)	4 (15%)
Infiltration cellular, histiocyte		1 (4%)	4 (14%)	1 (4%)
Lymph node, mediastinal	(37)	(45)	(48)	(49)
Angiectasis	–	–	1 (2%)	1 (2%)
Foreign body	–	32 (71%)	42 (88%)	48 (98%)
Hyperplasia, lymphoid	2 (5%)	8 (18%)	17 (35%)	34 (69%)
Infiltration cellular, histiocyte	–	4 (9%)	13 (27%)	34 (69%)
Artery, necrosis, fibrinoid	–	–	–	2 (4%)
Lymph node, mesenteric	(48)	(47)	(47)	(50)
Angiectasis	–	1 (2%)		1 (2%)
Ectasia	–	–	1 (2%)	–
Fibrosis	1 (2%)	–	–	–
Hyperplasia, lymphoid	3 (6%)	–	1 (2%)	2 (4%)
Infiltration cellular, histiocyte	–	–	–	2 (4%)
Infiltration cellular, mixed cell	–	2 (4%)	–	–
Infiltration cellular, plasma cell	–	4 (9%)	1 (2%)	–
Infiltration cellular, polymorphonuclear	–	–	2 (4%)	–
Inflammation, acute	–	–	1 (2%)	–
Artery, inflammation, chronic active	–	1 (2%)	–	–
Spleen	(49)	(50)	(50)	(50)
Angiectasis	–	1 (2%)	–	1 (2%)
Hematopoietic cell proliferation	13 (27%)	10 (20%)	10 (20%)	13 (26%)
Hyperplasia, lymphoid	4 (8%)	6 (12%)	6 (12%)	3 (6%)
Necrosis	–	–	1 (2%)	–
Artery, necrosis, fibrinoid	–	–	–	1 (2%)
Thymus	(41)	(38)	(43)	(39)

	Chamber Control	3 mg/m^3	10 mg/m^3	30 mg/m^3
Cyst	–	–	1 (2%)	1 (3%)
Depletion cellular	15 (37%)	14 (37%)	32 (74%)	32 (82%)
Thrombosis	–	–	1 (2%)	–
Medulla, hyperplasia, lymphoid	2 (5%)	1 (3%)	4 (9%)	2 (5%)
Integumentary System				
Mammary gland	(0)	(2)	(4)	(1)
Skin	(50)	(50)	(50)	(50)
Inflammation, chronic active	5 (10%)	2 (4%)	1 (2%)	3 (6%)
Necrosis	–	1 (2%)	–	–
Musculoskeletal System				
Bone	(50)	(50)	(49)	(50)
Necrosis	–	1 (2%)	–	–
Femur, fibro-osseous lesion	2 (4%)	2 (4%)	3 (6%)	2 (4%)
Maxilla, fibro-osseous lesion		1 (2%)	–	–
Maxilla, osteomalacia	–	–	–	1 (2%)
Synovial tissue, inflammation, chronic	–	–	–	1 (2%)
Skeletal muscle	(2)	(3)	(1)	(1)
Degeneration	1 (50%)	–	–	–
Metaplasia, cartilaginous	–	–	1 (100%)	–
Necrosis	–	1 (33%)	–	–
Artery, inflammation, chronic active	–	1 (33%)	–	–
Nervous System				
Brain	(50)	(50)	(50)	(50)
Hemorrhage	–	1 (2%)	1 (2%)	–
Inflammation, multifocal, acute	–	1 (2%)	–	–
Thrombosis	–	2 (4%)	1 (2%)	–
Arteriole, inflammation, chronic active	1 (2%)	2 (4%)	–	–
Cerebrum, inflammation, acute	–	1 (2%)	–	–
Cerebrum, inflammation, chronic	–	–	–	1 (2%)
Meninges, infiltration cellular, lymphoid	–	1 (2%)	1 (2%)	–
Peripheral nerve	(1)	(1)	(0)	(0)
Degeneration	1 (100%)	–	–	–
Spinal cord	(1)	(2)	(0)	(0)
Respiratory System				
Larynx	(50)	(50)	(50)	(50)

	Chamber Control	3 mg/m^3	10 mg/m^3	30 mg/m^3
Foreign body	–	15 (30%)	29 (58%)	44 (88%)
Inflammation, chronic active	8 (16%)	4 (8%)	7 (14%)	11 (22%)
Artery, inflammation, chronic active	–	–	–	1 (2%)
Respiratory epithelium, hyperplasia	1 (2%)	3 (6%)	15 (30%)	30 (60%)
Respiratory epithelium, inclusion body intracytoplasmic	–	–	–	1 (2%)
Respiratory epithelium, metaplasia, squamous	–	–	8 (16%)	18 (36%)
Respiratory epithelium, necrosis	–	–	–	1 (2%)
Squamous epithelium, hyperplasia	2 (4%)	–	4 (8%)	13 (26%)
Squamous epithelium, necrosis	–	–	–	1 (2%)
Lung	(50)	(50)	(50)	(50)
Foreign body	–	50 (100%)	50 (100%)	50 (100%)
Hemorrhage, acute	1 (2%)	–	–	–
Infiltration cellular, histiocyte	1 (2%)	–	–	–
Infiltration cellular, lymphocyte	13 (26%)	47 (94%)	48 (96%)	45 (90%)
Inflammation, focal, chronic	1 (2%)	–	–	–
Inflammation, chronic active	–	48 (96%)	50 (100%)	50 (100%)
Mineralization	–	1 (2%)	–	–
Necrosis	–	–	1 (2%)	–
Pigmentation, focal	1 (2%)	–	–	–
Proteinosis	–	–	1 (2%)	–
Thrombosis	1 (2%)	1 (2%)	–	–
Alveolar epithelium, hyperplasia	6 (12%)	39 (78%)	45 (90%)	49 (98%)
Alveolus, fibrosis	–	12 (24%)	30 (60%)	37 (74%)
Alveolus, infiltration cellular, histiocyte	2 (4%)	–	–	–
Artery, inflammation, chronic active	1 (2%)	1 (2%)	–	–
Bronchiole, epithelium, hyperplasia	–	32 (64%)	44 (88%)	44 (88%)
Bronchiole, epithelium, goblet cell, metaplasia	–	–	1 (2%)	–
Bronchus, epithelium, accumulation, hyaline droplet	–	–	–	2 (4%)
Bronchus, epithelium, hyperplasia	–	1 (2%)	1 (2%)	–
Bronchus, epithelium, metaplasia, squamous	–	–	1 (2%)	–
Bronchus, epithelium, necrosis	–	–	1 (2%)	–
Bronchus, epithelium, goblet cell, metaplasia	–	–	–	3 (6%)
Pleura, fibrosis	–	36 (72%)	46 (92%)	50 (100%)
Pleura, inflammation	1 (2%)	40 (80%)	47 (94%)	48 (96%)
Nose	(50)	(49)	(49)	(50)

	Chamber Control	3 mg/m^3	10 mg/m^3	30 mg/m^3
Foreign body	–	48 (98%)	48 (98%)	49 (98%)
Glands, olfactory epithelium, accumulation, hyaline droplet	–	–	–	1 (2%)
Glands, olfactory epithelium, dilatation	1 (2%)	–	–	–
Glands, olfactory epithelium, metaplasia, respiratory	1 (2%)	–	–	–
Nasolacrimal duct, hyperplasia, squamous	–	1 (2%)	–	–
Nasolacrimal duct, inflammation, acute	–	–	–	2 (4%)
Nasolacrimal duct, inflammation, chronic active	1 (2%)	1 (2%)	2 (4%)	3 (6%)
Nasopharyngeal duct, inflammation, chronic active	–	1 (2%)	–	–
Olfactory epithelium, accumulation, hyaline droplet	3 (6%)	2 (4%)	4 (8%)	4 (8%)
Olfactory epithelium, atrophy	–	1 (2%)	1 (2%)	–
Olfactory epithelium, inflammation, acute	–	–	1 (2%)	1 (2%)
Olfactory epithelium, metaplasia, respiratory	2 (4%)	4 (8%)	–	–
Olfactory epithelium, necrosis	–	–	–	1 (2%)
Respiratory epithelium, accumulation, hyaline droplet	9 (18%)	7 (14%)	7 (14%)	12 (24%)
Respiratory epithelium, erosion, acute	–	–	1 (2%)	–
Respiratory epithelium, hyperplasia	–	–	–	2 (4%)
Respiratory epithelium, inflammation, acute	1 (2%)	1 (2%)	3 (6%)	2 (4%)
Respiratory epithelium, inflammation, chronic active	3 (6%)	9 (18%)	9 (18%)	6 (12%)
Respiratory epithelium, metaplasia, squamous	–	2 (4%)	1 (2%)	2 (4%)
Respiratory epithelium, necrosis	–	–	–	2 (4%)
Respiratory epithelium, regeneration	–	–	1 (2%)	–
Respiratory epithelium, thrombosis	–	–	–	1 (2%)
Turbinate, inflammation, suppurative	–	–	–	2 (4%)
Pleura	(0)	(0)	(0)	(2)
Trachea	(49)	(50)	(50)	(50)
Foreign body	–	3 (6%)	1 (2%)	20 (40%)
Inflammation, chronic active	–	1 (2%)	–	–
Metaplasia, squamous	–	–	1 (2%)	–
Epithelium, hyperplasia	–	–	2 (4%)	5 (10%)
Epithelium, inclusion body intracytoplasmic	–	–	–	1 (2%)
Epithelium, metaplasia, squamous	–	–	–	1 (2%)
Glands, cyst	–	1 (2%)	–	–
Special Senses System				
Eye	(48)	(49)	(47)	(50)
Cataract	5 (10%)	4 (8%)	2 (4%)	2 (4%)

	Chamber Control	3 mg/m^3	10 mg/m^3	30 mg/m^3
Hemorrhage	–	–	1 (2%)	–
Retinal detachment	1 (2%)	–	–	–
Harderian gland	(49)	(50)	(50)	(50)
Hyperplasia	1 (2%)	–	2 (4%)	3 (6%)
Hypertrophy	2 (4%)	–	1 (2%)	–
Epithelium, hyperplasia	1 (2%)	–	–	–
Urinary System				
Kidney	(50)	(50)	(49)	(50)
Cyst	1 (2%)	1 (2%)	–	–
Hemorrhage	–	–	1 (2%)	–
Infarct	–	1 (2%)	1 (2%)	1 (2%)
Inflammation, acute	1 (2%)	–	1 (2%)	–
Metaplasia, osseous	1 (2%)	1 (2%)	2 (4%)	1 (2%)
Mineralization	2 (4%)	–	–	–
Nephropathy	41 (82%)	39 (78%)	38 (78%)	40 (80%)
Thrombosis	–	1 (2%)	–	–
Artery, inflammation, chronic active	–	2 (4%)	–	1 (2%)
Glomerulus, hyalinization	–	–	1 (2%)	–
Ureter	(1)	(0)	(0)	(0)
Urinary bladder	(50)	(50)	(48)	(50)
Calculus gross observation	1 (2%)	–	–	–
Inflammation, chronic active	1 (2%)	–	1 (2%)	–
Artery, inflammation, chronic active	–	2 (4%)	–	–

[a]Number of animals examined microscopically at the site and the number of animals with lesion.

Appendix D. Summary of Lesions in Female Mice in the Two-year Inhalation Study of Antimony Trioxide

Tables

Table D-1. Summary of the Incidence of Neoplasms in Female Mice in the Two-year Inhalation Study of Antimony Trioxide D-2
Table D-2. Statistical Analysis of Primary Neoplasms in Female Mice in the Two-year Inhalation Study of Antimony Trioxide D-10
Table D-3. Historical Incidence of Alveolar/Bronchiolar Neoplasms in Control Female B6C3F1/N Mice D-14
Table D-4. Historical Incidence of Malignant Lymphoma in Control Female B6C3F1/N Mice D-14
Table D-5. Historical Incidence of Squamous Cell Carcinoma of the Skin in Control Female B6C3F1/N Mice D-15
Table D-6. Historical Incidence of Benign Pheochromocytoma of the Adrenal Medulla in Control Female B6C3F1/N Mice D-15
Table D-7. Historical Incidence of Hepatocellular Adenoma or Carcinoma (combined) in Control Female B6C3F1/N Mice D-16
Table D-8. Summary of the Incidence of Nonneoplastic Lesions in Female Mice in the Two-year Inhalation Study of Antimony Trioxide D-16

Table D-1. Summary of the Incidence of Neoplasms in Female Mice in the Two-year Inhalation Study of Antimony Trioxide[a]

	Chamber Control	3 mg/m^3	10 mg/m^3	30 mg/m^3
Disposition Summary				
Animals initially in study	60	60	60	60
Twelve-month interim evaluation	10	10	10	10
Early deaths				
Accidental death	1	–	–	–
Moribund	10	11	16	27
Natural deaths	3	8	8	8
Survivors				
Terminal kill	36	31	26	15
Animals examined microscopically	60	60	60	60
Twelve-month Interim Evaluation				
Alimentary System				
Esophagus	(10)	(10)	(10)	(10)
Gallbladder	(10)	(10)	(10)	(10)
Intestine large, cecum	(10)	(10)	(10)	(10)
Intestine large, colon	(10)	(10)	(10)	(10)
Intestine large, rectum	(10)	(10)	(10)	(10)
Intestine small, duodenum	(10)	(10)	(10)	(10)
Intestine small, ileum	(10)	(10)	(10)	(10)
Intestine small, jejunum	(10)	(10)	(10)	(10)
Liver	(10)	(10)	(10)	(10)
Hepatocellular adenoma	–	2 (20%)	2 (20%)	4 (40%)
Pancreas	(10)	(10)	(10)	(10)
Salivary glands	(10)	(10)	(10)	(10)
Stomach, forestomach	(10)	(10)	(10)	(10)
Stomach, glandular	(10)	(10)	(10)	(10)
Tooth	(1)	(0)	(0)	(0)
Endocrine System				
Adrenal cortex	(10)	(10)	(10)	(10)
Adrenal medulla	(10)	(10)	(10)	(10)
Pheochromocytoma malignant	–	–	–	1 (10%)
Islets, pancreatic	(10)	(10)	(10)	(10)
Parathyroid gland	(8)	(9)	(6)	(8)

	Chamber Control	3 mg/m^3	10 mg/m^3	30 mg/m^3
Pituitary gland	(10)	(10)	(10)	(10)
Thyroid gland	(10)	(9)	(10)	(10)
Genital System				
Clitoral gland	(10)	(9)	(7)	(7)
Ovary	(10)	(10)	(10)	(10)
Luteoma	–	1 (10%)	–	–
Uterus	(10)	(10)	(10)	(10)
Respiratory System				
Larynx	(10)	(9)	(10)	(10)
Lung	(10)	(10)	(10)	(10)
Alveolar/bronchiolar adenoma	–	–	–	1 (10%)
Nose	(10)	(10)	(10)	(10)
Trachea	(10)	(10)	(10)	(10)
Systemic Lesions				
Multiple organs[b]	(10)	(10)	(10)	(10)
Histiocytic sarcoma	–	1 (10%)	–	–
Lymphoma malignant	–	–	–	3 (30%)
Systems Examined at 12 Months with No Neoplasms Observed				
Cardiovascular System				
General Body System				
Hematopoietic System				
Integumentary System				
Musculoskeletal System				
Nervous System				
Special Senses System				
Urinary System				
Two-year Study				
Alimentary System				
Esophagus	(50)	(50)	(50)	(50)
Gallbladder	(46)	(41)	(44)	(45)
Fibrosarcoma, metastatic, pancreas	–	1 (2%)	–	–
Hepatocholangiocarcinoma, metastatic, liver	–	1 (2%)	–	–
Intestine large, cecum	(47)	(44)	(48)	(47)
Hepatocholangiocarcinoma, metastatic, liver	–	1 (2%)	–	–
Polyp adenomatous	–	–	–	1 (2%)

	Chamber Control	3 mg/m^3	10 mg/m^3	30 mg/m^3
Intestine large, colon	(47)	(47)	(49)	(47)
Intestine large, rectum	(44)	(46)	(48)	(47)
Intestine small, duodenum	(47)	(44)	(45)	(45)
Fibrosarcoma, metastatic, pancreas	–	1 (2%)	–	–
Hepatocholangiocarcinoma, metastatic, liver	–	1 (2%)	–	–
Intestine small, ileum	(47)	(45)	(47)	(45)
Hemangiosarcoma	–	1 (2%)	–	–
Intestine small, jejunum	(47)	(43)	(46)	(44)
Adenoma	–	–	1 (2%)	1 (2%)
Carcinoma	–	1 (2%)	–	–
Liver	(50)	(50)	(50)	(50)
Fibrosarcoma, metastatic, pancreas	–	1 (2%)	–	–
Hemangioma	–	–	1 (2%)	–
Hemangiosarcoma	–	–	1 (2%)	–
Hepatocellular adenoma	9 (18%)	9 (18%)	11 (22%)	15 (30%)
Hepatocellular adenoma, multiple	2 (4%)	5 (10%)	5 (10%)	2 (4%)
Hepatocellular carcinoma	4 (8%)	10 (20%)	9 (18%)	3 (6%)
Hepatocellular carcinoma, multiple	2 (4%)	1 (2%)	3 (6%)	1 (2%)
Hepatocholangiocarcinoma	1 (2%)	2 (4%)	–	–
Mesentery	(9)	(12)	(16)	(7)
Fibrosarcoma, metastatic, pancreas	–	1 (8%)	–	–
Granulosa cell tumor malignant, metastatic, ovary	–	–	1 (6%)	–
Hepatocholangiocarcinoma, metastatic, liver	–	1 (8%)	–	–
Lipoma	1 (11%)	–	–	–
Pancreas	(50)	(50)	(50)	(50)
Fibrosarcoma	–	1 (2%)	–	–
Hemangiosarcoma, metastatic, liver	–	–	1 (2%)	–
Salivary glands	(50)	(50)	(50)	(50)
Myxosarcoma	1 (2%)	–	–	–
Stomach, forestomach	(50)	(50)	(50)	(50)
Hepatocholangiocarcinoma, metastatic, liver	–	1 (2%)	–	–
Squamous cell papilloma	1 (2%)	–	–	–
Stomach, glandular	(50)	(49)	(50)	(50)
Fibrosarcoma, metastatic, pancreas	–	1 (2%)	–	–
Hepatocholangiocarcinoma, metastatic, liver	–	1 (2%)	–	–

	Chamber Control	3 mg/m^3	10 mg/m^3	30 mg/m^3
Tongue	(0)	(1)	(0)	(0)
Tooth	(0)	(2)	(2)	(1)
Cardiovascular System				
Blood vessel	(50)	(48)	(47)	(46)
Alveolar/bronchiolar carcinoma, metastatic, lung	–	–	1 (2%)	–
Heart	(50)	(50)	(50)	(50)
Alveolar/bronchiolar carcinoma, metastatic, lung	–	1 (2%)	1 (2%)	1 (2%)
Pericardium, alveolar/bronchiolar carcinoma, metastatic, lung	–	–	1 (2%)	1 (2%)
Endocrine System				
Adrenal cortex	(50)	(50)	(50)	(50)
Adenoma	–	1 (2%)	–	–
Alveolar/bronchiolar carcinoma, metastatic, lung	–	–	–	1 (2%)
Capsule, fibrosarcoma, metastatic, pancreas	–	1 (2%)	–	–
Capsule, hepatocholangiocarcinoma, metastatic, liver	–	1 (2%)	–	–
Subcapsular, adenoma	1 (2%)	–	1 (2%)	–
Adrenal medulla	(50)	(50)	(48)	(49)
Pheochromocytoma benign	–	2 (4%)	–	3 (6%)
Islets, pancreatic	(50)	(49)	(49)	(49)
Adenoma	–	1 (2%)	1 (2%)	1 (2%)
Fibrosarcoma, metastatic, pancreas	–	1 (2%)	–	–
Parathyroid gland	(27)	(33)	(34)	(32)
Adenoma	–	–	–	1 (3%)
Pituitary gland	(49)	(50)	(50)	(50)
Pars distalis, adenoma	9 (18%)	10 (20%)	7 (14%)	3 (6%)
Pars distalis, carcinoma	–	–	1 (2%)	–
Pars intermedia, adenoma	–	1 (2%)	1 (2%)	–
Thyroid gland	(48)	(50)	(50)	(50)
Follicular cell, adenoma	–	–	–	1 (2%)
Follicular cell, carcinoma	–	–	1 (2%)	–
General Body System				
Peritoneum	(0)	(0)	(1)	(0)
Genital System				
Clitoral gland	(48)	(44)	(47)	(42)
Ovary	(50)	(49)	(50)	(50)

	Chamber Control	3 mg/m^3	10 mg/m^3	30 mg/m^3
Alveolar/bronchiolar carcinoma, metastatic, lung	–	1 (2%)	–	–
Cystadenoma	1 (2%)	2 (4%)	2 (4%)	–
Fibrosarcoma, metastatic, pancreas	–	1 (2%)	–	–
Granulosa cell tumor malignant	1 (2%)	–	1 (2%)	–
Granulosa-theca tumor malignant	–	1 (2%)	–	–
Hemangioma	–	1 (2%)	–	1 (2%)
Hemangiosarcoma	1 (2%)	–	1 (2%)	–
Hepatocholangiocarcinoma, metastatic, liver	–	1 (2%)	–	–
Luteoma	–	1 (2%)	–	–
Oviduct	(1)	(0)	(0)	(0)
Uterus	(50)	(50)	(50)	(50)
Carcinoma	–	–	1 (2%)	–
Granular cell tumor benign	1 (2%)	–	–	–
Hemangiosarcoma	1 (2%)	–	1 (2%)	–
Leiomyoma	–	2 (4%)	–	–
Polyp stromal	4 (8%)	2 (4%)	1 (2%)	2 (4%)
Endometrium, polyp stromal	–	–	–	1 (2%)
Hematopoietic System				
Bone marrow	(50)	(50)	(50)	(50)
Mast cell tumor NOS, metastatic, uncertain primary site	–	–	–	1 (2%)
Lymph node	(6)	(9)	(14)	(16)
Hemangioma	–	–	–	1 (6%)
Hepatocholangiocarcinoma, metastatic, liver	–	1 (11%)	–	–
Lumbar, hemangiosarcoma	1 (17%)	–	–	–
Lumbar, hepatocholangiocarcinoma, metastatic, liver	–	1 (11%)	–	–
Pancreatic, fibrosarcoma, metastatic, pancreas	–	1 (11%)	–	–
Pancreatic, granulosa cell tumor malignant, metastatic, ovary	–	–	1 (7%)	–
Pancreatic, hepatocholangiocarcinoma, metastatic, liver	–	1 (11%)	–	–
Lymph node, bronchial	(41)	(47)	(48)	(49)
Alveolar/bronchiolar carcinoma, metastatic, lung	–	2 (4%)	2 (4%)	–
Hepatocholangiocarcinoma, metastatic, liver	–	1 (2%)	–	–
Lymph node, mandibular	(41)	(28)	(38)	(39)
Lymph node, mediastinal	(46)	(48)	(49)	(50)

	Chamber Control	3 mg/m^3	10 mg/m^3	30 mg/m^3
Alveolar/bronchiolar carcinoma, metastatic, lung	–	2 (4%)	2 (4%)	–
Hepatocellular carcinoma, metastatic, liver	1 (2%)	–	–	–
Hepatocholangiocarcinoma, metastatic, liver	–	1 (2%)	–	–
Lymph node, mesenteric	(50)	(48)	(48)	(46)
Alveolar/bronchiolar carcinoma, metastatic, lung	–	1 (2%)	–	–
Fibrosarcoma, metastatic, pancreas	–	1 (2%)	–	–
Hemangiosarcoma	–	–	–	1 (2%)
Hepatocholangiocarcinoma, metastatic, liver	–	1 (2%)	–	–
Spleen	(50)	(50)	(50)	(50)
Hemangiosarcoma	–	1 (2%)	–	–
Thymus	(47)	(49)	(49)	(49)
Alveolar/bronchiolar carcinoma, metastatic, lung	–	2 (4%)	–	1 (2%)
Hemangioma	–	–	–	1 (2%)
Hepatocholangiocarcinoma, metastatic, liver	–	1 (2%)	–	–
Thymoma NOS	1 (2%)	–	–	–
Integumentary System				
Mammary gland	(50)	(50)	(50)	(50)
Carcinoma	1 (2%)	2 (4%)	–	–
Squamous cell carcinoma, metastatic, skin	–	–	–	1 (2%)
Skin	(50)	(50)	(50)	(50)
Fibrosarcoma	1 (2%)	1 (2%)	–	1 (2%)
Fibrous histiocytoma	1 (2%)	–	–	–
Hemangiosarcoma	1 (2%)	1 (2%)	–	1 (2%)
Hemangiosarcoma, metastatic, liver	–	–	1 (2%)	–
Hepatocholangiocarcinoma, metastatic, liver	–	1 (2%)	–	–
Squamous cell carcinoma	–	–	–	2 (4%)
Musculoskeletal System				
Bone	(50)	(50)	(49)	(50)
Femur, periosteum, alveolar/bronchiolar carcinoma, metastatic, lung	–	–	–	1 (2%)
Skeletal muscle	(4)	(1)	(4)	(3)
Alveolar/bronchiolar carcinoma, metastatic, lung	–	–	–	1 (33%)
Carcinoma, metastatic, mammary gland	–	1 (100%)	–	–
Granulosa cell tumor malignant, metastatic, ovary	–	–	1 (25%)	–

	Chamber Control	3 mg/m^3	10 mg/m^3	30 mg/m^3
Nervous System				
Brain	(50)	(50)	(50)	(50)
Peripheral nerve	(3)	(0)	(2)	(1)
Spinal cord	(4)	(0)	(2)	(1)
Respiratory System				
Larynx	(50)	(50)	(50)	(50)
Lung	(50)	(50)	(50)	(50)
Alveolar/bronchiolar adenoma	1 (2%)	7 (14%)	16 (32%)	7 (14%)
Alveolar/bronchiolar adenoma, multiple	–	3 (6%)	3 (6%)	1 (2%)
Alveolar/bronchiolar carcinoma	2 (4%)	7 (14%)	5 (10%)	7 (14%)
Alveolar/bronchiolar carcinoma, multiple	–	7 (14%)	6 (12%)	4 (8%)
Carcinoma, metastatic, harderian gland	1 (2%)	–	–	–
Granulosa-theca tumor malignant, metastatic, ovary	–	1 (2%)	–	–
Hepatocellular carcinoma, metastatic, liver	3 (6%)	3 (6%)	–	1 (2%)
Hepatocholangiocarcinoma, metastatic, liver	–	1 (2%)	–	–
Mast cell tumor NOS, metastatic, uncertain primary site	–	–	–	1 (2%)
Nose	(50)	(49)	(50)	(50)
Pleura	(0)	(2)	(0)	(2)
Alveolar/bronchiolar carcinoma, metastatic, lung	–	1 (50%)	–	–
Trachea	(50)	(50)	(50)	(50)
Special Senses System				
Ear	(0)	(0)	(0)	(1)
Eye	(49)	(47)	(49)	(49)
Harderian gland	(49)	(50)	(50)	(50)
Adenoma	3 (6%)	4 (8%)	6 (12%)	2 (4%)
Carcinoma	4 (8%)	–	–	2 (4%)
Zymbal’s gland	(0)	(0)	(0)	(1)
Carcinoma	–	–	–	1 (100%)
Urinary System				
Kidney	(50)	(50)	(50)	(50)
Alveolar/bronchiolar carcinoma, metastatic, lung	–	1 (2%)	1 (2%)	1 (2%)
Hepatocellular carcinoma, metastatic, liver	1 (2%)	–	–	–
Urinary bladder	(50)	(50)	(50)	(50)
Hemangioma	–	1 (2%)	–	–

	Chamber Control	3 mg/m^3	10 mg/m^3	30 mg/m^3
Systemic Lesions				
Multiple organs[b]	(50)	(50)	(50)	(50)
Histiocytic sarcoma	3 (6%)	6 (12%)	2 (4%)	3 (6%)
Lymphoma malignant	7 (14%)	17 (34%)	20 (40%)	27 (54%)
Neoplasm Summary				
Total animals with primary neoplasms[c]				
Twelve-month interim evaluation	–	3	2	6
Two-year study	35	47	46	45
Total primary neoplasms				
Twelve-month interim evaluation	–	4	2	9
Two-year study	66	111	108	97
Total animals with benign neoplasms				
Twelve-month interim evaluation	–	2	2	5
Two-year study	25	35	35	31
Total benign neoplasms				
Twelve-month interim evaluation	–	3	2	5
Two-year study	33	52	56	44
Total animals with malignant neoplasms				
Twelve-month interim evaluation	–	1	–	4
Two-year study	25	40	35	41
Total malignant neoplasms				
Twelve-month interim evaluation	–	1	–	4
Two-year study	32	59	52	53
Total animals with metastatic neoplasms				
Two-year study	7	13	5	7
Total metastatic neoplasms				
Two-year study	8	47	13	15
Total animals with uncertain neoplasms-benign or malignant				
Two-year study	1	–	–	–

[a]Number of animals examined microscopically at the site and the number of animals with neoplasm.
[b]Number of animals with any tissue examined microscopically.
[c]Primary neoplasms: all neoplasms except metastatic neoplasms.

Table D-2. Statistical Analysis of Primary Neoplasms in Female Mice in the Two-year Inhalation Study of Antimony Trioxide

	Chamber Control	3 mg/m^3	10 mg/m^3	30 mg/m^3
Adrenal Medulla: Benign Pheochromocytoma				
Overall rate[a]	0/50 (0%)	2/50 (4%)	0/48 (0%)	3/49 (6%)
Adjusted rate[b]	0.0%	4.6%	0.0%	8.4%
Terminal rate[c]	0/36 (0%)	2/31 (7%)	0/26 (0%)	2/15 (13%)
First incidence (days)	–[e]	731 (T)	–	701
Poly-3 test[d]	P = 0.078	P = 0.233	–[f]	P = 0.083
Harderian Gland: Adenoma				
Overall rate	3/50 (6%)	4/50 (8%)	6/50 (12%)	2/50 (4%)
Adjusted rate	6.7%	9.1%	14.5%	5.5%
Terminal rate	2/36 (6%)	3/31 (10%)	3/26 (12%)	1/15 (7%)
First incidence (days)	716	677	423	696
Poly-3 test	P = 0.463N	P = 0.492	P = 0.205	P = 0.591N
Harderian Gland: Carcinoma				
Overall rate	4/50 (8%)	0/50 (0%)	0/50 (0%)	2/50 (4%)
Adjusted rate	8.8%	0.0%	0.0%	5.5%
Terminal rate	2/36 (6%)	0/31 (0%)	0/26 (0%)	1/15 (7%)
First incidence (days)	472	–	–	628
Poly-3 test	P = 0.627N	P = 0.065N	P = 0.078N	P = 0.439N
Harderian Gland: Adenoma or Carcinoma				
Overall rate	7/50 (14%)	4/50 (8%)	6/50 (12%)	4/50 (8%)
Adjusted rate	15.4%	9.1%	14.5%	10.9%
Terminal rate	4/36 (11%)	3/31 (10%)	3/26 (12%)	2/15 (13%)
First incidence (days)	472	677	423	628
Poly-3 test	P = 0.465N	P = 0.278N	P = 0.571N	P = 0.392N
Liver: Hepatocellular Adenoma				
Overall rate	11/50 (22%)	14/50 (28%)	16/50 (32%)	17/50 (34%)
Adjusted rate	24.7%	31.6%	38.3%	43.1%
Terminal rate	11/36 (31%)	12/31 (39%)	10/26 (39%)	6/15 (40%)
First incidence (days)	731 (T)	645	521	470
Poly-3 test	P = 0.058	P = 0.312	P = 0.127	P = 0.056
Liver: Hepatocellular Carcinoma				
Overall rate	6/50 (12%)	11/50 (22%)	12/50 (24%)	4/50 (8%)
Adjusted rate	13.4%	24.6%	28.8%	10.8%
Terminal rate	4/36 (11%)	7/31 (23%)	6/26 (23%)	3/15 (20%)

	Chamber Control	3 mg/m^3	10 mg/m^3	30 mg/m^3
First incidence (days)	684	613	512	513
Poly-3 test	P = 0.252N	P = 0.139	P = 0.064	P = 0.496N
Liver: Hepatocellular Adenoma or Carcinoma				
Overall rate	14/50 (28%)	22/50 (44%)	22/50 (44%)	19/50 (38%)
Adjusted rate	31.2%	48.9%	51.1%	47.4%
Terminal rate	12/36 (33%)	17/31 (55%)	12/26 (46%)	7/15 (47%)
First incidence (days)	684	613	512	470
Poly-3 test	P = 0.213	P = 0.063	P = 0.042	P = 0.091
Lung: Alveolar/Bronchiolar Adenoma				
Overall rate	1/50 (2%)	10/50 (20%)	19/50 (38%)	8/50 (16%)
Adjusted rate	2.3%	22.8%	44.9%	20.3%
Terminal rate	1/36 (3%)	7/31 (23%)	12/26 (46%)	1/15 (7%)
First incidence (days)	731 (T)	708	519	404
Poly-3 test	P = 0.137	P = 0.003	P < 0.001	P = 0.009
Lung: Alveolar/Bronchiolar Carcinoma				
Overall rate	2/50 (4%)	14/50 (28%)	11/50 (22%)	11/50 (22%)
Adjusted rate	4.4%	31.2%	26.8%	28.8%
Terminal rate	1/36 (3%)	9/31 (29%)	7/26 (27%)	5/15 (33%)
First incidence (days)	472	511	526	493
Poly-3 test	P = 0.065	P < 0.001	P = 0.003	P = 0.002
Lung: Alveolar/Bronchiolar Adenoma or Carcinoma				
Overall rate	3/50 (6%)	22/50 (44%)	27/50 (54%)	18/50 (36%)
Adjusted rate	6.6%	48.8%	62.6%	43.5%
Terminal rate	2/36 (6%)	15/31 (48%)	17/26 (65%)	5/15 (33%)
First incidence (days)	472	511	519	404
Poly-3 test	P = 0.019	P < 0.001	P < 0.001	P < 0.001
Pituitary Gland (Pars Distalis): Adenoma				
Overall rate	9/49 (18%)	10/50 (20%)	7/50 (14%)	3/50 (6%)
Adjusted rate	20.7%	22.2%	17.1%	8.3%
Terminal rate	9/35 (26%)	6/31 (19%)	4/26 (15%)	3/15 (20%)
First incidence (days)	731 (T)	511	526	731 (T)
Poly-3 test	P = 0.065N	P = 0.535	P = 0.442N	P = 0.109N
Pituitary Gland (Pars Distalis): Adenoma or Carcinoma				
Overall rate	9/49 (18%)	10/50 (20%)	8/50 (16%)	3/50 (6%)
Adjusted rate	20.7%	22.2%	19.3%	8.3%
Terminal rate	9/35 (26%)	6/31 (19%)	4/26 (15%)	3/15 (20%)

	Chamber Control	3 mg/m^3	10 mg/m^3	30 mg/m^3
First incidence (days)	731 (T)	511	526	731 (T)
Poly-3 test	P = 0.069N	P = 0.535	P = 0.544N	P = 0.109N
Uterus: Stromal Polyp				
Overall rate	4/50 (8%)	2/50 (4%)	1/50 (2%)	3/50 (6%)
Adjusted rate	8.9%	4.6%	2.5%	8.2%
Terminal rate	3/36 (8%)	2/31 (7%)	0/26 (0%)	2/15 (13%)
First incidence (days)	614	731 (T)	519	572
Poly-3 test	P = 0.540	P = 0.349N	P = 0.211N	P = 0.607N
All Organs: Hemangioma				
Overall rate	0/50 (0%)	2/50 (4%)	1/50 (2%)	3/50 (6%)
Adjusted rate	0.0%	4.6%	2.5%	8.3%
Terminal rate	0/36 (0%)	2/31 (7%)	1/26 (4%)	2/15 (13%)
First incidence (days)	–	731 (T)	731 (T)	710
Poly-3 test	P = 0.095	P = 0.233	P = 0.478	P = 0.086
All Organs: Hemangiosarcoma				
Overall rate	4/50 (8%)	3/50 (6%)	3/50 (6%)	2/50 (4%)
Adjusted rate	9.0%	6.7%	7.5%	5.5%
Terminal rate	3/36 (8%)	1/31 (3%)	3/26 (12%)	1/15 (7%)
First incidence (days)	725	606	731 (T)	696
Poly-3 test	P = 0.408N	P = 0.499N	P = 0.560N	P = 0.434N
All Organs: Hemangioma or Hemangiosarcoma				
Overall rate	4/50 (8%)	5/50 (10%)	4/50 (8%)	5/50 (10%)
Adjusted rate	9.0%	11.2%	10.0%	13.7%
Terminal rate	3/36 (8%)	3/31 (10%)	4/26 (15%)	3/15 (20%)
First incidence (days)	725	606	731 (T)	696
Poly-3 test	P = 0.351	P = 0.501	P = 0.582	P = 0.377
All Organs: Histiocytic Sarcoma				
Overall rate	3/50 (6%)	6/50 (12%)	2/50 (4%)	3/50 (6%)
Adjusted rate	6.7%	13.3%	4.9%	8.0%
Terminal rate	1/36 (3%)	3/31 (10%)	0/26 (0%)	0/15 (0%)
First incidence (days)	614	559	526	488
Poly-3 test	P = 0.475N	P = 0.242	P = 0.546N	P = 0.574
All Organs: Malignant Lymphoma				
Overall rate	7/50 (14%)	17/50 (34%)	20/50 (40%)	27/50 (54%)
Adjusted rate	15.6%	38.1%	47.5%	60.7%
Terminal rate	5/36 (14%)	15/31 (48%)	12/26 (46%)	5/15 (33%)

	Chamber Control	3 mg/m^3	10 mg/m^3	30 mg/m^3
First incidence (days)	677	558	512	404
Poly-3 test	P < 0.001	P = 0.013	P < 0.001	P < 0.001
All Organs: Benign Neoplasms				
Overall rate	25/50 (50%)	35/50 (70%)	35/50 (70%)	31/50 (62%)
Adjusted rate	55.4%	76.5%	77.0%	72.1%
Terminal rate	22/36 (61%)	27/31 (87%)	20/26 (77%)	13/15 (87%)
First incidence (days)	614	511	423	404
Poly-3 test	P = 0.222	P = 0.022	P = 0.019	P = 0.068
All Organs: Malignant Neoplasms				
Overall rate	25/50 (50%)	40/50 (80%)	35/50 (70%)	41/50 (82%)
Adjusted rate	53.4%	81.9%	77.6%	86.5%
Terminal rate	16/36 (44%)	25/31 (81%)	19/26 (73%)	12/15 (80%)
First incidence (days)	472	511	512	404
Poly-3 test	P = 0.004	P = 0.002	P = 0.010	P < 0.001
All Organs: Benign or Malignant Neoplasms				
Overall rate	35/50 (70%)	47/50 (94%)	46/50 (92%)	46/50 (92%)
Adjusted rate	74.8%	95.9%	97.0%	94.3%
Terminal rate	26/36 (72%)	30/31 (97%)	26/26 (100%)	14/15 (93%)
First incidence (days)	472	511	423	404
Poly-3 test	P = 0.037	P = 0.002	P < 0.001	P = 0.006

(T) = terminal kill.
[a]Number of neoplasm-bearing animals/number of animals examined. Denominator is number of animals examined microscopically for adrenal gland, liver, lung, and pituitary gland; for other tissues, denominator is number of animals necropsied.
[b]Poly-3 estimated neoplasm incidence after adjustment for intercurrent mortality.
[c]Observed incidence at terminal kill.
[d]Beneath the chamber control incidence is the P value associated with the trend test. Beneath the exposed group incidence are the P values corresponding to pairwise comparisons between the chamber controls and that exposed group. The Poly-3 test accounts for differential mortality in animals that do not reach terminal kill. A negative trend or a lower incidence in an exposure group is indicated by **N**.
[e]Not applicable; no neoplasms in animal group.
[f]Value of statistic cannot be computed.

Table D-3. Historical Incidence of Alveolar/Bronchiolar Neoplasms in Control Female B6C3F1/N Mice[a]

Study (Study Start)	Adenoma	Carcinoma	Adenoma or Carcinoma
Historical Incidence: Inhalation Studies			
Antimony trioxide (October 2008)	1/50	2/50	3/50
CIMSTAR 3800 (May 2008)	1/50	4/50	4/50
Cobalt metal (May 2006)	3/49	5/49	8/49
Vinylidene chloride (June 2005)	3/50	1/50	4/50
Trim VX (August 2009)	4/50	5/50	9/50
Total (%)	12/249 (4.8%)	17/249 (6.8%)	28/249 (11.2%)
Mean ± standard deviation	4.8% ± 2.7%	6.8% ± 3.7%	11.3% ± 5.5%
Range	2%–8%	2%–10%	6%–18%
Overall Historical Incidence: All Routes			
Total (%)	27/549 (4.9%)	24/549 (4.4%)	50/549 (9.1%)
Mean ± standard deviation	4.9% ± 3.5%	4.4% ± 3.5%	9.1% ± 5.2%
Range	0%–10%	0%–10%	2%–18%

[a]Data as of June 2015.

Table D-4. Historical Incidence of Malignant Lymphoma in Control Female B6C3F1/N Mice[a]

Study (Study Start)	Incidence in Controls
Historical Incidence: Inhalation Studies	
Antimony trioxide (October 2008)	7/50
CIMSTAR 3800 (May 2008)	18/50
Cobalt (May 2006)	14/50
Vinylidene chloride (June 2005)	14/50
Trim VX (August 2009)	10/50
Total (%)	63/250 (25.2%)
Mean ± standard deviation	25.2% ± 8.4%
Range	14%–36%
Overall Historical Incidence: All Routes	
Total (%)	109/550 (19.8%)
Mean ± standard deviation	19.8% ± 7.9%
Range	12%–36%

[a]Data as of June 2015; may include data for histiocytic, lymphocytic, mixed, unspecified, or undifferentiated cell types.

Table D-5. Historical Incidence of Squamous Cell Carcinoma of the Skin in Control Female B6C3F1/N Mice[a]

Study (Study Start)	Incidence in Controls
Historical Incidence: Inhalation Studies	
Antimony trioxide (October 2008)	0/50
CIMSTAR 3800 (May 2008)	0/50
Cobalt metal (May 2006)	0/50
Vinylidene chloride (June 2005)	0/50
Trim VX (August 2009)	0/50
Total	0/250
Overall Historical Incidence: All Routes	
Total	0/550

[a]Data as of June 2015.

Table D-6. Historical Incidence of Benign Pheochromocytoma of the Adrenal Medulla in Control Female B6C3F1/N Mice[a]

Study (Study Start)	Incidence in Controls
Historical Incidence: Inhalation Studies	
Antimony trioxide (October 2008)	0/50
CIMSTAR 3800 (May 2008)	1/49
Cobalt metal (May 2006)	1/50
Vinylidene chloride (June 2005)	1/50
Trim VX (August 2009)	2/50
Total (%)	5/249 (2.0%)
Mean ± standard deviation	2.0% ± 1.4%
Range	0%–4%
Overall Historical Incidence: All Routes	
Total (%)	6/546 (1.1%)
Mean ± standard deviation	1.1% ± 1.4%
Range	0%–4%

[a]Data as of June 2015.

Table D-7. Historical Incidence of Hepatocellular Adenoma or Carcinoma (combined) in Control Female B6C3F1/N Mice[a]

Study (Study Start)	Incidence in Controls
Historical Incidence: Inhalation Studies	
Antimony trioxide (October 2008)	14/50
CIMSTAR 3800 (May 2008)	20/50
Cobalt metal (May 2006)	25/50
Vinylidene chloride (June 2005)	28/50
Trim VX (August 2009)	15/50
Total (%)	102/250 (40.8%)
Mean ± standard deviation	40.8% ± 12.2%
Range	28%–56%
Overall Historical Incidence: All Routes	
Total (%)	207/549 (37.7%)
Mean ± standard deviation	37.8% ± 16.6%
Range	16%–73%

[a]Data as of June 2015.

Table D-8. Summary of the Incidence of Nonneoplastic Lesions in Female Mice in the Two-year Inhalation Study of Antimony Trioxide[a]

	Chamber Control	3 mg/m^3	10 mg/m^3	30 mg/m^3
Disposition Summary				
Animals initially in study	60	60	60	60
Twelve-month interim evaluation	10	10	10	10
Early deaths				
Accidental death	1	–	–	–
Moribund	10	11	16	27
Natural deaths	3	8	8	8
Survivors				
Terminal kill	36	31	26	15
Animals examined microscopically	60	60	60	60
Twelve-month Interim Evaluation				
Alimentary System				
Esophagus	(10)	(10)	(10)	(10)
Gallbladder	(10)	(10)	(10)	(10)
Intestine large, cecum	(10)	(10)	(10)	(10)
Intestine large, colon	(10)	(10)	(10)	(10)

	Chamber Control	3 mg/m^3	10 mg/m^3	30 mg/m^3
Intestine large, rectum	(10)	(10)	(10)	(10)
Intestine small, duodenum	(10)	(10)	(10)	(10)
Intestine small, ileum	(10)	(10)	(10)	(10)
Intestine small, jejunum	(10)	(10)	(10)	(10)
Liver	(10)	(10)	(10)	(10)
Basophilic focus	–	1 (10%)	–	–
Clear cell focus	–	–	1 (10%)	–
Pancreas	(10)	(10)	(10)	(10)
Atrophy	–	–	1 (10%)	–
Salivary glands	(10)	(10)	(10)	(10)
Stomach, forestomach	(10)	(10)	(10)	(10)
Stomach, glandular	(10)	(10)	(10)	(10)
Tooth	(1)	(0)	(0)	(0)
Dysplasia	1 (100%)	–	–	–
Cardiovascular System				
Blood vessel	(10)	(9)	(10)	(10)
Adventitia, inflammation, chronic active	1 (10%)	–	–	–
Heart	(10)	(10)	(10)	(10)
Cardiomyopathy	–	1 (10%)	–	–
Artery, inflammation, chronic active	–	–	1 (10%)	–
Genital System				
Clitoral gland	(10)	(9)	(7)	(7)
Ovary	(10)	(10)	(10)	(10)
Follicle, cyst	1 (10%)	–	1 (10%)	1 (10%)
Uterus	(10)	(10)	(10)	(10)
Endometrium, hyperplasia, cystic	7 (70%)	9 (90%)	10 (100%)	9 (90%)
Hematopoietic System				
Bone marrow	(10)	(10)	(10)	(10)
Lymph node, bronchial	(5)	(10)	(9)	(10)
Foreign body	–	10 (100%)	9 (100%)	10 (100%)
Hyperplasia, lymphoid	–	6 (60%)	9 (100%)	10 (100%)
Infiltration cellular, histiocyte	–	1 (10%)	6 (67%)	4 (40%)
Lymph node, mandibular	(6)	(8)	(7)	(8)
Lymph node, mediastinal	(4)	(7)	(8)	(10)
Foreign body	–	2 (29%)	2 (25%)	9 (90%)

	Chamber Control	3 mg/m^3	10 mg/m^3	30 mg/m^3
Hyperplasia, lymphoid	–	1 (14%)	4 (50%)	4 (40%)
Infiltration cellular, histiocyte	–	–	2 (25%)	3 (30%)
Lymph node, mesenteric	(9)	(10)	(10)	(10)
Spleen	(10)	(10)	(10)	(10)
Hematopoietic cell proliferation	–	–	3 (30%)	2 (20%)
Hyperplasia, lymphoid	–	4 (40%)	6 (60%)	5 (50%)
Thymus	(10)	(9)	(10)	(9)
Medulla, hyperplasia, lymphoid	1 (10%)	4 (44%)	4 (40%)	3 (33%)
Integumentary System				
Mammary gland	(9)	(10)	(10)	(10)
Skin	(10)	(10)	(10)	(10)
Dermis, infiltration cellular, mixed cell	2 (20%)	1 (10%)	–	2 (20%)
Musculoskeletal System				
Bone	(10)	(10)	(10)	(10)
Femur, fibro-osseous lesion	1 (10%)	–	1 (10%)	–
Respiratory System				
Larynx	(10)	(9)	(10)	(10)
Foreign body	–	2 (22%)	7 (70%)	7 (70%)
Respiratory epithelium, hyperplasia	–	1 (11%)	4 (40%)	–
Respiratory epithelium, metaplasia, squamous	1 (10%)	–	1 (10%)	8 (80%)
Lung	(10)	(10)	(10)	(10)
Foreign body	–	10 (100%)	10 (100%)	10 (100%)
Infiltration cellular, lymphocyte	3 (30%)	10 (100%)	10 (100%)	9 (90%)
Inflammation, chronic active	–	10 (100%)	10 (100%)	10 (100%)
Alveolar epithelium, hyperplasia	–	8 (80%)	10 (100%)	10 (100%)
Alveolus, fibrosis	–	2 (20%)	6 (60%)	10 (100%)
Bronchiole, epithelium, hyperplasia	–	5 (50%)	10 (100%)	10 (100%)
Pleura, fibrosis	–	6 (60%)	9 (90%)	10 (100%)
Pleura, inflammation	–	7 (70%)	10 (100%)	10 (100%)
Nose	(10)	(10)	(10)	(10)
Foreign body	–	6 (60%)	9 (90%)	10 (100%)
Inflammation, acute	–	–	1 (10%)	–
Olfactory epithelium, accumulation, hyaline droplet	1 (10%)	–	–	–

	Chamber Control	3 mg/m^3	10 mg/m^3	30 mg/m^3
Olfactory epithelium, metaplasia, respiratory	–	–	–	1 (10%)
Respiratory epithelium, accumulation, hyaline droplet	6 (60%)	4 (40%)	3 (30%)	–
Respiratory epithelium, inflammation, acute	1 (10%)	–	–	–
Trachea	(10)	(10)	(10)	(10)
Foreign body	–	–	2 (20%)	4 (40%)
Inflammation, chronic active	–	1 (10%)	–	–
Special Senses System				
Eye	(10)	(10)	(10)	(10)
Harderian gland	(10)	(10)	(10)	(10)
Hyperplasia	1 (10%)	–	–	–
Urinary System				
Kidney	(10)	(10)	(10)	(10)
Nephropathy	2 (20%)	–	1 (10%)	1 (10%)
Urinary bladder	(10)	(10)	(10)	(10)
Systems Examined at 12 Months with No Lesions Observed				
Endocrine System				
General Body System				
Nervous System				
Two-year Study				
Alimentary System				
Esophagus	(50)	(50)	(50)	(50)
Gallbladder	(46)	(41)	(44)	(45)
Inflammation, chronic	–	1 (2%)	1 (2%)	–
Intestine large, cecum	(47)	(44)	(48)	(47)
Inflammation, chronic active	–	2 (5%)	2 (4%)	–
Intestine large, colon	(47)	(47)	(49)	(47)
Necrosis	–	–	1 (2%)	–
Intestine large, rectum	(44)	(46)	(48)	(47)
Intestine small, duodenum	(47)	(44)	(45)	(45)
Intestine small, ileum	(47)	(45)	(47)	(45)
Inflammation, chronic active	–	–	1 (2%)	–
Peyer’s patch, hyperplasia, lymphoid	–	–	1 (2%)	–
Intestine small, jejunum	(47)	(43)	(46)	(44)

	Chamber Control	3 mg/m^3	10 mg/m^3	30 mg/m^3
Inflammation	–	1 (2%)	–	–
Peyer's patch, hyperplasia, lymphoid	1 (2%)	–	–	–
Liver	(50)	(50)	(50)	(50)
Angiectasis	2 (4%)	1 (2%)	1 (2%)	2 (4%)
Basophilic focus	–	–	–	1 (2%)
Clear cell focus	6 (12%)	5 (10%)	3 (6%)	2 (4%)
Cyst	–	–	1 (2%)	–
Eosinophilic focus	2 (4%)	3 (6%)	2 (4%)	–
Fatty change	–	2 (4%)	1 (2%)	–
Hematopoietic cell proliferation	–	–	–	1 (2%)
Inflammation, chronic active	4 (8%)	3 (6%)	1 (2%)	2 (4%)
Mineralization	–	1 (2%)	–	–
Mixed cell focus	1 (2%)	–	1 (2%)	–
Necrosis	3 (6%)	2 (4%)	5 (10%)	2 (4%)
Tension lipidosis	4 (8%)	3 (6%)	3 (6%)	–
Thrombosis	–	1 (2%)	–	–
Centrilobular, fatty change	–	1 (2%)	–	–
Hepatocyte, periportal, hypertrophy	–	–	1 (2%)	–
Mesentery	(9)	(12)	(16)	(7)
Cyst	–	1 (8%)	–	–
Inflammation, suppurative	–	–	1 (6%)	–
Inflammation, chronic	–	–	–	1 (14%)
Necrosis, fatty	5 (56%)	9 (75%)	11 (69%)	4 (57%)
Artery, inflammation, chronic active	2 (22%)	–	2 (13%)	1 (14%)
Fat, necrosis	–	–	–	1 (14%)
Lymphatic, angiectasis	–	–	1 (6%)	–
Pancreas	(50)	(50)	(50)	(50)
Atrophy	–	3 (6%)	2 (4%)	–
Hypertrophy	–	1 (2%)	–	–
Inflammation	–	–	2 (4%)	–
Inflammation, chronic active	–	–	–	1 (2%)
Necrosis	–	–	1 (2%)	–
Artery, inflammation, chronic active	–	1 (2%)	–	1 (2%)
Duct, cyst	–	2 (4%)	1 (2%)	–
Salivary glands	(50)	(50)	(50)	(50)

	Chamber Control	3 mg/m^3	10 mg/m^3	30 mg/m^3
Inflammation, acute	–	1 (2%)	–	–
Artery, inflammation, chronic active	–	–	1 (2%)	1 (2%)
Stomach, forestomach	(50)	(50)	(50)	(50)
Hyperkeratosis	2 (4%)	–	–	–
Hyperplasia, squamous	–	–	–	1 (2%)
Inflammation, chronic active	–	1 (2%)	–	3 (6%)
Mineralization	–	1 (2%)	–	–
Perforation, chronic active	–	–	–	1 (2%)
Stomach, glandular	(50)	(49)	(50)	(50)
Inflammation, chronic active	1 (2%)	1 (2%)	3 (6%)	2 (4%)
Mineralization	2 (4%)	3 (6%)	2 (4%)	2 (4%)
Necrosis	–	1 (2%)	–	1 (2%)
Ulcer	–	–	–	1 (2%)
Artery, inflammation, chronic active	–	–	1 (2%)	–
Tongue	(0)	(1)	(0)	(0)
Hyperkeratosis	–	1 (100%)	–	–
Inflammation, chronic active	–	1 (100%)	–	–
Ulcer	–	1 (100%)	–	–
Tooth	(0)	(2)	(2)	(1)
Dysplasia	–	1 (50%)	1 (50%)	1 (100%)
Inflammation, chronic active	–	1 (50%)	–	–
Peridontal tissue, mineralization	–	–	1 (50%)	–
Cardiovascular System				
Blood vessel	(50)	(48)	(47)	(46)
Inflammation, chronic active	1 (2%)	–	2 (4%)	–
Mineralization	–	1 (2%)	–	–
Thrombosis	–	–	1 (2%)	–
Adventitia, inflammation, chronic active	–	–	2 (4%)	1 (2%)
Media, inflammation, chronic active	–	–	1 (2%)	1 (2%)
Media, mineralization	–	–	1 (2%)	–
Heart	(50)	(50)	(50)	(50)
Cardiomyopathy	11 (22%)	13 (26%)	6 (12%)	11 (22%)
Necrosis, acute	1 (2%)	–	–	–
Thrombosis	–	2 (4%)	–	–
Artery, inflammation, chronic active	10 (20%)	4 (8%)	11 (22%)	5 (10%)

	Chamber Control	3 mg/m^3	10 mg/m^3	30 mg/m^3
Artery, mineralization	–	1 (2%)	–	–
Epicardium, inflammation, chronic active	–	2 (4%)	7 (14%)	7 (14%)
Epicardium, myocardium, necrosis	–	–	1 (2%)	–
Myocardium, inflammation, acute	–	2 (4%)	1 (2%)	–
Myocardium, inflammation, chronic active	–	1 (2%)	–	–
Myocardium, necrosis	–	1 (2%)	–	–
Pericardium, hyperplasia, lymphoid	–	–	1 (2%)	–
Pericardium, inflammation, chronic active	–	–	1 (2%)	1 (2%)
Valve, inflammation, chronic active	1 (2%)	1 (2%)	1 (2%)	1 (2%)
Endocrine System				
Adrenal cortex	(50)	(50)	(50)	(50)
Necrosis	–	–	1 (2%)	–
Zona fasciculata, hypertrophy	12 (24%)	16 (32%)	11 (22%)	11 (22%)
Zona fasciculata, necrosis	–	–	1 (2%)	–
Zona glomerulosa, hyperplasia	–	–	–	1 (2%)
Adrenal medulla	(50)	(50)	(48)	(49)
Hyperplasia	9 (18%)	8 (16%)	9 (19%)	7 (14%)
Islets, pancreatic	(50)	(49)	(49)	(49)
Hyperplasia, adenomatous	1 (2%)	–	–	–
Parathyroid gland	(27)	(33)	(34)	(32)
Cyst	1 (4%)	–	–	–
Hypertrophy	1 (4%)	–	–	–
Pituitary gland	(49)	(50)	(50)	(50)
Pars distalis, angiectasis	–	–	1 (2%)	2 (4%)
Pars distalis, cyst	2 (4%)	1 (2%)	–	–
Pars distalis, hyperplasia	15 (31%)	6 (12%)	10 (20%)	14 (28%)
Pars nervosa, inflammation, acute	–	–	–	1 (2%)
Pars nervosa, thrombosis	–	–	1 (2%)	–
Thyroid gland	(48)	(50)	(50)	(50)
Inflammation, chronic active	–	–	1 (2%)	1 (2%)
Follicular cell, hyperplasia	1 (2%)	–	–	–
General Body System				
Peritoneum	(0)	(0)	(1)	(0)
Inflammation, suppurative	–	–	1 (100%)	–

	Chamber Control	3 mg/m^3	10 mg/m^3	30 mg/m^3
Genital System				
Clitoral gland	(48)	(44)	(47)	(42)
Inflammation, chronic active	1 (2%)	1 (2%)	–	1 (2%)
Ovary	(50)	(49)	(50)	(50)
Angiectasis	1 (2%)	–	2 (4%)	1 (2%)
Cyst	–	–	1 (2%)	–
Hemorrhage	–	–	1 (2%)	–
Inflammation, acute	1 (2%)	–	1 (2%)	1 (2%)
Inflammation, chronic active	1 (2%)	–	1 (2%)	1 (2%)
Mineralization	–	–	–	1 (2%)
Necrosis, fatty	–	–	–	1 (2%)
Artery, inflammation, chronic active	–	–	1 (2%)	–
Bursa, cyst	1 (2%)	1 (2%)	1 (2%)	3 (6%)
Follicle, cyst	7 (14%)	11 (22%)	13 (26%)	13 (26%)
Oviduct	(1)	(0)	(0)	(0)
Uterus	(50)	(50)	(50)	(50)
Angiectasis	2 (4%)	–	1 (2%)	1 (2%)
Hydrometra	–	–	1 (2%)	–
Inflammation, chronic active	1 (2%)	3 (6%)	1 (2%)	2 (4%)
Thrombosis	1 (2%)	–	–	–
Ulcer	–	–	–	1 (2%)
Endometrial glands, endometrium, hyperplasia	1 (2%)	–	–	–
Endometrium, hyperplasia, cystic	41 (82%)	43 (86%)	44 (88%)	41 (82%)
Lymphatic, angiectasis	–	–	1 (2%)	–
Serosa, cyst	–	1 (2%)	–	–
Hematopoietic System				
Bone marrow	(50)	(50)	(50)	(50)
Atrophy	–	–	–	1 (2%)
Hyperplasia	3 (6%)	5 (10%)	15 (30%)	28 (56%)
Myelofibrosis	1 (2%)	–	–	–
Necrosis	–	–	1 (2%)	–
Lymph node	(6)	(9)	(14)	(16)
Iliac, angiectasis	–	1 (11%)	1 (7%)	–
Iliac, hyperplasia	–	–	–	1 (6%)
Iliac, hyperplasia, lymphoid	–	–	1 (7%)	–

	Chamber Control	3 mg/m^3	10 mg/m^3	30 mg/m^3
Iliac, inflammation	–	–	–	1 (6%)
Lumbar, angiectasis	–	–	1 (7%)	–
Lumbar, ectasia	–	–	–	3 (19%)
Lumbar, hematopoietic cell proliferation	–	–	–	1 (6%)
Lumbar, hyperplasia, lymphoid	1 (17%)	–	–	–
Renal, angiectasis	–	3 (33%)	1 (7%)	–
Renal, hyperplasia, lymphoid	1 (17%)	–	–	1 (6%)
Lymph node, bronchial	(41)	(47)	(48)	(49)
Foreign body	–	34 (72%)	46 (96%)	43 (88%)
Hyperplasia, lymphoid	2 (5%)	15 (32%)	17 (35%)	11 (22%)
Infiltration cellular, histiocyte	–	2 (4%)	7 (15%)	7 (14%)
Infiltration cellular, plasma cell	–	–	–	1 (2%)
Inflammation, acute	1 (2%)	–	–	1 (2%)
Lymph node, mandibular	(41)	(28)	(38)	(39)
Angiectasis	–	1 (4%)	–	–
Foreign body	–	5 (18%)	9 (24%)	3 (8%)
Hyperplasia, lymphoid	7 (17%)	1 (4%)	2 (5%)	1 (3%)
Infiltration cellular, histiocyte	–	–	2 (5%)	1 (3%)
Lymph node, mediastinal	(46)	(48)	(49)	(50)
Angiectasis	–	1 (2%)	–	1 (2%)
Foreign body	–	28 (58%)	45 (92%)	44 (88%)
Hyperplasia, lymphoid	–	3 (6%)	16 (33%)	18 (36%)
Infiltration cellular, histiocyte	–	6 (13%)	11 (22%)	16 (32%)
Infiltration cellular, plasma cell	–	–	–	1 (2%)
Inflammation, acute	1 (2%)	–	–	–
Pigmentation	1 (2%)	–	–	–
Arteriole, necrosis	–	–	1 (2%)	–
Artery, inflammation, chronic active	–	1 (2%)	1 (2%)	–
Medullary sinuses, dilatation	1 (2%)	–	–	–
Lymph node, mesenteric	(50)	(48)	(48)	(46)
Angiectasis	–	2 (4%)	1 (2%)	–
Hematopoietic cell proliferation	–	–	–	1 (2%)
Hyperplasia, lymphoid	–	2 (4%)	3 (6%)	1 (2%)
Infiltration cellular, histiocyte	–	–	1 (2%)	–
Infiltration cellular, mixed cell	–	2 (4%)	1 (2%)	–

	Chamber Control	3 mg/m^3	10 mg/m^3	30 mg/m^3
Infiltration cellular, plasma cell	–	1 (2%)	–	1 (2%)
Inflammation, chronic	1 (2%)	–	–	–
Necrosis, acute	–	–	1 (2%)	–
Spleen	(50)	(50)	(50)	(50)
Angiectasis	–	1 (2%)	–	–
Hematopoietic cell proliferation	17 (34%)	19 (38%)	20 (40%)	35 (70%)
Hyperplasia, lymphoid	16 (32%)	6 (12%)	8 (16%)	7 (14%)
Inflammation, chronic active	–	1 (2%)	–	1 (2%)
Metaplasia, osseous	–	–	1 (2%)	–
Necrosis	–	1 (2%)	–	–
Thymus	(47)	(49)	(49)	(49)
Angiectasis	1 (2%)	1 (2%)	–	–
Cyst	–	–	1 (2%)	–
Depletion cellular	9 (19%)	18 (37%)	23 (47%)	29 (59%)
Foreign body	–	–	–	1 (2%)
Hyperplasia, lymphoid	–	–	1 (2%)	–
Inflammation, chronic active	1 (2%)	1 (2%)	2 (4%)	–
Medulla, hyperplasia, lymphoid	13 (28%)	12 (24%)	15 (31%)	16 (33%)
Integumentary System				
Mammary gland	(50)	(50)	(50)	(50)
Dilatation	–	–	1 (2%)	–
Hyperplasia	–	2 (4%)	–	1 (2%)
Hypertrophy	1 (2%)	4 (8%)	3 (6%)	1 (2%)
Inflammation, chronic active	–	2 (4%)	–	2 (4%)
Necrosis, acute	–	–	1 (2%)	–
Skin	(50)	(50)	(50)	(50)
Hyperplasia	–	–	–	2 (4%)
Inflammation, chronic active	2 (4%)	2 (4%)	2 (4%)	4 (8%)
Ulcer	–	–	–	1 (2%)
Musculoskeletal System				
Bone	(50)	(50)	(49)	(50)
Hyperostosis	–	–	1 (2%)	–
Femur, fibro-osseous lesion	21 (42%)	16 (32%)	10 (20%)	6 (12%)
Maxilla, fibro-osseous lesion	–	2 (4%)	1 (2%)	1 (2%)
Skeletal muscle	(4)	(1)	(4)	(3)

	Chamber Control	3 mg/m^3	10 mg/m^3	30 mg/m^3
Hemorrhage	1 (25%)	–	–	–
Inflammation, chronic	–	–	1 (25%)	–
Artery, inflammation, chronic active	1 (25%)	–	–	–
Nervous System				
Brain	(50)	(50)	(50)	(50)
Compression	2 (4%)	2 (4%)	2 (4%)	1 (2%)
Demyelination	1 (2%)	–	–	1 (2%)
Necrosis, acute	–	–	–	1 (2%)
Thrombosis	–	1 (2%)	1 (2%)	–
Arteriole, inflammation, chronic active	2 (4%)	–	2 (4%)	1 (2%)
Glial cell, hyperplasia	1 (2%)	–	–	–
Meninges, infiltration cellular, histiocyte	–	–	1 (2%)	–
Meninges, infiltration cellular, lymphoid	1 (2%)	2 (4%)	3 (6%)	1 (2%)
Peripheral nerve	(3)	(0)	(2)	(1)
Sciatic, degeneration	–	–	1 (50%)	–
Spinal cord	(4)	(0)	(2)	(1)
Hemorrhage	1 (25%)	–	–	–
Respiratory System				
Larynx	(50)	(50)	(50)	(50)
Foreign body	–	25 (50%)	39 (78%)	48 (96%)
Inflammation, chronic active	4 (8%)	3 (6%)	2 (4%)	4 (8%)
Mineralization	–	1 (2%)	–	–
Arteriole, inflammation, chronic active	1 (2%)	–	2 (4%)	–
Artery, inflammation, chronic active	–	1 (2%)	–	–
Cartilage, mineralization	–	2 (4%)	–	–
Respiratory epithelium, hyperplasia	2 (4%)	–	14 (28%)	18 (36%)
Respiratory epithelium, metaplasia, squamous	1 (2%)	–	5 (10%)	24 (48%)
Squamous epithelium, hyperplasia	4 (8%)	1 (2%)	1 (2%)	12 (24%)
Lung	(50)	(50)	(50)	(50)
Foreign body	–	50 (100%)	50 (100%)	50 (100%)
Hemorrhage	–	1 (2%)	–	–
Infiltration cellular, histiocyte	1 (2%)	–	–	–
Infiltration cellular, lymphocyte	7 (14%)	37 (74%)	37 (74%)	26 (52%)

	Chamber Control	3 mg/m^3	10 mg/m^3	30 mg/m^3
Inflammation, chronic active	1 (2%)	50 (100%)	50 (100%)	50 (100%)
Thrombosis	1 (2%)	1 (2%)		1 (2%)
Alveolar epithelium, hyperplasia	1 (2%)	36 (72%)	49 (98%)	48 (96%)
Alveolar epithelium, metaplasia, squamous	–	1 (2%)	–	2 (4%)
Alveolus, fibrosis	–	13 (26%)	30 (60%)	38 (76%)
Alveolus, infiltration cellular, histiocyte	–	–	–	1 (2%)
Alveolus, metaplasia, squamous	–	–	1 (2%)	–
Artery, inflammation, acute	1 (2%)	–	–	–
Bronchiole, epithelium, hyperplasia	1 (2%)	34 (68%)	48 (96%)	45 (90%)
Bronchiole, epithelium, goblet cell, metaplasia	–	–	1 (2%)	1 (2%)
Bronchus, epithelium, hyperplasia	–	–	1 (2%)	–
Bronchus, epithelium, goblet cell, metaplasia	–	–	–	2 (4%)
Mediastinum, inflammation, acute	1 (2%)	–	–	–
Mediastinum, necrosis, fatty	–	–	1 (2%)	–
Pleura, fibrosis	1 (2%)	39 (78%)	50 (100%)	50 (100%)
Pleura, inflammation	4 (8%)	27 (54%)	42 (84%)	38 (76%)
Nose	(50)	(49)	(50)	(50)
Foreign body	1 (2%)	44 (90%)	45 (90%)	48 (96%)
Artery, inflammation, chronic active	1 (2%)	–	–	–
Glands, dilatation	–	–	–	1 (2%)
Glands, olfactory epithelium, dilatation	1 (2%)	–	–	–
Glands, respiratory epithelium, accumulation, hyaline droplet	–	–	1 (2%)	–
Lumen, hyperkeratosis	1 (2%)	–	–	–
Nasolacrimal duct, inflammation, acute	–	–	–	1 (2%)
Nasolacrimal duct, inflammation, chronic active	–	1 (2%)	1 (2%)	–
Olfactory epithelium, accumulation, hyaline droplet	18 (36%)	9 (18%)	12 (24%)	8 (16%)
Olfactory epithelium, atrophy	–	2 (4%)	1 (2%)	1 (2%)
Olfactory epithelium, metaplasia, respiratory	–	1 (2%)	3 (6%)	–
Olfactory epithelium, necrosis	1 (2%)	–	–	–

	Chamber Control	3 mg/m^3	10 mg/m^3	30 mg/m^3
Respiratory epithelium, accumulation, hyaline droplet	29 (58%)	22 (45%)	25 (50%)	19 (38%)
Respiratory epithelium, hyperplasia	–	–	–	2 (4%)
Respiratory epithelium, inflammation, acute	2 (4%)	7 (14%)	7 (14%)	5 (10%)
Respiratory epithelium, inflammation, chronic active	2 (4%)	3 (6%)	4 (8%)	5 (10%)
Respiratory epithelium, metaplasia, squamous	–	3 (6%)	2 (4%)	4 (8%)
Respiratory epithelium, mineralization	–	–	1 (2%)	–
Respiratory epithelium, necrosis	1 (2%)	2 (4%)	–	–
Turbinate, inflammation, suppurative	1 (2%)	–	–	–
Turbinate, necrosis	–	–	1 (2%)	–
Vomeronasal organ, necrosis	1 (2%)	–	–	–
Pleura	(0)	(2)	(0)	(2)
Necrosis, fatty	–	1 (50%)	–	1 (50%)
Trachea	(50)	(50)	(50)	(50)
Foreign body	–	7 (14%)	14 (28%)	20 (40%)
Inflammation, chronic active	2 (4%)	4 (8%)	4 (8%)	–
Artery, inflammation, chronic active	1 (2%)	–	1 (2%)	–
Cartilage, metaplasia, osseous	–	1 (2%)	–	–
Epithelium, hyperplasia	–	–	–	1 (2%)
Epithelium, metaplasia, squamous	–	–	1 (2%)	1 (2%)
Epithelium, mineralization	–	2 (4%)	–	–
Glands, inflammation, acute	–	1 (2%)	–	–
Glands, metaplasia, cartilaginous	2 (4%)	–	–	–
Special Senses System				
Ear	(0)	(0)	(0)	(1)
Eye	(49)	(47)	(49)	(49)
Cataract	1 (2%)	4 (9%)	2 (4%)	4 (8%)
Cornea, inflammation, chronic active	–	–	–	1 (2%)
Retina, atrophy	1 (2%)	–	–	–
Harderian gland	(49)	(50)	(50)	(50)
Hyperplasia	2 (4%)	–	–	–
Inflammation, acute	–	–	1 (2%)	–
Zymbal’s gland	(0)	(0)	(0)	(1)

	Chamber Control	3 mg/m^3	10 mg/m^3	30 mg/m^3
Urinary System				
Kidney	(50)	(50)	(50)	(50)
Cyst	–	–	2 (4%)	–
Infarct	1 (2%)	3 (6%)	–	–
Inflammation, acute	–	2 (4%)	–	–
Metaplasia, osseous	1 (2%)	–	2 (4%)	1 (2%)
Mineralization	–	1 (2%)	–	–
Necrosis	–	1 (2%)	–	–
Nephropathy	35 (70%)	30 (60%)	29 (58%)	32 (64%)
Artery, inflammation, chronic active	–	–	1 (2%)	–
Urinary bladder	(50)	(50)	(50)	(50)
Hyperplasia, lymphoid	1 (2%)	–	1 (2%)	–
Infiltration cellular, lymphocyte, focal	–	–	–	1 (2%)
Artery, inflammation, chronic active	1 (2%)	–	2 (4%)	–

[a]Number of animals examined microscopically at the site and the number of animals with lesion.

Appendix E. Genetic Toxicology

Table of Contents

E.1. Rat and Mouse Peripheral Blood Micronucleus Test Protocol E-2
E.2. Comet Assay Protocol for DNA Damage Assessment in Peripheral Blood Leukocytes and Cells from the Lung E-2
E.3. Evaluation Protocol E-3
E.4. Results E-4

Tables

Table E-1. Frequency of Micronuclei in Peripheral Blood Erythrocytes of Rats Following Treatment with Antimony Trioxide by Inhalation for 12 Months E-5
Table E-2. Frequency of Micronuclei in Peripheral Blood Erythrocytes of Mice Following Treatment with Antimony Trioxide by Inhalation for 12 Months E-6
Table E-3. DNA Damage in the Blood and Lung of Rats Following Treatment with Antimony Trioxide by Inhalation for 12 Months E-7
Table E-4. DNA Damage in the Blood and Lung of Mice Following Treatment with Antimony Trioxide by Inhalation for 12 Months E-8

E.1. Rat and Mouse Peripheral Blood Micronucleus Test Protocol

A detailed discussion of this assay is presented by Torous et al.[94] and Witt et al.[95]. At the 12-month interim evaluation in the 2-year studies of antimony trioxide, small blood samples (approximately 120 µL) were obtained from male and female Wistar Han rats and B6C3F1/N mice in EDTA tubes. Samples were immediately refrigerated, and then shipped with cold packs by overnight courier to the analytical laboratory where they were immediately fixed in ultracold methanol[96] (MicroFlow® Basic Kits, Litron Laboratories, Rochester NY) and stored in a −80°C freezer until analysis. Flow cytometric analysis was conducted using a FACSCalibur flow cytometer (Becton Dickinson, San Jose, CA). Reticulocytes were identified by the presence of an active transferrin receptor (CD71+) on the cell surface; mature erythrocytes were identified as CD71-negative. For rat blood samples, the analysis was restricted to the youngest reticulocytes (i.e., the subpopulation of erythrocytes with the highest CD71 expression) to focus on the population of reticulocytes that were least altered by the efficient action of the rat spleen in sequestering and destroying micronucleated red blood cells[97]. Using flow cytometry, micronucleated cells were detected using the DNA staining dye propidium iodide (PI) in conjunction with RNase treatment. Therefore, micronucleated reticulocytes express high levels of CD71 (CD71+) and PI-associated fluorescence, while micronucleated erythrocytes are negative for CD71 (CD71−) and show PI-associated fluorescence. Twenty thousand CD71+ reticulocytes were scored per animal for the presence of micronuclei, and approximately 1×10^6 total erythrocytes were counted for the presence of micronuclei and to determine percentage of reticulocytes (percent reticulocytes) as a measure of chemical-induced bone marrow toxicity.

In this assay, the animal is the experimental unit and approximately 20,000 reticulocytes and/or 1×10^6 erythrocytes are evaluated per animal for the presence of micronuclei. In addition, the percent reticulocytes was determined in approximately 1×10^6 erythrocytes. The optimum number of cells to score for micronuclei using flow cytometric approaches was determined in earlier studies[98]. Data from each treatment group are summarized as the mean frequency of micronucleated reticulocytes per 1,000 reticulocytes, plus or minus the standard error of the mean. With the large number of cells counted by flow cytometry, it is assumed that the number of micronucleated cells is normally distributed. Levene's test is used to determine if variances among treatment groups were equal. When they are, linear regression analysis is used to test for linear trend and pairwise differences with the control group are evaluated using Williams' test, after linearizing the data by averaging data points that violate a linear trend. When variances are unequal, nonparametric methods are used to analyze the data: Jonckheere's test is used to evaluate linear trend and Dunn's test is used to assess the significance of pairwise differences with the control group. To maintain the overall significance level at $P \leq 0.05$, the trend as well as the pairwise differences from the control group are declared statistically significant if $P \leq 0.025$. Ultimately, the scientific staff determines the final call after considering the results of statistical analyses, reproducibility of any effects observed, and the magnitudes of those effects.

E.2. Comet Assay Protocol for DNA Damage Assessment in Peripheral Blood Leukocytes and Cells from the Lung

The same animals sampled for the peripheral blood micronucleus assay were sampled for assessment of DNA damage in cells from the blood and the lung. The general tissue sample preparation procedures have been described in detail previously[99]. In brief, at the 12-month

interim evaluation, lung and additional (approximately 50 µL) blood samples were collected for assessment of DNA damage using the comet assay[100-102]. Blood samples were placed into tubes containing 1 mL of mincing solution (Mg^{+2} and Ca^{+2} free Hank's Balanced Salt Solution with 20 mM EDTA, pH 7.4 to 7.7, and 10% v/v fresh DMSO). A small portion of the lung was placed in a cryovial containing 1 mL of mincing solution and rapidly minced. Blood and tissue samples for the comet assay were flash frozen in liquid nitrogen and stored at −80°C prior to shipping on dry ice to the genetic toxicology laboratory. Upon arrival at the genetic toxicology laboratory, frozen samples were stored in a −80°C freezer until thawing and processing for DNA damage analysis.

Thawed cell samples were diluted with phosphate buffered saline (PBS), mixed with 0.5% low melting point agarose at 37°C, layered onto slides, and placed in cold lysing solution (2.5 M NaCl, 100 mM Na2EDTA, 10 mM Tris, pH 10, with freshly added 10% DMSO and 1% Triton X-100) overnight. After rinsing in 0.4 M Trizma base, pH 7.5, slides were treated with cold alkali (300 mM NaOH, 1 mM Na2EDTA, pH>13) for 20 minutes, then electrophoresed at 4° to 10°C for 20 minutes at 1.0 V/cm, 300 mA. Slides were then neutralized with 0.4 M Trizma base (pH 7.5) for 5 minutes, incubated for 5 minutes in ice-cold 100% ethanol, and allowed to air dry. Slides were stained with SYBR® Gold and 100 cells were scored per tissue per animal using Comet Assay IV Imaging Software¸ Version 4.11 (Perceptive Instruments, Ltd., Suffolk, UK). For each cell, the extent of DNA migration was characterized using the percent tail DNA endpoint measurement (intensity of all tail pixels divided by the total intensity of all pixels in the comet, expressed as a percentage).

For each 100-cell sample per animal, the Shapiro-Wilk test was first used to assess normality of the control group. Data that were normally distributed were analyzed using an independent sample's t-test to compare each dose level to the concurrent control and linear regression to determine the presence of a dose response. Normally distributed data were also tested for homogeneity of variances using the F test; for data of unequal variances, the Welch's approximation for unequal variances t-test value was used for determination of a one-tailed significant ($P \leq 0.05$) increase in DNA migration. Data that were not normally distributed were analyzed by the Mann-Whitney test[103] comparing each dose level to the concurrent control, followed by the Kendall rank correlation test[104] to determine the presence of a dose response. Trend tests were considered statistically significant at $P \leq 0.025$ and pairwise comparisons were significant at $P \leq 0.008$ (0.025/3 dose groups) to correct for multiple comparisons.

E.3. Evaluation Protocol

These are the basic guidelines for arriving at an overall assay result for assays performed by the National Toxicology Program. Statistical as well as biological factors are considered. For an individual assay, the statistical procedures for data analysis have been described in the preceding protocols. There have been instances, however, in which multiple samples of a chemical were tested in the same assay, and different results were obtained among these samples and/or among laboratories. Results from more than one aliquot or from more than one laboratory are not simply combined into an overall result. Rather, all the data are critically evaluated, particularly with regard to pertinent protocol variations, in determining the weight of evidence for an overall conclusion of chemical activity in an assay. In addition to multiple aliquots, the in vitro assays have another variable that must be considered in arriving at an overall test result. In vitro assays are conducted with and without exogenous metabolic activation. Results obtained in the absence of activation are not combined with results obtained in the presence of activation; each testing

condition is evaluated separately. The summary table in the Abstract of this Technical Report presents a result that represents a scientific judgment of the overall evidence for activity of the chemical in an assay.

E.4. Results

In male and female Wistar Han rats, the reticulocyte population (polychromatic erythrocytes or PCEs), did not show an increase in micronucleated cells following 12 months of inhalation exposure to antimony trioxide (0, 3, 10, or 30 mg/m^3) (Table E-1). In addition, no significant alterations in the percent reticulocytes in peripheral blood were observed in either male or female rats, suggesting no bone marrow toxicity or effect on erythropoiesis associated with exposure to antimony trioxide.

Micronucleus frequencies in mature erythrocytes (normochromatic erythrocytes or NCEs) of male and female B6C3F1/N mice exposed to antimony trioxide (0, 3, 10, or 30 mg/m^3) for 12 months via inhalation were significantly increased, based on significant trend tests and significantly elevated frequencies of micronucleated erythrocytes at the highest exposure concentration (Table E-2). Using flow cytometry, approximately 1 million erythrocytes were scored per animal for the presence of micronuclei, making this a highly sensitive method of scoring and allowing small increases in the endpoint to be detected. In mice, the micronucleus response in the reticulocyte population, indicative of damage induced in the bone marrow within the last 48 hours prior to sampling, was slightly increased with increasing exposure concentration, but the increase was not statistically significant. However, the trend toward increased frequencies of micronucleated reticulocytes in the mice is supportive of the observations in the mature erythrocyte population. In addition, significant increases in the percent reticulocytes were seen in both male and female mice, suggesting a stimulation of erythropoiesis in mice exposed to antimony trioxide. It should be noted that stimulation of erythropoiesis may, in some instances, result in elevated levels of micronucleated red blood cells due to an increase in mitotic errors associated with rapid cell division, although in in vivo micronucleus studies conducted by the National Toxicology Program, no consistent association between increases in percent reticulocytes and increases in micronuclei has been observed.

In addition to evaluating the potential for chromosomal damage, manifested as micronuclei resulting from exposure to antimony trioxide, the potential for DNA damage was assessed using the comet assay in the same animals in which micronucleus induction was evaluated. DNA damage was assessed in blood leukocytes and lung tissue samples. No increases in DNA damage were seen in blood leukocytes or lung cell samples in male or female Wistar Han rats exposed to antimony trioxide (Table E-3). In male and female B6C3F1/N mice, significant increases in DNA damage, measured as percent tail DNA, were seen in lung tissue samples; no increases in percent tail DNA were observed in leukocytes (Table E-4).

In summary, exposure to antimony trioxide for 12 months by inhalation resulted in increases in micronucleated erythrocytes and lung cell DNA damage in male and female mice, but not in male or female rats.

Table E-1. Frequency of Micronuclei in Peripheral Blood Erythrocytes of Rats Following Treatment with Antimony Trioxide by Inhalation for 12 Months[a]

Concentration (mg/m^3)	Number of Rats with Erythrocytes Scored	Micronucleated PCEs/1,000 PCEs[b]	P Value[c]	Micronucleated NCEs/1,000 NCEs[b]	P Value[c]	PCEs[b] (%)	P Value[c]
Male							
Air[d]	5	0.98 ± 0.08		0.04 ± 0.01		0.632 ± 0.05	
3	5	0.81 ± 0.10	0.6885	0.06 ± 0.01	0.2690	0.702 ± 0.06	0.8511
10	5	1.11 ± 0.15	0.5738	0.06 ± 0.01	0.3234	0.651 ± 0.03	0.9499
30	5	0.86 ± 0.14	0.6068	0.05 ± 0.02	0.3447	0.588 ± 0.05	0.6547
		P = 0.642[e]		P = 0.467		P = 0.227	
Female							
Air	5	1.50 ± 0.37		0.05 ± 0.01		0.878 ± 0.21	
3	5	1.15 ± 0.33	0.8909	0.03 ± 0.00	0.9471	0.895 ± 0.11	1.0000
10	5	0.66 ± 0.08	0.9416	0.04 ± 0.01	0.9771	0.747 ± 0.06	0.9122
30	5	0.80 ± 0.15	0.9567	0.03 ± 0.00	0.9843	0.779 ± 0.13	0.9228
		P = 0.936		P = 0.892		P = 0.573	

[a]Study was performed at ILS, Inc. The detailed protocol is presented by Torous et al.[94] and Witt et al.[95]. NCE = normochromatic erythrocyte; PCE = polychromatic erythrocyte.
[b]Mean ± standard error.
[c]Pairwise comparison with the chamber control group; exposed group values are significant at $P \leq 0.025$ by Williams' test.
[d]Chamber control.
[e]Exposure concentration-related trend; significant at $P \leq 0.025$ by linear regression.

Table E-2. Frequency of Micronuclei in Peripheral Blood Erythrocytes of Mice Following Treatment with Antimony Trioxide by Inhalation for 12 Months[a]

Concentration (mg/m^3)	Number of Mice with Erythrocytes Scored	Micronucleated PCEs/1,000 PCEs[b]	P Value[c]	Micronucleated NCEs/1,000 NCEs[b]	P Value[c]	PCEs[b] (%)	P Value[d]
Male							
Air[e]	5	2.53 ± 0.14		1.55 ± 0.05		1.458 ± 0.07	
3	5	2.37 ± 0.13	0.6223	1.59 ± 0.03	0.3054	1.504 ± 0.09	0.8622
10	5	2.87 ± 0.23	0.1622	1.66 ± 0.02	0.1198	2.247 ± 0.34	0.0273
30	5	2.78 ± 0.21	0.1731	1.93 ± 0.10	0.0002	3.544 ± 0.57	0.0001
		P = 0.100[f]		P = 0.100[f]		P = 0.100[f]	
Female							
Air	5	2.17 ± 0.19		1.04 ± 0.02		1.131 ± 0.22	
3	5	1.77 ± 0.14	0.8408	1.08 ± 0.01	0.2750	1.215 ± 0.06	1.0000
10	5	2.21 ± 0.06	0.4985	1.13 ± 0.05	0.1462	1.398 ± 0.13	1.0000
30	5	2.38 ± 0.13	0.1931	1.38 ± 0.09	0.0002	2.660 ± 0.34	0.0069
		P < 0.001[f]		P < 0.001[f]		P = 0.001[g]	

[a]Study was performed at ILS, Inc. The detailed protocol is presented by Torous et al.94 and Witt et al.95. NCE = normochromatic erythrocyte; PCE = polychromatic erythrocyte.
[b]Mean ± standard error.
[c]Pairwise comparison with the chamber control group; exposed group values are significant at $P \leq 0.025$ by Williams' test.
[d]Pairwise comparison with the chamber control group; exposed group values are significant at $P \leq 0.025$ by Williams' (males) or Dunn's (females) test.
[e]Chamber control.
[f]Exposure concentration-related trend; significant at $P \leq 0.025$ by linear regression.
[g]Exposure concentration-related trend; significant at $P \leq 0.025$ by Jonckheere's test.

Table E-3. DNA Damage in the Blood and Lung of Rats Following Treatment with Antimony Trioxide by Inhalation for 12 Months[a]

	Dose (mg/m^3)	Number of Rats	Percent Tail DNA[b]	P Value[c]
Male				
Blood				
Air[d]	0	5	5.4 ± 1.04	
Antimony trioxide	3	5	7.9 ± 1.05	0.0476
	10	5	6.0 ± 1.23	0.4206
	30	5	4.5 ± 0.72	0.6548
			P = 0.4194[e]	
Lung				
Air	0	5	31.0 ± 2.32	
Antimony trioxide	3	5	34.7 ± 2.42	0.1518
	10	5	25.8 ± 2.61	0.9142
	30	5	29.3 ± 1.00	0.7412
			P = 0.6636	
Female				
Blood				
Air	0	5	2.5 ± 0.51	
Antimony trioxide	3	5	1.7 ± 0.14	0.9047
	10	5	3.3 ± 1.08	0.2575
	30	5	2.2 ± 0.34	0.6689
			P = 0.9566	
Lung				
Air	0	5	32.2 ± 1.20	
Antimony trioxide	3	5	30.1 ± 1.28	0.8753
	10	5	28.9 ± 4.03	0.7653
	30	5	29.2 ± 3.03	0.8116
			P = 0.4813	

[a]Study was performed at ILS, Inc. The detailed protocol is presented by Recio et al.[99].
[b]Mean ± standard error.
[c]Pairwise comparison with the chamber control group; exposed group values are significant at $P \leq 0.008$ by Student's t-test, except male blood by the Mann-Whitney test.
[d]Chamber control.
[e]Exposure concentration-related trend; significant at $P \leq 0.025$ by linear regression, except male blood by the Kendall Rank Correlation test.

Table E-4. DNA Damage in the Blood and Lung of Mice Following Treatment with Antimony Trioxide by Inhalation for 12 Months[a]

	Dose (mg/m^3)	Number of Mice	Percent Tail DNA[b]	P Value[c]
Male				
Blood				
Air[d]	0	5	3.3 ± 0.74	
Antimony trioxide	3	5	3.6 ± 0.27	0.3888
	10	5	3.0 ± 0.41	0.6526
	30	5	4.1 ± 1.24	0.3065
			P = 0.4538[e]	
Lung				
Air	0	5	25.6 ± 0.78	
Antimony trioxide	3	5	33.7 ± 2.62	0.0165
	10	5	33.5 ± 2.02	0.0033
	30	5	37.5 ± 2.28	0.0005
			P = 0.0076	
Female				
Blood				
Air	0	5	3.5 ± 0.68	
Antimony trioxide	3	5	3.8 ± 0.40	0.3735
	10	5	2.5 ± 0.20	0.8953
	30	5	2.4 ± 0.28	0.9139
			P = 0.9566	
Lung				
Air	0	5	32.8 ± 1.11	
Antimony trioxide	3	5	35.8 ± 2.09	0.1181
	10	5	36.4 ± 2.65	0.1220
	30	5	45.5 ± 2.32	0.0006
			P = 0.0002	

[a]Study was performed at ILS, Inc. The detailed protocol is presented by Recio et al.[99].
[b]Mean ± standard error.
[c]Pairwise comparison with the chamber control group; exposed group values are significant at $P \leq 0.008$ by Student's t-test.
[d]Chamber control.
[e]Exposure concentration-related trend; significant at $P \leq 0.025$ by linear regression.

Appendix F. Organ Weights and Organ-Weight-To-Body-Weight Ratios

Tables

Table F-1. Organ Weights and Organ-Weight-to-Body-Weight Ratios for Rats in the Two-week Inhalation Study of Antimony Trioxide F-2
Table F-2. Organ Weights and Organ-Weight-to-Body-Weight Ratios for Rats at the 12-month Interim Evaluation in the Two-year Inhalation Study of Antimony Trioxide F-4
Table F-3. Organ Weights and Organ-Weight-to-Body-Weight Ratios for Mice in the Two-week Inhalation Study of Antimony Trioxide F-5
Table F-4. Organ Weights and Organ-Weight-to-Body-Weight Ratios for Mice at the 12-month Interim Evaluation in the Two-year Inhalation Study of Antimony Trioxide F-7

Table F-1. Organ Weights and Organ-Weight-to-Body-Weight Ratios for Rats in the Two-week Inhalation Study of Antimony Trioxide[a]

	Chamber Control	3.75 mg/m^3	7.5 mg/m^3	15 mg/m^3	30 mg/m^3	60 mg/m^3
n	5	5	5	5	5	5
Male						
Necropsy body wt.	227 ± 6	217 ± 5	226 ± 5	220 ± 5	210 ± 7	224 ± 9
Heart						
Absolute	0.91 ± 0.03	0.85 ± 0.04	0.87 ± 0.02	0.87 ± 0.02	0.83 ± 0.03	0.85 ± 0.02
Relative	4.033 ± 0.157	3.910 ± 0.123	3.848 ± 0.092	3.975 ± 0.113	3.982 ± 0.109	3.790 ± 0.079
R. Kidney						
Absolute	0.99 ± 0.04	0.94 ± 0.03	0.99 ± 0.04	0.96 ± 0.04	0.91 ± 0.03	0.98 ± 0.04
Relative	4.370 ± 0.142	4.338 ± 0.054	4.406 ± 0.199	4.357 ± 0.139	4.362 ± 0.090	4.368 ± 0.039
Liver						
Absolute	10.05 ± 0.25	8.53 ± 0.32	8.84 ± 0.39	8.55 ± 0.47	8.56 ± 0.56	9.40 ± 0.41
Relative	44.330 ± 1.402	39.406 ± 1.436	39.133 ± 1.363*	38.715 ± 1.306*	40.698 ± 1.534	41.859 ± 0.728
Lung						
Absolute	1.99 ± 0.11	1.93 ± 0.14	2.04 ± 0.15	2.08 ± 0.12	2.28 ± 0.19	2.56 ± 0.10**
Relative	8.758 ± 0.530	8.919 ± 0.592	9.038 ± 0.609	9.416 ± 0.402	10.871 ± 0.806*	11.423 ± 0.351**
R. Testis						
Absolute	1.465 ± 0.034	1.312 ± 0.056	1.420 ± 0.045	1.404 ± 0.052	1.293 ± 0.047	1.443 ± 0.078
Relative	6.458 ± 0.157	6.051 ± 0.184	6.287 ± 0.124	6.382 ± 0.239	6.195 ± 0.294	6.436 ± 0.267
Thymus						
Absolute	0.759 ± 0.068	0.698 ± 0.030	0.896 ± 0.075	0.731 ± 0.053	0.739 ± 0.029	0.792 ± 0.044
Relative	3.346 ± 0.303	3.236 ± 0.176	3.953 ± 0.287	3.308 ± 0.178	3.525 ± 0.066	3.559 ± 0.290

	Chamber Control	3.75 mg/m^3	7.5 mg/m^3	15 mg/m^3	30 mg/m^3	60 mg/m^3
Female						
Necropsy body wt.	158 ± 3	160 ± 3	160 ± 3	156 ± 5	156 ± 1	158 ± 7
Heart						
Absolute	0.67 ± 0.02	0.64 ± 0.03	0.66 ± 0.01	0.63 ± 0.02	0.67 ± 0.02	0.64 ± 0.03
Relative	4.226 ± 0.072	4.007 ± 0.108	4.115 ± 0.149	4.045 ± 0.069	4.308 ± 0.110	4.064 ± 0.106
R. Kidney						
Absolute	0.72 ± 0.02	0.67 ± 0.03	0.72 ± 0.02	0.67 ± 0.02	0.70 ± 0.03	0.75 ± 0.03
Relative	4.545 ± 0.061	4.194 ± 0.099	4.544 ± 0.211	4.299 ± 0.064	4.501 ± 0.207	4.803 ± 0.155
Liver						
Absolute	5.96 ± 0.14	5.62 ± 0.32	5.96 ± 0.23	5.68 ± 0.21	5.78 ± 0.15	5.93 ± 0.31
Relative	37.850 ± 0.518	35.041 ± 1.537	37.401 ± 2.077	36.303 ± 0.606	37.070 ± 0.918	37.602 ± 0.881
Lung						
Absolute	1.39 ± 0.09	1.33 ± 0.08	1.52 ± 0.15	1.51 ± 0.11	1.70 ± 0.07*	1.71 ± 0.10*
Relative	8.849 ± 0.511	8.320 ± 0.391	9.508 ± 0.927	9.626 ± 0.445	10.911 ± 0.385*	10.865 ± 0.388*
Thymus						
Absolute	0.614 ± 0.040	0.570 ± 0.027	0.619 ± 0.056	0.567 ± 0.037	0.588 ± 0.019	0.633 ± 0.056
Relative	3.909 ± 0.286	3.555 ± 0.116	3.889 ± 0.391	3.615 ± 0.144	3.774 ± 0.121	3.995 ± 0.212

*Significantly different ($P \leq 0.05$) from the chamber control group by Williams' or Dunnett's test.
**$P \leq 0.01$.
[a]Organ weights (absolute weights) and body weights are given in grams; organ-weight-to-body-weight ratios (relative weights) are given as mg organ weight/g body weight (mean ± standard error).

Table F-2. Organ Weights and Organ-Weight-to-Body-Weight Ratios for Rats at the 12-month Interim Evaluation in the Two-year Inhalation Study of Antimony Trioxide[a]

	Chamber Control	3 mg/m^3	10 mg/m^3	30 mg/m^3
n	10	10	10	10
Male				
Necropsy body wt.	522 ± 16	531 ± 17	540 ± 20	534 ± 13
Heart				
Absolute	1.21 ± 0.05	1.24 ± 0.04	1.21 ± 0.02	1.29 ± 0.05
Relative	2.321 ± 0.053	2.337 ± 0.077	2.252 ± 0.073	2.410 ± 0.070
R. Kidney				
Absolute	1.42 ± 0.04	1.39 ± 0.05	1.49 ± 0.05	1.46 ± 0.03
Relative	2.724 ± 0.080	2.623 ± 0.073	2.769 ± 0.105	2.746 ± 0.062
Liver				
Absolute	14.08 ± 0.64	14.78 ± 0.43	15.81 ± 0.61	15.75 ± 0.70
Relative	26.908 ± 0.582	27.910 ± 0.458	29.294 ± 0.508*	29.452 ± 0.886**
Lung				
Absolute	2.79 ± 0.18	3.65 ± 0.19*	4.32 ± 0.28**	6.57 ± 0.29**
Relative	5.368 ± 0.326	6.897 ± 0.312*	8.040 ± 0.490**	12.313 ± 0.484**
R. Testis				
Absolute	1.854 ± 0.113	1.628 ± 0.177	1.917 ± 0.055	1.958 ± 0.055
Relative	3.559 ± 0.198	3.071 ± 0.329	3.592 ± 0.173	3.683 ± 0.113
Thymus				
Absolute	0.474 ± 0.037	0.512 ± 0.025	0.508 ± 0.028	0.477 ± 0.020
Relative	0.906 ± 0.057	0.977 ± 0.063	0.946 ± 0.054	0.896 ± 0.038
Female				
Necropsy body wt.	278 ± 10	293 ± 11	272 ± 7	278 ± 6
Heart				
Absolute	0.82 ± 0.03	0.86 ± 0.03	0.82 ± 0.02	0.85 ± 0.03
Relative	2.957 ± 0.075	2.956 ± 0.076	3.030 ± 0.054	3.052 ± 0.037
R. Kidney				
Absolute	0.91 ± 0.02	0.96 ± 0.02	0.92 ± 0.03	0.93 ± 0.03
Relative	3.309 ± 0.104	3.294 ± 0.119	3.381 ± 0.078	3.342 ± 0.058
Liver				
Absolute	7.61 ± 0.19	8.54 ± 0.35	7.97 ± 0.41	7.81 ± 0.25
Relative	27.588 ± 0.781	29.218 ± 0.728	29.201 ± 1.044	28.087 ± 0.629
Lung				
Absolute	1.78 ± 0.09	2.89 ± 0.16**	4.20 ± 0.22**	5.48 ± 0.28**
Relative	6.451 ± 0.335	9.898 ± 0.448**	15.528 ± 0.975**	19.719 ± 0.901**
Thymus				
Absolute	0.346 ± 0.025	0.348 ± 0.024	0.343 ± 0.018	0.346 ± 0.017
Relative	1.246 ± 0.074	1.184 ± 0.057	1.264 ± 0.071	1.245 ± 0.056

*Significantly different ($P \leq 0.05$) from the chamber control group by Williams' test.
**$P \leq 0.01$.
[a]Organ weights (absolute weights) and body weights are given in grams; organ-weight-to-body-weight ratios (relative weights) are given as mg organ weight/g body weight (mean ± standard error).

Table F-3. Organ Weights and Organ-Weight-to-Body-Weight Ratios for Mice in the Two-week Inhalation Study of Antimony Trioxide[a]

	Chamber Control	3.75 mg/m^3	7.5 mg/m^3	15 mg/m^3	30 mg/m^3	60 mg/m^3
n	5	5	5	5	5	5
Male						
Necropsy body wt.	25.0 ± 0.2	25.3 ± 0.1	26.4 ± 0.5	25.9 ± 0.6	25.5 ± 0.6	26.6 ± 0.8
Heart						
Absolute	0.12 ± 0.00	0.13 ± 0.00	0.13 ± 0.01	0.13 ± 0.01	0.12 ± 0.01	0.12 ± 0.00
Relative	4.796 ± 0.114	4.973 ± 0.162	4.838 ± 0.141	4.999 ± 0.176	4.704 ± 0.137	4.598 ± 0.143
R. Kidney						
Absolute	0.21 ± 0.01	0.23 ± 0.00	0.23 ± 0.01	0.24 ± 0.02	0.21 ± 0.01	0.23 ± 0.01
Relative	8.390 ± 0.169	8.999 ± 0.093	8.849 ± 0.181	9.071 ± 0.397	8.315 ± 0.153	8.653 ± 0.259
Liver						
Absolute	1.20 ± 0.04	1.12 ± 0.03	1.19 ± 0.05	1.21 ± 0.08	1.11 ± 0.06	1.16 ± 0.03
Relative	47.938 ± 1.448	44.364 ± 1.189	45.125 ± 1.498	46.366 ± 2.182	43.536 ± 1.251	43.723 ± 1.222
Lung						
Absolute	0.17 ± 0.01	0.21 ± 0.02	0.22 ± 0.01*	0.21 ± 0.01*	0.21 ± 0.01*	0.23 ± 0.01**
Relative	6.939 ± 0.267	8.086 ± 0.835	8.184 ± 0.443	8.076 ± 0.321	8.147 ± 0.232	8.725 ± 0.209**
R. Testis						
Absolute	0.096 ± 0.002	0.094 ± 0.002	0.094 ± 0.002	0.096 ± 0.005	0.091 ± 0.003	0.099 ± 0.002
Relative	3.827 ± 0.066	3.709 ± 0.068	3.574 ± 0.145	3.714 ± 0.204	3.572 ± 0.145	3.733 ± 0.084
Thymus						
Absolute	0.040 ± 0.004	0.045 ± 0.004	0.049 ± 0.004	0.046 ± 0.004	0.048 ± 0.005	0.052 ± 0.004
Relative	1.589 ± 0.143	1.768 ± 0.155	1.844 ± 0.159	1.772 ± 0.156	1.882 ± 0.208	1.948 ± 0.131
Female						
Necropsy body wt.	21.2 ± 0.3	20.9 ± 0.2	20.6 ± 0.4	20.9 ± 0.2	21.0 ± 0.3	21.1 ± 0.4
Heart						

	Chamber Control	3.75 mg/m^3	7.5 mg/m^3	15 mg/m^3	30 mg/m^3	60 mg/m^3
Absolute	0.11 ± 0.00	0.11 ± 0.00	0.11 ± 0.00	0.12 ± 0.00	0.11 ± 0.00	0.11 ± 0.00
Relative	5.187 ± 0.103	5.369 ± 0.072	5.363 ± 0.219	5.645 ± 0.199	5.235 ± 0.146	5.216 ± 0.101
R. Kidney						
Absolute	0.16 ± 0.01	0.16 ± 0.00	0.16 ± 0.00	0.16 ± 0.00	0.17 ± 0.00	0.16 ± 0.00
Relative	7.455 ± 0.264	7.579 ± 0.200	7.800 ± 0.316	7.656 ± 0.217	7.901 ± 0.118	7.776 ± 0.178
Liver						
Absolute	1.00 ± 0.04	0.93 ± 0.03	0.93 ± 0.03	1.02 ± 0.02	0.99 ± 0.02	1.03 ± 0.03
Relative	46.932 ± 1.037	44.760 ± 1.054	45.306 ± 0.747	48.750 ± 0.409	47.003 ± 0.565	48.841 ± 0.663
Lung						
Absolute	0.16 ± 0.00	0.18 ± 0.01	0.18 ± 0.00	0.20 ± 0.01**	0.20 ± 0.01**	0.22 ± 0.01**
Relative	7.656 ± 0.185	8.736 ± 0.336*	8.734 ± 0.131*	9.546 ± 0.308**	9.659 ± 0.229**	10.320 ± 0.397**
Thymus						
Absolute	0.074 ± 0.002	0.071 ± 0.002	0.067 ± 0.003	0.067 ± 0.005	0.072 ± 0.005	0.075 ± 0.003
Relative	3.481 ± 0.083	3.412 ± 0.093	3.257 ± 0.099	3.194 ± 0.261	3.410 ± 0.226	3.558 ± 0.117

*Significantly different ($P \leq 0.05$) from the chamber control group by Williams' test.
**$P \leq 0.01$.
[a]Organ weights (absolute weights) and body weights are given in grams; organ-weight-to-body-weight ratios (relative weights) are given as mg organ weight/g body weight (mean ± standard error).

Table F-4. Organ Weights and Organ-Weight-to-Body-Weight Ratios for Mice at the 12-month Interim Evaluation in the Two-year Inhalation Study of Antimony Trioxide[a]

	Chamber Control	3 mg/m^3	10 mg/m^3	30 mg/m^3
n	10	10	10	10
Male				
Necropsy body wt.	51.4 ± 0.3	51.3 ± 0.9	51.5 ± 0.6	51.9 ± 0.8
Heart				
Absolute	0.21 ± 0.01	0.21 ± 0.00	0.22 ± 0.01	0.23 ± 0.01
Relative	4.161 ± 0.108	4.077 ± 0.079	4.197 ± 0.130	4.474 ± 0.153
R. Kidney				
Absolute	0.42 ± 0.01	0.41 ± 0.01	0.41 ± 0.01	0.42 ± 0.01
Relative	8.068 ± 0.188	7.913 ± 0.232	7.946 ± 0.244	8.095 ± 0.196
Liver				
Absolute	2.51 ± 0.19	2.29 ± 0.10	2.51 ± 0.25	2.70 ± 0.25
Relative	48.720 ± 3.637	44.824 ± 2.426	48.812 ± 5.098	52.084 ± 4.884
Lung				
Absolute	0.24 ± 0.01	0.33 ± 0.01**	0.46 ± 0.01**	0.66 ± 0.04**
Relative	4.703 ± 0.113	6.396 ± 0.131*	8.862 ± 0.289**	12.857 ± 0.855**
R. Testis				
Absolute	0.120 ± 0.002	0.120 ± 0.002	0.119 ± 0.001	0.120 ± 0.002
Relative	2.332 ± 0.035	2.332 ± 0.051	2.314 ± 0.022	2.309 ± 0.037
Thymus				
Absolute	0.114 ± 0.005	0.126 ± 0.006	0.147 ± 0.008**	0.173 ± 0.011**
Relative	2.219 ± 0.102	2.450 ± 0.091	2.840 ± 0.151**	3.317 ± 0.170**
Female				
Necropsy body wt.	47.3 ± 2.1	55.4 ± 1.7*	50.5 ± 2.1	49.8 ± 1.7
Heart				
Absolute	0.17 ± 0.00	0.17 ± 0.00	0.17 ± 0.00	0.19 ± 0.01**
Relative	3.552 ± 0.129	3.120 ± 0.062*	3.423 ± 0.120	3.770 ± 0.119
R. Kidney				
Absolute	0.24 ± 0.01	0.25 ± 0.01	0.25 ± 0.01	0.25 ± 0.01
Relative	5.060 ± 0.223	4.485 ± 0.133	4.913 ± 0.219	4.998 ± 0.242
Liver				
Absolute	1.73 ± 0.07	1.91 ± 0.06	1.83 ± 0.06	1.94 ± 0.06*
Relative	36.653 ± 0.588	34.465 ± 0.634	36.531 ± 1.129	39.158 ± 1.118
Lung				
Absolute	0.23 ± 0.01	0.33 ± 0.01**	0.42 ± 0.02**	0.79 ± 0.03**
Relative	4.799 ± 0.126	5.913 ± 0.169	8.331 ± 0.320**	16.000 ± 0.857**
Thymus				
Absolute	0.080 ± 0.005	0.116 ± 0.009*	0.112 ± 0.012*	0.129 ± 0.010**
Relative	1.681 ± 0.062	2.069 ± 0.126	2.216 ± 0.232*	2.554 ± 0.127**

*Significantly different ($P \leq 0.05$) from the chamber control group by Williams' or Dunnett's test.
**$P \leq 0.01$.
[a]Organ weights (absolute weights) and body weights are given in grams; organ-weight-to-body-weight ratios (relative weights) are given as mg organ weight/g body weight (mean ± standard error).

Appendix G. Tissue Burden Results

Table of Contents

G.1. Blood and Lung Deposition and Clearance Equations Used in the Two-week Inhalation Studies of Antimony Trioxide G-3

G.2. Lung Deposition and Clearance Equations Used in the Two-year Inhalation Studies of Antimony Trioxide G-3

G.3. Lung Overload Evaluation Used in the Two-year Inhalation Studies of Antimony Trioxide G-4

Tables

Table G-1. Lung Weights, Antimony Concentrations and Burdens, and Antimony Trioxide Burdens for Rats in the Two-week Inhalation Study of Antimony Trioxide G-8

Table G-2. Lung Deposition and Clearance Parameter Estimates for Female Rats in the Two-week Inhalation Study of Antimony Trioxide G-10

Table G-3. Lung Weights, Antimony Concentrations and Burdens, and Antimony Trioxide Burdens for Female Rats in the Two-year Inhalation Study of Antimony Trioxide G-11

Table G-4. Lung Deposition and Clearance Parameter Estimates for Female Rats in the Two-year Inhalation Study of Antimony Trioxide G-13

Table G-5. Lung Burden Overload Parameter Estimates for Female Rats in the Two-year Inhalation Study of Antimony Trioxide G-13

Table G-6. Lung Weights, Antimony Concentrations and Burdens, and Antimony Trioxide Burdens for Mice in the Two-week Inhalation Study of Antimony Trioxide G-14

Table G-7. Blood and Lung Deposition and Clearance Parameter Estimates for Female Mice in the Two-week Inhalation Study of Antimony Trioxide G-16

Table G-8. Lung Weights, Antimony Concentrations and Burdens, and Antimony Trioxide Burdens for Female Mice in the Two-year Inhalation Study of Antimony Trioxide G-17

Table G-9. Retained Lung Antimony Trioxide Burden Volumes and Surface Areas in Female Mice in the Two-year Inhalation Study of Antimony Trioxide G-19

Figures

Figure G-1. Lung Antimony Trioxide Burdens in 3, 10, and 30 mg/m^3 Female Rats in the Two-year Inhalation Study of Antimony Trioxide G-20

Figure G-2. Lung Antimony Trioxide Burdens in 3 mg/m^3 Female Mice in the Two-year Inhalation Study of Antimony Trioxide Including All Time Points (Top) and with Day 551 Data Removed (Bottom) G-21

Figure G-3. Lung Antimony Trioxide Burdens in 10 mg/m^3 Female Mice in the Two-year Inhalation Study of Antimony Trioxide Including All Time Points (Top) and with Day 551 Data Removed (Bottom) G-22

Figure G-4. Lung Antimony Trioxide Burdens in 30 mg/m^3 Female Mice in the Two-year Inhalation Study of Antimony Trioxide Including All Time Points (Top) and with Day 551 Data Removed (Bottom)..... G-23

G.1. Blood and Lung Deposition and Clearance Equations Used in the Two-week Inhalation Studies of Antimony Trioxide

Lung and blood clearance rates were calculated using Equation (1):

Equation (1): $A_{(t)} = A_o(e^{-kt})$

where, $A_{(t)}$ is the lung burden (μg Sb_2O_3/lung) or blood concentration (μg Sb/g) at time t (t = 4 weeks postexposure), A_o is the lung burden or blood concentration at terminal sacrifice (0 days postexposure), and k is the lung or blood clearance rate constant [fraction cleared per day (day^{-1})].

Lung and blood clearance half-lives in days ($t_{½}$) were calculated from Equation (2), where ln 2 is the Naperian logarithm of 2:

Equation (2): $t_{½} = \ln 2/k$

Deposition rates were calculated from lung burdens using Equation (3). The lung antimony trioxide burden at terminal sacrifice and the calculated lung clearance rate constant were used to solve for the deposition rate, α (μg Sb_2O_3/day).

Equation (3):$A_{(t)} = \alpha/k(1 - e^{-kt})$

In Equation (3), $A_{(t)}$ is the lung burden at time t [t = 16 (rats) or 17 (mice) days on study]; α is the antimony trioxide deposition rate; and k is the first-order clearance rate constant derived from Equation (1). Steady-state or equilibrium lung burdens A_e (μg Sb_2O_3/lung) were calculated according to Equation (4):

Equation (4): $A_e = \alpha/k$

G.2. Lung Deposition and Clearance Equations Used in the Two-year Inhalation Studies of Antimony Trioxide

The lung burden model used for these studies assumed a zero-order (constant) deposition rate and a first-order (with respect to lung burden) clearance rate as shown in Equation (5):

Equation (5): $L_{(t)} = (D/k)(1 - e^{-kt})$

In Equation (5), $L_{(t)}$ is the retained antimony trioxide lung burden (μg Sb_2O_3/lung) at any time t (days on study); D represents the deposition rate (μg Sb_2O_3/lung per day); and k is the lung clearance rate constant ($days^{-1}$). The equation also contains a boundary condition that at t = 0, the mass of antimony trioxide in the lung is zero.

This model was fit to the antimony trioxide lung burden data collected during the in-life part of the chronic studies. The model was fit to the individual animal data from each exposure group using KaleidaGraph (Synergy Software, Reading, PA). All results are presented from model fits using 1/variance weighting.

The model did not fit the mouse data well; when all the data were included the model would not calculate meaningful deposition and clearance parameters. Accordingly, the mouse data were

remodeled excluding the day 551 data, but the model still fit the data poorly and thus no calculated deposition and clearance parameter estimates are provided for the mouse study.

For the rat study, the model fits provided direct estimates of D and k along with their standard errors for each exposure group. Parameters estimated by the model fit were used to calculate additional quantities for each exposure group along with their standard errors using propagation of error techniques and Equations (6) and (7):

Equation (6): $t_{1/2} = \ln 2/k$

Equation (7): $L_{SS} = D/k$

In Equations (6) and (7), $t_{1/2}$ is the clearance half-life in days; ln 2 is the Naperian logarithm of 2; and L_{SS} is the predicted steady-state lung burden (µg Sb_2O_3/lung).

The deposition efficiency (%E) was calculated for each exposure group as defined in Equation (8):

Equation (8): $\%E = [D/(0.33C \times 360)] \times 100\%$

In Equation (8), D is the deposition rate (µg Sb_2O_3/lung per day) determined from the model fit; 0.33 is the minute volume of a mature Sprague Dawley rat[73] in L/minute; C is the exposure concentration (µg Sb_2O_3/L); and 360 is the exposure duration in minutes/day. Because their minute volumes are expected to be similar, the minute volume for Sprague Dawley rats was used in the calculations, even though Wistar Han rats were used for the current tissue burden study.

The total lung dose (in mg Sb_2O_3/lung) administered to each exposed group was calculated as defined in Equation (9):

Equation (9): $\text{Total dose} = 551 \times D/1{,}000$

In Equation (9), 551 is the total number of study days for tissue burden study rats; D is the deposition rate; and dividing by 1,000 converts from µg to mg. Also calculated for each exposure group was the total amount of antimony trioxide cleared from the lungs during the study, which was the difference between the calculated dose (in mg Sb_2O_3/lung) and the calculated lung burden (in mg Sb_2O_3/lung) on study day 551. This was expressed as both an absolute value and as a percentage relative to the total dose.

G.3. Lung Overload Evaluation Used in the Two-year Inhalation Studies of Antimony Trioxide

Lung overload refers to the situation in which respirable, relatively insoluble particles are deposited in the lungs at a rate in excess of the rate at which the alveolar macrophages (AM) can clear the particles from the lung[74; 75; 105; 106]. Morrow[74] proposed a mechanism by which such overload may occur. Based on empirical observation, when the volume of particulate material in the lung reaches approximately 6% of the total volume available in the lung AM pool, the mobility of the AM begins to become compromised and lung clearance of deposited particulate material slows. This is a progressive process; as more particulate material is deposited in the lung, the lung AM become increasingly engorged with particles, and AM mediated clearance becomes increasingly slower up to the point where the volume of particulate material in the lung

reaches approximately 60% of the total volume available in the AM pool. At this point, AM mediated particle clearance essentially ceases. As clearance slows, the particle burden in the lung continues to increase with increased exposure. Thus, very long lung clearance half-lives and dramatically increased lung burdens are hallmarks of lung overload.

Data on the macrophage pool volume in F344 rat lungs have been reported[74; 107; 108] based on experimental observations, and similar data have been reported by other investigators using different strains of rat[109; 110]. Morrow[74] estimated the AM pool in the F344 rat lung is approximately 2.5×10^7 cells, each with a volume of around 1,000 μm^3/AM. Taking 6% of this volume as 60 μm^3 and multiplying by the number of cells in the rat lung AM pool, the lung burden volume at which overload begins to occur is 1.5×10^9 μm^3. The lung burden volume at which clearance ceases is 10 times greater (600 μm^3/AM) or 1.5×10^{10} μm^3. As pointed out by Morrow[74], for a particulate material with a density of 1.0 g/cm^3 the volume of 1.5×10^9 μm^3 (onset of overload) corresponds to a lung burden of approximately 1.5 mg/lung. Ten times this amount would be a lung burden of 15 mg/lung and would correspond to the condition when the volume of the lung burden is 60% of the available volume in the AM pool (clearance ceases). As burdens increase from 1.5 to 15 mg, particle clearance is expected to become progressively slower.

However, it is noteworthy that the amounts of 1.5 and 15 mg given above apply only to a material of unit density. Because the antimony trioxide used in these studies has a density of 5.47 g/cm^3 the test chemical occupies a smaller volume per unit mass than a material of unit density. Additionally, the above hypothesis is based on the macrophage population in the lungs of F344 rats. Masse et al.[109] estimated that the AM population in 300 g Sprague Dawley rats is approximately 3.0×10^7 cells. Thus, the above calculations can be made more specific to the test systems in this study by using the AM volume for the Sprague Dawley rat, which is similar to the Wistar Han, and accounting for the density of antimony trioxide. Assuming a pool of 3.0×10^7 cells, each with a volume of 1,000 μm^3/cell, gives a total AM pool volume of 3.0×10^{10} μm^3. Using 6% of this the total AM volume gives a volume for onset of overload of 1.8×10^9 μm^3. Given an antimony trioxide density of 5,470 mg/cm^3, this would correspond to 9.8 mg of antimony trioxide in the lungs. Similarly 60% of the AM pool volume (where lung clearance ceases) would be 1.8×10^{10} μm^3 and would correspond to an antimony trioxide lung burden of 98 mg.

No literature values for AM populations in mouse lungs were found. The AM population in B6C3F1 mice was estimated to be approximately 4.0×10^6 cells. This value was calculated by multiplying the Sprague Dawley rat AM population by the mean lung weight ratio of B6C3F1 mice to Wistar Han rats from chamber control animals from the 18-month time point in the 2-year antimony trioxide studies. Wistar Han rats were assumed to have a similar AM population as Sprague Dawley rats. Thus, the above calculations can be made more specific to the test systems in this study by using the estimated AM volume for the B6C3F1 mouse and accounting for the density of antimony trioxide. Assuming a pool of 4.0×10^6 cells, each with a volume of 1,000 μm^3/cell, gives a total AM pool volume of 4.0×10^9 μm^3. Using 6% of the total AM volume gives a volume for onset of overload of 2.4×10^8 μm^3. Given an antimony trioxide density of 5,470 mg/cm^3, this would correspond to 1.3 mg of antimony trioxide in the lungs. Similarly 60% of the AM pool volume (where lung clearance ceases) would be 2.4×10^9 μm^3 and would correspond to an antimony trioxide lung burden of 13 mg.

As described above a model was fit to the antimony trioxide lung burden data to estimate the deposition and clearance rates of antimony trioxide during the current study. This model was employed to calculate retained lung burdens over the course of the study. In rats, these calculated lung burdens were converted to an equivalent volume of antimony trioxide and compared to the threshold volume required to reach overload. In mice, the mean measured lung burden values at each collection time point were converted to an equivalent volume of antimony trioxide and compared to the threshold volume required to reach overload.

Lung burdens in these tissue burden studies did not achieve steady state, as evidenced by very high lung burdens in both rats and mice by the end of the studies. These results indicated the possibility that lung overload may have occurred in some of the exposed groups, and additional calculations were undertaken to evaluate this possibility. In this evaluation, lung burdens of antimony trioxide at each collection time point were converted to equivalent volumes and surface areas of antimony trioxide and compared to the thresholds required to reach lung overload.

Using Equation (10), the density of antimony trioxide and the measured lung burden were used to calculate the total volume of antimony trioxide (μm^3) in the lungs for each time point:

Equation (10): $V_p(t) = [10^{-3} \times L(t)/\rho] \times 10^{12}$

In Equation (10), $V_p(t)$ is the volume of the retained lung burden in μm^3 at any time t (days on study); L(t) is the measured lung burden (converted to mg by multiplying by 10^{-3} mg/μg) at time t; ρ is the density of antimony trioxide (5,470 mg/cm^3); and the factor 10^{12} converts cm^3 to μm^3.

Through an iterative calculation, the ratio R(t) was calculated using Equation (11):

Equation (11): $R(t) = V_p(t)/V^*$

In Equation (11), $V_p(t)$ is the volume of retained antimony trioxide lung burden at time t, and V* is the threshold volume required for the onset of lung overload [6% of the alveolar macrophage (AM) pool volume]; V* is estimated to be 1.8×10^9 μm^3 in the Sprague Dawley rat and 2.4×10^8 μm^3 in the B6C3F1/N mouse.

These calculated ratios were used to determine the time of onset of lung overload and the extent of overload achieved over the course of the studies. The time of onset of the overload condition (t*, days) was determined as the earliest time (days on study) for which R(t) > 1.0. Thus, t* is the time point when the volume of the lung burden first exceeded 6% of the volume of the AM pool. The maximum value of the ratio (R_{max}) was used to determine the extent of overload that occurred by the end of the study. Since lung burdens increased throughout the studies, R_{max} was necessarily the value of R at 551 days on study (the terminal sacrifice for tissue burden study animals).

As noted above, the time point when the volume of retained lung burden first exceeds 6% of the AM pool volume or when the overload condition first occurs during the study is defined at t*. Experimental studies have indicated that this should occur at an antimony trioxide lung burden slightly greater than 9.8 mg/lung in Wistar Han rats and at slightly greater than 1.3 mg/lung in B6C3F1/N mice. R_{max} is the multiplicative factor by which the threshold volumes were exceeded over the duration of the studies. For example, a value of R_{max} of 10 would indicate a lung burden

volume that is 60% of the AM pool volume, which would occur near lung burdens of 98 mg Sb_2O_3/lung in Wistar Han rats or 13 mg Sb_2O_3/lung in B6C3F1/N mice.

As discussed by Tran et al.[76], in some cases the surface area of the retained lung burden (as opposed to the volume) has been a more robust indicator of whether overload has occurred. In this regard, these investigators determined that the threshold for lung overload in rats occurs when the surface area of the retained lung burden reaches 200 to 300 cm^2/lung; no corresponding value is available for mice in the literature, but for the current study, the threshold surface area for lung overload in mice was estimated to be 40 cm^2/lung. This value was calculated by multiplying the threshold surface area value for rats (300 cm^2/lung) by the mean lung weight ratio of B6C3F1/N mice to Wistar Han rats from chamber control animals in the current 2-year antimony trioxide studies.

The surface area of retained lung burdens was calculated using Equation (12):

Equation (12): $\alpha(t) = 2.54[L(t)/10^3] \times 10^4$

In Equation (12), $\alpha(t)$ is the surface area (cm^2 Sb_2O_3/lung) of the retained lung burden at time t (days on study); 2.54 is the specific surface area of the antimony trioxide test chemical in m^2/g; L(t) is the measured lung burden (mg Sb_2O_3/lung) at time t; 10^3 converts mg to g; and 10^4 converts m^2 to cm^2.

The ratio of $\alpha(t)$ to the determined or estimated threshold surface areas (300 and 40 cm^2/lung for rats and mice, respectively) was calculated and determined the time point when this ratio first exceeded 1.0 as the time point when the overload threshold surface area was first exceeded. This ratio was also calculated at 551 days to determine to what extent the threshold surface area was exceeded by the end of the study.

Table G-1. Lung Weights, Antimony Concentrations and Burdens, and Antimony Trioxide Burdens for Rats in the Two-week Inhalation Study of Antimony Trioxide[a]

	Chamber Control	3.75 mg/m^3	7.5 mg/m^3	15 mg/m^3	30 mg/m^3	60 mg/m^3
n	5	5	5	5	5	5
Male						
Blood						
µg Sb/g blood						
Day 16	0.020 ± 0.001	1.297 ± 0.045**	2.405 ± 0.141**	3.967 ± 0.227**	6.148 ± 0.405**	11.802 ± 0.649**
µg Sb/g blood per mg Sb_2O_3/m^3						
Day 16	NA	0.346 ± 0.012	0.321 ± 0.019	0.264 ± 0.015	0.205 ± 0.014	0.197 ± 0.011
Lung[b]						
Absolute lung wt. (g)						
Day 16	1.985 ± 0.109	1.934 ± 0.144	2.043 ± 0.150	2.078 ± 0.120	2.282 ± 0.186	2.559 ± 0.102**
µg Sb/g lung						
Day 16	0.052 ± 0.010	142.568 ± 13.635**	301.569 ± 25.638**	546.957 ± 54.568**	728.835 ± 64.918**	1,444.030 ± 55.892**
µg Sb/lung						
Day 16	0.105 ± 0.023	270.211 ± 18.232**	602.680 ± 25.519**	1,112.528 ± 59.870**	1,616.755 ± 23.888**	3,687.600 ± 166.239**
µg Sb_2O_3/lung						
Day 16	0.126 ± 0.028	323.490 ± 21.827**	721.514 ± 30.551**	1,331.890 ± 71.675**	1,935.538 ± 28.598**	4,414.702 ± 199.017**
µg Sb_2O_3/lung per mg Sb_2O_3/m^3						
Day 16	NA	86.264 ± 5.820	96.202 ± 4.073	88.793 ± 4.778	64.518 ± 0.953	73.578 ± 3.317
Female						
Blood						
µg Sb/g blood						
Day 16	0.027 ± 0.004	1.368 ± 0.037**	2.710 ± 0.084**	4.473 ± 0.301**	7.362 ± 0.339**	13.342 ± 0.850**
Week 4 PE	0.037 ± 0.007	2.594 ± 0.116**	4.874 ± 0.318**	7.605 ± 0.318**	12.174 ± 0.389**	21.589 ± 1.186**
µg Sb/g blood per mg Sb_2O_3/m^3						
Day 16	NA	0.365 ± 0.010	0.361 ± 0.011	0.298 ± 0.020	0.245 ± 0.011	0.222 ± 0.014

	Chamber Control	3.75 mg/m^3	7.5 mg/m^3	15 mg/m^3	30 mg/m^3	60 mg/m^3
Week 4 PE	NA	0.692 ± 0.031	0.650 ± 0.042	0.507 ± 0.021	0.406 ± 0.013	0.360 ± 0.020
Lung[b]						
Absolute lung wt. (g)						
Day 16	1.394 ± 0.085	1.334 ± 0.080	1.517 ± 0.145	1.511 ± 0.111	1.702 ± 0.065*	1.711 ± 0.095*
Week 4 PE	1.539 ± 0.133	1.736 ± 0.108	1.984 ± 0.175*	2.023 ± 0.066*	2.309 ± 0.134**	2.147 ± 0.111**
µg Sb/g lung						
Day 16	0.042 ± 0.000	165.730 ± 10.218**	338.480 ± 32.598**	638.542 ± 38.782**	968.788 ± 51.547**	1,865.036 ± 81.633**
Week 4 PE	0.051 ± 0.009	108.658 ± 7.337**	210.955 ± 21.354**	360.035 ± 10.640**	612.160 ± 49.834**	1,201.76 ± 75.166**
µg Sb/lung						
Day 16	0.059 ± 0.004	218.212 ± 6.318**	495.395 ± 21.259**	948.774 ± 20.889**	1,637.570 ± 51.105**	3,175.977 ± 159.404**
Week 4 PE	0.078 ± 0.014	186.169 ± 7.635**	404.222 ± 14.954**	727.562 ± 26.171**	1,390.39 ± 64.499**	2,552.45 ± 84.325**
µg Sb_2O_3/lung						
Day 16	0.070 ± 0.004	261.238 ± 7.563**	593.075 ± 25.451**	1,135.848 ± 25.007**	1,960.458 ± 61.182**	3,802.200 ± 190.835**
Week 4 PE	0.094 ± 0.017	222.877 ± 9.141**	483.924 ± 17.903**	871.019 ± 31.331**	1,664.54 ± 77.216**	3,055.73 ± 100.951**
µg Sb_2O_3/lung per mg Sb_2O_3/m^3						
Day 16	NA	69.663 ± 2.017	79.077 ± 3.394	75.723 ± 1.667	65.349 ± 2.040	63.370 ± 3.181
Week 4 PE	NA	59.434 ± 2.438	64.523 ± 2.387	58.068 ± 2.089	55.485 ± 2.574	50.929 ± 1.682

*Significantly different ($P \leq 0.05$) from the chamber control group by Williams' test.
**Significantly different ($P \leq 0.01$) from the chamber control group by Williams' test (lung weights) or Shirley's test (tissue concentrations and burdens).
[a]Data are presented as mean ± standard error. Statistical tests were performed only on data that were not normalized. NA = not applicable; PE = postexposure.
[b]Lung burdens were calculated using the weights of the total lung with mainstem bronchi at collection and antimony concentrations measured in the right lung (terminal sacrifice) or the right and left lung (recovery). Lung antimony trioxide burdens (µg Sb_2O_3/lung) were calculated by dividing the lung antimony burden (µg Sb/lung) by the fraction of antimony in antimony trioxide (0.8353).

Table G-2. Lung Deposition and Clearance Parameter Estimates for Female Rats in the Two-week Inhalation Study of Antimony Trioxide[a]

Exposure Concentration (mg/m^3)	k ($days^{-1}$)	$t_{1/2}$ (days)	α (μg Sb_2O_3/day)	Ae (μg Sb_2O_3)
3.75	0.0057	122	17	3,011
7.5	0.0073	95	39	5,405
15	0.0095	73	77	8,070
30	0.0058	119	128	21,962
60	0.0078	89	253	32,385

[a]Statistical analyses of these data were not performed due to the limited number of time points and data points within some time points. K = first-order clearance rate constant; $t_{½}$ = clearance half-life; α = lung deposition rate; A_e = steady-state lung burden.

Table G-3. Lung Weights, Antimony Concentrations and Burdens, and Antimony Trioxide Burdens for Female Rats in the Two-year Inhalation Study of Antimony Trioxide[a]

	Chamber Control	3 mg/m^3	10 mg/m^3	30 mg/m^3
n	5	5	5	5
Blood				
µg Sb/g blood				
Day 61	0.139 ± 0.012	7.352 ± 0.375**	18.079 ± 0.793**	43.574 ± 1.741**
Day 124	0.050 ± 0.002	16.135 ± 0.995**	40.350 ± 1.543**	96.082 ± 3.940**
Day 271	0.077 ± 0.002	39.590 ± 3.915**	88.833 ± 2.210**	175.437 ± 6.471**
Day 369	0.084 ± 0.008	50.917 ± 2.296**	102.083 ± 2.738**	200.239 ± 10.302**
Day 551	0.066 ± 0.005	63.297 ± 3.906**	149.192 ± 8.472**[b]	231.934 ± 8.681**
µg Sb/g blood per mg Sb_2O_3/m^3				
Day 61	NA	2.451 ± 0.125	1.808 ± 0.079	1.452 ± 0.058
Day 124	NA	5.378 ± 0.332	4.035 ± 0.154	3.203 ± 0.131
Day 271	NA	13.197 ± 1.305	8.883 ± 0.221	5.848 ± 0.216
Day 369	NA	16.972 ± 0.765	10.208 ± 0.274	6.675 ± 0.343
Day 551	NA	21.099 ± 1.302	14.919 ± 0.847[b]	7.731 ± 0.289
Lung[c]				
Absolute lung wt. (g)				
Day 61	1.112 ± 0.041	1.558 ± 0.098**	1.750 ± 0.086**	1.936 ± 0.069**
Day 124	1.356 ± 0.099	1.999 ± 0.096**	2.346 ± 0.050**	2.851 ± 0.095**
Day 271	1.474 ± 0.095	2.631 ± 0.177**	3.374 ± 0.100**	4.233 ± 0.254**
Day 369	1.693 ± 0.174	2.990 ± 0.355	3.887 ± 0.234**	5.409 ± 0.778**
Day 551	1.539 ± 0.079	2.748 ± 0.186	5.830 ± 1.106**[b]	9.641 ± 1.148**
µg Sb/g lung				
Day 61	0.128 ± 0.046	436.686 ± 14.015**	1,202.69 ± 51.447**	2,894.85 ± 87.000**
Day 124	0.042 ± 0.000	689.305 ± 49.265**	1,571.00 ± 59.097**	3,750.99 ± 144.557**

	Chamber Control	3 mg/m^3	10 mg/m^3	30 mg/m^3
Day 271	0.285 ± 0.074	837.475 ± 40.496**	1,983.17 ± 92.267**	4,610.22 ± 363.095**
Day 369	0.302 ± 0.031	765.002 ± 179.148**	1,976.06 ± 92.704**	4,256.31 ± 344.828**
Day 551	0.163 ± 0.020	978.770 ± 86.114**	1,801.06 ± 277.723**[b]	3,261.79 ± 535.308**
µg Sb/lung				
Day 61	0.146 ± 0.055	677.161 ± 35.177**	2,098.68 ± 104.802**	5,589.54 ± 158.053**
Day 124	0.057 ± 0.004	1,360.25 ± 48.652**	3,686.32 ± 157.588**	10,706.2 ± 596.172**
Day 271	0.427 ± 0.113	2,190.88 ± 143.007**	6,675.12 ± 264.985**	19,215.3 ± 924.889**
Day 369	0.493 ± 0.021	2,052.99 ± 136.950**	7,596.49 ± 167.389**	22,447.0 ± 2,309.92**
Day 551	0.249 ± 0.025	2,631.38 ± 129.598**	9,599.82 ± 393.455**[b]	29,011.6 ± 1,437.94**
µg Sb_2O_3/lung				
Day 61	0.175 ± 0.066	810.681 ± 42.113**	2,512.49 ± 125.466**	6,691.65 ± 189.217**
Day 124	0.068 ± 0.005	1,628.46 ± 58.245**	4,413.16 ± 188.660**	12,817.1 ± 713.722**
Day 271	0.512 ± 0.135	2,622.87 ± 171.204**	7,991.29 ± 317.233**	23,004.1 ± 1,107.25**
Day 369	0.591 ± 0.025	2,457.79 ± 163.953**	9,094.32 ± 200.394**	26,873.0 ± 2,765.38**
Day 551	0.298 ± 0.030	3,150.22 ± 155.152**	11,492.7 ± 471.034**[b]	34,731.9 ± 1,721.47**
µg Sb_2O_3/lung per mg Sb_2O_3/m^3				
Day 61	NA	270.227 ± 14.038	251.249 ± 12.547	223.055 ± 6.307
Day 124	NA	542.819 ± 19.415	441.316 ± 18.866	427.238 ± 23.791
Day 271	NA	874.288 ± 57.068	799.129 ± 31.723	766.803 ± 36.908
Day 369	NA	819.264 ± 54.651	909.432 ± 20.039	895.765 ± 92.179
Day 551	NA	1,050.07 ± 51.717	1,149.27 ± 47.103[b]	1,157.73 ± 57.382

**Significantly different ($P \leq 0.01$) from the chamber control group by Williams' test (lung weights) or Shirley's test (tissue concentrations and burdens).
[a]Data are presented as mean ± standard error. Statistical tests were performed only on data that were not normalized. NA = not applicable.
[b]n = 4.
[c]Lung burdens were calculated using the weights of the total lung with mainstem bronchi at collection and measured concentrations of antimony in the total lung. Lung antimony trioxide burdens (µg Sb_2O_3/lung) were calculated by dividing the lung antimony burden (µg Sb/lung) by the fraction of antimony in antimony trioxide (0.8353).

Table G-4. Lung Deposition and Clearance Parameter Estimates for Female Rats in the Two-year Inhalation Study of Antimony Trioxide[a]

Parameter	3 mg/m^3	10 mg/m^3	30 mg/m^3
D (µg Sb_2O_3/total lung per day)	16.7 ± 0.7	44.2 ± 1.9	119.1 ± 3.8
k (days^{-1})	0.0051 ± 0.0005	0.0034 ± 0.0003	0.0026 ± 0.0003
$t_{½}$ (days)	136 ± 11	203 ± 18	262 ± 26
Lss (µg Sb_2O_3/total lung)	3,281 ± 326	12,964 ± 1,348	44,997 ± 5,226

[a]Data are presented as mean ± standard error. D = deposition rate; k = first-order lung clearance rate constant; $t_{½}$ = lung clearance half-life; L_{SS} = steady-state lung burden.

Table G-5. Lung Burden Overload Parameter Estimates for Female Rats in the Two-year Inhalation Study of Antimony Trioxide

Parameter	3 mg/m^3	10 mg/m^3	30 mg/m^3
t* = Time when R(t) > 1 (days)	NA	418	94
L(t*) = lung burden at t* (mg Sb_2O_3/lung)	NA	9.8	9.9
Rmax = maximum R(t) at 551 days (unitless)	0.3	1.1	3.5
Lung burden at Rmax = L(t) at 551 days (mg Sb_2O_3/lung)	3.1	11.0	34.5
Total dose = deposited Sb_2O_3 at 551 days (mg/lung)	9.2	24.4	65.6
Total Sb_2O_3 cleared = cleared Sb_2O_3 up through 551 days (mg/lung)	6.1	13.4	31.1
% Total Sb_2O_3 cleared = total Sb_2O_3 cleared/total dose) × 100 (unitless)	66	55	47

R(t) = ratio of the volume of retained Sb_2O_3 lung burden at time t to the threshold volume required for the onset of lung overload; NA = not applicable.

Table G-6. Lung Weights, Antimony Concentrations and Burdens, and Antimony Trioxide Burdens for Mice in the Two-week Inhalation Study of Antimony Trioxide[a]

	Chamber Control	3.75 mg/m^3	7.5 mg/m^3	15 mg/m^3	30 mg/m^3	60 mg/m^3
n	5	5	5	5	5	5
Male						
Blood						
µg Sb/g blood						
Day 17	0.001 ± 0.000	0.023 ± 0.001**[b]	0.040 ± 0.002**[b]	0.061 ± 0.001**	0.084 ± 0.001**	0.178 ± 0.066**[b]
µg Sb/g blood per mg Sb_2O_3/m^3						
Day 17	NA	0.006 ± 0.000b	0.005 ± 0.000b	0.004 ± 0.000	0.003 ± 0.000	0.003 ± 0.001b
Lung[c]						
Absolute lung wt. (g)						
Day 17	0.174 ± 0.008	0.205 ± 0.021	0.217 ± 0.013*	0.210 ± 0.010*	0.208 ± 0.009*	0.231 ± 0.005**
µg Sb/g lung						
Day 17	0.455 ± 0.000	317.011 ± 34.763**	574.255 ± 39.327**	1,229.622 ± 63.691**	2,010.842 ± 69.131**	3,572.798 ± 153.853**
µg Sb/lung						
Day 17	0.079 ± 0.004	62.195 ± 3.222**	122.395 ± 3.209**	255.787 ± 9.064**	415.521 ± 5.836**	825.632 ± 32.596**
µg Sb_2O_3/lung						
Day 17	0.095 ± 0.004	74.459 ± 3.857**	146.528 ± 3.843**	306.222 ± 10.851**	497.451 ± 6.987**	988.425 ± 39.023**
µg Sb_2O_3/lung per mg Sb_2O_3/m^3						
Day 17	NA	19.856 ± 1.029	19.537 ± 0.512	20.415 ± 0.723	16.582 ± 0.233	16.474 ± 0.650
Female						
Blood						
µg Sb/g blood						
Day 17	0.001 ± 0.000b	0.027 ± 0.001*	0.042 ± 0.001**	0.070 ± 0.006**	0.088 ± 0.004**b	0.140 ± 0.016**
Week 4 PE	0.001 ± 0.000	0.011 ± 0.001**	0.021 ± 0.000**	0.034 ± 0.001**	0.048 ± 0.002**	0.068 ± 0.002**

	Chamber Control	3.75 mg/m^3	7.5 mg/m^3	15 mg/m^3	30 mg/m^3	60 mg/m^3
μg Sb/g blood per mg Sb/m^3						
Day 17	NA	0.007 ± 0.000	0.006 ± 0.000	0.005 ± 0.000	0.003 ± 0.000b	0.002 ± 0.000
Week 4 PE	NA	0.003 ± 0.000	0.003 ± 0.000	0.002 ± 0.000	0.002 ± 0.000	0.001 ± 0.000
Lung[c]						
Absolute lung wt. (g)						
Day 17	0.162 ± 0.004	0.182 ± 0.006	0.180 ± 0.004	0.200 ± 0.007**	0.203 ± 0.005**	0.218 ± 0.010**
Week 4 PE	0.200 ± 0.008	0.181 ± 0.004	0.204 ± 0.008	0.255 ± 0.023**	0.271 ± 0.004**	0.342 ± 0.009**
μg Sb/g lung						
Day 17	0.455 ± 0.000	294.205 ± 16.022**	635.327 ± 18.297**	1,073.105 ± 28.121**[b]	1,871.826 ± 80.026**	3,111.101 ± 173.398**
Week 4 PE	0.637 ± 0.182	194.627 ± 5.879**	409.191 ± 19.625**	613.924 ± 54.525**	1,011.90 ± 27.660**	1,408.27 ± 58.728**
μg Sb/lung						
Day 17	0.074 ± 0.002	53.307 ± 2.208**	113.836 ± 1.662**	213.298 ± 11.923**[b]	381.127 ± 23.682**	673.947 ± 28.796**
Week 4 PE	0.131 ± 0.042	35.247 ± 0.943**	83.042 ± 1.892**	151.673 ± 4.355**	273.437 ± 4.895**	480.060 ± 12.981**
μg Sb_2O_3/lung						
Day 17	0.088 ± 0.002	63.818 ± 2.643**	136.282 ± 1.990**	255.355 ± 14.274**[b]	456.276 ± 28.351**	806.832 ± 34.474**
Week 4 PE	0.157 ± 0.051	42.197 ± 1.129**	99.415 ± 2.265**	181.579 ± 5.214**	327.351 ± 5.860**	574.715 ± 15.541**
μg Sb_2O_3/g lung per mg Sb_2O_3/m^3						
Day 17	NA	17.018 ± 0.705	18.171 ± 0.265	17.024 ± 0.952b	15.209 ± 0.945	13.447 ± 0.575
Week 4 PE	NA	11.253 ± 0.301	13.255 ± 0.302	12.105 ± 0.348	10.912 ± 0.195	9.578 ± 0.259

*Significantly different ($P \leq 0.05$) from the chamber control group by Williams' test (lung weights) or Shirley's test (tissue concentrations and burdens).
**$P \leq 0.01$.
[a]Data are presented as mean ± standard error. Statistical tests were performed only on data that were not normalized. NA = not applicable; PE = postexposure.
[b]n = 4.
[c]Lung burdens were calculated using the weights of the total lung with mainstem bronchi at collection and antimony concentrations measured in the right lung (terminal sacrifice) or the right and left lung (recovery). Lung antimony trioxide burdens (μg Sb_2O_3/lung) were calculated by dividing the lung antimony burden (μg Sb/lung) by the fraction of antimony in antimony trioxide (0.8353).

Table G-7. Blood and Lung Deposition and Clearance Parameter Estimates for Female Mice in the Two-week Inhalation Study of Antimony Trioxide[a]

Tissue	Exposure Concentration (mg/m^3)	k ($days^{-1}$)	$t_{1/2}$ (days)	α (μg Sb_2O_3/day)	A_e (μg Sb_2O_3)
Blood	3.75	0.032	22	NA	NA
	7.5	0.026	27	NA	NA
	15	0.026	27	NA	NA
	30	0.022	32	NA	NA
	60	0.026	27	NA	NA
Lung	3.75	0.015	47	4	287
	7.5	0.011	62	9	782
	15	0.012	57	17	1,366
	30	0.012	58	30	2,499
	60	0.012	57	53	4,335

[a]Statistical analyses of these data were not performed due to the limited number of time points and data points within some time points. k = first-order clearance rate constant; $t_{½}$ = clearance half-life; α = lung deposition rate; A_e = steady-state lung burden; NA = not applicable.

Table G-8. Lung Weights, Antimony Concentrations and Burdens, and Antimony Trioxide Burdens for Female Mice in the Two-year Inhalation Study of Antimony Trioxide[a]

	Chamber Control	3 mg/m^3	10 mg/m^3	30 mg/m^3
n	5	5	5	5
Blood				
µg Sb/g blood				
Day 61	0.001 ± 0.000	0.043 ± 0.002**	0.083 ± 0.002**	0.141 ± 0.003**
Day 124	0.001 ± 0.001	0.058 ± 0.001**	0.089 ± 0.002**	0.148 ± 0.005**
Day 269	0.001 ± 0.000	0.053 ± 0.006**	0.091 ± 0.002**	0.163 ± 0.008**[b]
Day 369	0.001 ± 0.000	0.052 ± 0.003**	0.088 ± 0.003**	0.137 ± 0.007**
Day 551	0.001 ± 0.000	0.061 ± 0.010**	0.087 ± 0.004**	0.163 ± 0.006**[b]
µg Sb/g blood per mg Sb_2O_3/m^3				
Day 61	NA	0.014 ± 0.001	0.008 ± 0.000	0.005 ± 0.000
Day 124	NA	0.019 ± 0.000	0.009 ± 0.000	0.005 ± 0.000
Day 269	NA	0.017 ± 0.002	0.009 ± 0.000	0.005 ± 0.000[b]
Day 369	NA	0.017 ± 0.001	0.009 ± 0.000	0.005 ± 0.000
Day 551	NA	0.020 ± 0.003	0.009 ± 0.000	0.005 ± 0.000[b]
Lung[c]				
Absolute lung wt. (g)				
Day 61	0.202 ± 0.006	0.263 ± 0.008**	0.335 ± 0.017**	0.398 ± 0.008**
Day 124	0.182 ± 0.003	0.279 ± 0.014**	0.367 ± 0.004**	0.517 ± 0.020**
Day 269	0.184 ± 0.008	0.268 ± 0.006*	0.353 ± 0.005**	0.646 ± 0.056**[b]
Day 369	0.187 ± 0.003	0.281 ± 0.009**	0.354 ± 0.012**	0.701 ± 0.025**
Day 551	0.204 ± 0.006	0.306 ± 0.022**	0.435 ± 0.032**	0.617 ± 0.026**[b]
µg Sb/g lung				
Day 61	0.455 ± 0.000	560.526 ± 11.741**	1,233.12 ± 42.424**	2,687.32 ± 56.076**

	Chamber Control	3 mg/m^3	10 mg/m^3	30 mg/m^3
Day 124	0.455 ± 0.000	682.534 ± 59.310**	1,475.78 ± 32.782**	2,954.05 ± 95.408**
Day 269	0.455 ± 0.000	801.719 ± 22.118**	2,678.08 ± 135.202**	4,132.91 ± 667.094**[b]
Day 369	0.455 ± 0.000	978.803 ± 53.661**	3,797.88 ± 231.550**	3,892.00 ± 248.070**
Day 551	0.455 ± 0.000	1,471.76 ± 115.654**	4,188.07 ± 608.706**	8,398.33 ± 609.402**[b]
µg Sb/lung				
Day 61	0.092 ± 0.003	146.980 ± 3.155**	410.431 ± 12.314**	1,069.07 ± 32.882**
Day 124	0.083 ± 0.001	187.387 ± 8.950**	541.373 ± 15.157**	1,532.01 ± 95.506**
Day 269	0.084 ± 0.004	215.420 ± 9.629**	943.736 ± 40.072**	2,558.37 ± 180.94**[b]
Day 369	0.085 ± 0.002	275.448 ± 18.393**	1,336.04 ± 56.473**	2,716.81 ± 157.964**
Day 551	0.093 ± 0.003	441.294 ± 13.534**	1,744.56 ± 188.559**	5,136.49 ± 155.895**[b]
µg Sb_2O_3/lung				
Day 61	0.110 ± 0.004	175.960 ± 3.777**	491.358 ± 14.741**	1,279.86 ± 39.365**
Day 124	0.099 ± 0.002	224.335 ± 10.714**	648.118 ± 18.146**	1,834.09 ± 114.338**
Day 269	0.100 ± 0.004	257.896 ± 11.527**	1,129.82 ± 47.974**	3,062.82 ± 216.617**[b]
Day 369	0.102 ± 0.002	329.760 ± 22.020**	1,599.48 ± 67.608**	3,252.50 ± 189.110**
Day 551	0.111 ± 0.003	528.306 ± 16.202**	2,088.54 ± 225.738**	6,149.27 ± 186.634**[b]
µg Sb_2O_3/lung per mg Sb_2O_3/m^3				
Day 61	NA	58.653 ± 1.259	49.136 ± 1.474	42.662 ± 1.312
Day 124	NA	74.778 ± 3.571	64.812 ± 1.815	61.136 ± 3.811
Day 269	NA	85.965 ± 3.842	112.982 ± 4.797	102.094 ± 7.221[b]
Day 369	NA	109.920 ± 7.340	159.948 ± 6.761	108.417 ± 6.304
Day 551	NA	176.102 ± 5.401	208.854 ± 22.574	204.976 ± 6.221[b]

*Significantly different ($P \leq 0.05$) from the chamber control group by Williams' test.
**Significantly different ($P \leq 0.01$) from the chamber control group by Williams' test (lung weights) or Shirley's test (tissue concentrations and burdens).
[a]Data are presented as mean ± standard error. Statistical tests were performed only on data that were not normalized. NA = not applicable.
[b]n = 4.
[c]Lung burdens were calculated using the weights of the total lung with mainstem bronchi at collection and measured concentrations of antimony in the total lung. Lung antimony trioxide burdens (µg Sb_2O_3/lung) were calculated by dividing the lung antimony burden (µg Sb/lung) by the fraction of antimony in antimony trioxide (0.8353).

Table G-9. Retained Lung Antimony Trioxide Burden Volumes and Surface Areas in Female Mice in the Two-year Inhalation Study of Antimony Trioxide

Parameter	3 mg/m^3	10 mg/m^3	30 mg/m^3
Volume of retained lung burden (μm^3 Sb_2O_3/lung)			
Day 61	3.22 × 107	8.98 × 107	2.34 × 108
Day 124	4.10 × 107	1.18 × 108	3.35 × 108
Day 269	4.71 × 107	1.98 × 108	5.60 × 108
Day 369	6.03 × 107	2.92 × 108	5.95 × 108
Day 551	9.66 × 107	4.23 × 108	1.12 × 109
Ratio of retained volume to threshold volume (μm^3 Sb_2O_3/lung)/(2.4 × 108 μm^3)[a]			
Day 61	0.13	0.37	0.97
Day 124	0.17	0.49	1.40
Day 269	0.20	0.82	2.33
Day 369	0.25	1.22	2.48
Day 551	0.40	1.76	4.68
Surface area of retained lung burden (cm^2 Sb_2O_3/lung)			
Day 61	4	12	33
Day 124	6	16	47
Day 269	7	27	78
Day 369	8	41	83
Day 551	13	59	156
Ratio of retained surface area to threshold surface area (cm^2 Sb_2O_3/lung)/(40 cm^2/lung)[b]			
Day 61	0.11	0.31	0.81
Day 124	0.14	0.41	1.16
Day 269	0.16	0.69	1.94
Day 369	0.21	1.02	2.07
Day 551	0.34	1.47	3.90

[a]2.4×10^8 μm^3 is the estimated threshold alveolar macrophage pool volume when overload should occur.
[b]40 cm^2/lung is the estimated threshold lung surface area when overload should occur.

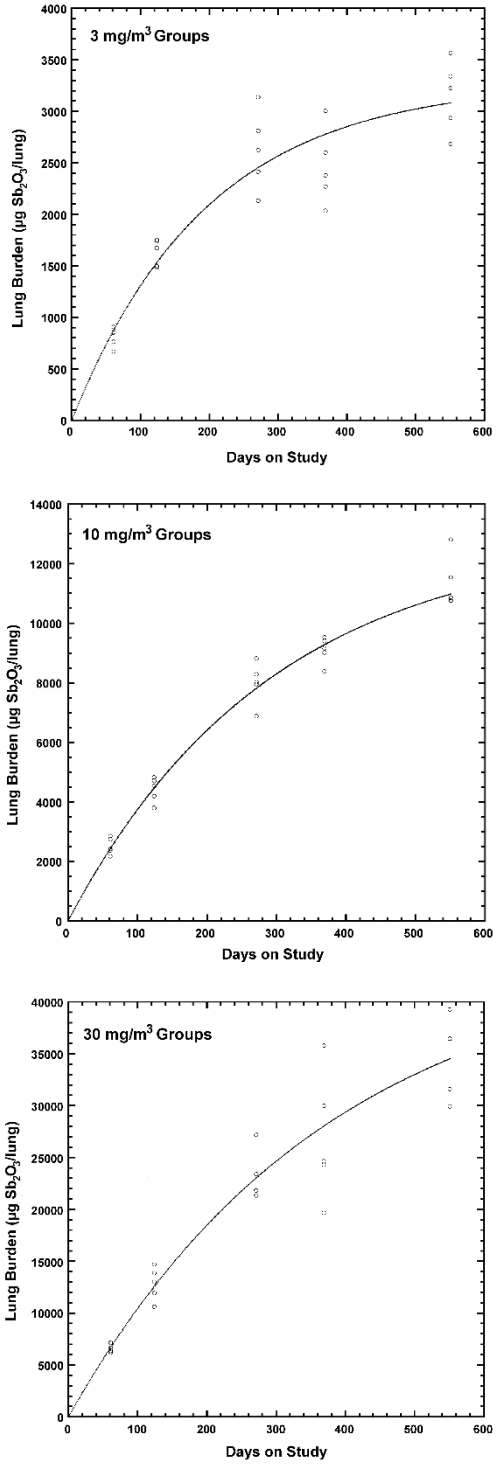

Figure G-1. Lung Antimony Trioxide Burdens in 3, 10, and 30 mg/m^3 Female Rats in the Two-year Inhalation Study of Antimony Trioxide

The lines represent the fit of the lung deposition and clearance model to the data.

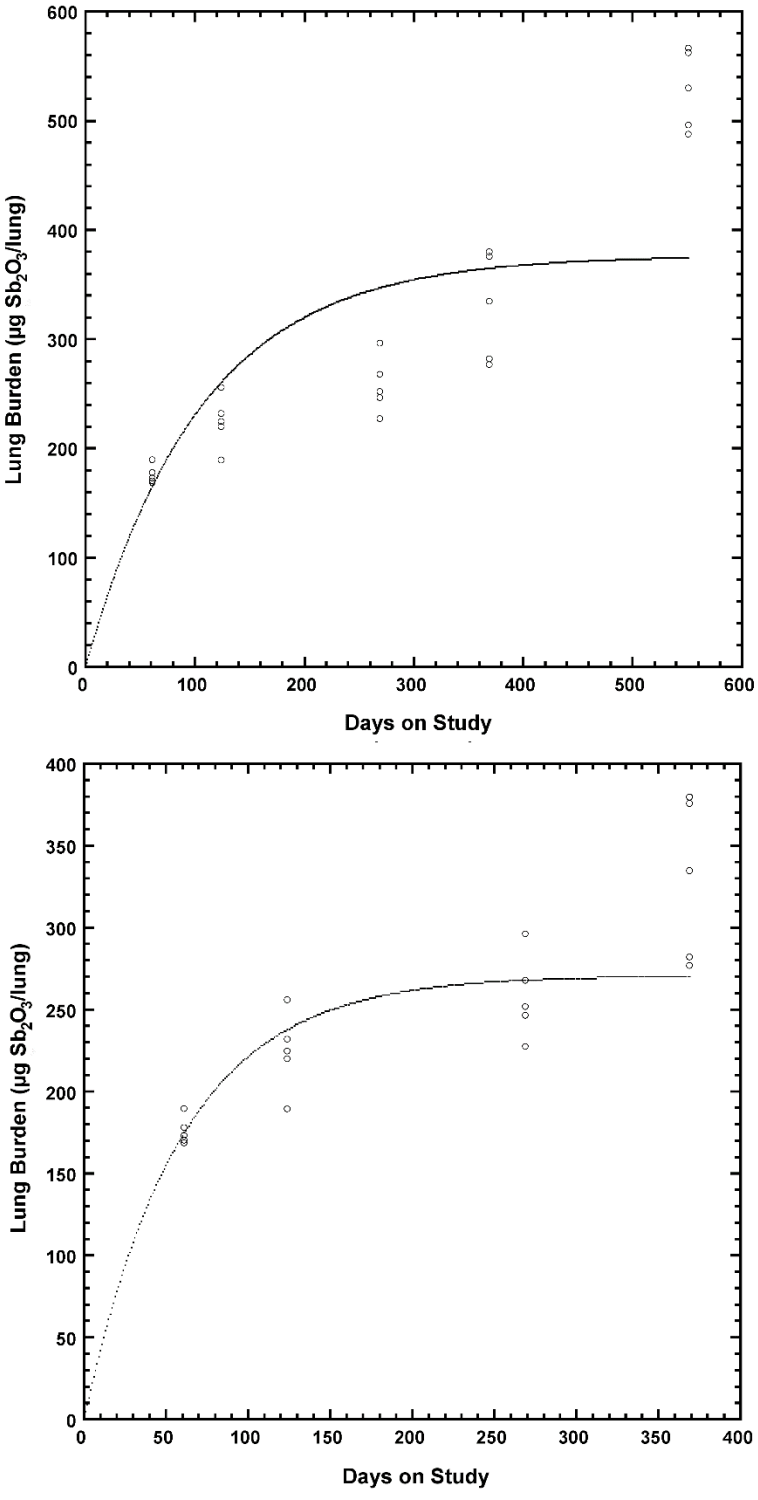

Figure G-2. Lung Antimony Trioxide Burdens in 3 mg/m^3 Female Mice in the Two-year Inhalation Study of Antimony Trioxide Including All Time Points (Top) and with Day 551 Data Removed (Bottom)

The lines represent the fit of the lung deposition and clearance model to the data.

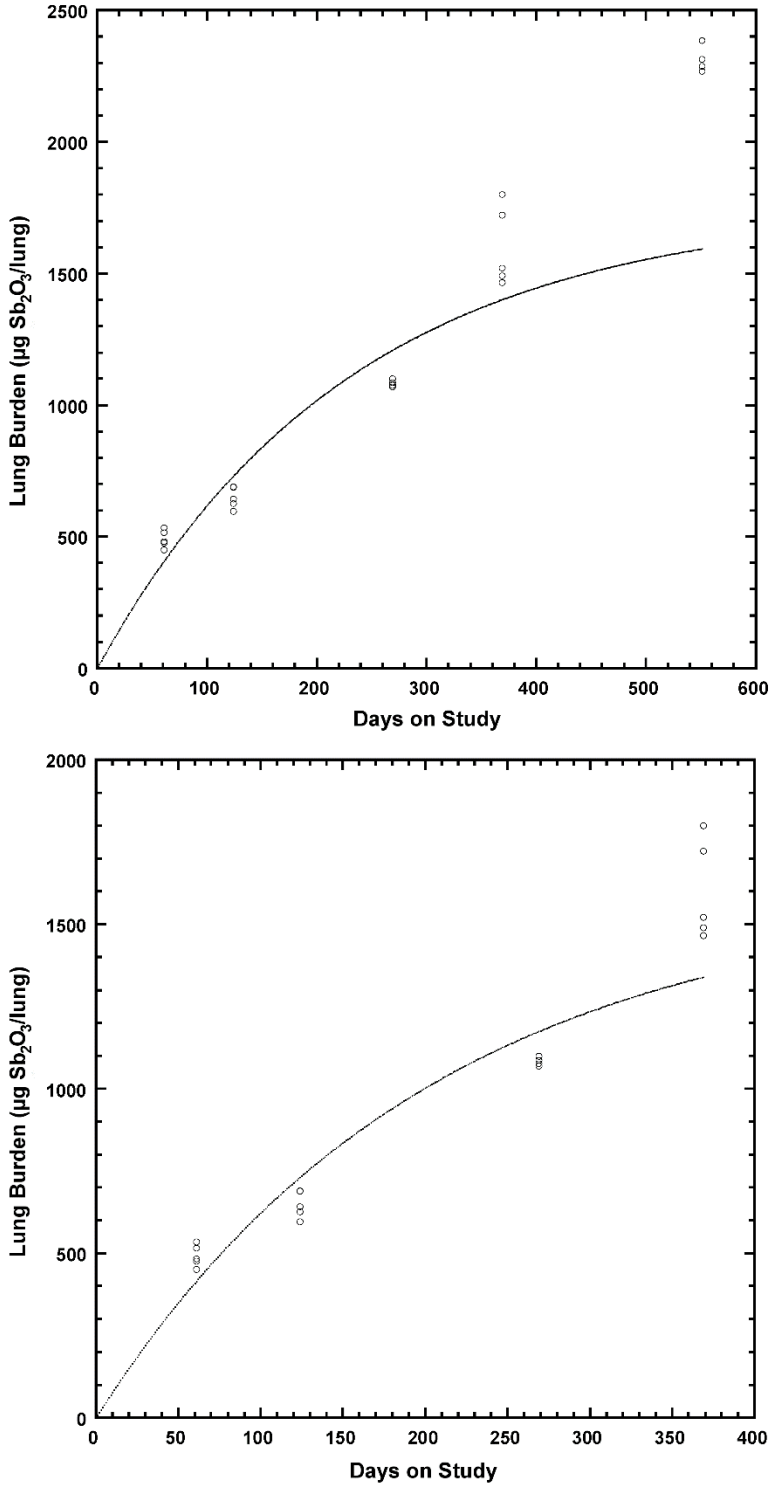

Figure G-3. Lung Antimony Trioxide Burdens in 10 mg/m^3 Female Mice in the Two-year Inhalation Study of Antimony Trioxide Including All Time Points (Top) and with Day 551 Data Removed (Bottom)

The lines represent the fit of the lung deposition and clearance model to the data.

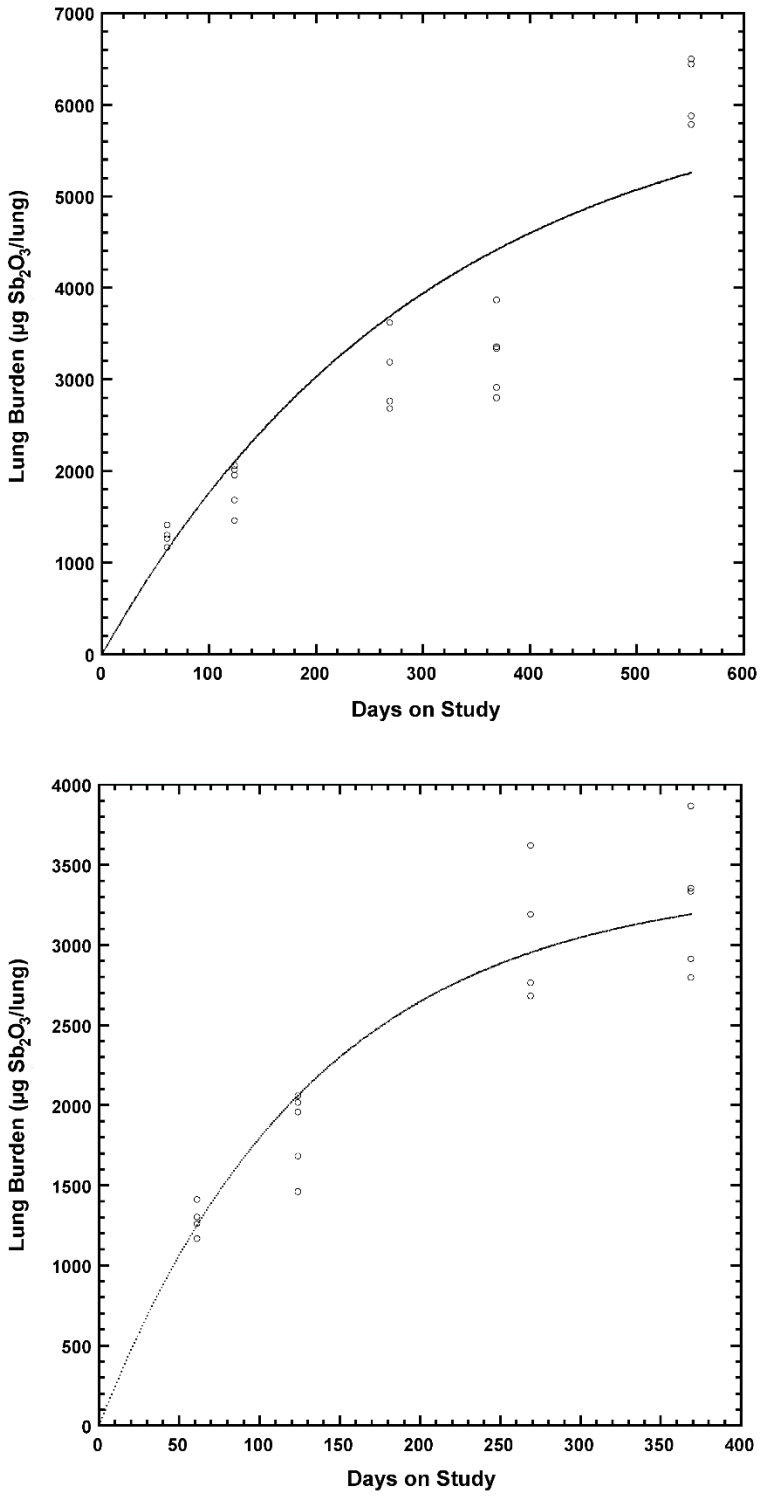

Figure G-4. Lung Antimony Trioxide Burdens in 30 mg/m^3 Female Mice in the Two-year Inhalation Study of Antimony Trioxide Including All Time Points (Top) and with Day 551 Data Removed (Bottom)

The lines represent the fit of the lung deposition and clearance model to the data.

Appendix H. Chemical Characterization and Generation of Chamber Concentrations

Table of Contents

H.1. Procurement and Characterization of Antimony Trioxide H-2
H.2. Aerosol Generation and Exposure System H-3
H.3. Aerosol Concentration Monitoring H-4
H.4. Chamber Atmosphere Characterization H-5

Tables

Table H-1. Summary of Chamber Concentrations in the Two-week Inhalation Studies of Antimony Trioxide H-7
Table H-2. Summary of Chamber Concentrations in the Two-year Inhalation Studies of Antimony Trioxide H-7
Table H-3. Summary of Aerosol Size Measurements for the Rat and Mouse Exposure Chambers in the Two-week Inhalation Studies of Antimony Trioxide H-7
Table H-4. Summary of Aerosol Size Measurements for the Male Rat Exposure Chambers in the Two-year Inhalation Study of Antimony Trioxide H-8
Table H-5. Summary of Aerosol Size Measurements for the Female Rat and Male and Female Mouse Exposure Chambers in the Two-year Inhalation Studies of Antimony Trioxide H-10

Figures

Figure H-1. X-ray Diffraction Pattern of Antimony Trioxide H-12
Figure H-2. Schematic of the Aerosol Generation and Delivery System in the Inhalation Studies of Antimony Trioxide. H-13

H.1. Procurement and Characterization of Antimony Trioxide

Antimony trioxide was obtained from 3N International, Inc. (Akron, OH), in one lot (3N-06159) that was used in the 2-week and 2-year studies. Identity and purity analyses were conducted by the analytical chemistry laboratories at H&M Analytical Services, Inc. [Allentown, NJ; X-ray diffraction (XRD)], and Chemir Analytical Services, Inc. [Maryland Heights, MO; redox titration and ultraviolet (UV) spectrophotometry], and by the study laboratory at Battelle Toxicology Northwest [Richland, WA; inductively coupled plasma/atomic emission spectroscopy (ICP/AES)]. Reports on analyses performed in support of the antimony trioxide studies are on file at the National Institute of Environmental Health Sciences.

Lot 3N-06159 of the chemical, a finely divided white powder, was identified as antimony trioxide by the analytical chemistry laboratory using XRD. XRD patterns were consistent with library reference patterns (Joint Center for Powder Diffraction Studies/International Centre for Diffraction Data) for the diamond cubic structure of antimony trioxide, senarmontite, at 99.9%, with a trace amount of lead dioxide (0.1%) based on the XRD Rietveld method. A representative XRD pattern is presented in Figure H-1.

The purity of lot 3N-06159 was determined using ICP/AES by system A. In addition, redox titration and UV spectrophotometry of bulk chemical samples dissolved in hydrochloric acid (HCl) determined the oxidation state of antimony in the test article. Redox titration was performed with a standardized iodine solution and a freshly prepared starch indicator solution. UV spectrophotometry measured absorbance (330 nm) of iodoantimonous acid formed by the addition of potassium iodide reagent to the antimony tartrate salt of the test article.

A) For ICP/AES, samples were dissolved in concentrated HCl. National Institute of Standards and Technology (NIST)-traceable standards of yttrium (224.306 nm) and indium (325.609 nm) were added to each sample as internal standards for analyses of antimony (206.833 nm) and 18 minor elemental contaminants (aluminum, arsenic, beryllium, cadmium, cobalt, chromium, copper, iron, magnesium, manganese, molybdenum, nickel, lead, sulfur, selenium, tin, tungsten, and zirconium), respectively. Analyses were performed on a Thermo Elemental IRIS Intrepid II inductively coupled plasma/atomic emission spectrometer (Thermo Electron Corporation, Waltham, MA), and the results were normalized against those of NIST-traceable reference standards.

For lot 3N-06159, ICP/AES analysis by system A indicated a purity of 101.9% based on a theoretical content of 83.5% antimony in antimony trioxide. Of the 18 minor elements measured by ICP/AES, only arsenic (~0.019%) and lead (~0.016%) were detected above 0.01% relative to antimony trioxide. Redox titration and UV spectroscopy confirmed that antimony was present in the +3 oxidation state, consistent with antimony trioxide. The overall purity of lot 3N-06159 was determined to be greater than 99.9%.

To ensure stability, the bulk chemical was stored at room temperature in amber glass containers with Teflon®-lined lids. Periodic reanalyses of the bulk chemical were performed by the study laboratory using ICP/AES by system A and the analytical chemistry laboratory using XRD and no degradation of the bulk chemical was detected.

H.2. Aerosol Generation and Exposure System

A schematic diagram of the antimony trioxide generation and distribution system used during the 2-week and 2-year studies is shown in Figure H-2. For the 2-year studies, male and female rats were housed in separate chambers; female rat chambers also housed male and female mice from the concurrent study. The generation system used a linear feed device designed and built by Battelle to meter antimony trioxide into a Trost jet mill (Garlock, Inc., Newtown, PA) for aerosolization and particle size reduction. The linear feed device consisted of a slide bar, a body, a delivery tube, and a test article reservoir.

The compressed air driven slide bar slid back and forth during generation. As the slide bar moved to the filling position, the metering port on the shuttle bar was aligned with the reservoir opening and was filled with a small metered amount of test article. A stainless steel screen at the bottom of the metering port held the material within the port. A slight vacuum was applied to the metering port to assist with filling. As the slide bar moved to the dispersing position, the metering port was aligned with a compressed air port in the body. A puff of air from the port dispersed the test article from the metering port. The output of the linear feeder was regulated by adjusting the shuttle bar cadence.

Initial particle size reduction was accomplished within the Trost jet mill. Opposing nitrogen and air gas streams drove the jet mill. All components of the generation system were housed within a glove box located within the exposure control center.

From the jet mill, aerosol was directed to the main distribution line where it was diluted with humidified air then conveyed from the exposure control center to the exposure room where it passed through a cyclone separator to further reduce particle size. On exiting the cyclone, the aerosol-laden air was directed to either of two smaller branch lines. The main distribution and branch lines were made of stainless steel, bonded and grounded to prevent the buildup of electrostatic charge. The distribution line pressure was continuously monitored and maintained slightly negative to the exposure room.

From the branch line, aerosol was delivered to each exposure chamber by a sampling tube. The flow through the sampling tube was induced by a stainless steel ejector pump designed and fabricated at Battelle. The flow rate and configuration of the ejector pumps were chosen to optimize the efficiency of the delivery system. The aerosol then entered the chamber inlet duct where it was further diluted with conditioned chamber air to achieve the desired exposure concentration.

During exposure periods, there was a small excess of aerosol in each branch line over that needed to maintain chamber concentrations. This additional aerosol was available for making adjustments to the chamber aerosol delivery flow rates and was controlled using house vacuum regulated by a filter-protected flow meter. A second flow control system was available during off-exposure periods. This system consisted of a vacuum transducer pump (Air-Vac Engineering Company, Inc., Seymour, CT) of higher flow capacity positioned in parallel with each branch line flow meter control assembly that became operational only during critical shut-down periods. This backup pump was intended to create sufficient vacuum in the branch line to overcome the negative pressure in the chambers and prevent the flow of aerosol-laden air from the branch line to the chambers as the air supply to each chamber ejector pump was shut off. A high-efficiency

particulate air (HEPA) filter was placed before the endline flow control assembly of each branch to remove aerosol from the airstream prior to exhausting from the room.

The study laboratory designed the inhalation exposure chambers (Lab Products, Inc., Seaford, DE) so that uniform aerosol concentrations could be maintained throughout the chambers with the catch pans in place. The total volume of each chamber was 2.3 m^3 with an active mixing volume of 1.7 m^3. There were three levels of caging, each level split into two tiers that were offset from each other and from the chamber walls. Drawer-like stainless steel cage units composed of individual animal cages were suspended in the space above each tier. Stainless steel catch pans for the collection of urine and feces were suspended below each cage unit.

Incoming air that contained a uniform mixture of test chemical was diverted so that it flowed vertically along the inner surfaces of the chambers. Eddies were formed at each tier as the aerosol flowed past the catch pans. Stagnant zones that would normally exist above each pair of catch pans were cleared by exhaust flow through the space between the tiers. Aerosol reaching the lowest level was deflected across the bottom tiers by metal strips in the space between the catch pan and the wall. Tests showed that aerosol concentration could be reliably maintained homogenous within 8% throughout the chambers, provided the aerosol was uniformly mixed before passing through the chamber inlet and provided the test material did not react to a significant extent with animals, animal excrement, or the chamber interior[41].

H.3. Aerosol Concentration Monitoring

Summaries of the chamber aerosol concentrations are given in Table H-1 and Table H-2. The concentration of antimony trioxide in the exposure chambers and room air was monitored using three real-time aerosol monitors (RAMs) (MicroDust *pro*, Casella USA, Amherst, NH). The monitors were connected to the chambers by a sampling system designed by Battelle incorporating a valve that multiplexed each RAM to a 0 mg/m^3 chamber or the room, a HEPA-filtered air blank, and two exposure chambers. The output (voltage) of the RAM was recorded by a program designed by Battelle (Battelle Exposure Data Acquisition and Control) to select the correct sample stream and acquire a raw voltage signal from each RAM. Equations for the calibration curves resided within the program and were used to convert the measured RAM voltages to exposure chamber concentrations. Concentration control limits within the program were compared to each measured concentration and, if limits were exceeded, an audible alarm was triggered or, in extreme cases, exposure was terminated.

Each RAM was calibrated by constructing a response curve using the measured RAM voltages (voltage readings were corrected by subtracting the RAM zero-offset voltage from measured RAM voltages) and antimony concentrations that were determined by analyzing duplicate 25 mm Pallflex TX40HI20WW Emfab, 0.45 µm Teflon®-coated, glass-fiber filters (Pall Corporation, East Hills, NY) collected daily from the exposure chambers. Antimony trioxide was extracted from the filters with concentrated hydrochloric acid, sonicated, and analyzed using ICP/AES by system A.

The ICP/AES instrument was calibrated against serially diluted NIST-traceable 10 mg/mL spectrometric standards of antimony trioxide and the internal standard yttrium. Quality control standards and a reagent blank were analyzed after calibration, after approximately every tenth sample, and at the end of the analysis to determine accuracy and calibration drift during analysis.

H.4. Chamber Atmosphere Characterization

Particle size distribution was determined once prior to the 2-week and 2-year studies, once during the 2-week studies, and monthly during the 2-year studies. Cascade impactor samples were taken from each exposure chamber using a Mercer-style seven-stage impactor (In-Tox Products, Moriarty, NM) and the stages [22 mm glass coverslips lightly coated with silicone to prevent particle bounce for stages 1 to 7, or 25 mm Pallflex TX40HI20WW Emfab Teflon®-coated glass-fiber filters (Pall Corporation) for stage 8] were analyzed for antimony using ICP/AES by system A after antimony trioxide was extracted from the slides or filters with concentrated HCl and sonication. The mass of antimony trioxide collected was calculated based on the theoretical percent of antimony in antimony trioxide (83.5%). The relative mass of test article collected on each stage was analyzed by the NEWCAS impactor analysis program developed at Battelle based on probit analysis[42]. The resulting estimates of the mass median aerodynamic particle diameter and the geometric standard deviation of each set of samples are given in Table H-3, Table H-4, and Table H-5. All samples were within the 1 to 3 µm range required by the protocol.

Buildup and decay rates for chamber aerosol concentrations were determined with (all studies) and without (2-year studies) animals present in the chambers. At a chamber airflow rate of 15 air changes per hour, the theoretical value for the time to achieve 90% of the target concentration after the beginning of aerosol generation (T90) and the time for the chamber concentration to decay to 10% of the target concentration after aerosol generation was terminated (T10) was approximately 9.4 minutes. For rats and mice in the 2-week studies with animals present, T90 values ranged from 8 to 12 minutes; T10 values ranged from 7 to 10 minutes. For rats and mice in the 2-year studies, T90 values ranged from 11 to 18 minutes without animals present and from 12 to 17 minutes with animals; T10 values ranged from 5 to 10 minutes without animals present and from 8 to 12 minutes with animals. A T90 value of 12 minutes was selected for all studies.

The uniformity of aerosol concentration in the inhalation exposure chambers without animals present was evaluated before each of the studies began; in addition, concentration uniformity with animals present in the chambers was measured once during the 2-week studies, and every 2 to 3 months during the 2-year studies. Aerosol concentrations were measured using the on-line monitor with the stream-selection valve fixed in one position to allow continuous monitoring from a single input line. Concentrations were measured at all 12 sample ports; one in front and one in back for each of six possible cage unit positions per chamber. Chamber concentration uniformity was maintained throughout the studies.

The persistence of antimony trioxide in the exposure chambers after aerosol delivery ended was determined by monitoring the aerosol concentration in the 60 mg/m^3 chambers in the 2-week studies with animals present and the 30 mg/m^3 chambers in the 2-year studies, with and without animals present. In the 2-week studies, the concentration decreased to 1% of the starting concentration within 17 minutes. In the 2-year study of male rats, the concentration decreased to 1% of the starting concentration within approximately 23 minutes with animals present and within 18 minutes without animals. In the 2-year studies of female rats and male and female mice, the concentration decreased to 1% of the starting concentration within 16 minutes with animals present and within 15 minutes without animals.

Stability studies of antimony trioxide in the generation and exposure system were performed before (2-year studies only) and during the studies by the study laboratory (ICP/AES) and H&M Analytical Services, Inc. (XRD). On each sample collection day, a sample of antimony trioxide powder was collected before filling the generator reservoir, and a sample of the powdered test article from the generator reservoir was collected at the end of the generation day; additional test material was added to the generator each day. Before (except for the 2-week studies) and during each study, microporous filters [25 mm A/E glass-fiber filters (Pall Corporation)] were collected from the aerosol distribution line and the 3.75 mg/m^3 and 60 mg/m^3 chambers (2-week studies) or the 3 mg/m^3 and 30 mg/m^3 chambers (2-year studies) to obtain samples for XRD analyses. Separate sets of filters [25 mm GH Polypro, 0.45 µm (Pall Corporation)] were collected from the distribution line and the same chambers to obtain samples for ICP/AES analyses. Generator reservoir and filter samples were analyzed using multiple but similar XRD systems and ICP/AES by system A to determine if inorganic impurities were introduced into the test atmosphere by the exposure generation system. Powder and filter samples for XRD analyses required no additional processing; those for ICP/AES analyses were dissolved in concentrated HCl and assayed for antimony and 18 minor elemental contaminants as in the initial bulk chemical purity assessment.

During the 2-week studies, XRD with Rietveld analysis indicated that the samples taken from the generation and exposure system contained antimony trioxide (99.6% to 99.9%) and lead dioxide (0.1% to 0.4%). Relative to antimony trioxide, ICP/AES detected aluminum, arsenic, beryllium, cadmium, chromium, copper, manganese, selenium, tungsten, and zirconium at less than 0.1%, cobalt, iron, magnesium, molybdenum, nickel, lead, and tin at less than 0.2%, and sulfur at less than 0.3%.

Before the 2-year studies, XRD with Rietveld analysis indicated the presence of a single crystalline phase of antimony trioxide, the diamond cubic structure senarmontite. The detection limits were approximately 0.1%, 0.2%, and 1.0% for the generator reservoir bulk material samples, the chamber filter samples, and the distribution line filter samples, respectively. Relative to antimony trioxide, ICP/AES detected sulfur at less than 0.2 % and the other 17 measured minor elemental contaminants at less than 0.1%.

XRD analyses of test chemical stability in the generation and exposure system were performed at 2 (mice) or 4 (rats) weeks, 1 year, and the end of the 2-year studies. XRD with Rietveld analysis of the generator reservoir bulk material and filter samples indicated a single crystalline phase, that of antimony trioxide in the diamond cubic structure senarmontite. The detection limit for impurity phases ranged from 0.05% to 0.1% for the powder samples and 0.1% to 0.3% for the filter samples. ICP/AES analyses of test chemical stability in the generation and exposure system were performed on generator reservoir bulk material and filter samples collected at 2 (mice) or 4 (rats) weeks during the 2-year studies; all 18 measured minor elemental contaminants were detected at less than or equal to 0.1% relative to antimony trioxide.

Taken together, these results demonstrated that the exposure atmosphere and generator reservoir samples were in good agreement with the bulk test article, the composition of antimony trioxide was stable in the exposure system, and contamination from metal materials in the exposure system did not occur.

Table H-1. Summary of Chamber Concentrations in the Two-week Inhalation Studies of Antimony Trioxide

	Target Concentration (mg/m^3)	Total Number of Readings	Average Concentration[a] (mg/m^3)
Rat Chambers	3.75	113	3.72 ± 0.26
	7.5	116	7.42 ± 0.40
	15	113	14.7 ± 1.0
	30	113	30.2 ± 1.4
	60	116	59.5 ± 2.9
Mouse Chambers	3.75	123	3.71 ± 0.27
	7.5	126	7.43 ± 0.39
	15	123	14.7 ± 1.1
	30	123	30.2 ± 1.4
	60	126	59.4 ± 2.9

[a]Mean ± standard deviation.

Table H-2. Summary of Chamber Concentrations in the Two-year Inhalation Studies of Antimony Trioxide

	Target Concentration (mg/m^3)	Total Number of Readings	Average Concentration[a] (mg/m^3)
Male Rat Chambers	3	4,914	3.0 ± 0.2
	10	4,916	9.9 ± 0.7
	30	4,937	29.7 ± 2.1
Female Rat Chambers	3	4,953	3.0 ± 0.2
	10	4,951	9.9 ± 0.6
	30	4,932	30.1 ± 1.9
Mouse Chambers	3	4,947	3.0 ± 0.2
	10	4,945	9.9 ± 0.6
	30	4,928	30.1 ± 1.9

[a]Mean ± standard deviation.

Table H-3. Summary of Aerosol Size Measurements for the Rat and Mouse Exposure Chambers in the Two-week Inhalation Studies of Antimony Trioxide

Target Concentration (mg/m^3)	Mass Median Aerodynamic Diameter (μm)	Geometric Standard Deviation
3.75	1.4	1.9
7.5	1.3	1.9
15	1.5	1.9
30	1.4	1.9
60	1.4	1.9

Table H-4. Summary of Aerosol Size Measurements for the Male Rat Exposure Chambers in the Two-year Inhalation Study of Antimony Trioxide

Date of Test	Target Concentration (mg/m^3)	Mass Median Aerodynamic Diameter (µm)	Geometric Standard Deviation
September 2008	3	1.1	2.2
	10	1.2	2.0
	30	1.3	1.8
November 2008	3	1.4	2.2
	10	1.1	2.0
	30	1.1	1.9
December 2008	3	1.2	1.8
	10	1.2	2.0
	30	1.2	2.0
January 2009	3	1.2	1.9
	10	1.2	1.9
	30	1.2	1.9
February 2009	3	1.1	1.9
	10	1.1	2.0
	30	1.2	1.9
March 2009	3	1.1	1.9
	10	1.1	1.9
	30	1.2	1.8
April 2009	3	1.1	2.0
	10	1.2	1.9
	30	1.1	1.9
May 2009	3	1.0	1.9
	10	1.1	1.9
	30	1.1	1.9
June 2009	3	1.1	1.9
	10	1.2	1.9
	30	1.3	1.9
July 2009	3	1.2	1.9
	10	1.3	1.9
	30	1.4	1.9
August 2009	3	1.1	2.0
	10	1.2	2.0
	30	1.4	1.9

Date of Test	Target Concentration (mg/m^3)	Mass Median Aerodynamic Diameter (µm)	Geometric Standard Deviation
September 2009	3	1.1	2.0
	10	1.1	1.9
	30	1.2	1.9
October 2009	3	1.2	1.9
	10	1.3	2.0
	30	1.3	1.9
November 2009	3	1.1	1.9
	10	1.3	1.9
	30	1.3	1.9
December 2009	3	1.2	2.0
	10	1.3	1.9
	30	1.3	1.9
January 2010	3	1.2	1.9
	10	1.3	1.8
	30	1.3	1.9
February 2010	3	1.3	1.8
	10	1.2	2.0
	30	1.4	1.9
March 2010	3	1.1	1.9
	10	1.2	1.9
	30	1.1	1.9
April 2010	3	1.2	2.1
	10	1.3	2.0
	30	1.3	1.9
May 2010	3	1.2	2.0
	10	1.3	1.9
	30	1.3	1.9
June 2010	3	1.2	1.9
	10	1.3	2.0
	30	1.4	1.8
July 2010	3	1.3	1.9
	10	1.2	2.0
	30	1.3	1.9
August 2010	3	1.2	2.0
	10	1.3	1.9

Date of Test	Target Concentration (mg/m^3)	Mass Median Aerodynamic Diameter (µm)	Geometric Standard Deviation
	30	1.4	1.9
September 2010	3	1.2	1.9
	10	1.2	1.9
	30	1.3	1.9
Range	3	1.0–1.4	1.8–2.2
	10	1.1–1.3	1.8–2.0
	30	1.1–1.4	1.8–2.0

Table H-5. Summary of Aerosol Size Measurements for the Female Rat and Male and Female Mouse Exposure Chambers in the Two-year Inhalation Studies of Antimony Trioxide

Date of Test	Target Concentration (mg/m^3)	Mass Median Aerodynamic Diameter (µm)	Geometric Standard Deviation
October 2008	3	1.3	1.8
	10	1.3	1.9
	30	1.2	1.9
November 2008	3	0.9	2.0
	10	1.1	1.9
	30	0.9	2.0
December 2008	3	1.3	1.9
	10	1.3	1.9
	30	1.3	1.9
January 2009	3	1.2	1.9
	10	1.3	1.9
	30	1.3	1.8
February 2009	3	1.1	2.0
	10	1.2	1.9
	30	1.2	2.0
March 2009	3	1.2	1.9
	10	1.3	1.9
	30	1.2	1.9
April 2009	3	1.1	1.9
	10	1.1	2.0
	30	1.2	2.0
May 2009	3	1.1	2.0
	10	1.1	2.0

Date of Test	Target Concentration (mg/m^3)	Mass Median Aerodynamic Diameter (µm)	Geometric Standard Deviation
	30	1.3	2.0
June 2009	3	1.1	1.9
	10	1.2	2.0
	30	1.3	2.0
July 2009	3	1.1	1.9
	10	1.2	1.9
	30	1.2	2.0
August 2009	3	1.2	2.0
	10	1.0	2.0
	30	1.1	2.0
September 2009	3	1.4	1.9
	10	1.0	2.0
	30	1.3	1.9
October 2009	3	1.1	2.0
	10	1.1	2.0
	30	1.2	1.9
November 2009	3	1.2	2.0
	10	1.4	1.7
	30	1.2	2.0
December 2009	3	1.2	1.9
	10	1.3	1.9
	30	1.4	1.9
January 2010	3	1.0	2.0
	10	1.1	2.0
	30	1.2	1.9
February 2010	3	1.2	1.9
	10	1.4	2.0
	30	1.2	1.9
March 2010	3	1.4	1.9
	10	1.3	2.0
	30	1.3	2.0
April 2010	3	1.1	2.0
	10	1.2	1.9
	30	1.0	2.1
May 2010	3	1.1	2.0

Date of Test	Target Concentration (mg/m^3)	Mass Median Aerodynamic Diameter (µm)	Geometric Standard Deviation
	10	1.3	1.9
	30	1.4	1.9
June 2010	3	1.4	2.1
	10	1.3	1.9
	30	1.4	1.9
July 2010	3	1.2	1.9
	10	1.3	2.0
	30	1.3	2.0
August 2010	3	1.5	2.0
	10	1.4	1.9
	30	1.5	1.9
September 2010	3	1.2	1.9
	10	1.2	1.9
	30	1.3	1.8
Range	3	0.9–1.5	1.8–2.1
	10	1.0–1.4	1.7–2.0
	30	0.9–1.5	1.8–2.1

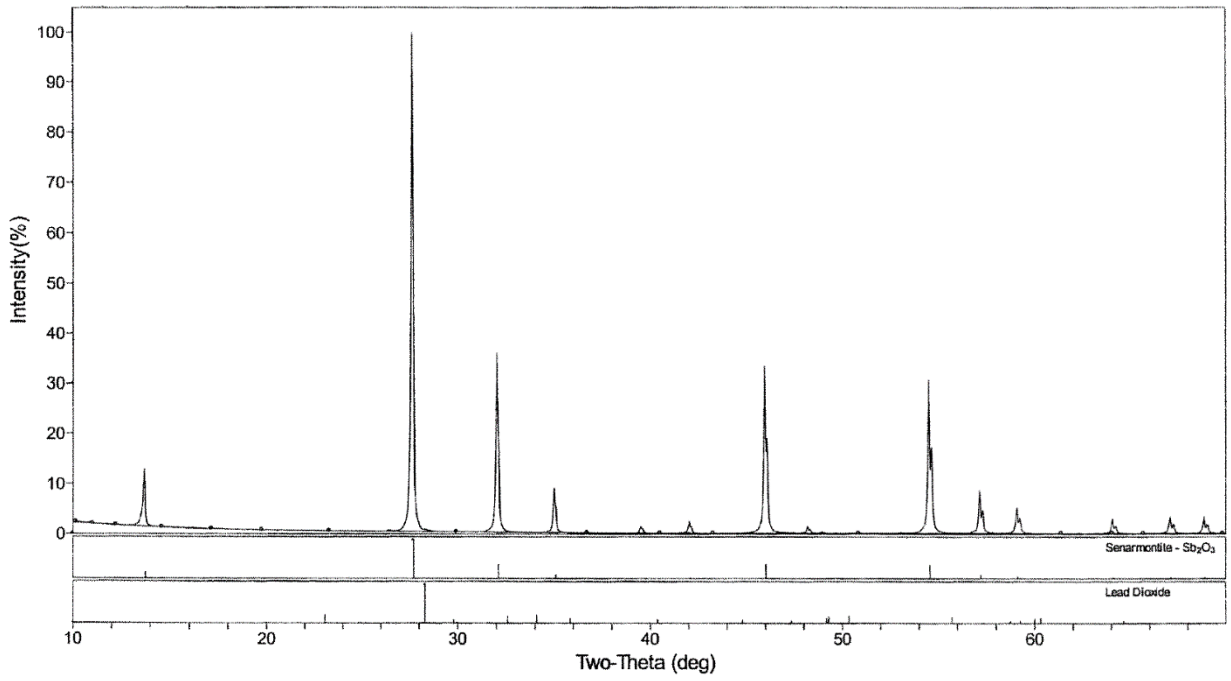

Figure H-1. X-ray Diffraction Pattern of Antimony Trioxide

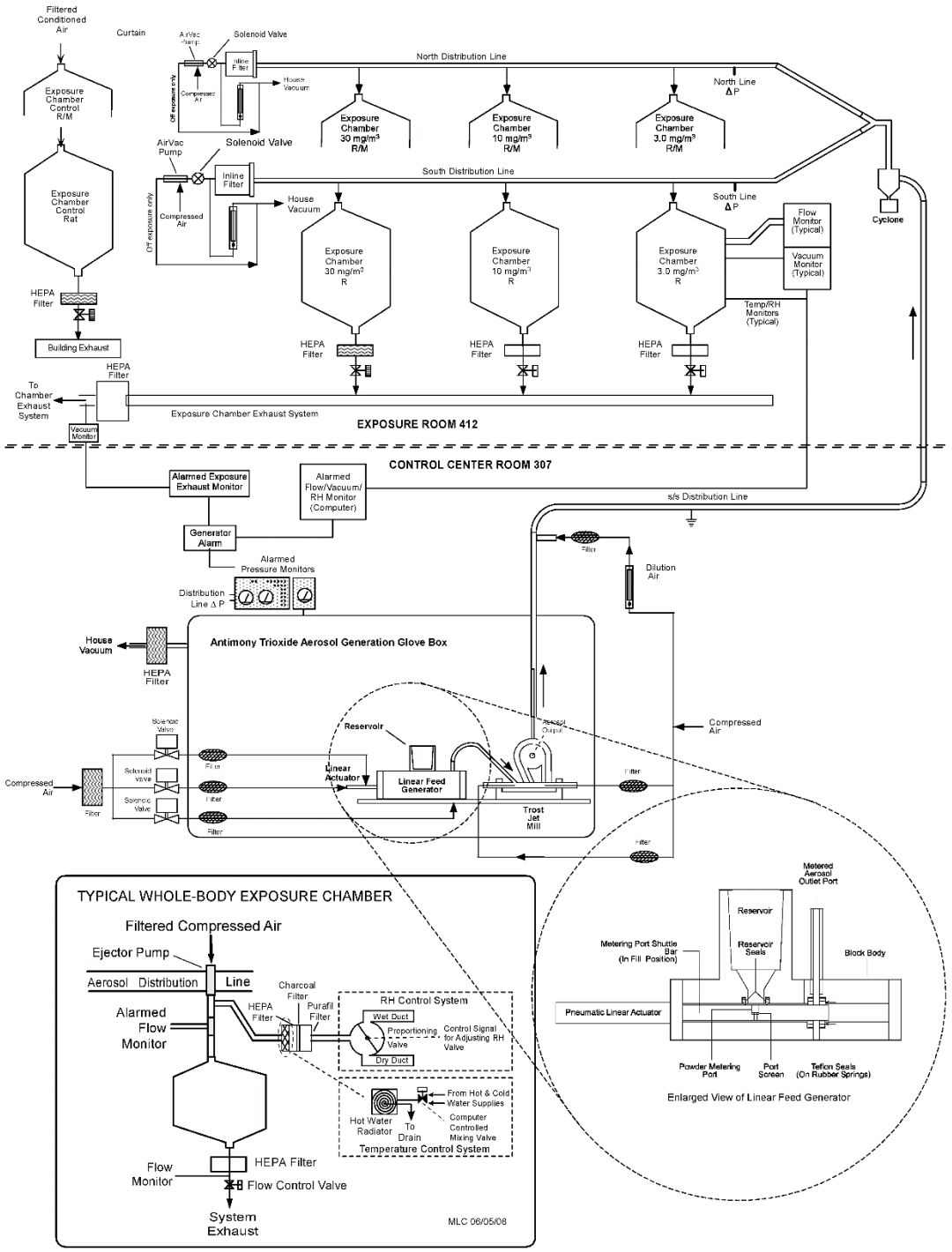

Figure H-2. Schematic of the Aerosol Generation and Delivery System in the Inhalation Studies of Antimony Trioxide

The exposure chamber configuration shown is for the 2-year studies.

Appendix I. Ingredients, Nutrient Composition, and Contaminant Levels in NTP-2000 Rat and Mouse Ration

Tables

Table I-1. Ingredients of NTP-2000 Rat and Mouse Ration.....I-2
Table I-2. Vitamins and Minerals in NTP-2000 Rat and Mouse Ration I-2
Table I-3. Nutrient Composition of NTP-2000 Rat and Mouse Ration.....I-3
Table I-4. Contaminant Levels in NTP-2000 Rat and Mouse Ration.....I-4

Table I-1. Ingredients of NTP-2000 Rat and Mouse Ration

Ingredients	Percent by Weight
Ground hard winter wheat	22.26
Ground #2 yellow shelled corn	22.18
Wheat middlings	15.0
Oat hulls	8.5
Alfalfa meal (dehydrated, 17% protein)	7.5
Purified cellulose	5.5
Soybean meal (49% protein)	5.0
Fish meal (60% protein)	4.0
Corn oil (without preservatives)	3.0
Soy oil (without preservatives)	3.0
Dried brewer's yeast	1.0
Calcium carbonate (USP)	0.9
Vitamin premix[a]	0.5
Mineral premix[b]	0.5
Calcium phosphate, dibasic (USP)	0.4
Sodium chloride	0.3
Choline chloride (70% choline)	0.26
Methionine	0.2

[a]Wheat middlings as carrier.
[b]Calcium carbonate as carrier.

Table I-2. Vitamins and Minerals in NTP-2000 Rat and Mouse Ration[a]

	Amount	Source
Vitamins		
A	4,000 IU	Stabilized vitamin A palmitate or acetate
D	1,000 IU	D-activated animal sterol
K	1.0 mg	Menadione sodium bisulfite complex
α-Tocopheryl acetate	100 IU	–
Niacin	23 mg	–
Folic acid	1.1 mg	–
d-Pantothenic acid	10 mg	*d*-Calcium pantothenate
Riboflavin	3.3 mg	–
Thiamine	4 mg	Thiamine mononitrate
B12	52 µg	–
Pyridoxine	6.3 mg	Pyridoxine hydrochloride
Biotin	0.2 mg	*d*-Biotin

	Amount	Source
Minerals		
Magnesium	514 mg	Magnesium oxide
Iron	35 mg	Iron sulfate
Zinc	12 mg	Zinc oxide
Manganese	10 mg	Manganese oxide
Copper	2.0 mg	Copper sulfate
Iodine	0.2 mg	Calcium iodate
Chromium	0.2 mg	Chromium acetate

[a]Per kg of finished product.

Table I-3. Nutrient Composition of NTP-2000 Rat and Mouse Ration

Nutrient	Mean ± Standard Deviation	Range	Number of Samples
Protein (% by weight)	14.6 ± 0.53	13.7–15.9	26
Crude fat (% by weight)	8.3 ± 0.24	7.7–8.6	26
Crude fiber (% by weight)	9.3 ± 1.02	7.1–11.8	26
Ash (% by weight)	5.1 ± 0.14	4.9–5.4	26
Amino Acids (% of total diet)			
Arginine	0.789 ± 0.071	0.67–0.97	24
Cystine	0.219 ± 0.023	0.15–0.25	24
Glycine	0.700 ± 0.039	0.62–0.80	24
Histidine	0.349 ± 0.075	0.27–0.68	24
Isoleucine	0.546 ± 0.042	0.43–0.66	24
Leucine	1.095 ± 0.064	0.96–1.24	24
Lysine	0.703 ± 0.114	0.31–0.86	24
Methionine	0.409 ± 0.044	0.26–0.49	24
Phenylalanine	0.628 ± 0.038	0.54–0.72	24
Threonine	0.507 ± 0.041	0.43–0.61	24
Tryptophan	0.151 ± 0.028	0.11–0.20	24
Tyrosine	0.409 ± 0.064	0.28–0.54	24
Valine	0.664 ± 0.042	0.55–0.73	24
Essential Fatty Acids (% of total diet)			
Linoleic	3.96 ± 0.250	3.49–4.55	24
Linolenic	0.30 ± 0.031	0.21–0.35	24
Vitamins			
Vitamin A (IU/kg)	3,795 ± 92	2,110–5,720	26
Vitamin D (IU/kg)	1,000[a]	–	–

Nutrient	Mean ± Standard Deviation	Range	Number of Samples
α-Tocopherol (ppm)	79.7 ± 21.28	27.0–124.0	24
Thiamine (ppm)[b]	7.3 ± 1.17	5.3–11.0	26
Riboflavin (ppm)	7.9 ± 2.96	4.20–17.50	24
Niacin (ppm)	78.9 ± 8.86	66.4–98.2	24
Pantothenic acid (ppm)	27 ± 12.08	17.4–81.0	24
Pyridoxine (ppm)[b]	9.58 ± 1.91	6.44–13.7	24
Folic acid (ppm)	1.6 ± 0.47	1.15–3.27	24
Biotin (ppm)	0.32 ± 0.10	0.20–0.704	24
Vitamin B12 (ppb)	52.8 ± 38.0	18.3–174.0	24
Choline (ppm)[b]	2,733 ± 608	1,160–3,790	24
Minerals			
Calcium (%)	0.910 ± 0.043	0.810–0.994	26
Phosphorus (%)	0.557 ± 0.031	0.490–0.630	26
Potassium (%)	0.669 ± 0.031	0.626–0.733	24
Chloride (%)	0.384 ± 0.038	0.300–0.474	24
Sodium (%)	0.193 ± 0.024	0.160–0.283	24
Magnesium (%)	0.217 ± 0.059	0.185–0.490	24
Sulfur (%)	0.170 ± 0.029	0.116–0.209	14
Iron (ppm)	188 ± 38.3	135–311	24
Manganese (ppm)	51.2 ± 9.99	21.0–73.1	24
Zinc (ppm)	59.02 ± 27.84	43.3–184	24
Copper (ppm)	7.28 ± 2.635	3.21–16.3	24
Iodine (ppm)	0.504 ± 0.197	0.158–0.972	24
Chromium (ppm)	0.683 ± 0.270	0.330–1.380	24
Cobalt (ppm)	0.242 ± 0.162	0.094–0.864	24

[a]From formulation.
[b]As hydrochloride (thiamine and pyridoxine) or chloride (choline).

Table I-4. Contaminant Levels in NTP-2000 Rat and Mouse Ration[a]

	Mean ± Standard Deviation[b]	Range	Number of Samples
Contaminants			
Arsenic (ppm)	0.24 ± 0.039	0.16–0.31	26
Cadmium (ppm)	0.06 ± 0.010	0.04–0.01	26
Lead (ppm)	0.1 ± 0.160	0.06–0.89	26
Mercury (ppm)	<0.02	–	26
Selenium (ppm)	0.2 ± 0.045	0.14–0.34	26
Aflatoxins (ppb)	<5.00	–	26

	Mean ± Standard Deviation[b]	Range	Number of Samples
Nitrate nitrogen (ppm)c	19.89 ± 7.81	10.0–35.9	26
Nitrite nitrogen (ppm)c	<0.61	–	26
BHA (ppm)d	<1.0	–	26
BHT (ppm)d	<1.0	–	26
Aerobic plate count (CFU/g)	10 ± 0.0	10	26
Coliform (MPN/g)	3.0 ± 0.0	3.0	26
Escherichia coli (MPN/g)	<10	–	26
Salmonella (MPN/g)	Negative	–	26
Total nitrosoamines (ppb)e	9.5 ± 4.20	2.0–17.2	26
N-Nitrosodimethylamine (ppb)e	2.9 ± 2.70	0.9–11.1	26
N-Nitrosopyrrolidine (ppb)e	7.2 ± 2.80	1.0–11.2	26
Pesticides (ppm)			
α-BHC	<0.01	–	26
β-BHC	<0.02	–	26
γ-BHC	<0.01	–	26
δ-BHC	<0.01	–	26
Heptachlor	<0.01	–	26
Aldrin	<0.01	–	26
Heptachlor epoxide	<0.01	–	26
DDE	<0.01	–	26
DDD	<0.01	–	26
DDT	<0.01	–	26
HCB	<0.01	–	26
Mirex	<0.01	–	26
Methoxychlor	<0.05	–	26
Dieldrin	<0.01	–	26
Endrin	<0.01	–	26
Telodrin	<0.01	–	26
Chlordane	<0.05	–	26
Toxaphene	<0.10	–	26
Estimated PCBs	<0.20	–	26
Ronnel	<0.01	–	26
Ethion	<0.02	–	26
Trithion	<0.05	–	26
Diazinon	<0.10	–	26
Methyl chlorpyrifos	0.131 ± 0.120	0.020–0.553	26

	Mean ± Standard Deviation[b]	Range	Number of Samples
Methyl parathion	<0.02	–	26
Ethyl parathion	<0.02	–	26
Malathion	0.117 ± 0.094	0.02–0.40	26
Endosulfan I	<0.01	–	26
Endosulfan II	<0.01	–	26
Endosulfan sulfate	<0.03	–	26

[a]All samples were irradiated. CFU = colony-forming units; MPN = most probable number; BHC = hexachlorocyclohexane or benzene hexachloride.
[b]For values less than the limit of detection, the detection limit is given as the mean.
[c]Sources of contamination: alfalfa, grains, and fish meal.
[d]Sources of contamination: soy oil and fish meal.
[e]All values were corrected for percent recovery.

Appendix J. Sentinel Animal Program

Table of Contents

J.1. Methods J-2
J.2. Results J-4

Tables

Table J-1. Laboratory Methods and Agents Tested for in the Sentinel Animal Program J-2

J.1. Methods

Rodents used in the National Toxicology Program are produced in optimally clean facilities to eliminate potential pathogens that may affect study results. The Sentinel Animal Program is part of the periodic monitoring of animal health that occurs during the toxicologic evaluation of test compounds. Under this program, the disease state of the rodents is monitored via sera or feces from extra (sentinel) or dosed animals in the study rooms. The sentinel animals and the study animals are subject to identical environmental conditions. Furthermore, the sentinel animals come from the same production source and weanling groups as the animals used for the studies of test compounds.

Blood samples were collected from each animal and allowed to clot and the serum was separated. Additionally, fecal samples were collected and tested for *Helicobacter* species. All samples were processed appropriately with serology testing performed in-house or sent to the Research Animal Diagnostic Laboratory, University of Missouri, Columbia, MO, for determination of the presence of pathogens. The laboratory methods and agents for which testing was performed are tabulated below; the times at which samples were collected during the studies are also listed.

Blood was collected from five animals per sex per time point except for the following: 18-month collection – five male rats and four female rats; 18-month collection – four male mice and five female mice.

Table J-1. Laboratory Methods and Agents Tested for in the Sentinel Animal Program

Method and Test	Time of Collection
Rats	
Two-week Study	
ELISA	
Mycoplasma pulmonis	2 weeks
PVM (pneumonia virus of mice)	2 weeks
RCV/SDA(rat coronavirus/sialodacryoadenitis virus)	2 weeks
RPV (rat parvovirus)	2 weeks
Sendai	2 weeks
Two-year Study	
ELISA	
M. pulmonis	2 weeks
PVM	2 weeks
RCV/SDA	2 weeks
RPV	2 weeks
Sendai	2 weeks
Multiplex Fluorescent Immunoassay	
KRV (Kilham's rat virus)	6, 12, and 18 months, study termination

Method and Test	Time of Collection
M. pulmonis	6, 12, and 18 months, study termination
Parvo NS-1	6, 12, and 18 months, study termination
PVM	6, 12, and 18 months, study termination
RCV/SDA	6, 12, and 18 months, study termination
RMV (rat minute virus)	6, 12, and 18 months, study termination
RPV	6, 12, and 18 months, study termination
RTV (rat theilovirus)	6, 12, and 18 months, study termination
Sendai	6, 12, and 18 months, study termination
TMEV (Theiler's murine encephalomyelitis virus)	6, 12, and 18 months, study termination
Toolan's H-1 virus	6, 12, and 18 months, study termination
Immunofluorescence Assay	
KRV	Study termination
RTV	Study termination
Mice	
Two-week Study	
ELISA	
MHV (mouse hepatitis virus)	2 weeks
MPV (mouse parvovirus)	2 weeks
M. pulmonis	2 weeks
PVM	2 weeks
Sendai	2 weeks
TMEV GDVII (Theiler's murine encephalomyelitis virus – mouse poliovirus, strain GDVII)	2 weeks
Two-year Study	
ELISA	
MHV	2 weeks
MPV	2 weeks
M. pulmonis	2 weeks
PVM	2 weeks
Sendai	2 weeks
TMEV GDVII	2 weeks
Multiplex Fluorescent Immunoassay	
Ectromelia virus	6, 12, and 18 months, study termination
EDIM (epizootic diarrhea of infant mice)	6, 12, and 18 months, study termination
LCMV (lymphocytic choriomeningitis virus)	6, 12, and 18 months, study termination
M. pulmonis	6, 12, and 18 months, study termination

Method and Test	Time of Collection
MHV	6, 12, and 18 months, study termination
MNV (mouse norovirus)	6, 12, and 18 months, study termination
Parvo NS-1	6, 12, and 18 months, study termination
MPV	6, 12, and 18 months, study termination
MVM (minute virus of mice)	6, 12, and 18 months, study termination
PVM	6, 12, and 18 months, study termination
Reovirus	6, 12, and 18 months, study termination
Sendai	6, 12, and 18 months, study termination
TMEV GDVII	6, 12, and 18 months, study termination
Immunofluorescence Assay	
MNV	18 months
TMEV GDVII	18 months
EDIM	Study termination
MVM	Study termination
Polymerase Chain Reaction	
Helicobacter species	18 months

J.2. Results

All test results were negative.

Appendix K. Analysis of *Kras* and *Egfr* Mutations in Wistar Han Rat and B6C3F1/N Mouse Alveolar/Bronchiolar Tumors Resulting from Chronic Inhalation Exposure to Antimony Trioxide

H.L. Hong[1], T.V. Ton[1], G.P. Flake[1], M.D. Stout[2], G.E. Kissling[3], R.C. Kovi[4], R.C. Sills[1], and A.R. Pandiri[1]

[1]Cellular and Molecular Pathology Branch, DNTP, NIEHS, Research Triangle Park, North Carolina, USA

[2]Program Operations Branch, DNTP, NIEHS, Research Triangle Park, North Carolina, USA

[3]Biostatistics and Computational Biology Branch, DIR, NIEHS, Research Triangle Park, North Carolina, USA

[4]Experimental Pathology Laboratories, Inc., Durham, North Carolina, USA

Table of Contents

K.1. Introduction K-3

K.2. Materials and Methods K-4

K.3. Results K-5

K.4. Discussion K-6

Tables

Table K-1. Primers Used to Amplify the Hot Spot Regions of Rat *Kras* and *Egfr* Genes K-7
Table K-2. Primers Used to Amplify the Hot Spot Regions of Mouse *Kras* and *Egfr* Genes K-8
Table K-3. Summary of *Kras* and *Egfr* Mutations in Nontumor Lung Tissue and Alveolar/Bronchiolar Adenomas and Carcinomas from Wistar Han Rats in the Two-year Inhalation Study of Antimony Trioxide K-9
Table K-4. *Kras* and *Egfr* Mutations in Nontumor Lung Tissue and Alveolar/Bronchiolar Adenomas and Carcinomas from Male Wistar Han Rats in the Two-year Inhalation Study of Antimony Trioxide K-9
Table K-5. *Kras* and *Egfr* Mutations in Alveolar/Bronchiolar Adenomas and Carcinomas from Female Wistar Han Rats in the Two-year Inhalation Study of Antimony Trioxide K-11
Table K-6. Summary of *Kras* and *Egfr* Mutations in Nontumor Lung Tissue and Alveolar/Bronchiolar Carcinomas from B6C3F1/N Mice in the Two-year Inhalation Study of Antimony Trioxide K-12

Table K-7. *Kras* and *Egfr* Mutations in Nontumor Lung Tissue and Alveolar/Bronchiolar Carcinomas from Male B6C3F1/N Mice in the Two-year Inhalation Study of Antimony Trioxide K-12
Table K-8. *Kras* and *Egfr* Mutations in Alveolar/Bronchiolar Carcinomas from Female B6C3F1/N Mice in the Two-year Inhalation Study of Antimony Trioxide K-18

K.1. Introduction

In the current studies, chronic exposure of Wistar Han rats and B6C3F1/N mice to antimony trioxide particulates for 2 years resulted in increased incidences of alveolar/bronchiolar adenomas and carcinomas. The incidences of alveolar/bronchiolar adenoma or carcinoma (combined) in Wistar Han rats (males and females, respectively) from each exposure group were 0 mg/m^3 (6%, 0%), 3 mg/m^3 (8%, 4%), 10 mg/m^3 (16%, 12%), and 30 mg/m^3 (16%, 10%) (Table A-2 and Table B-2). The incidences of alveolar/bronchiolar carcinoma in B6C3F1/N mice (males and females, respectively) from each exposure group were 0 mg/m^3 (8%, 4%), 3 mg/m^3 (36%, 28%), 10 mg/m^3 (40%, 22%), and 30 mg/m^3 (54%, 22%) (Table C-2 and Table D-2).

Somatic mutations in some oncogenes such as *Kras* and *Egfr* are commonly noted in human lung cancers. These mutations are also observed in rodent lung tumors that either arise spontaneously or are due to chemical exposure. Most often, the mutation spectra are conserved in tumors resulting from certain chemical exposures and these signatures often serve as biomarkers of exposure and disease. For example, G to T transversions in codon 12 of *Kras* genes are commonly noted in lung cancers resulting from tobacco smoke exposure and also in rodent lung tumors resulting from chronic oxidative stress.

In human non-small cell lung cancer, the incidence of *Kras* mutations is approximately 26% (67/254)[111]. Of these, 86% of the mutations arise within codon 12, and 14% occur in codon 13. Point mutations in codons 12, 13, and 61 of *Kras* are activating mutations that result in constitutive activation of the KRAS protein, making it refractory to the inhibitory GTPase activating proteins, which results in stimulus-independent, persistent activation of downstream effectors, in particular the RAF-MEK-ERK cascade. Constitutive activation of this kinase cascade results in promotion of cellular proliferation and transformation[112; 113].

The incidence of *Egfr* mutations in the non-small cell lung cancer subtype of adenocarcinoma in humans is about 9% (22/254) with the majority (70%) of the mutations located within exons 19 and 21111. EGFR is a transmembrane receptor, which upon ligand binding, dimerizes and activates the cytosolic kinase domain of the receptor tyrosine kinase resulting in activation of signaling pathways that support cancer development and progression. These signaling pathways include the PI3K pathway, which when activated leads to AKT activation and apoptosis inhibition, and the GRB2-SOS pathways, which lead to activation of P21RAS, resulting in cell cycle progression[114].

In the current studies, increased lung weights in the exposed animals were related to the antimony trioxide exposure concentration and duration (Table F-2, Table F-4, Table G-3, and Table G-8). Antimony trioxide lung burden modeling studies in female Wistar Han rats and B6C3F1/N mice suggested that mid and high exposure concentration groups (10 and 30 mg/m^3) in both species may have approached the threshold needed for pulmonary overload (Appendix G). Pulmonary overload is characterized by prolonged pulmonary clearance half-lives, markedly increased lung burdens of the inhaled particulates, and subsequent compromise of pulmonary function. Reduced clearance and marked pulmonary inflammation resulting from inhalation of very high doses of minimally soluble particulates may contribute to neoplasia in the rat[93; 115].

The objective of this study was to determine the somatic point mutations relevant to human lung cancer in lung tumors occurring in rats and mice due to chronic inhalation of antimony trioxide

and also to evaluate any differences in mutations in lung tumors arising in the exposed groups that may have approached the threshold for pulmonary overload.

K.2. Materials and Methods

K.2.1. Lung Tumors

After inhalation exposure to antimony trioxide for 2 years, alveolar/bronchiolar adenomas and carcinomas were obtained from male Wistar Han rats and female B6C3F1/N mice, and alveolar/bronchiolar carcinomas were obtained from female Wistar Han rats and male B6C3F1/N mice. In addition, spontaneous alveolar/bronchiolar neoplasms and nontumor normal lung tissues were acquired from chamber control animals at study termination. Formalin-fixed, paraffin-embedded (FFPE) tissues were used for mutation analysis. The mouse tumors that were selected for mutation analysis were generally greater than 5 mm in diameter, whereas the rat tumors were smaller and scattered throughout the pulmonary parenchyma. The alveolar/bronchiolar tumors were selected for molecular biology analysis based on their overall size and viability (minimal to no necrosis or hemorrhage microscopically) in order to maximize the amount and quality of DNA obtained from the FFPE sections. DNA quality was measured using a Nanodrop spectrophotometer (Thermo Scientific, Wilmington, DE) to calculate the 260/280 nm absorbance ratio, and DNA samples with a purity range of 1.7 to 2.0 were used for analysis. Samples falling outside of this range were reisolated from FFPE sections until a suitable purity measure was obtained or were discarded.

K.2.2. DNA Extraction, Polymerase Chain Reaction, Autosequencing, and Mutation Analysis

Alveolar/bronchiolar tumors (carcinomas from B6C3F1/N mice; adenomas and carcinomas from Wistar Han rats) representing all antimony trioxide exposed groups, spontaneous alveolar/bronchiolar tumors (2 rat adenomas and 9 mouse carcinomas), and nontumor lung tissue from chamber control rats (11) and mice (10) were evaluated for hot spot mutations within specific codons or exons in *Kras* and *Egfr* genes that are relevant in human lung cancer. FFPE sections at 10 µm thickness were collected on glass slides. The neoplasms (single or multiple from the same lung) were dissected with a sharp microtome blade and collected into screw-top tubes. In some cases (especially in rats) where the alveolar/bronchiolar tumors had a miliary distribution and were scattered throughout the pulmonary parenchyma, the entire lung section was used for DNA isolation. DNA was isolated from these FFPE dissected neoplasm tissue sections with the DNeasy® Tissue Kit (Qiagen, Valencia, CA). Amplification reactions were carried out by seminested polymerase chain reaction (PCR) using primer sets designed for *Kras* (exons 1 and 2), and *Egfr* (exons 18 to 21) (Table K-1 and Table K-2). Controls lacking template DNA were run with all sets of reactions. PCR products were purified using a QIAquick® Gel Extraction Kit (Qiagen). The purified products were cycled with Terminal Ready Reaction Mix-Big Dye® (PerkinElmer, Foster City, CA), and the extension products were purified with the DyeEx® 2.0 SpinKit (Qiagen). The lyophilized PCR products were sequenced with an automatic sequencer (Perkin-Elmer ABI Model 3100)116. The resulting electropherograms were compared to identify mutations in alveolar/bronchiolar neoplasms that either arose spontaneously or were due to antimony trioxide exposure.

K.2.3. Statistics

To test for significance of exposure concentration-related trends in the incidences of mutations, a one-sided Cochran-Armitage trend test was conducted. One-sided Fisher's exact tests were conducted to test for significant differences in the proportions of mutations between the chamber control and various exposed groups.

K.3. Results

K.3.1. Rats

The incidences of *Kras* and *Egfr* mutations in alveolar/bronchiolar tumors in Wistar Han rats exposed to antimony trioxide by inhalation for 2 years were 4% (1/26) and 50% (13/26), respectively (Table K-3, Table K-4, and Table K-5). No *Kras* or *Egfr* mutations were noted in alveolar/bronchiolar tumors that arose spontaneously or in age-matched nontumor lung tissues. The *Kras* mutation (A to G transition) that occurred in the single antimony trioxide exposed alveolar/bronchiolar tumor was in exon 1, codon 16, a non-hot spot location for *Kras* mutations. The *Egfr* mutations were localized within exons 18 to 21 and all of them were transition mutations.

The tissue burden modeling studies (Appendix G) estimated that the mid- and high-exposure concentration groups may have approached the threshold for pulmonary overload. The incidences of *Kras* mutations in alveolar/bronchiolar tumors in groups without (3 mg/m^3) and with (10 and 30 mg/m^3) pulmonary overload were 0% (0/5) and 5% (1/21), respectively, whereas, the incidences of *Egfr* mutations in alveolar/bronchiolar tumors in groups without (3 mg/m^3) and with (10 and 30 mg/m^3) pulmonary overload were 60% (3/5) and 48% (10/21), respectively (Table K-3).

K.3.2. Mice

The incidences of *Kras* and *Egfr* mutations in alveolar/bronchiolar tumors in B6C3F1/N mice exposed to antimony trioxide by inhalation for 2 years were 43% (34/80) and 46% (37/80), respectively (Table K-3, Table K-7, and Table K-8). The majority of the *Kras* mutations were located in codon 12 and were G to A transitions. The *Egfr* mutations were mainly located within exons 18 and 20 and were transition mutations. The incidences of *Kras* mutations were 33% (3/9) and 0% (0/10) in spontaneous alveolar/bronchiolar carcinomas and age-matched nontumor lung tissues, respectively. All three *Kras* mutations in spontaneous alveolar/bronchiolar carcinomas were G to A transitions. No *Egfr* mutations were noted in either spontaneous alveolar/bronchiolar carcinomas or non-tumor lung tissues.

The tissue burden modeling studies (Appendix G) estimated that the mid- and high-dose groups may have approached the threshold for pulmonary overload. The incidences of *Kras* mutations in alveolar/bronchiolar tumors in groups without (3 mg/m^3) and with (10 and 30 mg/m^3) pulmonary overload were 32% (9/28) and 48% (25/52), respectively, whereas, the incidences of *Egfr* mutations in alveolar/bronchiolar tumors in groups without (3 mg/m^3) and with (10 and 30 mg/m^3) pulmonary overload were 39% (11/28) and 50% (26/52), respectively (Table K-6).

K.4. Discussion

Kras mutations were common in antimony trioxide-exposed alveolar/bronchiolar tumors in B6C3F1/N mice but not in alveolar/bronchiolar tumors in Wistar Han rats. The only *Kras* mutation in the single alveolar/bronchiolar tumor in the rats was present in the atypical codon 16. In contrast, *Kras* mutations in mouse alveolar/bronchiolar tumors that occurred due to chronic exposure to antimony trioxide were located mainly in codon 12 and were mainly G to A transitions. These G to A transitions of *Kras* mutations are also common in spontaneous alveolar/bronchiolar carcinomas[116] and suggest that antimony trioxide exposure may have enhanced the proliferation of clones harboring the spontaneous mutations. Rat and mouse alveolar/bronchiolar adenomas and carcinomas from exposures that did and did not approach the threshold for pulmonary overload did not have significant differences in the incidences or types of *Kras* or *Egfr* mutations.

Interestingly, the alveolar/bronchiolar tumors resulting from chronic antimony trioxide exposure in both rats and mice harbored mutations in the *Egfr* gene. Both KRAS and EGFR are major components of the MAPK signaling pathway, but the antimony trioxide induced tumors seem to preferentially harbor *Egfr* mutations in both species. These results suggest that EGFR signaling plays an important role in the pulmonary carcinogenesis resulting from chronic antimony trioxide exposure in both rats and mice. These findings may be relevant in the context of human lung cancers since the demographics, etiology, and prognosis of lung cancers harboring *Egfr* mutations are different from those harboring *Kras* mutations[117-119].

Table K-1. Primers Used to Amplify the Hot Spot Regions of Rat *Kras* and *Egfr* Genes

Exon	Codon	Primer	Strand	Sequence
1	*Kras*-12-13	R*Kras*F25849	Sense	5′-AAAGTACTTGATAATTCTTGTGTGG-3′
		R*Kras*R25489	Antisense	5′-AGAAGTGGGGTTCCTTGCACCG-3′
		R*Kras*R25497	Antisense	5′-GGTTCCTTGCACCGATGGTTCCC-3′
2	*Kras*-61	R*Kras*F14399	Sense	5′-GCTCTGCCTATTTGGACTGGG-3′
		R*Kras*F14444	Sense	5′-CGAGTGCTTGCTGACCACTTG-3′
		R*Kras*R13986	Antisense	5′-CAGGAATTCTACATACTTGACAC-3′
18	*Egfr*-689-729	R*Egfr*18F144600	Sense	5′-TGCGTGTAGCATATTGTG-3′
		R*Egfr*18F144640	Sense	5′-GTCTGCTCCCTTCTTCAC-3′
		R*Egfr*18R144843	Antisense	5′-GGAGAGTACAGCAAATAC-3′
		R*Egfr*18R144823	Antisense	5′-GTTCCCAGAAGCCTAGTC-3′
19	*Egfr*-730-762	R*Egfr*19F146377	Sense	5′-ACAAGGCAACATGCTGCTG-3′
		R*Egfr*19F146412	Sense	5′-TTAATGTCAGCCCTCTTC-3′
		R*Egfr*19R146605	Antisense	5′-ACACAAACTAAGGAAGCAAGAC-3′
		R*Egfr*19R146583	Antisense	5′-TGACTATAGGAAACCGTG-3′
20	*Egfr*-763-824	R*Egfr*20F150643	Sense	5′-ACATGTGTTGTCCTTACC-3′
		R*Egfr*20R150924	Antisense	5′-ATTCATCCTGCTTCTGAAACC-3′
		R*Egfr*20R150905	Antisense	5′-CCTGCTATTGGCTCTTTG-3′
21	*Egfr*-825-876	R*Egfr*21F162616	Sense	5′-TGGTTCACTTCCCTCACTG-3′
		R*Egfr*21R162634	Antisense	5′-AAGCGTCTTCTGTGTTTC-3′
		R*Egfr*21R162838	Antisense	5′-ATGCTTCCTGACTTATTCTC-3′

Table K-2. Primers Used to Amplify the Hot Spot Regions of Mouse *Kras* and *Egfr* Genes

Exon	Codon	Primer	Strand	Sequence
1	*Kras*-12-13	M*Kras*12AOS	Sense	5′-TTATTGTAAGGCCTGCTGAA-3′
		M*Kras*12AOA	Antisense	5′-GCAGCGTTACCTCTATCGTA-3′
		M*Kras*12AIS	Sense	5′-ATGACTGAGTATAAACTTGT-3′
		M*Kras*12AIA	Antisense	5′-TCGTACTCATCCACAAAGTG-3′
2	*Kras*-61	M*Kras*61OS	Sense	5′-TTCTCAGGACTCCTACAGGA-3′
		M*Kras*61OA	Antisense	5′-ACCCACCTATAATGGTGAAT-3′
		MAPK61IS	Sense	5′-TACAGGAAACAAGTAGTAATTGATGGAGAA-3′
		MAPK61IA	Antisense	5′-ATAATGGTGAATATCTTCAAATGATTTAGT-3′
18	*Egfr*-688-728	M*Egfr*18F138871	Sense	5′-ATGCTATTAGGAGTTGGA-3′
		M*Egfr*18F138893	Sense	5′-CTGGCTCAGAATGAATCTAC-3′
		M*Egfr*18R139205	Antisense	5′-CACAGCAAACACTGGTTC-3′
		M*Egfr*18R139157	Antisense	5′-GTCTCCAGGAAGCCTAGT-3′
19	*Egfr*-729-761	M*Egfr*19F140736	Sense	5′-CCAGCTCACAAGGCAACA-3′
		M*Egfr*19F140773	Sense	5′-TCAAGTTAATGTCAGCCC-3′
		M*Egfr1*9R140986	Antisense	5′-GAACTAAGGAAGCAAGATTG-3′
20	*Egfr*-762-823	M*Egfr*20F144618	Sense	5′-CCAGAAAGGGATATGCGT-3′
		M*Egfr*20F144669	Sense	5′-CATCTATTGTCCTTACCTTG-3′
		M*Egfr*20R144989	Antisense	5′-GGAAGACCACAAGTCAAAG-3′
		M*Egfr*20R144917	Antisense	5′-CTTTGGGTACTTCAGTGG-3′
21	*Egfr*-824-875	M*Egfr*21F152001	Sense	5′-GTGGATTTAACCCTGTGTTC-3′
		M*Egfr*21F152063	Sense	5′-GATGGTTCACTCCCTCAC-3′
		M*Egfr*21R152302	Antisense	5′-TGGGCTGTCAGGAAAATG-3′

Table K-3. Summary of *Kras* and *Egfr* Mutations in Nontumor Lung Tissue and Alveolar/Bronchiolar Adenomas and Carcinomas from Wistar Han Rats in the Two-year Inhalation Study of Antimony Trioxide[a]

Tissue:	Antimony Trioxide Concentration	Mutation Frequency[b]		*Kras* Codon	*Egfr* Exons			
		Kras	*Egfr*	16	18	19	20	21
Nontumor lung:	0 mg/m^3	0/11 (0)	0/11 (0)	0	0	0	0	0
Lung tumors:	0 mg/m^3	0/4 (0)	0/4 (0)	0	0	0	0	0
	3 mg/m^3	0/5 (0)	3[c]/5 (60)	0	2	2	0	1
	10 mg/m^3	1/11 (9)	6/11 (55)	1	2	2	1	1
	30 mg/m^3	0/10 (0)	4/10 (40)	0	0	1	2	1
All exposed groups combined		1/26 (4)	13[c]/26 (50)	1	4	5	3	3
Without pulmonary overload		0/5 (0)	3[c]/5 (60)	0	2	2	0	1
With pulmonary overload		1/21 (5)	10/21 (48)	1	2	3	3	2

[a]Male and female Wistar Han rats were exposed to 0, 3, 10, or 30 mg/m^3 antimony trioxide daily by inhalation for 2 years. Silent mutations are not included. There were no significant differences from the chamber control group by the one-sided Fisher's exact test and no significant exposure-concentration trend by the Cochran-Armitage trend test.
[b]Number of tissues with mutations/number of tissues assayed (% with mutation).
[c]Same animal with double mutations (M246 with *Egfr* 19 and 21; M257 with *Egfr* 18 and 19).

Table K-4. *Kras* and *Egfr* Mutations in Nontumor Lung Tissue and Alveolar/Bronchiolar Adenomas and Carcinomas from Male Wistar Han Rats in the Two-year Inhalation Study of Antimony Trioxide[a]

Sample/ Animal #	Dose (mg/m^3)/ Dx	*Kras*		*Egfr*			
		Codon 16	Codon 57	Exon 18	Exon 19	Exon 20	Exon 21
1/M4	0 N	NM	NM	NM	NM	NM	NM
2/M12	0 N	NM	NM	NM	NM	NM	NM
3/M14	0 N	NM	NM	NM	NM	NM	NM
4/M15	0 N	NM	NM	NM	NM	NM	NM
5/M16	0 N	NM	NM	NM	NM	NM	NM
6/M17	0 N	NM	NM	NM	NM	NM	NM
7/M25	0 N	NM	NM	NM	NM	NM	NM
8/M21	0 N	NM	NM	NM	NM	NM	NM
9/M22	0 N	NM	NM	NM	NM	NM	NM
10/M50	0 N	NM	NM	NM	NM	NM	NM
11/M20	0 Ad	NM	NM	NM	NM	NM	NM
12/M24	0 Ad	NM	NM	NM	**Codon 736** GGC→GGT (Gly→Gly)	NM	NM
13/M59	0 N	NM	NM	NM	NM	NM	NM

Sample/ Animal #	Dose (mg/m^3)/ Dx	*Kras*		*Egfr*			
		Codon 16	**Codon 57**	**Exon 18**	**Exon 19**	**Exon 20**	**Exon 21**
14/M246	3 Ad	NM	NM	NM	**Codon 761** CTT→CCT (Leu→Pro)	NM	**Codon 858** GGA→AGA (Gly→Arg)
15/M257	3 Ad	NM	NM	**Codon 720** GGT→AGT (Gly→Ser)	**Codon 749** AGA→AAA (Arg→Lys)	NM	NM
16/M426	10 Ad	NM	NM	**Codon 691** GAA→AAA (Glu→Lys)	NM	NM	NM
17/M452	10 Ad	NM	NM	**Codon 723** GCA→GTA (Ala→Val)	NM	NM	**Codon 870** TAC→TAT (Tyr→Tyr)
18/M404	10 Ca	NM	NM	NM	**Codon 742** CCT→CTT (Pro→Leu)	NM	NM
19/M412	10 Ad	NM	NM	NM	NM	NM	NM
20/M417	10 Ca	NM	NM	NM	NM	NM	NM
21/M425	10 Ad	NM	NM	NM	NM	**Codon 787** GTC→GCC (Val→Ala)	NM
22/M611	30 Ad	NM	GAC→GAT (Asp→Asp)	NM	NM	NM	NM
23/M624	30 Ad	NM	NM	NM	**Codon 742** CCT→CTT (Pro→Leu)	NM	NM
24/M626	30 Ad	NM	NM	NM	NM	NM	**Codon 836** CAC→CGC (His→Arg)
25/M632	30 Ad	NM	NM	NM	NM	NM	NM
26/M658	30 Ad	NM	NM	NM	NM	NM	NM

[a]Rats were exposed to 0, 3, 10, or 30 mg/m^3 antimony trioxide daily by inhalation for 2 years. Alveolar/bronchiolar adenomas and carcinomas were included.
N = no neoplasm; NM = no mutation; Ad = adenoma; Ca = carcinoma. No *Kras* mutations were detected at codon 12, 13, or 61.

Table K-5. *Kras* and *Egfr* Mutations in Alveolar/Bronchiolar Adenomas and Carcinomas from Female Wistar Han Rats in the Two-year Inhalation Study of Antimony Trioxide[a]

Sample/ Animal #	Dose (mg/m^3)/ Dx	*Kras*		*Egfr*			
		Codon 16	Codon 57	Exon 18	Exon 19	Codon 16	Codon 57
1/F316	3/Ad	NM	NM	**Codon 697** GGA→GAA (Gly→Glu)	NM	NM	NM
2/F319	3/Ad	NM	NM	NM	NM	NM	NM
3/F342	3/Ad*	NM	NM	NM	**Codon 755** AAA→AAG (Lys→Lys)	NM	NM
4/F512	10/Ad	NM	NM	NM	**Codon 741** ATC→ACC (Ile→Thr)	**Codon 804** CGA→AGA (Arg→Arg)	NM
5/F529	10/Ad	NM	NM	NM	NM	NM	NM
6/F535	10/Ad	NM	NM	NM	NM	NM	NM
7/F541	10/Ad	AAG→GAG (Lys→Glu)	NM	NM	NM	NM	**Codon 861** AAA→GAA (Lys→Glu)
8/F512	10/Ad	NM	NM	NM	NM	NM	NM
9/F737	30/Ad	NM	NM	NM	NM	NM	NM
10/F720	30/Ad	NM	NM	NM	NM	NM	NM
11/F725	30/Ad	NM	NM	NM	NM	**Codon 808** GAC→GGC (Asp→Gly)	NM
12/F760	30/Ca*	NM	NM	NM	NM	**Codon 820** GTG→ATG (Val→Met)	NM
13/F711	30/Ad	NM	NM	NM	NM	NM	NM

[a]Rats were exposed to 0, 3, 10, or 30 mg/m^3 antimony trioxide daily by inhalation for 2 years. Alveolar/bronchiolar adenomas and carcinomas were included.
NM = no mutation; Ad = adenoma; Ca = carcinoma.
*Pathology Working Group downgraded the diagnosis to marked hyperplasia. No *Kras* mutations were detected at codon 12, 13, or 61.

Table K-6. Summary of *Kras* and *Egfr* Mutations in Nontumor Lung Tissue and Alveolar/Bronchiolar Carcinomas from B6C3F1/N Mice in the Two-year Inhalation Study of Antimony Trioxide[a]

Tissue:	Antimony Trioxide Concentration	Mutation Frequency[b]		*Kras* Codons					*Egfr* Exons			
		Kras	*Egfr*	12	13	14	60	61	18	19	20	21
Nontumor lung:	0 mg/m^3	0/10 (0)	0/10 (0)	0	0	0	0	0	0	0	0	0
Lung tumors:	0 mg/m^3	3/9 (33)	0/9 (0)[#]	3	0	0	0	0	0	0	0	0
	3 mg/m^3	9/28 (32)	11/28 (39)*	4	0	0	1	4	5	0	4	2
	10 mg/m^3	15/26 (58)	11[c]/26 (42)*	11	0	0	0	4	2	1	8	1
	30 mg/m^3	10/26 (38)	15[c]/26 (58)**	8	1	1	0	0	4	7	4	1
All exposed groups combined		34/80 (43)	37[c]/80 (46)**	23	1	1	1	8	11	8	16	4
Without pulmonary overload		9/28 (32)	11/28 (39)*	4	0	0	0	4	5	0	4	2
With pulmonary overload		25/52 (48)	26[c]/52 (50)**	19	1	1	0	4	6	8	12	2

*Significantly different ($P \leq 0.05$) from the chamber control group by the one-sided Fisher's exact test.
**$P \leq 0.005$.
[#]Significant exposure-concentration trend ($P \leq 0.01$) by the Cochran-Armitage trend test.
[a]Male and female B6C3F1/N mice were exposed to 0, 3, 10, or 30 mg/m^3 antimony trioxide daily by inhalation for 2 years. Silent mutations are not included.
[b]Number of tissues with mutation/number of tissues assayed (% with mutation).
[c]Same animal with double mutations (M449 with *Egfr* 20 and 21; M623 with *Egfr* 19 and 21).

Table K-7. *Kras* and *Egfr* Mutations in Nontumor Lung Tissue and Alveolar/Bronchiolar Carcinomas from Male B6C3F1/N Mice in the Two-year Inhalation Study of Antimony Trioxide[a]

Sample/ Animal #	Dose (mg/m^3)/ Dx	*Kras*			*Egfr*			
		Codon 12	Codon 13	Codon 61	Exon 18	Exon 19	Exon 20	Exon 21
1/M14	0/N	NM	NM	NM	NM	NM	NM	NM
2/M15	0/N	NM	NM	NM	NM	NM	NM	NM
3/M20	0/N	NM	NM	NM	NM	NM	NM	NM
4/M22	0/N	NM	NM	NM	NM	NM	NM	NM
5/M26	0/N	NM	NM	NM	NM	NM	NM	NM
6/M28	0/N	NM	NM	NM	NM	NM	NM	NM

Sample/ Animal #	Dose (mg/m^3)/ Dx	*Kras*			*Egfr*			
		Codon 12	**Codon 13**	**Codon 61**	**Exon 18**	**Exon 19**	**Exon 20**	**Exon 21**
7/M33	0/N	NM	NM	NM	NM	NM	NM	NM
8/M34	0/N	NM	NM	NM	NM	NM	NM	NM
9/M40	0/N	NM	NM	NM	NM	NM	NM	NM
10/M47	0/N	NM	NM	NM	NM	NM	NM	NM
11/M10	0/Ca	NM	NM	NM	NM	NM	NM	NM
12/M13	0/Ca	GGT→GAT (Gly→Asp)	NM	NM	NM	NM	NM	NM
13/M25	0/Ca	NM	NM	NM	NM	NM	NM	NM
14/M58	0/Ca	NM	NM	NM	NM	NM	NM	NM
15/M205	3/Ca	NM	NM	NM	NM	NM	NM	NM
16/M210	3/Ca	NM	NM	NM	**Codon 723** GGA→AGA (Gly→Arg)	NM	NM	NM
17/M211	3/Ca	NM	NM	NM	NM	NM	NM	NM
18/M219	3/Ca	NM	NM	NM	**Codon 713** GAA→AAA (Glu→Lys)	NM	NM	NM
19/M220	3/Ca	NM	NM	NM	NM	NM	NM	NM
20/M225	3/Ca	NM	NM	NM	NM	NM	NM	NM
21/M228	3/Ca	NM	NM	NM	NM	NM	NM	NM
22/M242	3/Ca	NM	NM	NM	NM	NM	NM	**Codon 859** GGG→AGG (Gly→Arg)

Sample/ Animal #	Dose (mg/m^3)/ Dx	*Kras*			*Egfr*			
		Codon 12	**Codon 13**	**Codon 61**	**Exon 18**	**Exon 19**	**Exon 20**	**Exon 21**
23/M247	3/Ca	NM	NM	NM	NM	NM	**Codon 796** CCC→CCT (Pro→Pro)	NM
24/M251	3/Ca	GGT→GAT (Gly→Asp)	NM	NM	NM	NM	NM	**Codon 866** GCT→ACT (Ala→Thr)
25/M252	3/Ca	NM	NM	**Codon 60** GGT→GAT (Gly→Asp)	**Codon 713** GAA→AAA (Glu→Lys)	NM	NM	NM
26/M253	3/Ca	NM	NM	NM	NM	NM	NM	NM
27/M255	3/Ca	NM	NM	NM	NM	NM	NM	**Codon 876** GGC→GGT (Gly→Gly)
28/M256	3/Ca	NM	NM	CAA→CTA (Gln→Leu)	NM	NM	NM	NM
29/M259	3/Ca	NM	NM	NM	NM	NM	NM	NM
30/M402	10/Ca	NM	NM	NM	NM	NM	NM	NM
31/M404	10/Ca	GGT→GTT (Gly→Val)	NM	CAA→CAT (Gln→His)	NM	NM	NM	NM
32/M406	10/Ca	NM	NM	NM	NM	NM	**Codon 772** GAC→GAT (Asp→Asp)	NM
33/M418	10/Ca	NM	NM	NM	NM	NM	**Codon 782** ATC→ACC	NM

Sample/ Animal #	Dose (mg/m^3)/ Dx	*Kras*			*Egfr*			
		Codon 12	**Codon 13**	**Codon 61**	**Exon 18**	**Exon 19**	**Exon 20**	**Exon 21**
							(Ile→Thr)	
34/M421	10/Ca	NM	NM	NM	NM	NM	NM	NM
35/M422	10/Ca	NM	NM	NM	NM	NM	**Codon 807** CAC→TAC (His→Tyr)	NM
36/M424	10/Ca	GGT→GAT (Gly→Asp)	NM	NM	NM	NM	NM	NM
37/M426	10/Ca	GGT→GAT (Gly→Asp)	NM	NM	NM	NM	NM	NM
38/M429	10/Ca	GGT→GAT (Gly→Asp)	NM	NM	NM	NM	**Codon 810** AAC→CAC (Asn→His)	NM
39/M435	10/Ca	NM	NM	NM	NM	NM	**Codon 771** GTG→GAG (Val→Glu)	**Codon 837** CAC→CAT (His→His)
40/M437	10/Ca	NM	NM	NM	NM	**Codon 752** GCC→GAC (Ala→Asp)	NM	NM
41/M445	10/Ca	NM	NM	CAA→CTA (Gln→Leu)	NM	NM	**Codon 807** CAC→TAC (His→Tyr)	NM
42/M449	10/Ca	NM	NM	NM	NM	NM	**Codon 799** TCG→CGC (Cys→Arg)	**Codon 870** GAA→AAA (Glu→Lys)

Sample/ Animal #	Dose (mg/m^3)/ Dx	*Kras*			*Egfr*			
		Codon 12	**Codon 13**	**Codon 61**	**Exon 18**	**Exon 19**	**Exon 20**	**Exon 21**
43/M451	10/Ca	NM	NM	NM	NM	NM	NM	NM
44/M456	10/Ca	NM	NM	CAA→CAC (Gln→His)	NM	NM	**Codon 813** TCC→CCC (Ser→Pro)	NM
45/M458	10/Ca	NM	NM	NM	NM	NM	NM	NM
46/M602	30/Ca*	NM	NM	NM	NM	**Codon 758** AAC→AAT (Asn→Asn)	NM	NM
47/M605	30/Ca	GGT→GAT (Gly→Asp)	NM	NM	**Codon 691** GTG→GAG (Val→Glu)	NM	NM	NM
48/M614	30/Ca	NM	NM	NM	NM	NM	**Codon 788** GTC→GTA (Val→Val)	NM
49/M615	30/Ca	NM	GGC→CGC Gly→Arg)	NM	NM	NM	NM	NM
50/M620	30/Ca	GGT→GAT (Gly→Asp)	NM	NM	NM	NM	**Codon 810** CAC→AAC (His→Asn)	NM
51/M622	30/Ca	GGT→GAT (Gly→Asp)	NM	NM	NM	NM	**Codon 771** GTG→GTA (Val→Val)	**Codon 849** ACA→ACG (Thr→Thr)
52/M623	30/Ca	NM	NM	NM	NM	**Codon 751** GAA→GGA	NM	**Codon 841** GCA→GTA

Sample/ Animal #	Dose (mg/m³)/ Dx	*Kras*			*Egfr*			
		Codon 12	**Codon 13**	**Codon 61**	**Exon 18**	**Exon 19**	**Exon 20**	**Exon 21**
						(Glu→Gly)		(Ala→Val)
53/M628	30/Ca	GGT→GAT (Gly→Asp)	NM	NM	NM	**Codon 744** GTG→GAG (Val→Glu)	NM	NM
54/M633	30/Ca	NM	NM	NM	NM	**Codon 737** GGT→GAT (Gly→Asp)	NM	**Codon 859** GGG→GGT (Gly→Gly)
55/M641	30/Ca	NM	NM	NM	**Codon 706** TTG→CTG (Leu→Leu)	NM	**Codon 799** TGC→CGC (Cys→Arg)	NM
56/M642	30/Ca	GGT→GTT (Gly→Val)	NM	**Codon 14** GTA→ATA (Val→Ile)	NM	NM	NM	NM
57/M643	30/Ca	GGT→GAT (Gly→Asp)	NM	NM	NM	**Codon 752** GCC→GAC (Ala→Asp)	NM	NM
58/M644	30/Ca	NM	NM	NM	NM	NM	**Codon 812** GGC→GGT (Gly→Gly) **Codon 813** TCC→CCC (Ser→Pro)	NM
59/M646	30/Ca	NM	NM	NM	NM	**Codon 732** CTC→CTT	NM	NM

Sample/ Animal #	Dose (mg/m³)/ Dx	*Kras*				*Egfr*		
		Codon 12	**Codon 13**	**Codon 61**	**Exon 18**	**Exon 19**	**Exon 20**	**Exon 21**
60/M656	30/Ca	NM	NM	NM	NM	(Leu→Leu) **Codon 745** GCC→GTC (Ala→Val)	NM	NM
61/M657	30/Ca	NM	NM	NM	NM	NM	NM	**Codon 877** AAA→AAG (Lys→Lys)

[a]Mice were exposed to 0, 3, 10, or 30 mg/m³ antimony trioxide daily by inhalation for 2 years. Alveolar/bronchiolar carcinomas were included.
N = no neoplasm; NM = no mutation; Ca = carcinoma; *Pathology Working Group downgraded the diagnosis to hyperplasia.

Table K-8. *Kras* and *Egfr* Mutations in Alveolar/Bronchiolar Carcinomas from Female B6C3F1/N Mice in the Two-year Inhalation Study of Antimony Trioxide[a]

Sample/ Animal #	Dose (mg/m³)/ Dx	*Kras*				*Egfr*		
		Codon 12	**Codon 13**	**Codon 61**	**Exon 18**	**Exon 19**	**Exon 20**	**Exon 21**
1/F113	0/Ca	GGT→GAT (Gly→Asp)	NM	NM	NM	**Codon 758** AAC→AAT (Asn→Asn)	NM	NM
2/F122	0/Ca	NM	NM	NM	NM	NM	NM	NM
3/F147	0/Ca	NM	NM	NM	NM	NM	NM	NM
4/F155	0/Ca	GGT→GAT (Gly→Asp)	NM	NM	NM	NM	NM	NM
5/F156	0/Ca	NM	NM	NM	NM	NM	**Codon 815** TAC→TAT (Tyr→Tyr)	NM
6/F303	3/Ca	NM	NM	NM	NM	NM	**Codon 801** CTG→CAG	**Codon 861** GCC→GCT

Sample/ Animal #	Dose (mg/m^3)/ Dx	*Kras*			*Egfr*			
		Codon 12	**Codon 13**	**Codon 61**	**Exon 18**	**Exon 19**	**Exon 20**	**Exon 21**
							(Leu→Gln)	(Ala→Ala)
7/F310	3/Ca	NM	NM	NM	NM	NM	NM	NM
8/F312	3/Ca	NM	NM	CAA→CAT (Gln→His)	NM	NM	**Codon 822** CAG→CGG (Gln→Arg)	NM
9/F318	3/Ca	GGT→GAT (Gly→Asp)	NM	CAA→CAG Gln→Gln)	NM	NM	NM	NM
10/F326	3/Ca	GGT→GAT (Gly→Asp)	NM	CAA→CTA (Gln→Leu)	NM	NM	NM	NM
11/F333	3/Ca	NM	NM	NM	NM	NM	NM	NM
12/F334	3/Ca	NM	NM	CAA→CAC (Gln→His)	NM	NM	**Codon 811** ATT→ACT (Ile→Thr)	NM
13/F338	3/Ca	NM	NM	NM	NM	NM	NM	NM
14/F339	3/Ca	NM	NM	NM	**Codon 696** CCC→GCC (Pro→Ala)	NM	NM	NM
15/F353	3/Ca	NM	NM	NM	NM	NM	**Codon 815** TAC→TCC (Ile→Thr)	NM
16/F354	3/Ca	NM	NM	NM	NM	NM	NM	NM
17/F355	3/Ca	GGT→GTT (Gly→Val)	NM	NM	**Codon 690** CTC→TTC (Leu→Phe)	NM	NM	NM
18/F356	3/Ca	NM	NM	NM	NM	NM	NM	NM
19/F503	10/Ca	GGT→GAT	NM	CAA→CAG	NM	NM	NM	NM

Sample/ Animal #	Dose (mg/m^3)/ Dx	*Kras*			*Egfr*			
		Codon 12	**Codon 13**	**Codon 61**	**Exon 18**	**Exon 19**	**Exon 20**	**Exon 21**
		(Gly→Asp)		(Gln→Gln)				
20/F504	10/Ca	GGT→GTT	NM	NM	NM	NM	NM	NM
		(Gly→Val)						
21/F508	10/Ca	NM	NM	NM	**Codon 724**	NM	NM	NM
					GCA→GTA			
					(Ala→Val)			
22/F516	10/Ca	GGT→GAT	NM	NM	NM	NM	NM	NM
		(Gly→Asp)						
23/F523	10/Ca	GGT→GAT	NM	CAA→CGA	NM	NM	**Codon 801**	NM
		(Gly→Asp)		(Gln→Arg)			CTG→CAG	
							(Leu→Gln)	
24/F525	10/Ca	NM	NM	NM	NM	NM	NM	NM
25/F538	10/Ca	GGT→GAT	NM	NM	NM	NM	NM	NM
		(Gly→Asp)						
26/F555	10/Ca	GGT→GAT	NM	NM	NM	NM	NM	NM
		(Gly→Asp)						
27/F556	10/Ca	NM	NM	NM	**Codon 701**	NM	NM	NM
					CCA→TCA			
					(Pro→Ser)			
28/F558	10/Ca	GGT→GAT	NM	NM	NM	NM	NM	NM
		(Gly→Asp)						
29/F706	30/Ca	NM	NM	NM	NM	NM	NM	NM
30/F707	30/Ca	NM	NM	NM	NM	**Codon 747**	NM	NM
						AAG→AGG		
						(Lys→Arg)		
31/F725	30/Ca	GGT→CGT	NM	NM	NM	**Codon 752**	NM	NM

Sample/ Animal #	Dose (mg/m^3)/ Dx	*Kras*				*Egfr*		
		Codon 12	**Codon 13**	**Codon 61**	**Exon 18**	**Exon 19**	**Exon 20**	**Exon 21**
		(Gly→Arg)				GCC→GTC (Ala→Val)		
32/F740	30/Ca	NM	NM	NM	NM	NM	NM	NM
33/F742	30/Ca	NM	NM	NM	NM	NM	**Codon 812** GGC→GGT (Gly→Gly) **Codon 813** TCC→CCC (Ser→Pro)	NM
34/F744	30/Ca	NM	NM	NM	**Codon 691** GTG→GAG (Val→Glu)	NM	NM	NM
35/F749	30/Ca	NM	NM	NM	NM	NM	NM	NM
36/F753	30/Ca	GGT→GTT (Gly→Val)	NM	NM	NM	NM	NM	NM
37/F755	30/Ca	NM	NM	NM	**Codon 806** GAA→GGA (Glu→Gly)	NM	NM	NM
38/F759	30/Ca	NM	NM	NM	**Codon 712** ACA→ATA (Thr→Ile)	NM	NM	NM

[a]Mice were exposed to 0, 3, 10, or 30 mg/m^3 antimony trioxide daily by inhalation for 2 years. Alveolar/bronchiolar carcinomas were included.
NM = no mutation; Ca = carcinoma.

Appendix L. Summary of Peer Review Panel Comments

On February 16, 2016, the draft Technical Report on the toxicology and carcinogenesis studies of antimony trioxide received public review by the National Toxicology Program's Technical Reports Peer Review Panel. The review meeting was held at the National Institute of Environmental Health Sciences, Research Triangle Park, NC.

Dr. M.D. Stout, NIEHS, introduced the toxicology and carcinogenesis studies of antimony trioxide by describing the uses of the chemical, the study designs, and the results of the studies in rats and mice, including nonneoplastic and neoplastic lesions in test animals. The proposed conclusions were *some evidence of carcinogenic activity* of antimony trioxide in male and female Wistar Han rats and *clear evidence of carcinogenic activity* of antimony trioxide in male and female B6C3F1/N mice.

Dr. Pino, the first primary reviewer, stated the studies in both rats and mice were well conducted, and the results overall supported NTP's conclusions regarding the long-term toxicity and carcinogenicity of antimony trioxide. He suggested adding mention of foreign body in the summary findings in the abstract, providing solubility of antimony trioxide in water, clarifying the paragraph about animal source, and discussing whether or not cataracts observed in female mice were considered related to exposure. He also suggested giving the reasons why the findings in the prostate gland and skin of rats and the adrenal medullary pheochromocytomas in mice were not considered exposure related. He disagreed that the incidence of mammary gland carcinoma in rats was meaningfully decreased. He also made several specific editorial corrections and comments. He suggested changes to the report's conclusions, including rewriting a sentence in the first paragraph to indicate that the incidence of fibrous histiocytoma alone is also increased and replacing "lesions of" with "findings in" in the second paragraph. He noted that there was no increase in reticulocytes in the micronucleus test in rats at 12 months to correlate with the bone marrow increase in erythroid precursors at 2 years. This was in contrast to observations in the mouse. He suggested hematology should have been performed to determine what was happening with circulating erythrocytes. He agreed with the discussion in the report that significance of increased micronuclei in mice was of questionable significance. Dr. Pino suggested that a brief sentence discussing foreign body observations would be helpful. Dr. Stout concurred. For Dr. Pino's other suggestions, Dr. Stout agreed with his comments and noted that sections of the report would be updated accordingly. Dr. Pinkerton, the second primary reviewer, stated the study design, conduct, and findings were excellent. He noted that the conclusions made by NTP were scientifically sound and logical. While he did not recommend deleting any information from the report, he suggested that tables should be adjusted to provide a clear designation of the total number of animals examined. He suggested adding a definition of "thinness" for the animals. He asked for more information on inflammation of the pleura and appreciated the report's inclusion of the rationale for changing the rat model. Dr. Stout said he would ensure that the number of animals is included in all tables. Regarding "thinness," he said it is a general body shape observation. Dr. G.P. Flake, NIEHS, discussed pleural inflammation, stating that particles in or below the pleura appeared to cause the fibrosis that had been observed. Dr. Pinkerton asked if it was dose related. Dr. Flake replied that it was.

Dr. Singal, the third primary reviewer, stated that overall the study design was appropriate and suggested improvements to enhance the report's thoroughness and additional endpoints that

could have been added to the studies. She asked for more information about how the material affected the system as a whole. She suggested that urinary excretion could have been added. She asked for further evaluation of the difference in thymus weight increases between rats and mice. She suggested lung lavage data would have been informative of the proteinaceous/cellular changes in the lungs. She asked for further evaluation of the observation regarding karyorrhectic debris, as well as evaluation of lymphocytic infiltrates in rats. She noted that skin lesions had been observed in mice and suggested that future studies should include a more detailed evaluation of dermal changes due to the relevance for effects observed in humans. She suggested further investigation of hyaline droplet formation in the kidney. She suggested inclusion of comet assay data, as it is mentioned in the text and not shown, to allow a basis for comparison of the differing DNA damage results in mice and rats. In reference to the discussion in the report about potential intrinsic toxicity of antimony trioxide, she noted that particle surface chemistry may contribute to free radical generation and asked for further investigation. Regarding microscopic image slides, she asked for more information about the collection and fixing process and the method of sectioning. She suggested adding proper labeling with magnification information. She recommended adding images of sections of the upper respiratory tract. She noted that there was reference to deposition and clearance modeling without data or methodology. She said her observations would enhance the report and not detract from the study's findings. Dr. Stout stated that urinary excretion is not typically assessed in these types of studies and acknowledged that it might have been useful in this case. He said that lung lavage data are typically obtained in satellite studies. Dr. Flake addressed Dr. Singal's comment regarding arterial inflammation, noting that the cause was unknown and there are several possibilities. Regarding Dr. Singal's question about pulmonary edema, he noted that the associated histologic changes were not observed. He proposed the vascular changes were most likely related to increased blood volume. Regarding the karyorrhectic debris, he said it was related to the neutrophils and alveolar macrophages in the lung, which tend to form aggregates and ultimately break down to form the debris seen. Regarding the lymphocytic infiltrates in the rats, he said it was a less prominent reaction than in the mice. Dr. Stout concurred about cytokine analysis being useful to include; however, he said the molecular analyses were retrospective; therefore, there was not an opportunity to collect specimens for cytokine analysis. He agreed that the skin effects warranted further investigation. He said Dr. Singal's suggestion regarding hyaline droplet accumulation was noteworthy. Regarding the DNA damage results, he noted that the genotoxicity data are publicly available on the website and that there were no observed explanations for the difference between the results in the rats and the mice. He said that the issue of particle surface chemistry in the study of metal particles could be important to investigate in better understanding the toxicity. He said that the final magnification was not shown on the photos because it could be different when it is published. He stated that collecting and fixing sections of the lungs followed standard NTP practices. He agreed that it would be helpful to add more detail about the inflation fixing pressure and that images of the upper respiratory tract would be helpful. He noted that deposition and clearance information had been included in the report's appendix and would be checked for completeness.

Dr. Mirsalis noted receipt and distribution to the panel of written comments from Dr. Craig Boreiko of CJB Risk Analysis, LLC on behalf of the International Antimony Association. He then recognized Dr. Boreiko for oral public comments. Dr. Boreiko spoke on behalf of the International Antimony Association and noted he would be touching on highlights of the written comments he had previously submitted. He said there was no question that something was

happening in the mouse; however, he proposed that the question of why remained largely unresolved in the report. He was surprised by the results in the rat. He speculated that deep alveolar loading was likely to be significantly greater in the rat studies than that seen in previous studies. He noted that particle overload had been discussed in the body of the report; however it was not in the abstract. He questioned interpretation of the comet assay data, and asked whether the micronucleus data were actually biologically significant. He questioned the conclusion of clear evidence of lymphoma in female mice.

Dr. Brock asked whether the panelists' discussions and reviews would be captured and processed for inclusion in the final reports and future studies. Dr. C.R. Blystone, NIEHS, replied that all comments are discussed and addressed, and suggestions are taken into account. Dr. Brock asked if there was a process for protocol review. Dr. Blystone said that there are multiple steps for protocol review and reviewer comments are considered. Dr. Brock said that he had found the exposure concentration justification weak given the results of the study. He suggested enhancing the justification in the report.

Dr. Elwell asked whether the adenoma in the nose (listed in the summary tables in the appendix) of one of the highest exposure male rats should be mentioned in the body of the report, given that it was at a target site. He asked about the incidence of adenomas in males at the highest dose in the lung; the table in the report indicated that there were eight, which did not seem to agree with the incidence in the summary table of the report. Dr. Stout noted that eight is the correct number.

Dr. Mirsalis stated that following standard regulatory guidelines, the genotoxicity data would be considered negative. Regarding the micronucleus data, he said that it is important to consider the historical control data for comparison. He emphasized that contrary to language in the report, there was a lack of genotoxic carcinogen response. He recommended toning down that section of the report. Ms. Kristine Witt, NIEHS, genetic toxicology group leader in the Biomolecular Screening Branch of DNTP, noted that the report reflected what had been observed. The level of response was low, and the historic control data were taken into account.

Dr. Brock moved to accept the conclusions as written, and Dr. Pinkerton seconded the motion. Dr. Pino suggested adding the phrase "incidence of fibrous histiocytoma and the" to the second bullet point under the male mice. In the discussion of nonneoplastic issues, Dr. Pino suggested changing the word "lesions" to "findings," and the addition of "the kidney and" between "and" and "eye" later in the sentence.

Given Dr. Pino's suggestions, Dr. Brock withdrew his original motion. Dr. Pino moved to accept the conclusions as revised. Dr. Pinkerton seconded the motion. Dr. Mirsalis called for a vote on the motion. The panel voted unanimously to accept the motion.

National Toxicology Program

NTP Central Data Management, MD EC-03
National Institute of Environmental Health Sciences
P.O. Box 12233
Research Triangle Park, NC 27709

http://ntp.niehs.nih.gov

ISSN 2378-8925